BIOSYNTHESIS AND USE OF COBAMIDES BY PROKARYOTES

by

ELIZABETH ANNE VILLA

(Under the Direction of JORGE C. ESCALANTE-SEMERENA)

ABSTRACT

Cobamides are used as cofactors by diverse enzymes across all domains of life to catalyze numerous reactions including carbon skeleton rearrangements, methylations and eliminations. Cobamides are modified tetrapyrroles, and belong to a family of coenzymes known as the “pigments of life” which includes chlorophylls, bilins, heme and coenzyme F_{430}. As such, cobamides are one of the most complex molecules produced in nature, and are composed of a cobalt-containing cyclic tetrapyrrole with an upper (*Co*β) and lower (*Co*α) ligand. Perhaps one of the best-known cobamides is coenzyme B_{12}, or adenosylcobalamin, which critical to numerous metabolic reactions including methionine synthesis, methanogenesis, and catabolism of ethanolamine and 1,2-propanediol.

De novo biosynthesis of coenzyme B_{12} requires approximately 30 enzymes, and is only performed by some prokaryotes. Two different pathways have been defined for synthesis of the central corrin ring, in which the Co^{+2} may be inserted “early” or “late” in the pathway. These pathways are further differentiated by a requirement for molecular oxygen in the “late” insertion pathway, while the “early” insertion pathway occurs under anaerobic conditions. Once the corrin ring is formed, the axial ligands are attached. The final steps of biosynthesis include the activation and attachment of the lower ligand

through a process known as nucleotide loop assembly (NLA). Many prokaryotes are incapable of *de novo* corrin ring biosynthesis, but are capable of salvaging ring precursors into a complete coenzyme using this pathway.

In this work, we investigate the biosynthesis and use of coenzyme B_{12} in a number of prokaryotes. We identified a metabolosome-free system for ethanolamine utilization in *Acinetobacter baumannii*. We investigate the interactions between the NLA enzymes CobU and the integral membrane protein CobS, and propose that the *cis* bond formed between Glu^{80} and Cys^{81} of CobU is involved in facilitating this interaction. We further characterize CbiS, a fusion protein identified in *Methanopyrus kandleri* that catalyzes both amidohydrolase and phosphatase reactions necessary for precursor salvaging in archaea. This work expands our understanding of the physiological role of enzymes that make and require cobamides in multiple prokaryotic species.

INDEX WORDS: *Acinetobacter,* Cobamide, Coenzyme B_{12}, ethanolamine, *Salmonella*, *Methanopyrus*

BIOSYNTHESIS AND USE OF COBAMIDES BY PROKARYOTES

by

ELIZABETH ANNE VILLA

B.S., VIRGINIA POLYTECHNIC INSTITUTE AND STATE UNIVERSITY

M.S., APPALACHIAN STATE UNIVERSITY

A Dissertation Submitted to the Graduate Faculty of The University of Georgia in Partial Fulfillment of the Requirements for the Degree

DOCTOR OF PHILOSOPHY

ATHENS, GEORGIA

2022

BIOSYNTHESIS AND USE OF COBAMIDES BY PROKARYOTES

by

ELIZABETH ANNE VILLA

Major Professor:	Jorge C. Escalante-Semerena
Committee:	Diana Downs M. Stephen Trent Robert Maier

Electronic Version Approved:

Ron Walcott
Vice Provost for Graduate Education and Dean of the Graduate School
The University of Georgia
December 2022

DEDICATION

This dissertation is dedicated to my husband, Daniel, and our cat Dexter and dog Finn. I am lucky to come home to you three every day.

ACKNOWLEDGEMENTS

First, I would like to acknowledge the members of the Escalante lab who have influenced my growth as a scientist during my time in graduate school. Thank you, Jorge, for fostering an environment where curiosity is encouraged. I consider myself very lucky to have had a mentor who allowed me so much freedom and flexibility in my research.

I thank my husband Daniel for being a constant source of support through all of our years together. When things get overwhelming, I can always count on you to make me laugh, and am so fortunate to have you as my partner.

A huge thank you to my family, especially my parents Mary and John, who provided me with so many opportunities. Thank you for always supporting and encouraging my endeavors. I would also like to thank Linda and Rodney for being such supportive in-laws. As this chapter closes, Daniel and I are looking forward to moving closer to both of our families.

Thank you to my friends, both old and new. I am grateful to have an amazing group of friends who keep me motivated through disappointments and celebrate my successes.

And thank you for reading!

TABLE OF CONTENTS

LIST OF TABLES

Page

LIST OF FIGURES

Page

CHAPTER 1

INTRODUCTION TO THE BIOSYNTHESIS AND USE OF COBAMIDES BY PROKARYOTES

1.1 OVERVIEW OF COBAMIDE STRUCTURE AND FUNCTION

Modified tetrapyrroles, sometimes referred to as the “pigments of life”, act as cofactors for a diverse array of enzymes across all domains of life (1). This group of metal-containing tetrapyrroles includes heme, coenzyme F_{430}, chlorophylls, bilins, and cobamides (2). Cobamide cofactors are large molecules that contain the characteristic corrin ring, a cyclic tetrapyrrole ring with a central cobalt ion equatorially chelated to the nitrogen atoms of the pyrrole rings. In the biologically active coenzyme, a Co-C bond secures the upper ligand (*Co*β) 5’-deoxyadenosine to the corrin ring structure. The covalent bond is relatively weak and responsible for the radical chemistry associated with cobamide coenzymes. In a complete cobamide, a lower (Coα) ligand extends from the opposite face of the ring in which a nucleobase is tethered to the ring by a structure known as the nucleotide loop. Perhaps the best known cobamide, coenzyme B_{12}, contains 5,6-dimethylbenzimidazole (DMB) in this position. Various nucleobases may be substituted at this position, and specificity may depend on the organism or environment in which the coenzyme is formed. The structure of coenzyme B_{12} is illustrated in Figure 1.1.

Cobamides are used by enzymes to catalyze a diverse array of biological reactions including carbon skeleton rearrangements, methyl transfers, and eliminations (2). In prokaryotes, catabolism of ethanolamine, 1,2-propanediol, and glycerol are cobamide-dependent (3-5). Cobamides are also critical cofactors for methanogenesis (6, 7). Humans require coenzyme B_{12}; therefore, cobamides are relevant to human healthcare. The human methylmalonyl-CoA mutase requires coenzyme B_{12}, and a B_{12}-deficiency can lead to severe neurological problems and even death (8). Pathogenic bacteria including *Listeria monocytogenes, Salmonella enterica* serovar Typhimurium (*S.* Typhimurium) and *Escherichia coli* utilize cobamide-dependent ethanolamine metabolism during the course of infection. This metabolic capability enhances infection and adaptation within the human host (9-13).

1.2 BIOSYNTHESIS OF COENZYME B_{12}

Despite the widespread distribution of cobamide-dependent enzymes in living organisms, *de novo* cobamide synthesis is restricted to a subset of prokaryotes. A recent study identified that 86% genomes from gut bacteria encode cobamide-dependent enzymes; however, only 37% of these genomes also encode the genes necessary to synthesize the complete coenzyme (14). Coenzyme B_{12} is one of the most complex molecules produced in nature, and as such the process is extremely energy-intensive. Depending on the organism, this process requires the involvement of approximately 30 enzymes. The *de novo* synthesis pathway of the central corrin ring is illustrated in Figure 1.2.

Like other modified tetrapyrroles such as heme, uroporphyrinogen III (uro'gen III) serves as the template scaffold for cobamide macrocycles (15). Uro'gen III is synthesized from glutamic acid, and six enzymes are required for this conversion. This process is illustrated in Figure 1.2. Glutamic acid is first charged with tRNA, and this glutamyl-tRNA is then reduced to form glutamate semialdehyde (GSA). GSA is then converted into 5-aminolevulinic acid (ALA) (15-18). Two molecules of ALA are condensed to form the pyrrole-containing porphobilinogen (PBG) (19). Four molecules of PBG are polymerized to form the linear tetrapyrrole hydroxymethylbilane, which is then cyclized by an additional enzyme to yield uro'gen III (20-23).

In some organisms, like *Salmonella*, *de novo* ring biosynthesis can only take place in the absence of oxygen (Figure 1.2, left) (24, 25). Alternatively, some organisms require molecular oxygen to synthesize the corrinoid ring. This pathway has been well-studied in *Pseudomonas denitrificans* (Figure 1.2, right) (26). These two pathways also distinctly differ in the timing of insertion of the cobalt atom into the ring; the anaerobic pathway is also known as the "early" insertion pathway, and genes are named with the *cbi* prefix. In this case, uro'gen III is modified by methylation and dehydrogenation by a single enzyme, CysG. At this point, the cobalt ion is inserted by a cobaltochelatase. Contraction of the methylene bridge between ring A and D occurs subsequently (Figure 1.1). The aerobic pathway implements "late" insertion, and these genes have a *cob* prefix. In this case, a number of modifications are made to the pyrrole moieties, and ring contraction takes place late in the pathway but prior to insertion of the cobalt ion (26, 27).

The completed cobalt-containing ring structure produced in this process is known as cobyric acid, which is further modified with upper and lower ligands to produce the

biologically active coenzyme. Many organisms are not capable of synthesizing the corrin ring, but produce the proteins necessary to import the corrin ring-containing precursors and attach the upper and lower ligands to form a cobamide, a process known as "salvaging" (14). The salvaging process is briefly described here based on studies in *S.* Typhimurium. More information on salvaging and remodeling of corrin precursors and cobamides, as well as alternative enzymes found in other organisms can be found in Chapter 3.

Following ring synthesis, the upper (*Coβ)* ligand is attached. This reaction is catalyzed by an ATP:Co(I)rrinoid adenosyltransferase (ACAT, PF01923). In *S.* Typhimurium, CobA is the housekeeping adenosyltransferase (EC 2.5.1.17) (28, 29). Two additional classes of ACAT enzymes, EutT and PduO, are utilized for ethanolamine and 1,2-propanediol, respectively (30-32). Adenosylation requires two single-electron reductions of the cobalt ion to take place. In *S.* Typhimurium, the first reduction of Co^{+3} to Co^{+2} can be performed nonenzymatically by free dihydroflavins (33). The second reduction of Co^{+2} to Co^{+1} is carried out by the ACAT, which then facilitates the nucleophilic attack of Co^{+1} to the 5'-C of ATP, forming a Co-C bond and releasing phosphate (34-36).

The nucleotide loop is assembled and attached late in the cobamide biosynthetic pathway. The *S.* Typhimurium pathway is discussed here. Homologous enzymes in other organisms are illustrated in Figure 1.3 and discussed further in Chapter 3. In *S.* Typhimurium, NLA enzymes are specific for adenosylated intermediates (37). In the first step of nucleotide loop assembly (NLA), an aminopropanol (AP) linker is attached to the corrin ring. In *S.* Typhimurium, synthesis of AP is catalyzed by CobD (EC 4.1.1.81) (38). This AP moiety is synthesized from L-threonine-phosphate by PduX (EC 2.7.1.177) (39).

CbiB (EC 6.3.1.10) attaches AP to cobyric acid to form adenosylcobinimade-phosphate (AdoCbi-P). Subsequent nucleotide loop attachment requires the products of the *cobUST* operon (40-42). CobU (EC 2.7.1.156, 2.7.7.62) is a bifunctional kinase/guanylyltransferase, which activates the ring in an essential step in both *de novo* synthesis and salvaging and generates adenosylcobinamide-GDP (40, 43, 44). If cobinamide is to be salvaged, the substrate is first phosphorylated and subsequently guanylylated by CobU (43, 45). During *de novo* synthesis, the CbiB product (AdoCbi-P) is already phosphorylated, so only the guanylyltransferase activity is required. CobT (EC 2.4.2.21) is a phosphoribosyltransferase, which generates the α-ribazole-phosphate (α-RP) of the nucleotide loop from a nucleotide base and NaMN. The base is 5,6-dimethylbenzimidazole in the case of coenzyme B_{12} (46, 47). It is important to note that while we focus on coenzyme B_{12}, a number of bases may be used in the nucleotide loop (48). These include other benzimidazoles, purine analogues, and phenolic compounds (49-51). The synthase CobS (EC 2.7.8.26) condenses the activated ring and nucleobase, forming adenosylcobalamin-5'-phosphate (52-55). The final step of nucleotide loop assembly entails the removal of the 5'-phosphate of the ribose moiety by CobC (EC 3.1.3.73) to yield the biologically active coenzyme (56).

1.3 DISSERTATION OUTLINE

This dissertation details my work to expand our knowledge of both biosynthesis and use of coenzyme B_{12} and cobamides by various prokaryotes. Chapter 2 details the identification and verification of a metabolosome-free ethanolamine utilization system in the pathogen *Acinetobacter baumannii*. Ethanolamine catabolism depends on a

cobamide cofactor for the ethanolamine-ammonia lyase (EAL) enzyme complex. Typically, this process takes place within a protein shell known as a metabolosome. We identified a unique, metabolosome-free mechanism in this organism. Intriguingly, the EAL enzyme complex localizes to the membrane in both *A. baumannii* and *S.* Typhimurium. *A. baumannii* is also capable of salvaging the precursor cobinamide, and can produce various cobamide analogues. EAL can utilize a number of these analogues as a coenzyme. This work expands our knowledge of B_{12} utilization into a new organism, and provides insight into the physiology and metabolism of this pathogen.

Chapter 3 is a review discussing the current literature on salvaging and remodeling systems in archaea and bacteria. All subsequent chapters will focus on precursor salvaging and/or remodeling. I discuss cobamides-dependent enzymes in various organisms, the nucleotide loop assembly pathway, and currently identified remodeling enzymes.

Chapter 4 describes a method for reconstitution of cobamide synthase CobS into a proteoliposome. This method facilitates improved study of CobS, and may be useful in the study of other integral membrane proteins. Use of this method has enhanced our ability to study the interactions between NLA enzymes, which will be discussed in the subsequent chapter.

In Chapter 5, I report findings from studies to investigate interactions between *S.* Typhimurium NLA enzymes CobS and CobU. An intriguing aspect of cobamide synthesis is the common association with the membrane. I discuss investigations of interactions between CobS, the cobalamin-phosphate synthase and an integral membrane protein, and the adenosylcobinamide kinase/ adenosylcobinamide-phosphate

guanylyltransferase CobU. We propose a model in which CobS and other integral membrane proteins such as CbiB act as anchor points in the membrane around which other NLA enzymes can localize to facilitate efficient exchange of intermediates.

Chapter 6 describes studies of the amidohydrolase CbiS from *Methanopyrus kandleri*. This enzyme is of particular interest because it is a fusion of CbiZ and CobZ, which represent the “first” and “last” enzyme activities necessary for archaeal salvage and/or remodeling processes. Intriguingly, this fusion is only found in extremophilic organisms, suggesting that an advantage to stability or activity under extreme conditions may be enhanced by fusing these two enzymes.

In Chapter 7, concise conclusions of the findings reported in this work are reiterated. Recommendations for future directions are proposed.

1.4 REFERENCES

1. Battersby AR. 2000. Tetrapyrroles: the pigments of life. Nat Prod Rep 17:507-526.
2. Bryant DA, Hunter CN, Warren MJ. 2020. Biosynthesis of the modified tetrapyrroles-the pigments of life. J Biol Chem 295:6888-6925.
3. Toraya T, Honda S, Kuno S, Fukui S. 1978. Coenzyme B_{12}-dependent diol dehydratase: regulation of apoenzyme synthesis in Klebsiella pneumoniae (Aerobacter aerogenes) ATCC 8724. J Bacteriol 135:726-9.
4. Daniel R, Bobik TA, Gottschalk G. 1998. Biochemistry of coenzyme B12-dependent glycerol and diol dehydratases and organization of the encoding genes. FEMS Microbiol Rev 22:553-66.
5. Roof DM, Roth JR. 1988. Ethanolamine utilization in *Salmonella typhimurium*. J Bacteriol 170:3855-3863.
6. DiMarco AA, Bobik TA, Wolfe RS. 1990. Unusual coenzymes of methanogenesis. Annu Rev Biochem 59:355-94.
7. Grahame DA. 1989. Different isozymes of methylcobalamin:2-mercaptoethanesulfonate methyltransferase predominate in methanol- versus acetate-grown *Methanosarcina barkeri*. J Biol Chem 264:12890-12894.
8. Banerjee R, Chowdhury S. 1999. Methylmalonyl-CoA mutase, p 707-729. *In* Banerjee R (ed), Chemistry and Biochemistry of B_{12}. John Wiley & Sons, Inc., New York.
9. Joseph B, Przybilla K, Stuhler C, Schauer K, Slaghuis J, Fuchs TM, Goebel W. 2006. Identification of *Listeria monocytogenes* genes contributing to intracellular replication by expression profiling and mutant screening. J Bacteriol 188:556-568.

10. Anderson CJ, Clark DE, Adli M, Kendall MM. 2015. Ethanolamine signaling promotes *Salmonella* niche recognition and adaptation during infection. PLoS Pathog 11:e1005278.
11. Anderson CJ, Kendall MM. 2016. Location, location, location. *Salmonella* senses ethanolamine to gauge distinct host environments and coordinate gene expression. Microb Cell 3:89-91.
12. Foster DB, Philpott D, Abul-Milh M, Huesca M, Sherman PM, Lingwood CA. 1999. Phosphatidylethanolamine recognition promotes enteropathogenic E. coli and enterohemorrhagic E. coli host cell attachment. Microbial pathogenesis 27:289-301.
13. Wu Y, Lau B, Smith S, Troyan K, Barnett Foster D. 2004. Enteropathogenic Escherichia coli infection triggers host phospholipid metabolism perturbations. Infection and immunity 72:6764-6772.
14. Shelton AN, Seth EC, Mok KC, Han AW, Jackson SN, Haft DR, Taga ME. 2019. Uneven distribution of cobamide biosynthesis and dependence in bacteria predicted by comparative genomics. ISME J 13:789-804.
15. Warren MJ, Scott AI. 1990. Tetrapyrrole assembly and modification into the ligands of biologically functional cofactors. Trends Biochem Sci 15:486-491.
16. Beale SI, Castelfranco PA. 1974. The biosynthesis of 5-aminolevulinic acid in higher plants. II. Formation of 5-amino[14C]levulinic acid for labelled precursors in greening plants tissues. Plant Physiol 53:291-296,.
17. Li JM, Brathwaite O, Cosloy SD, Russell CS. 1989. 5-Aminolevulinic acid synthesis in *Escherichia coli*. J Bacteriol 171:2547-2552.

18. Jahn D, Michelsen U, Soll D. 1991. Two glutamyl-tRNA reductase activities in *Escherichia coli*. J Biol Chem 266:2542-2548.

19. Li JM, Russell CS, Cosloy SD. 1989. The structure of the Escherichia coli *hemB* gene. Gene 75:177-184.

20. Battersby AR, McDonald E, Cornforth JW, Frydman B. 1976. Biosynthesis of Porphyrins and Corrins [and Discussion]. Phil Transac Royal Soc London Series B, Biol Sci 273:161-180.

21. Thomas SD, Jordan PM. 1986. Nucleotide sequence of the hemC locus encoding uroporhybilinogen deaminase of Escherichia coli K-12. Nucleic Acids Res 14:6215-6225.

22. Sasarman A, Nepveu A, Echelard Y, Dymetryszyn J, Drolet M, Goyer C. 1987. Molecular cloning and sequencing of the hemD gene of Escherichia coli and preliminary data on the Uro operon. J BActeriol 169:4257-4262.

23. Jordan PM, Mgbeje BIA, Thomas SD, Alwan AF. 1988. Nucleotide sequence for the hemD gene of Escherichia coli encoding uroporphyrinogen III synthase and initial evidence for a hem operon. Biochem J 249:613-616.

24. Jeter RM, Olivera BM, Roth JR. 1984. *Salmonella typhimurium* synthesizes cobalamin (vitamin B_{12}) de novo under anaerobic growth conditions. J Bacteriol 159:206-213.

25. Moore SJ, Lawrence AD, Biedendieck R, Deery E, Frank S, Howard MJ, Rigby SE, Warren MJ. 2013. Elucidation of the anaerobic pathway for the corrin component of cobalamin (vitamin B12). Proc Natl Acad Sci U S A 110:14906-14911.

26. Thibaut D, Blanche F, Debussche L, Leeper FJ, Battersby AR. 1990. Biosynthesis of vitamin B12: structure of precorrin-6x octamethyl ester. Proc Natl Acad Sci U S A 87:8800-8804.

27. Müller G, Zipfel F, Hliney K, Savvidis E, Hertle R, Traub-Eberhard U, Scott AI, Williams HJ, Stolowich NJ, Santander PJ, Warren M, Blanche F, Thibaut D. 1991. Timing of cobalt insertion in vitamin B12 biosynthesis. J Amer Chem Soc 113:9893-9895.

28. Suh S, Escalante-Semerena JC. 1995. Purification and initial characterization of the ATP:corrinoid adenosyltransferase encoded by the *cobA* gene of *Salmonella typhimurium*. J Bacteriol 177:921-925.

29. Suh SJ, Escalante-Semerena JC. 1993. Cloning, sequencing and overexpression of *cobA* which encodes ATP:corrinoid adenosyltransferase in *Salmonella typhimurium*. Gene 129:93-97.

30. Buan NR, Escalante-Semerena JC. 2006. Purification and initial biochemical characterization of ATP:Cob(I)alamin adenosyltransferase (EutT) enzyme of *Salmonella enterica*. J Biol Chem 281:16971-16977.

31. Buan NR, Suh SJ, Escalante-Semerena JC. 2004. The *eutT* gene of *Salmonella enterica* encodes an oxygen-labile, metal-containing ATP:corrinoid adenosyltransferase enzyme. J Bacteriol 186:5708-5714.

32. Johnson CL, Pechonick E, Park SD, Havemann GD, Leal NA, Bobik TA. 2001. Functional genomic, biochemical, and genetic characterization of the *Salmonella pduO* gene, an ATP:cob(I)alamin adenosyltransferase gene. J Bacteriol 183:1577-1584.

33. Fonseca MV, Escalante-Semerena JC. 2000. Reduction of cob(III)alamin to cob(II)alamin in *Salmonella enterica* Serovar Typhimurium LT2. J Bacteriol 182:4304-4309.

34. Stich TA, Brooks AJ, Buan NR, Brunold TC. 2003. Spectroscopic and computational studies of Co(3+)-corrinoids: spectral and electronic properties of the B(12) cofactors and biologically relevant precursors. J Am Chem Soc 125:5897-5914.

35. Stich TA, Buan NR, Brunold TC. 2004. Spectroscopic and computational studies of Co(2+)corrinoids: spectral and electronic properties of the biologically relevant base-on and base-off forms of Co(2+)cobalamin. J Am Chem Soc 126:9735-9749.

36. Stich TA, Buan NR, Escalante-Semerena JC, Brunold TC. 2005. Spectroscopic and computational studies of the ATP:Corrinoid adenosyltransferase (CobA) from *Salmonella enterica*: Insights into the mechanism of adenosylcobalamin biosynthesis. J Am Chem Soc 127:8710-8719.

37. Escalante-Semerena JC, Suh SJ, Roth JR. 1990. *cobA* function is required for both de novo cobalamin biosynthesis and assimilation of exogenous corrinoids in *Salmonella typhimurium*. J Bacteriol 172:273-280.

38. Brushaber KR, O'Toole GA, Escalante-Semerena JC. 1998. CobD, a novel enzyme with L-threonine-*O*-3-phosphate decarboxylase activity, is responsible for the synthesis of (*R*)-1-amino-2-propanol *O*-2-phosphate, a proposed new intermediate in cobalamin biosynthesis in *Salmonella typhimurium* LT2. J Biol Chem 273:2684-2691.

39. Fan C, Bobik TA. 2008. The PDUX enzyme of *Salmonella enterica* is an L-threonine kinase used for coenzyme B_{12} synthesis. J Biol Chem 283:11322-11329.

40. O'Toole GA, Rondon MR, Escalante-Semerena JC. 1993. Analysis of mutants of defective in the synthesis of the nucleotide loop of cobalamin. J Bacteriol 175:3317-3326.

41. Woodson JD, Zayas CL, Escalante-Semerena JC. 2003. A new pathway for salvaging the coenzyme B_{12} precursor cobinamide in archaea requires cobinamide-phosphate synthase (CbiB) enzyme activity. J Bacteriol 185:7193-7201.

42. Zayas CL, Claas K, Escalante-Semerena JC. 2007. The CbiB protein of *Salmonella enterica* is an integral membrane protein involved in the last step of the de novo corrin ring biosynthetic pathway. J Bacteriol 189:7697-7708.

43. O'Toole GA, Escalante-Semerena JC. 1995. Purification and characterization of the bifunctional CobU enzyme of *Salmonella typhimurium* LT2. Evidence for a CobU-GMP intermediate. J Biol Chem 270:23560-23569.

44. Blanche F, Debussche L, Famechon A, Thibaut D, Cameron B, Crouzet J. 1991. A bifunctional protein from *Pseudomonas denitrificans* carries cobinamide kinase and cobinamide phosphate guanylyltransferase activities. J Bacteriol 173:6052-6057.

45. Thomas MG, Thompson TB, Rayment I, Escalante-Semerena JC. 2000. Analysis of the adenosylcobinamide kinase/adenosylcobinamide-phosphate guanylyltransferase (CobU) enzyme of *Salmonella typhimurium* LT2. Identification of residue His-46 as the site of guanylylation. J Biol Chem 275:27576-27586.

46. Trzebiatowski JR, Escalante-Semerena JC. 1997. Purification and characterization of CobT, the nicotinate-mononucleotide:5,6-dimethylbenzimidazole phosphoribosyltransferase enzyme from *Salmonella typhimurium* LT2. J Biol Chem 272:17662-17667.

47. Trzebiatowski JR, O'Toole GA, Escalante-Semerena JC. 1994. The *cobT* gene of *Salmonella typhimurium* encodes the NaMN: 5,6-dimethylbenzimidazole phosphoribosyltransferase responsible for the synthesis of N^1-(5-phospho-alpha-D-ribosyl)-5,6-dimethylbenzimidazole, an intermediate in the synthesis of the nucleotide loop of cobalamin. J Bacteriol 176:3568-3575.

48. Cheong CG, Escalante-Semerena JC, Rayment I. 2001. Structural investigation of the biosynthesis of alternative lower ligands for cobamides by nicotinate mononucleotide: 5,6-dimethylbenzimidazole phosphoribosyltransferase from *Salmonella enterica*. J Biol Chem 276:37612-37620.

49. Chan CH, Escalante-Semerena JC. 2011. ArsAB, a novel enzyme from *Sporomusa ovata* activates phenolic bases for adenosylcobamide biosynthesis. Mol Microbiol 81:952-967.

50. Stupperich E, Eisinger HJ, Kräutler B. 1989. Identification of phenolyl cobamide from the homoacetogenic bacterium *Sporomusa ovata*. Eur J Biochem 186:657-661.

51. Keck B, Munder M, Renz P. 1998. Biosynthesis of cobalamin in *Salmonella typhimurium*: transformation of riboflavin into the 5,6-dimethylbenzimidazole moiety. Arch Microbiol 171:66-68.

52. Maggio-Hall LA, Claas KR, Escalante-Semerena JC. 2004. The last step in coenzyme B(12) synthesis is localized to the cell membrane in bacteria and archaea. Microbiology 150:1385-1395.

53. Zayas CL, Escalante-Semerena JC. 2007. Reassessment of the late steps of coenzyme B_{12} synthesis in *Salmonella enterica*: Evidence that dephosphorylation of adenosylcobalamin-5'-phosphate by the CobC phosphatase is the last step of the pathway. J Bacteriol 189:2210-2218.

54. Jeter VL, Escalante-Semerena JC. 2021. Insights into the relationship between cobamide synthase and the cell membrane. mBio 12.

55. Jeter VL, Escalante-Semerena JC. 2022. Elevated levels of an enzyme involved in coenzyme B12 biosynthesis kills *Escherichia coli*. mBio 13:e0269721.

56. O'Toole GA, Trzebiatowski JR, Escalante-Semerena JC. 1994. The *cobC* gene of *Salmonella typhimurium* codes for a novel phosphatase involved in the assembly of the nucleotide loop of cobalamin. J Biol Chem 269:26503-26511.

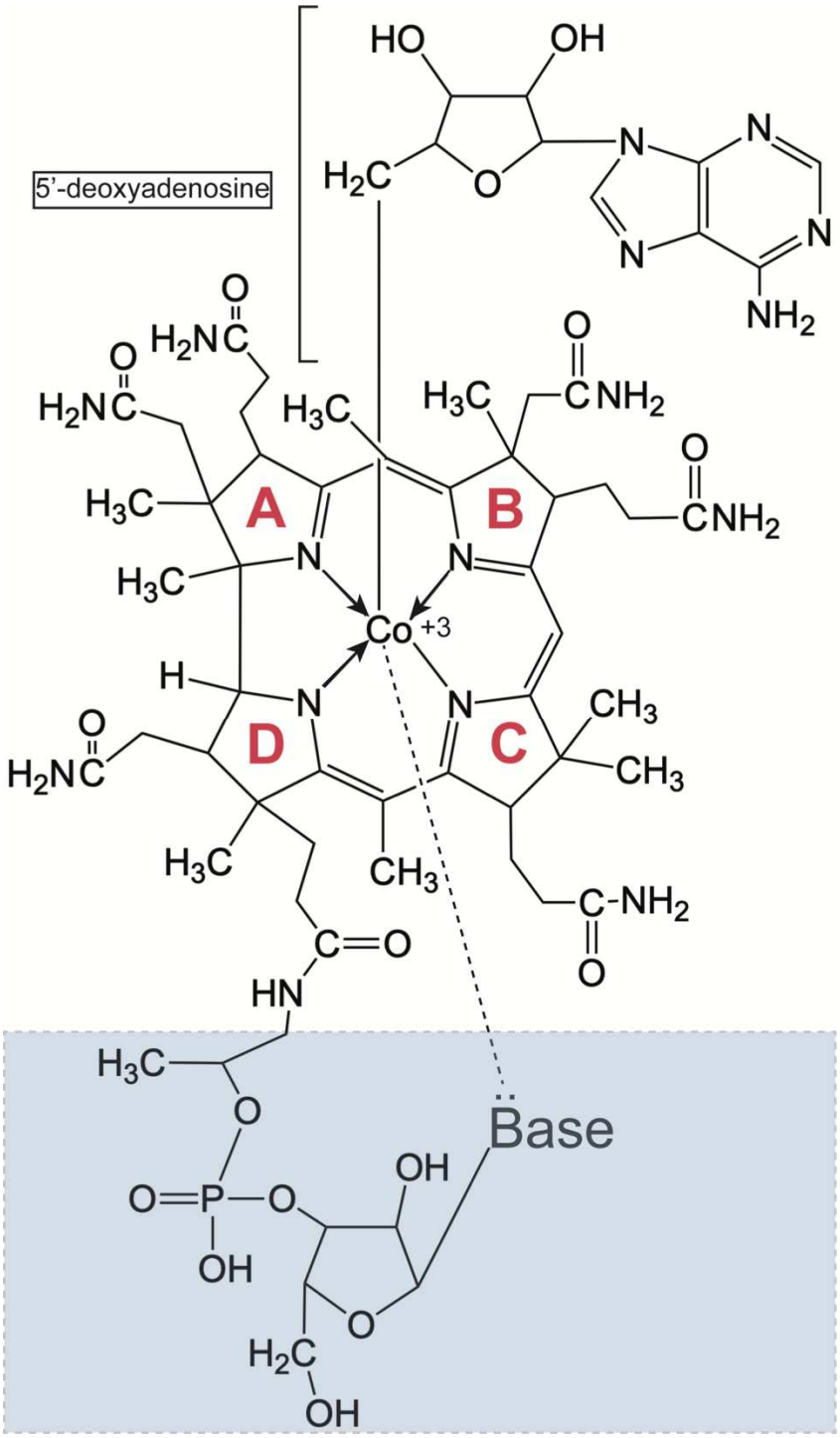

Figure 1.1. The structure of coenzyme B_{12}. The individual pyrrole rings of the corrin moiety are labeled in red. The *Co*β ligand, 5'-deoxyadenosine, is shown in brackets. The nucleotide loop (*Co*α ligand) is highlighted in a blue box. "Base" denotes variable bases that may be incorporated into the nucleotide loop at this position.

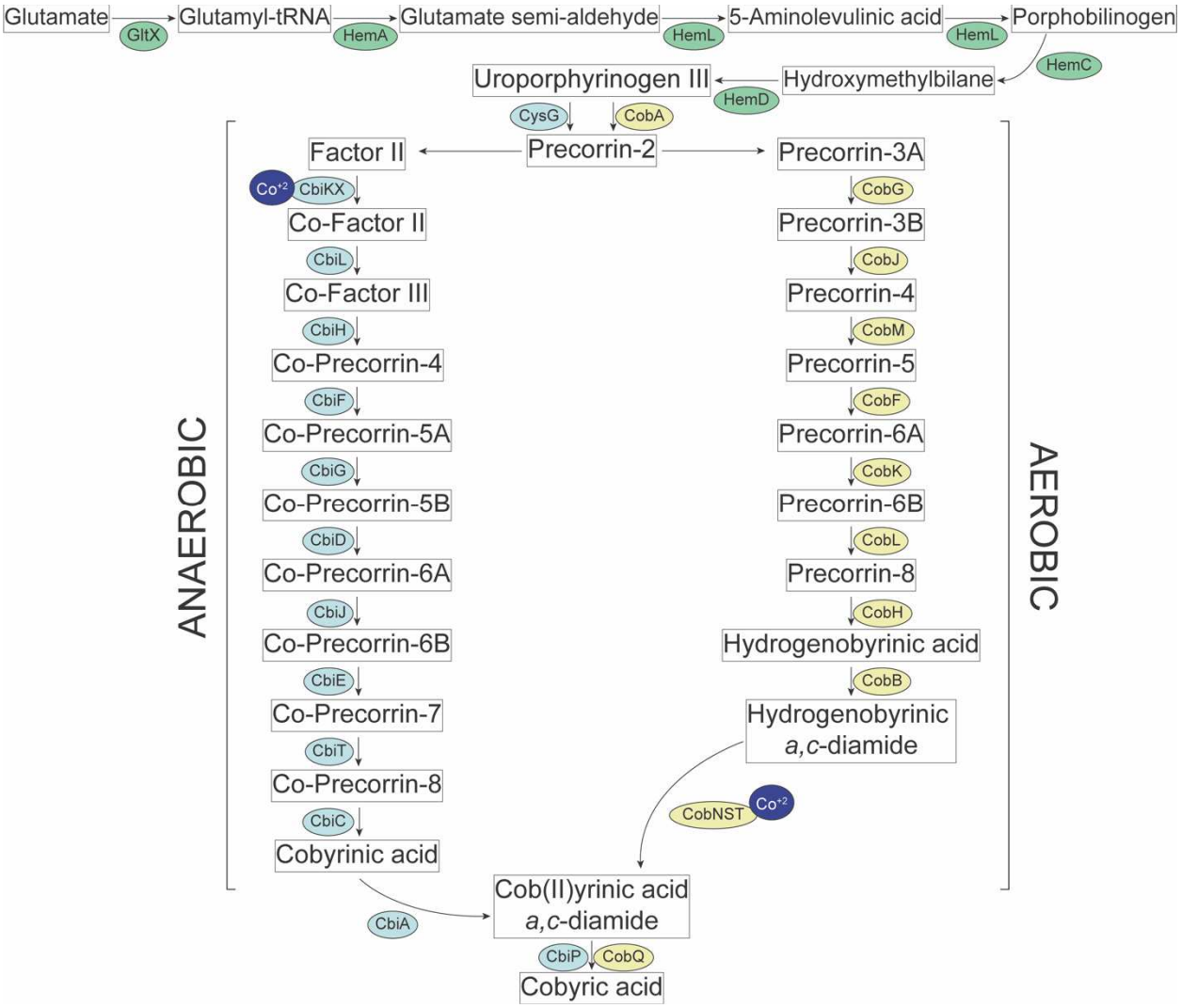

Figure 1.2. *De novo* cobamide biosynthesis. Enzymes involved in uro'gen III synthesis are shown in green circles. The early and late cobalt insertion pathways are illustrated. The anaerobic pathway (early insertion) intermediates are depicted on the left with enzymes shown in light blue circles. The aerobic (late insertion) pathway intermediates are shown on the right with enzymes shown in yellow circles. The cobalt insertion step is denoted by Co^{+2} shown in dark blue circles.

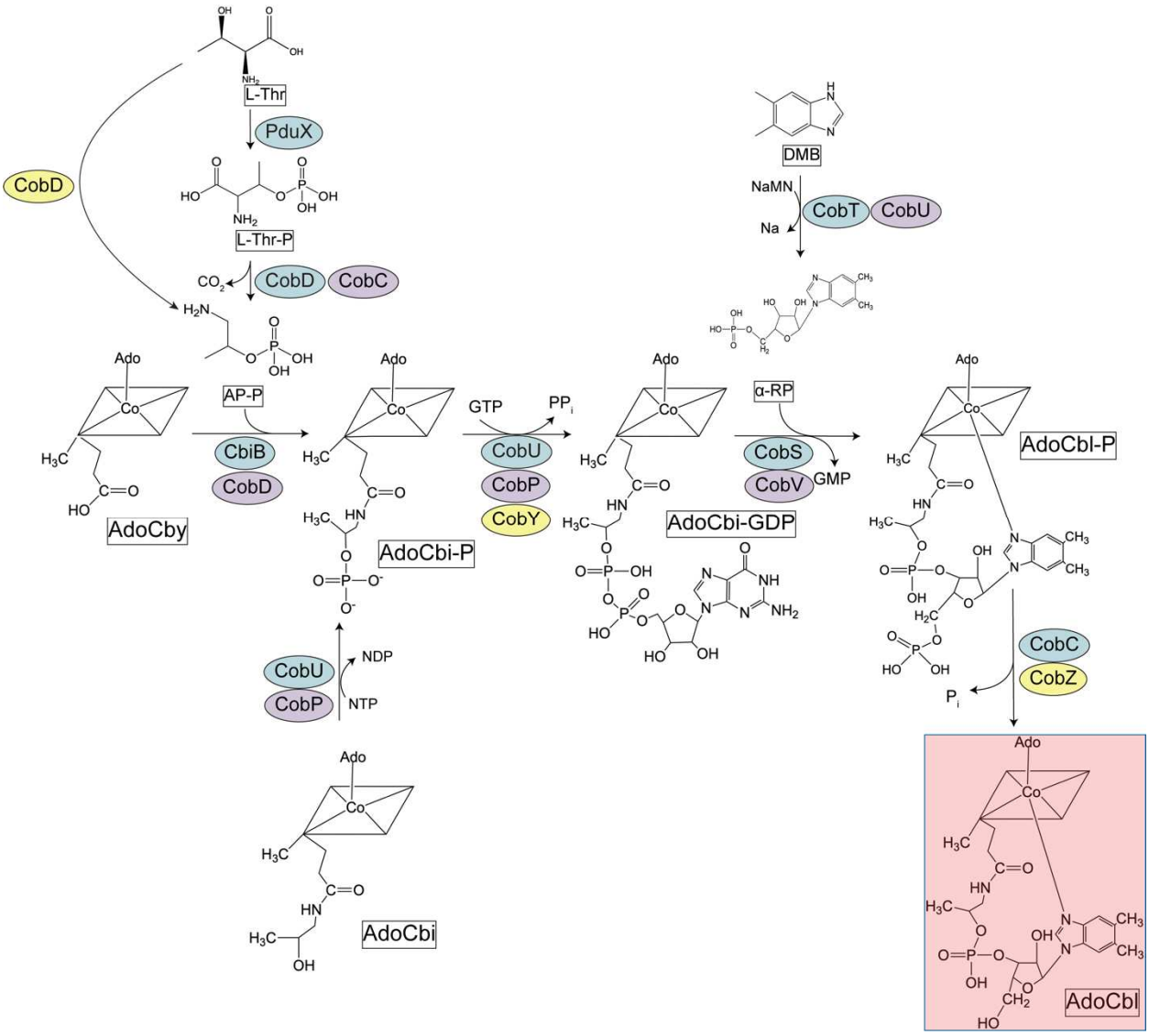

Figure 1.3. Nucleotide loop assembly in bacteria and archaea. The structures of pathway intermediates are shown. *S.* Typhimurium enzymes are shown in blue. *P. denitrificans* homologues are shown in purple. Archaeal homologues are shown in yellow. AdoCbl (coenzyme B_{12}) is shown in a red box. Abbreviations are as follows: L-Thr, L-threonine; L-Thr-P, L-threonine-phosphate; AP-P, aminopropanol-phosphate; AdoCby, adenosylcobyric acid; AdoCbi, adenosylcobinamide; AdoCbi-P, adocobinamide-phosphate; AdoCbi-GDP, adenosylcobinamide-GDP; DMB, 5,6-dimethylbenzimidazole; α-RP, a-ribazole-phosphate; AdoCbl-P, adenosylcobalamin-phosphate; AdoCbl, adenosylcobalamin.

CHAPTER 2

ACINETOBACTER BAUMANNII CATABOLIZES ETHANOLAMINE IN THE ABSENCE OF A METABOLOSOME AND CONVERTS COBINAMIDE INTO ADENOSYLATED COBAMIDES[1]

[1]Villa E.A. and Escalante-Semerena, J.C. 2022. *mBio. 13:*e01793-22.

Reprinted here with permission from the publisher.

2.1 ABSTRACT

Acinetobacter baumannii is an opportunistic pathogen typically associated with hospital-acquired infections. Our understanding of the metabolism and physiology of *A. baumannii* is limited. Here we report that *A. baumannii* uses ethanolamine (EA) as the sole source of nitrogen, and can use this aminoalcohol as a source of carbon and energy if the expression of the *eutBC* genes encoding ethanolamine ammonia-lyase (EAL) is increased. A strain with an IS*Aba1* element upstream of the *eutBC* genes efficiently used EA as carbon and energy source. The *A. baumannii* EAL (*Ab*EAL) enzyme supported growth of a strain of *Salmonella* lacking the entire *eut* operon. Remarkably, growth of the aforementioned *Salmonella* strain did not require the metabolosome, the reactivase EutA enzyme, the EutE acetaldehyde dehydrogenase, nor the addition of glutathione to the medium. Transmission electron micrographs showed that when *S.* Typhimurium synthesized *Ab*EAL the protein localized to the cell membrane. We also report that the *A. baumannii* genome encodes all the enzymes needed for the assembly of the nucleotide loop of cobamides, and that it uses these enzymes to synthesize different cobamides from the precursor cobinamide and several nucleobases. In the absence of exogenous nucleobases, the most abundant cobamide produced by *A. baumannii* was cobalamin.

2.2 IMPORTANCE

Acinetobacter baumannii is a Gram-negative bacterium commonly found in soil and water. *A. baumannii* is an opportunistic human pathogen, considered by the CDC to be a serious threat to human health due to the multi-drug resistances commonly associated with this bacterium. Knowledge of the metabolic capabilities of *A. baumannii*

is limited. The importance of the work reported here lies on the identification of ethanolamine catabolism occurring in the absence of a metabolosome structure. In other bacteria, this structure protects the cell against damage by acetaldehyde generated by the deamination of ethanolamine. In addition, the ethanolamine ammonia-lyase (EAL) enzyme of this bacterium is unique in that it does not require a reactivase enzyme to remain active. Importantly, we also demonstrate that the *A. baumannii* genome encodes the functions needed to assemble adenosylcobamide, the coenzyme of EAL, from the precursor cobinamide.

2.3 INTRODUCTION

Acinetobacter baumannii is a non-motile Gram-negative bacillus of concern to public health due to its ability to rapidly develop resistance to antibiotics, leading to multidrug resistant strains that are difficult to treat. At present, *A. baumannii* is listed as a high-priority pathogen for research and development of new antibiotics by the World Health Organization.

A goal of this study was to determine whether *A. baumannii* could catabolize ethanolamine (EA), and if so, which enzymes were required to degrade this aminoalcohol. Inspection of the genome of this bacterium suggested that EA could be catabolized and used as a source of carbon, energy and nitrogen. In pathogens such as *Salmonella enterica* subsp. *enterica* sv. Typhimurium str. LT2 (hereafter *S.* Typhimurium), EA catabolism plays an important role in cell fitness, survival, and infection (1-3).

Bioinformatics analysis of the *A. baumannii* genome provided a very intriguing picture of how EA may be catabolized in this bacterium. We identified homologues to

some of the genes required for EA degradation in *S.* Typhimurium, where such metabolic capability has been studied in detail (4). The genome of *S.* Typhimurium contains a 16-gene operon (*eutSPQTDMNEJGHABCLK*) that encodes functions needed for the safe breakdown of EA inside a structure that is referred to as the Eut metabolosome (5, 6). *S.* Typhimurium controls the expression of the *eut* operon with an AraC-like protein known as EutR, which binds AdoCbl and EA before it activates expression of the *eut* operon (Fig. 2.1A). In contrast, the *A. baumannii* genome encodes only a putative 4-gene *eut* operon (locus tags A1S_2102, 2103, 2104, and 2106, respectively) and a divergently transcribed regulator (*eatR,* locus tag A1S_2101)*,* encoding a σ^{54} enhancer binding protein (7) (Fig. 2.1B). Two additional genes immediately upstream and divergently transcribed from the putative regulator may also participate in the catabolism of EA. If this were the case, six functions would be needed to breakdown EA in *A. baumannii* (Fig. 2.1B, Fig. 2.2). Notably, the genome does not encode the shell proteins that comprise the *S.* Typhimurium metabolosome. This fact is important because it suggests that EA catabolism in *A. baumannii* is not contained within a metabolosome, raising the question of how this bacterium controls reactive intermediates generated during EA catabolism in the absence of such physical structure.

The first step of EA catabolism is catalyzed by the adenosylcobalamin (AdoCbl)-dependent EA ammonia-lyase (EAL) encoded by the *eutBC* genes (8-10) (Figure 2.3). As mentioned above, in *S.* Typhimurium this metabolic pathway occurs inside of the metabolosome (6) to prevent cell damage by acetaldehyde, and to sequester and concentrate substrates, enzymes, and coenzymes needed for the efficient catabolism of EA (*e.g.,* AdoCbl, NAD^+, CoA) (11, 12). Previous studies in *S.* Typhimurium demonstrated

that under certain conditions, EAL alone was sufficient for ethanolamine catabolism only when exogenous glutathione was provided to mitigate the damaging effects of acetaldehyde (6).

Figure 2.3 depicts two steps pertinent to the work reported herein, namely, the conversion of Co(II)Cbl to AdoCbl by EutT ('AdoCbl biosynthesis' in the figure), and the exchange of AdoCbl for Co(II)Cbl by EutA ('EAL activation' in the figure). Notably, the *A. baumannii* genome lacks a EutT-type ATP:Co(I)rrinoid adenosyltransferase (ACAT) (13-17) needed for the synthesis of an adenosylcobamide (AdoCba), the cofactor of the EAL enzyme. We have identified a putative PduO-type ACAT elsewhere on the chromosome (locus tag A1S_2878) (Figure 2.4). PduO ACATs are the most widespread ACATs in prokaryotes, and homologues are the only ACAT found in humans (18-20).

The absence of most *eut* genes in *A. baumannii* suggest that this organism may have evolved a new way of breaking down EA that does not expose the cell to acetaldehyde damage. Furthermore, lack of an identifiable EutA reactivase structural homologue presents two possibilities; either *Ab*EAL better protects AdoCbl from inactivation than *S.* Typhimurium EAL, or there is a functional homologue for the *S.* Typhimurium EutA reactivase yet to be discovered in *A. baumannii.*

While the *A. baumannii* genome does not encode functions for the *de novo* synthesis of the corrin ring of AdoCba, it does encode homologues of enzymes required for the assembly of the nucleotide loop of AdoCba. The alluded genes are *cobU* (A1S_1659)*, cobS* (A1S_1663)*, cobT* (A1S_1660) and *cobC* (A1S_1661) (Fig. 2.5, 2.6), and their products activate the corrin ring and the nucleobase, condense the activated precursors and dephosphorylate the last intermediate to yield biologically active

cobamides (Fig. 2.7) (21). Collectively, the presence of these putative functions suggested that *A. baumannii* could salvage incomplete corrinoids and convert them into biologically active coenzymes.

In this work, we i) experimentally validate the ability of *A. baumannii* to utilize ethanolamine as a sole carbon, nitrogen and energy source, ii) show that increased expression of *eutBC* is required for *A. baumannii* to utilize ethanolamine as a sole carbon source, iii) show that *Ab*EAL is sufficient to support ethanolamine utilization in the absence of all other Eut proteins, iv) determine that *Ab*EutBC localizes to the cell membrane of *A. baumannii* and *S.* Typhimurium, v) show that ethanolamine catabolism relies on the availability of an adenosylcobamide (AdoCba), and that *A. baumannii* genome encodes functions needed to assemble the nucleotide loop of an AdoCba from a precursor such as cobinamide, vi) show that *A. baumannii* synthesizes a functional PduO-type ATP:Co(I)rrinoid adenosyltransferase, vii) showed that the *A. baumannii* ethanolamine ammonia-lyase (*Ab*EutBC) can utilize various adenosylcobamides, and that *A. baumannii* predominantly makes cobalamin from cobinamide in the absence of exogeneous base supplementation.

2.4 RESULTS

Chromosomal expression of *eutBC* allows *A. baumannii* to use ethanolamine as a sole nitrogen source, but not as a carbon and energy source. To determine whether *A. baumannii* could use EA as a nitrogen source, growth was assessed in minimal medium containing M9 salts made without NH_4Cl, but was supplemented with ethanolamine as the sole source of nitrogen (Fig. 2.8A). To determine whether *A.*

baumannii could use EA as a carbon and energy source, M9 minimal medium (containing NH_4Cl) was supplemented with ethanolamine as the sole source of carbon and energy (Fig. 2.8B). Growth of *A. baumannii* with ethanolamine depended on wild-type alleles of the *eutBC* genes (Fig. 2.8A, 2.8B, grey squares), which encode the subunits of the adenosylcobalamin (AdoCbl)-dependent EAL enzyme subunits. Chromosomal levels of *eutBC* expression were sufficient to support growth on ethanolamine as a nitrogen source (Fig. 2.8A, yellow squares). When *eutBC* was overexpressed *in trans*, the cultures reached a higher density (Fig. 2.8A, blue circles). In contrast, *A. baumannii* grew with ethanolamine as the sole source of carbon and energy in medium supplemented with CNCbl only when *eutBC* was overexpressed (Fig. 2.8B, blue circles *vs* yellow squares).

Spontaneous *A. baumannii* mutant strains grow robustly on ethanolamine when *eutBC* expression is driven by the IS*Aba1* element. We isolated spontaneous strains of *A. baumannii* that abolished the extended lag time of the wild-type strain growing on ethanolamine as carbon and energy source. The putative mutants were obtained after ~100 h of incubation on liquid medium at 37 ºC. To test the stability of the causative mutation(s) we passaged the mutant strain several times on solid and liquid rich medium. This strain maintained the ability to rapidly grow with ethanolamine as carbon and energy source. These results suggested that the phenotype was the result of one or more stable mutations. To determine the nature of the mutation(s), we sequenced the genome of the mutant strain, and the analysis of the sequence revealed an insertion of the IS*Aba1* transposable element upstream of the *eutBC* genes, between the 3' end of the *eutH* gene (encodes a putative ethanolamine permease) and the start of *eutB* (encodes the putative

large subunit of ethanolamine ammonia-lyase) (Fig. 2.9, 2.10). This element was inserted immediately after the final nucleotide of *eutH*, leaving the 16-bp length upstream of *eutB* undisrupted.

Previous reports have shown that the IS*Aba1* element contains a σ^{70} promoter at the 3' end of the gene, and that this promoter is used to increase the expression of downstream genes (22). This element is frequently associated with increased expression of antibiotic resistance genes in a clinical setting (22-26). The predicted σ^{70} sites found in IS*Aba1* are illustrated in Fig. 2.10.

We used the strain with the IS*Aba1* element driving the synthesis of *Ab*EutBC to determine the optimal concentrations of ethanolamine as a sole carbon source and CNCbl during growth in minimal medium (Fig. 2.116A, 2.11B). Strong growth was observed at 10 nM CNCbl and 75 mM ethanolamine as the sole source of carbon and energy (Fig. 2.11A, blue squares, and Fig. 2.11B, blue circles). As little as 0.5 nM CNCbl and 10 mM EA promoted robust growth when EA was used as the sole source of nitrogen by the *A. baumannii* parental strain (Fig. 2.11C, yellow squares and Fig. 2.11D, blue circles).

Assessment of *A. baumannii* EutBC function in a heterologous host. We used well-characterized *eut* mutant strains of *S.* Typhimurium to assess the level of activity of the *Ab*EutBC enzyme in different genetic backgrounds, namely, a D*eutBC* strain, a D*eutABC* strain, or a strain carrying a deletion of the entire *eut* operon (D*eut*) (Fig. 2.12). *Ab*EutBC supported growth of a *S.* Typhimurium D*eutBC* strain with EA as the sole source of nitrogen as well as *Se*EutBC did (Fig. 2.12A, orange squares *vs* green circles). Notably,

the *Ab*EutBC enzyme remained active in the absence of the *Se*EutA reactivase (Fig. 2.12B, green circles), whilst, as expected, the *Se*EutBC enzyme did not support growth in the absence of *Se*EutA (Fig. 2.12B, orange squares). Most intriguingly, *Ab*EutBC alone supported ethanolamine utilization in a *S.* Typhimurium strain in which the entire *eut* operon was deleted. Consistent for the need for *Se*EutA and other *eut* operon gene products, *Se*EutBC supported poor growth of the D*eut* strain (Fig. 2.12C, green circles *vs* orange squares). *Se*EutBC components (49.4 and 32.1 kDa, respectively) were detected at higher levels in crude lysate (Fig. 2.12E, lanes 2-4) compared to *Ab*EutBC (50.6 and 30.1 kDa, respectively) (Fig. 2.12E lanes 5-8). This was likely due to a stronger reaction of the a-EAL, as this antibody was generated against *Se*EutBC. The reduced signal observed for *Ab*EutC was likely due to protein instability under the tested conditions, as the theoretical pI of *Ab*EutC is 6.96. The loading buffer and gel stacking layer in this experiment were both pH 6.8.

Genes associated with ethanolamine utilization are co-transcribed. To test whether the putative *eut* genes were co-transcribed, primers were generated to amplify the intergenic regions between *ald1* and *eutH*, *eutH* and *eutB*, and *eutB* and *eutC* (Fig. 2.13A). As previously shown in *Pseudomonas aeruginosa*, all four genes were transcribed as a polycistronic mRNA and expressed from a promoter upstream of *ald1* wild-type *A. baumannii* (Fig. 2.13B) (7). We used RT-qPCR to determine that the evolved strain (ES) overexpresses *eutBC* (Fig. 2.13C). In the absence of EA, wild-type *A. baumannii* produced extremely low levels of *eutBC* transcript (Fig. 2.13C, yellow striped bars). The evolved strain carrying an Is*Aba1* insertion upstream of *eutBC* grown with

ethanolamine as a sole carbon source showed a significant increase in *eutBC* expression (100-fold and 64-fold, respectively) compared to the parental strain, while *eutH* levels were very low in both strains and conditions tested. We tested the expression of the upstream *ald1* gene to determine whether this might act as an acetaldehyde dehydrogenase and aid in management of reactive intermediates during EA catabolism. Interestingly, *ald1* was expressed at high levels in wild-type *A. baumannii* even in the absence of EA (Fig. 2.13D); therefore, fluctuations in gene expression in response to EA may not be detectible under the conditions used. This suggested that under some conditions, *ald1-eutHBC* were co-transcribed, but expression of *ald1* may be subject to other regulatory mechanisms.

Transmission electron microscopy reveals the absence of metabolosome structures in *A. baumannii* grown with ethanolamine. We used TEM and immunogold labeling to localize the *Ab*EutBC proteins within the *A. baumannii* cell. Previous reports have shown that *Se*EutBC was associated with the metabolosome (27), which can be visualized by TEM (6). No similar structures were visible in *A. baumannii* cells in the presence of EA as a sole carbon source (Fig. 2.14A, Fig. 2.15A, B). In addition, *Ab*EutBC primarily localized to the periphery of cells, with some protein apparently interspersed throughout the cytosol. We further investigated localization within the cell by overexpressing *Ab*EutBC in a *S.* Typhimurium Δ*eutBC* strain (Fig. 2.14B, Fig. 2.15C, D). It is important to note that the genome of this strain of *S.* Typhimurium encodes the genes for the metabolosome shell. When expressed in the presence of the *eut* metabolosome, *Ab*EutBC did not associate with the metabolosome structure; strikingly it was exclusively

associated with the cell membrane (Fig. 2.14B). No EAL was detected in control samples treated with secondary antibody only (Fig. 2.16).

***A. baumannii* synthesizes cobamides from the precursor cobinamide.** The *Se*EutBC enzyme requires adenosylcobalamin (AdoCbl) as its cofactor (28). Our bioinformatics analysis of the *A. baumannii* genome indicated that this bacterium lacked the functions needed for *de novo* synthesis of the corrin ring of cobamides, but appeared to encode the function needed to adenosylate the corrin ring, *i.e.,* attach the adenosyl (Ado) moiety from ATP to the Co ion of the ring, and the functions required for the assembly of the nucleotide loop (29).

Forming a complete coenzyme from the precursor cobinamide requires the nucleotide loop assembly (NLA) pathway (Fig. 2.7). Under the conditions tested, *A. baumannii* salvaged the precursor cobinamide and other nitrogenous bases to form a functional coenzyme and facilitate the growth on EA, demonstrating that NLA pathway enzymes were functional (Fig. 2.17A), We also tested for activity of NLA enzymes using heterologous expression in a MetH-dependent *S.* Typhimurium strain. *A. baumannii* NLA enzymes CobU, CobS, and CobT compensated for the absence of the *cobU, cobS* and *cobT* genes of *S.* Typhimurium (Fig. 2.17B, 10C). Furthermore, the *A. baumannii pduO*-type ACAT supported EA metabolism in a *S.* Typhimurium ACAT null strain. The NLA enzymes CobU and CobS require adenosylated substrates (30, 31), thus, salvaging of the precursor cobinamide depended on the function of the *A. baumannii* ACAT under these conditions (Fig. 2.17B, C). These results demonstrated that *A. baumannii* NLA and ACAT homologues were functional.

Cobalamin is produced by *A. baumannii* in the absence of nucleobase supplementation. Prokaryotes can utilize numerous nucleobases to yield a functional coenzyme (32). As shown in Figure 2.17A, various bases can be used by *A. baumannii* to form a functional coenzyme. Salvaging was performed in the absence of exogeneous nucleobase, however this led to diminished growth (Fig. 2.17A, purple circles). To determine the identity of this cobamide produced by *A. baumannii* in the absence of exogeneous nucleobase, we extracted cobamides and separated them using RP-HPLC as described in *Materials and Methods*. A compound eluted off the column 33 min after sample injection. The retention time was equal to the retention time of commercially available CNCbl (Fig. 2.18A, B). This peak was collected, cleaned and analyzed using MALDI-TOF mass spectrometry, confirming that cobalamin, the cobamide containing 5,6-dimethylbenzimidazole as its nucleobase was the cobamide synthesized by *A. baumannii* in the absence of exogenous nucleobases (Fig. 2.18C).

2.5 DISCUSSION

***A. baumannii* catabolizes ethanolamine as a source of carbon and nitrogen.** Based on the data presented here we surmised that the wild-type strain of *A. baumannii* used in this work synthesizes insufficient *Ab*EutBC to support growth with EA as the sole carbon and energy source. It is possible, however, that in its natural environment, *A. baumannii* uses EA mainly as a source of nitrogen, and for that purpose enough EAL is produced from chromosomal expression levels. Our data show that *A. baumannii* can use the IS*Aba1* element to increase the expression of *eutBC* if a selective pressure for the use of ethanolamine as carbon and energy source arises in its environment. Previous studies have identified IS*Aba1* upstream of antibiotic resistance genes in patient samples,

suggesting that this is a clinically relevant adaptive mechanism used by this organism during human infection (23). The insertion of an IS*Aba1* element does not affect the expression of the upstream *eutH* and *ald1* genes. The low level of *eutH* even in the presence of EA, suggesting that under the conditions tested, active transport is not required, and that sufficient EA diffuses across the membrane into the cell. We have shown that the requirement for both cobamide and EA concentrations are lower in *A. baumannii* than in *S.* Typhimurium. The reduced need may reflect faster access of enzymes to these molecules due to the lack of restriction by the metabolosome.

***Ab*EAL is sufficient to support ethanolamine metabolism in the absence of a metabolosome or EAL reactivase.** We did not identify genes encoding homologues of metabolosome shell proteins in the *A. baumannii* genome, suggesting to us that *A. baumannii* may be able to perform this metabolism without containment in a microcompartment. The N-terminus of *Se*EutC contains a signal sequence involved in localization to the microcompartment (33). Consistent with the lack of any genes encoding microcompartment shell proteins, the *Ab*EutC sequence also lacks any predicted N-terminal signal sequence (Fig. 2.2D). We showed here that *Ab*EAL does not require a reactivase; furthermore, *Ab*EAL alone can support EA utilization in the absence of the entire *S.* Typhimurium *eut* operon. This suggests that either the *Ab*EAL enzyme directly quenches the acetaldehyde generated from EA or *A. baumannii* reduces cellular damage caused by acetaldehyde using an alternative mechanism. The mechanism by which *Ab*EAL functions in the absence of a physical metabolosome is intriguing. Using TEM, we showed that *A. baumannii* does not form metabolosomes, and that the enzyme does not

associate with metabolosomes when expressed in *S.* Typhimurium (Fig. 2.14). Based on these data, we surmise that the *Ab*EAL enzyme acts independently of other Eut components in *S.* Typhimurium. The membrane association of *Ab*EAL was more pronounced when expressed in *S.* Typhimurium. It is possible that this is due to the association of *Ab*EAL with other B_{12}-related enzymes not found in *A. baumannii.* We hypothesize that in *A. baumannii* other enzymes, such as the co-transcribed aldehyde dehydrogenase, associate with *Ab*EAL to facilitate swift quenching of reactive molecules and prevent cellular damage. To our knowledge, this is the first report of ethanolamine metabolism occurring in an organism that does not form a metabolosome.

Multiple cobamides can be formed by the *A. baumannii* salvaging pathway and used as a coenzyme by *Ab*EAL. *A. baumannii* encodes the genes for nucleotide loop assembly, as well as a functional PduO-type ACAT. Due to the apparent absence of other genes relating to propanediol metabolism, we instead refer to this protein as a general ACAT (AcaT). The unique organization of these genes in *A. baumannii* is notable, as *cobUST* are typically organized immediately adjacent to each other. We have shown experimental evidence that the *cobU, cobT* and *cobS* gene products facilitate use of various nucleobases to form the nucleotide loop, and that the resulting cobamides function as coenzymes for *Ab*EAL. This is consistent with a previous report in which *Se*EAL was shown to also use pseudocobalamin (34). Structural studies would provide insight into the ability of this enzyme complex to utilize multiple cobamide coenzymes.

Ethanolamine metabolism and pathogenesis. Understanding the metabolic capabilities of *A. baumannii* is of great interest as we attempt to combat antimicrobial resistance. EA has been shown to play a role in environmental sensing and pathogenesis of *S.* Typhimurium and *Escherichia coli* (3, 35, 36). Although *A. baumannii* is not generally associated with gastrointestinal disease or as part of a normal gut microbiome, it has been found to inhabit the digestive tract of long-term ICU patients (37) indicating that the intestine may be a possible reservoir for this nosocomial pathogen. EA breakdown may be an important metabolic capability for *A. baumannii* during the course of colonization or infection, and if so, the enzymes studied herein could serve as effective therapeutic targets.

2.6 MATERIALS & METHODS

Bacterial strains and growth conditions. All *A. baumannii* strains used were derivatives of *A. baumannii* ATCC 17978. All *S.* Typhimurium strains used were derivatives of *S. enterica* subsp. *enterica* sv Typhimurium strain LT2 (*S.* Typhimurium). *E. coli* DH5α was used for plasmid construction. All cultures were grown at 37 ºC. *A. baumannii* was grown in lysogeny broth (LB) (38, 39) or M9 minimal medium (40). To test EA as a carbon source, M9 minimal medium was supplemented with $MgSO_4$ (1 mM), $CaCl_2$ (10 mM), EA•HCL (90 mM, unless otherwise noted), LB (1%, v/v), and cyanocobalamin (CNCbl, 100 nM, unless otherwise noted). To test EA as a nitrogen source, *A. baumannii* was grown in nitrogen-free M9 salts supplemented with $MgSO_4$ (1 mM) $CaCl_2$ (10 mM), sodium pyruvate (20 mM), CNCbl (10 nM, unless otherwise noted) and EA•HCl (30 mM, unless otherwise noted). *S.* Typhimurium strains were grown on Nutrient Broth (NB, Difco)

or no carbon essential (NCE) minimal medium (41); *E. coli* was grown in LB. When antibiotics were used, their concentration was indicated for each experiment. Unless otherwise noted, isopropyl b-D-1-thiogalactopyranoside (IPTG) was used at 1 mM, and L-(+)-arabinose was used as inducer of gene expression at 0.5 mM. Unless otherwise specified, all chemicals were purchased from Sigma-Aldrich Chemical Company.

Construction of *A. baumannii* deletion strains. Deletions were constructed as described elsewhere (42, 43). *A. baumannii* harboring plasmid pRecABtet was transformed with a fragment containing flanking regions of the gene of interest fused to the kanamycin resistance gene from plasmid pKD4 by electroporation. Cells were recovered using Super Optimal broth with Catabolite (SOC) repression medium (tryptone [20 g/L w/v], yeast extract [5 g/L], NaCl [0.5 g/L], glucose [20 mM]) at 37 °C with shaking at 220 rpm for 2-4 h. Following incubation, cells were plated on lysogeny broth (LB, Difco) agar plates containing kanamycin (Km, 25 μg/mL) and IPTG (2 mM). Kanamycin-resistant (Km^R) transformants were patched to plates containing tetracycline (Tc, 10 μg/mL), and tetracycline-sensitive (Tc^S) Km^R colonies were analyzed further. To resolve the kanamycin cassette, plasmid pFLPtet was moved into the strains by electroporation. Cells were recovered with SOC medium (2 mL) for 2-4 h at 37 °C with shaking at 220 rpm and plated on LB agar containing tetracycline (10 μg/mL). Cells were streaked for isolation on plates containing tetracycline (10 μg/mL) and IPTG (2 mM) to induce expression of *flp*. Isolated colonies were streaked on LB, then patched to LB agar containing kanamycin (30 μg/mL) or tetracycline (10 μg/mL). We isolated genomic DNA from Tc^S Km^S colonies

as described elsewhere (42), followed by PCR amplification and DNA sequencing to verify the disruption of the gene of interest and loss of the Km resistance cassette.

Plasmid construction. To test complementation in *S.* Typhimurium, each gene of interest from *A. baumannii* was cloned into cloning vector pCV1 (44) using BspQI restriction sites and electroporated into *E. coli* DH5α. Plasmids were miniprepped using a Wizard Plus SV Minipreps DNA Purification System (VWR) and sequenced to verify each insert. Positive plasmids were electroporated into a *S.* Typhimurium strain carrying a deletion of the homologous gene. Cells containing the plasmid were selected for by addition of ampicillin (100 μg/mL) to the growth medium.

Complementation studies in *A. baumannii* were performed as described elsewhere (45). *A. baumannii eutBC* was inserted into pMMB67EH using EcoRI and SalI (ThermoFisher) restriction digests, then ligating using T4 DNA ligase (ThermoFisher) following the manufacturer's instructions. Chemically competent *E. coli* DH5α was transformed and plated on Tc (10 μg/mL). Selected colonies were miniprepped and sequenced to verify insertion. Verified plasmids were used to transform electrocompetent *A. baumannii* Δ*eutBC* was transformed as described above, recovered in SOC medium for 2-4 h, and plated on LB agar containing tetracycline.

Analysis of EA catabolism in *A. baumannii.* *A. baumannii* strains were grown in LB overnight and sub-cultured (5%, v/v) into M9 minimal medium or nitrogen-free M9 minimal medium. Growth analyses were performed using a 96-well microtiter dish (Falcon) with 200 μL per well, incubated at 37 °C with shaking and increases in cell density were monitored at 630 nm for 24 h. Each growth analysis consisted of three biological

replicates in technical triplicate. Concentrations of CNCbl or ethanolamine were varied where indicated to assess the minimal requirements of *A. baumannii* for these nutrients.

Complementation studies in *S.* Typhimurium. Heterologous expression of *A. baumannii* genes was performed in *S.* Typhimurium to test EAL, NLA and ACAT function. NB was inoculated with a single colony and grown overnight at 37 °C. The following day, 1% (v/v) of an overnight culture (~16-h old) was transferred into minimal medium in a 96-well microtiter plate. *S.* Typhimurium growth experiments were performed in no-carbon essential (NCE) minimal medium (41) containing Wolfe's trace minerals (46), $MgSO_4$ (1 mM), glycerol (22 mM), and ampicillin (100 μg/mL). Cobamide precursor salvaging was performed by assessing growth with the addition of dicyanocobinamide [$(CN)_2$Cbi] and 5,6-dimethylbenzimidazole (DMB, 150 mM). Gene expression was induced with L-(+)-arabinose (0.5 mM). Growth of cultures in microtiter plates was monitored every hour at 630 nm during incubation at 37 °C in a BioTek Elx808 microplate reader. To test *A. baumannii eutBC* complementation, minimal medium contained no-nitrogen NCE medium (47) with ethanolamine (30 mM) provided as the sole source of nitrogen. In each case, growth analysis was performed on three biological replicates in technical triplicate.

Sequencing of *A. baumannii* genomes. Strains of *A. baumannii* able to grow on ethanolamine as the sole source of carbon and energy were grown overnight in LB (10 mL) at 37 °C with shaking at 180 rpm. Cells were harvested by centrifuging at 3,000 x *g* using a table-top Eppendorf 5810R centrifuge for 30 min at room temperature. Genomic DNA was isolated using Blood and Cell Culture DNA Midi Kit and Genomic DNA Buffer Set (Qiagen) following the manufacturer's protocol for preparation of Gram-negative

samples. Genomic DNA quality was measured using an Invitrogen Qubit Model 4 fluorometer and only samples containing >10% (w/v) double-stranded DNA were used for whole-genome sequencing (WGS). DNA-end repair was performed using NEBNext FFPE DNA Repair Mix and NEBNext Ultra II End Repair (New England Biolabs) following manufacturer's instructions. The repair reaction was allowed to proceed for 30 min at 20 °C and 30 min at 65 °C. DNA isolated by mixing with AMPure XP beads, washing with 70% (v/v) ethanol, and eluting off of beads with Ambion™ nuclease-free water. Eluate containing end-repaired DNA was quantified using a Qubit fluorometer. Barcodes were attached using NEB Blunt/TA Ligase and Master Mix (New England Biolabs) following manufacturer's instructions and incubated at 25 °C for 15 min. DNA was purified from reaction mix using AMPure beads as described by the manufacturer and eluted in 25 μL nuclease-free water. Barcoded DNA was quantified using a Qubit fluorometer. Equimolar amounts of barcoded samples were pooled to a total of 1050 ng in 65 μL. Adapters were attached to barcoded DNA using Adapter Mix, NEBNext Ligation Buffer and NEBNext Quick T4 DNA Ligase (New England Biolabs) incubated at 20 °C for 15 min. Following incubation, DNA was isolated from the reaction mixture using AMPure XP beads as described. Beads were washed with long fragment buffer (Nanopore) twice before elution with elution buffer (Nanopore). The final concentration of the library was quantified using a Qubit fluorometer. Libraries were loaded into a R10.3 flow cell on MinION Mk1C (Nanopore Technologies).

Antibody preparation. Purified *S.* Typhimurium EAL was provided to Envigo (Envigo, PA) for production of rabbit polyclonal antibodies. Anti-serum was pre-cleared against

JE8094 (D*eutBC*). Cells were grown at 37 °C with shaking at 180 rpm in minimal NCE containing ribose (20 mM), EA (30 mM), and CNCbl (200 nM) to OD_{600}= ~ 1.0. Cells were incubated on ice for 15 min, then harvested by centrifuging at 2,000 x *g* for 15 min in a 5810 R centrifuge (Eppendorf). Cells were resuspended in 100 mL Tris•HCl buffer (50 mM pH 7.5 at 4 °C) containing SDS (2%, w/v). To lyse cells, the suspension was boiled for 5 min, then incubated on ice for 10 min. The solution was brought to a final volume of 1 mL with Tris•HCl buffer (50 mM, pH 7.5 at 4 °C). Anti-serum was added at a 1:100 dilution and incubated at 4 °C for 36 h. Pre-cleared antibody was obtained by centrifuging at 16,000 x *g* for 10 min and removing the supernatant. Pre-cleared antibody was flash frozen in liquid N_2 and stored at -80 °C until used.

Western Blotting. *S.* Typhimurium strains were grown in NCE or NCN containing EA (30 mM) as the sole source of nitrogen. Each medium was supplemented with Wolfe's trace minerals, $MgSO_4$ (1 mM), glycerol (22 mM), CNCbl (150 nM), ampicillin (100 μg/mL), and L-(+)-arabinose (0.5 mM). Cultures were inoculated with LB (2%, w/v) overnight culture and grown with shaking at 180 rpm at 37 °C to an OD_{600} = 0.45-0.65. Cells were harvested 5810 R centrifuge (Eppendorf) at 2,220 x *g* for 15 min and stored at -80 °C. Cells were resuspended in 1 mL sterile PBS (10 mM sodium phosphate pH 7.4, 0.9% w/v) NaCl) and centrifuged at 4,000 x *g* for 10 min in a 5415 D centrifuge (Eppendorf) at 4 °C. Cell pellets were resuspended in B-PER (300 mL, ThermoFisher) and vortexed for 1 min to lyse cells. The protein concentration of the crude lysate was quantified using Bradford Protein Assay Dye (Bio-Rad Laboratories) following the manufacturer's instructions. Bovine gamma globulin (ThermoFisher) was used to generate a standard curve. Cell lysates were diluted

to 500 ng/μL in PBS and incubated with loading buffer [Tris pH 6.8 (300 mM), glycerol (60%, v/v), 12 mM ethylenediaminotetracetic acid (EDTA, 12 mM), 2-mercaptoethanol (0.85 M), and bromophenol blue (0.05% w/v)] for 5 min at 95 °C. Crude lysate was loaded in duplicate to a 15% (w/v) SDS-PAGE gel (48). Gels were loaded with Precision-Plus Protein Standards (Bio-Rad Laboratories) or SuperSignal Molecular Weight Protein Ladder (ThermoFisher). Gels intended for Coomassie staining were loaded with 5 mg crude lysate; gels intended for Western blot were loaded with 5 μg for strains complemented with *Ab*EutBC or VOC and 1.25 μg for strains complemented with *Se*EutBC. A constant voltage of 200 V was applied to gels for approximately 35 min. Gels loaded with Precision-Plus Protein Standards were stained with Brilliant Blue R dye to visualize proteins. Gels loaded with SuperSignal Molecular Weight Protein Ladder were transferred to a PVDF membrane using a Trans-Blot Turbo system (Bio-Rad Laboratories). Following transfer, the membrane was incubated in blocking buffer composed of 0.5% (w/v) nonfat milk in PBST [phosphate-buffered saline pH 7.4 containing 0.1% v/v Tween 20 (Millipore Sigma)] for 1 hour at room temperature on an Advanced Digital Shaker (VWR). The primary antibody generated against *S.* Typhimurum EAL was diluted 1:2,000 in blocking buffer, and the membrane was incubated in this solution at 4 °C overnight on a tabletop shaker. The following morning, the membrane was washed thrice with PBST. The membrane as incubated in PBST containing goat anti-rabbit IgG horseradish peroxidase conjugate (1:20,000, Invitrogen) for 1 h at room temperature on a tabletop shaker. The membrane was washed thrice with PBST, then incubated with SuperSignal West Pico PLUS Chemiluminescent Substrate

(ThermoFisher) for 10 min at room temperature, and imaged using a UVP ChemStudio (analytikjena) with an exposure time of 5 sec.

RNA isolation. RNA was isolated as described (49). An overnight culture in LB medium inoculated with a single colony was sub-cultured (2.5%, v/v) into 10 mL minimal medium. Cultures grown for RT-qPCR analyses were grown in M9 minimal medium containing either ethanolamine (90 mM) or pyruvate (20 mM) as a sole carbon and energy source. For cultures used in experiments aimed at determining whether the *A. baumannii* putative *eut* genes were co-transcribed, wild-type *A. baumannii* (JE25551) was grown in no-nitrogen (NoN) M9 minimal medium supplemented with 30 mM ethanolamine and 20 mM pyruvate. In all cases, cultures were incubated with shaking (200 rpm) at 37 °C to an OD_{600} 0.4-0.5, and harvested using a 5810 R centrifuge (Eppendorf) at 3,220 x *g* for 10 min. The supernatant was removed and cells were stored at -80 °C until processed. Cell pellets were lysed by resuspending in boil solution (ethylenediaminetetraacetic acid, EDTA, [18 mM], SDS [0.025% v/v], 2-mercaptoethanol [1% v/v], formamide [95% v/v], Rnase-free water [to final volume]) and heating at 95 °C for 7 min. The cell suspension was centrifuged at 16,000 x *g* for 5 min at room temperature, and 100 μL of the supernatant was removed into a new tube. RNase-free water (400 μL) was added to dilute the culture and sodium acetate was added to a final concentration of 0.3 M. Ice-cold ethanol (100%) was added (1650 μL) and samples were vortexed briefly to mix, then incubated at -80 °C overnight. Samples were centrifuged for 30 min at 16,000 x *g* at 4 °C and the supernatant was discarded. The remaining pellet was washed with 300 μL of ice-cold 70% ethanol and centrifuged at 8,000 x *g* for 5 min at 4 °C. The supernatant was

discarded and the pellet was allowed to air-dry. RNA pellets were resuspended in 100 μL RNase-free water, centrifuged for 1 min at 16,000 x *g* to remove any insoluble contaminants, and 90 μL was transferred into a new tube. A DNA digest was performed using the rigorous DNase treatment described for TURBO DNase (ThermoFisher). Following DNase treatment and inactivation, samples were centrifuged at 10,000 x *g* for 1.5 minutes, and 90 μL was transferred into a new tube. A second sodium acetate/ethanol precipitation was performed as described above. RNA yield and quality was analyzed using a Qubit 4 Fluorometer using the RNA BR Assay Kit and RNA IQ Assay Kit, respectively (Invitrogen). Samples with an RNA IQ value of 6 or higher were used for RT-qPCR experiments.

cDNA synthesis and RT-qPCR. RNA to be used as cDNA template was diluted to a final concentration of 12.5 ng/μL and cDNA was synthesized using iScript cDNA Synthesis Kit (BioRad) following the manufacturer's protocol. cDNA was diluted to 2.5 ng/μL when used for RT-qPCR experiments. RT-qPCR reactions were performed in a 96-well plate. In each well 20 μL of reaction mix was added containing 10 μL FastSYBR Green Master Mix (Life Technologies), gene-specific primers (500 nM) and cDNA (10 ng). Gene-specific primers were designed using Primer3 software. The *A. baumannii* 16S rRNA gene was used as an internal control. RT-qPCR reactions were run using a 7500 Fast real-time PCR system (Applied Biosystems). Three biological replicates each in technical triplicate were analyzed for each strain. Cycle threshold (C_T) was normalized against 16S values and these values were transformed using $2(e\text{-}DC_T)/10^{-6}$ and reported as arbitrary expression units (EU). The mean EU of each biological replicate was used to calculate standard error

in Prism software v9 (Graphpad). Statistical significance was determined using Welch's t-test in Prism software v9 (GraphPad).

Operon PCR. Intergenic primers were generated to amplify regions between genes within the putative operon. To each reaction, 5 μL of iScript reaction product with (+ RT) or without (- RT) reverse transcriptase. Genomic DNA (gDNA) was diluted to 12.5 ng/μL, and 5 μL was added to each control reaction. PCR was performed using GoTaq Green Master Mix (Promega) following the manufacturer's instructions. Products were analyzed on a 1% agarose (w/v) DNA gel.

Cell preparation for transmission electron microscopy. *A. baumannii* was grown in M9 minimal medium containing EA as a sole carbon source. *S.* Typhimurium was grown in NCN medium supplemented with glycerol (22 mM), and EA (30 mM). In both cases, cultures were harvested at OD_{600} (~0.6) in a 5810 R centrifuge (Eppendorf) at 3,220 x *g* for 10 min. Cell pellets were resuspended in Sorensen's phosphate buffer (0.1 M sodium phosphate, pH 7.4) containing 4% paraformaldehyde and 0.2% glutaraldehyde and incubated at room temperature for 15 min. Fixed cells were centrifuged at 6,000 x g for 2 min. The supernatant was removed and cells were washed twice in Sorensen's phosphate buffer. Cells were enrobed in melted, 60 °C Noble agar (4% In Sorensen's buffer pH 7.4) and cut into 2mm blocks for dehydration.

Samples were dehydrated by treating with the following steps: 50% ethanol for 15 min; 70% ethanol for 15 min; 80% ethanol for 10 min. Each step was incubated on a slow rotator set at a 45° angle at room temperature. Cells were incubated with a mixture of LR

White resin (London Resin Company, LTD) and 80% ethanol (2:1 v/v) for one hour at room temperature. Cells were then incubated with LR White resin (100%) thrice for one hour each. Each incubation was performed at room temperature on a slow rotator set at 45°. Cells were embedded in LR White resin in gelatin capsules incubated at 50 ºC for 14-16 h. Sections of 30-50 nm were cut using a DiaTOME Ultra diamond knife mounted on an RMC-MT-X microtome. Sections were placed on gold grids coated with formvar and carbon until immunogold labeling.

Grids were incubated top down on a 25 μL drop of blocking buffer containing 20 mM Tris pH 7.4, 150 mM NaCl, and 1% w/v bovine serum albumin (BSA) for 10 min, then washed by repeatedly dipping in a beaker containing 10 mL blocking buffer for 1 min. Grids were incubated top down on a 25 μL drop of blocking buffer containing primary antibody (rabbit polyclonal antibody generated against *S.* Typhimurium EAL) diluted to 1:50 overnight at room temperature. Grids were washed by dipping in a beaker containing 10 mL blocking buffer for 1 min, then incubated top down on a 25 μL drop of blocking buffer for 15 min. Grids were then transferred top own to a 25 μL drop of goat-anti-rabbit IgG-gold antibody (Millipore Sigma) and incubated for 1 h at room temperature. A final wash was performed by dipping repeatedly in a beaker containing 10 mL blocking buffer for 0.5 min, then dipping repeatedly in a beaker containing 10 mL water for 0.5 min. Where indicated, grids were post-stained by incubating on a droplet of filtered 4% aqueous uranyl acetate for 20 min, washed thoroughly by dipping in a beaker of DI H_2O thirty times, then incubated on a drop of filtered DI H_2O for 1 min. Negative controls were treated exclusively with secondary antibody. Imaging was performed using a JEOL 1011 Transmission Electron Microscope (JEOL USA, Peabody MA).

Cobamide extraction and identification. Isolation and identification of cobamides was performed as described elsewhere (32). Briefly, 100 mL of M9 minimal medium containing ethanolamine (90 mM) as the sole source of carbon and energy and cobinamide (100 nM) was inoculated with 2.5% (v/v) from an LB liquid culture and grown overnight at 37 °C with shaking at 180 rpm. The following morning, cultures were harvested using a 5810 R centrifuge (Eppendorf) at 3,220 x *g* for 20 min. The cell pellet was resuspended in 10 mL Buffer A (50 mM KH_2PO_4 pH 6.5, 5 mM KCN) and 20 mL methanol, then incubated at 65 °C for 2 hours with shaking (220 rpm). Cell debris was removed by centrifuging at 30,000 x *g* in an Avanti JP20-XVI centrifuge equipped with a JA-25.50 rotor for 1 h. A SepPak C18 Plus (360 mg sorbent per cartridge, 55-105 mm particle, Waters) was activated with methanol (10 mL) and water (10 mL). The supernatant was diluted 1:5 in water and passed over the activated SepPak. Cobamides bound to the SepPak were washed with water (20 mL), and eluted using methanol (100% (v/v), 1.5 mL). Cobamides were dried overnight in a Vacfuge Plus (Eppendorf) and resuspended in Buffer A (200 mL). KCN was added to a final concentration of 25 mM and incubated for 10 min in a sand bath kept at 90 °C. Cobamides were then passed over a Spin-X centrifuge tube filter (Corning) for 5 min at 13,000 x *g*. Cleaned reactions were separated by RP-HPLC on a Shimadzu Prominence UFLC SPD-M30A equipped with a Synergi 4m Hydro-RP 80A 150 x 4.6 mm column. The following method was used to separate cobamides: The column was equilibrated with 97% mobile phase A (MP A) [KH_2PO_4 (0.1 M), pH 6.5, KCN (10 mM)]/3% mobile phase B (MP B) [KH_2PO_4 (0.1 M), pH 8, KCN (10 mM): acetonitrile in a 1:1 ratio]. Sample injection was followed by a 5 min linear gradient to 75% MP A/ 25% MP B, followed by a 15 min linear gradient to 65% MP A/ 35% MP B, followed by a 5 min

isocratic step at 65% MP A/ 35% MP B, followed by a 2.5 min linear gradient to 100% MP B, concluding with a 5 min isocratic step at 100% B. Cobamides were identified by measuring the absorbance at 367 nm. Fractions containing cobamides were collected, desalted using a SepPak C18 cartridge, and dried overnight in a VacFuge Plus. Cobamide fractions were resuspended in sterile water and sent for MALDI-TOF mass spectrometry analysis.

ACKNOWLEDGEMENTS

The authors do not have conflicts of interest to declare.

We thank Michael Paxhia and Diana Downs (UGA) for help with whole-genome sequencing and use of MinION Mk1C. We thank M. Stephen Trent at UGA for strains and plasmids used in this work, and methods to work with *A. baumannii.* We thank John Shields and Mary Ard at the Georgia Electron Microscopy (GEM) facility at UGA for preparing samples and obtaining the reported TEM images. We also thank Dennis Phillips and Chau-Wen Chou at the Proteomics and Mass Spectrometry (PAMS) facility at UGA for obtaining the reported mass spectrum.

This work was supported by USPHS Grant from the National Institute of Health (R35-130399 awarded to J.C.E.-S.). The funders had no role in study design, data collection and interpretation, or the decision to submit the work for publication.

J.C.E.-S. conceived the project. E.A.V. performed the experiments. J.C.E.-S. and E.A.V. designed experiments, analyzed the data, and wrote the manuscript.

2.7 REFERENCES

1. Winter SE, Thiennimitr P, Winter MG, Butler BP, Huseby DL, Crawford RW, Russell JM, Bevins CL, Adams LG, Tsolis RM, Roth JR, Baumler AJ. 2010. Gut inflammation provides a respiratory electron acceptor for *Salmonella*. Nature 467:426-4269.
2. Baumler AJ, Winter SE, Thiennimitr P, Casadesus J. 2011. Intestinal and chronic infections: *Salmonella* lifestyles in hostile environments. Environ Microbiol Rep 3:508-517.
3. Anderson CJ, Clark DE, Adli M, Kendall MM. 2015. Ethanolamine signaling promotes *Salmonella* niche recognition and adaptation during infection. PLoS Pathog 11:e1005278.
4. Kaval KG, Garsin DA. 2018. Ethanolamine utilization in bacteria. MBio 9:e00066-18.
5. Kofoid E, Rappleye C, Stojiljkovic I, Roth J. 1999. The 17-gene ethanolamine (*eut*) operon of *Salmonella typhimurium* encodes five homologues of carboxysome shell proteins. J Bacteriol 181:5317-5329.
6. Brinsmade SR, Paldon T, Escalante-Semerena JC. 2005. Minimal functions and physiological conditions required for growth of *Salmonella enterica* on ethanolamine in the absence of the metabolosome. J Bacteriol 187:8039-8046.
7. Lundgren BR, Sarwar Z, Pinto A, Ganley JG, Nomura CT. 2016. Ethanolamine catabolism in *Pseudomonas aeruginosa* PAO1 is regulated by the enhancer-binding protein EatR (PA4021) and the alternative sigma factor RpoN. J Bacteriol 198:2318-2329.

8. Roof DM, Roth JR. 1989. Functions required for vitamin B12-dependent ethanolamine utilization in *Salmonella typhimurium*. J Bacteriol 171:3316-3323.
9. Chang GW, Chang JT. 1975. Evidence for the B12-dependent enzyme ethanolamine deaminase in *Salmonella*. Nature 254:150-151.
10. Faust LR, Connor JA, Roof DM, Hoch JA, Babior BM. 1990. Cloning, sequencing, and expression of the genes encoding the adenosylcobalamin-dependent ethanolamine ammonia-lyase of *Salmonella typhimurium*. J Biol Chem 265:12462-12466.
11. Costa FG, Deery E, Warren M, Escalante-Semerena JC. 2020. Insights into the biosynthesis of cobamides and their use, p 364-394. *In* Liu H-W, Begley TP (ed), Comprehensive Natural Products III: Chemistry and Biology, ed vol 5. Elsevier,
12. Huseby DL, Roth JR. 2013. Evidence that a metabolic microcompartment contains and recycles private cofactor pools. J Bacteriol 195:2864-2879.
13. Buan NR, Escalante-Semerena JC. 2006. Purification and initial biochemical characterization of ATP:Cob(I)alamin adenosyltransferase (EutT) enzyme of *Salmonella enterica*. J Biol Chem 281:16971-16977.
14. Costa FG, Escalante-Semerena JC. 2018. A new class of EutT ATP:Co(I)rrinoid adenosyltransferases found in *Listeria monocytogenes* and other *Firmicutes* does not require a metal Ion for activity. Biochemistry 57:5076-5087.
15. Moore TC, Mera PE, Escalante-Semerena JC. 2014. the EutT enzyme of *Salmonella enterica* is a unique ATP:Cob(I)alamin adenosyltransferase metalloprotein that requires ferrous ions for maximal activity. J Bacteriol 196:903-910.

16. Buan NR, Suh SJ, Escalante-Semerena JC. 2004. The *eutT* gene of *Salmonella enterica* encodes an oxygen-labile, metal-containing ATP:corrinoid adenosyltransferase enzyme. J Bacteriol 186:5708-5714.

17. Sheppard DE, Penrod JT, Bobik T, Kofoid E, Roth JR. 2004. Evidence that a B12-adenosyl transferase is encoded within the ethanolamine operon of *Salmonella enterica*. J Bacteriol 186:7635-7644.

18. Schubert HL, Hill CP. 2006. Structure of ATP-bound human ATP:cobalamin adenosyltransferase. Biochemistry 45:15188-15196.

19. Mera PE, Maurice MS, Rayment I, Escalante-Semerena JC. 2007. Structural and functional analyses of the human-type corrinoid adenosyltransferase (PduO) from *Lactobacillus reuteri*. Biochemistry 46:13829-13836.

20. Johnson CL, Pechonick E, Park SD, Havemann GD, Leal NA, Bobik TA. 2001. Functional genomic, biochemical, and genetic characterization of the *Salmonella pduO* gene, an ATP:cob(I)alamin adenosyltransferase gene. J Bacteriol 183:1577-1584.

21. Escalante-Semerena JC. 2007. Conversion of cobinamide into adenosylcobamide in bacteria and archaea. J Bacteriol 189:4555-4560.

22. Heritier C, Poirel L, Nordmann P. 2006. Cephalosporinase over-expression resulting from insertion of IS*Aba1* in *Acinetobacter baumannii*. Clin Microbiol Inf:123-130.

23. Potron A, Vuillemenot J, Puja H, Triponney P, Bour M, Valot B, Amara M, Cavalié L, Bernard C, Parmeland L. 2019. IS*Aba1*-dependent overexpression of *eptA* in clinical strains of *Acinetobacter baumannii* resistant to colistin. J Antimicrob Chemother 74:2544-2550.

24. Segal H, Nelson EC, Elisha BG. 2004. Genetic environment and transcription of *ampC* in an *Acinetobacter baumannii* clinical isolate. Antimicrob Agents Chemother 48:612-614.

25. Segal H, Thomas R, Elisha BG. 2003. Characterization of class 1 integron resistance gene cassettes and the identification of a novel IS-like element in *Acinetobacter baumannii*. Plasmid 49:169-178.

26. Corvec S, Caroff N, Espaze E, Giraudeau C, Drugeon H, Reynaud A. 2003. AmpC cephalosporinase hyperproduction in *Acinetobacter baumannii* clinical strains. J AntimicrobChemother 52:629-635.

27. Choudhary S, Quin MB, Sanders MA, Johnson ET, Schmidt-Dannert C. 2012. Engineered protein nano-compartments for targeted enzyme localization. PLoS One 7:e33342.

28. Hull WE, Mauck L, Babior BM. 1975. Mechanism of action of ethanolamine ammonia-lyase, an adenosylcobalamin-dependent enzyme. Proton nuclear magnetic resonance studies of the binding of adenine nucleosides and substrate to ethanolamine ammonia-lyase. J Biol Chem 250:8023-8029.

29. Escalante-Semerena JC, Warren MJ. 2008. Biosynthesis and use of cobalamin (B_{12}). *In* Böck A, Curtiss III R, Kaper JB, Karp PD, Neidhardt FC, Nyström T, Slauch

JM, Squires CL (ed), *EcoSal - Escherichia coli* and *Salmonella*: cellular and molecular biology. ASM Press, Washington, D. C.

30. Escalante-Semerena JC, Suh SJ, Roth JR. 1990. *cobA* function is required for both de novo cobalamin biosynthesis and assimilation of exogenous corrinoids in *Salmonella typhimurium*. J Bacteriol 172:273-280.

31. O'Toole GA, Escalante-Semerena JC. 1993. *cobU*-dependent assimilation of nonadenosylated cobinamide in cobA mutants of *Salmonella typhimurium*. J Bacteriol 175:6328-6336.

32. Chan CH, Escalante-Semerena JC. 2011. ArsAB, a novel enzyme from *Sporomusa ovata* activates phenolic bases for adenosylcobamide biosynthesis. Mol Microbiol 81:952-967.

33. Fan C, Cheng S, Liu Y, Escobar CM, Crowley CS, Jefferson RE, Yeates TO, Bobik TA. 2010. Short N-terminal sequences package proteins into bacterial microcompartments. Proc Natl Acad Sci U S A 107:7509-7514.

34. Anderson PJ, Lango J, Carkeet C, Britten A, Kräutler B, Hammock BD, Roth JR. 2008. One pathway can incorporate either adenine or dimethylbenzimidazole as an alpha-axial ligand of B_{12} cofactors in *Salmonella enterica*. J Bacteriol 190:1160-1171.

35. Rowley CA, Anderson CJ, Kendall MM. 2018. Ethanolamine influences human commensal *Escherichia coli* growth, gene expression, and competition with enterohemorrhagic *E. coli* O157: H7. MBio:1-5.

36. Anderson CJ, Kendall MM. 2016. Location, location, location. *Salmonella* senses ethanolamine to gauge distinct host environments and coordinate gene expression. Microb Cell 3:89-91.

37. Corbella X, Pujol M, Ayats J, Sendra M, Ardanuy C, Dominguez MA, Linares J, Ariza J, Gudiol F. 1996. Relevance of digestive tract colonization in the epidemiology of nosocomial infections due to multiresistant Acinetobacter baumannii. Clinical Infectious Diseases 23:329-334.

38. Bertani G. 1951. Studies on lysogenesis. I. The mode of phage liberation by lysogenic *Escherichia coli*. J Bacteriol 62:293-300.

39. Bertani G. 2004. Lysogeny at mid-twentieth century: P1, P2, and other experimental systems. J Bacteriol 186:595-600.

40. Davis RW, Botstein D, Roth JR. 1980. A manual for genetic engineering: advanced bacterial genetics. Cold Spring Harbor Laboratory Press, Cold Spring Harbor, NY.

41. Berkowitz D, Hushon JM, Whitfield HJ, Jr., Roth J, Ames BN. 1968. Procedure for identifying nonsense mutations. J Bacteriol 96:215-220.

42. Tucker AT, Powers MJ, Trent MS, Davies BW. 2019. RecET-mediated recombineering in *Acinetobacter baumannii*. Methods Mol Biol 1946:107-113.

43. Datsenko KA, Wanner BL. 2000. One-step inactivation of chromosomal genes in *Escherichia coli* K-12 using PCR products. Proc Natl Acad Sci U S A 97:6640-6645.

44. VanDrisse CM, Escalante-Semerena JC. 2016. New high-cloning-efficiency vectors for complementation studies and recombinant protein overproduction in *Escherichia coli* and *Salmonella enterica*. Plasmid 86:1-6.

45. Tucker AT, Nowicki EM, Boll JM, Knauf GA, Burdis NC, Trent MS, Davies BW. 2014. Defining gene-phenotype relationships in *Acinetobacter baumannii* through one-step chromosomal gene inactivation. MBio 5:e01313-14.

46. Balch WE, Wolfe RS. 1976. New approach to the cultivation of methanogenic bacteria: 2-mercaptoethanesulfonic acid (HS-CoM)-dependent growth of *Methanobacterium ruminantium* in a pressurized atmosphere. Appl Environ Microbiol 32:781-791.

47. Ratzkin P, Roth JR. 1978. Cluster of genes controlling proline degradation in *Salmonella typhimurium*. J Bacteriol 133:744-754.

48. Laemmli UK. 1970. Cleavage of structural proteins during the assembly of the head of bacteriophage T4. Nature 227:680-685.

49. Stead MB, Agrawal A, Bowden KE, Nasir R, Mohanty BK, Meagher RB, Kushner SR. 2012. RNAsnap: a rapid, quantitative and inexpensive, method for isolating total RNA from bacteria. Nucleic Acids Res 40:e156.

50. Boll JM, Crofts AA, Peters K, Cattoir V, Vollmer W, Davies BW, Trent MS. 2016. A penicillin-binding protein inhibits selection of colistin-resistant, lipooligosaccharide-deficient *Acinetobacter baumannii*. Proc Nat Acad Sci U S A 113:E6228-E6237.

51. Cronan JE. 2006. A family of arabinose-inducible *Escherichia coli* expression vectors having pBR322 copy control. Plasmid 55:152-157.

52. Mera PE, Escalante-Semerena JC. 2010. Multiple roles of ATP:cob(I)alamin adenosyltransferases in the conversion of B(12) to coenzyme B (12). Appl Microbiol Biotechnol 88:41-48.

Table 2.1. Strains used in this study[a]		
Strain	**Genotype**	**Reference/source**
***Salmonella enterica* subsp. *enterica* sv. Typhimurium str. LT2 strains**		
JE6583	*metE205 araB9*	
JE7088	Δ*metE2702 araB9*	
Derivatives of strain JE6583		
JE8248	Δ*cobS1313*	Lab collection
JE8249	Δ*cobU1315*	Lab collection
JE8268	Δ*cobU1315* Δ*ycfN112*	Lab collection
JE15888	Δ*cobS1313* / pCOBS69 (*Se*CobS)	Lab collection
JE16852	Δ*cobS1313* / pBAD24	Lab collection
JE22175	Δ*eutSPQTDMNEJGHABCLK* (*zfa3648**Tn*10***zfa3649*)	Lab collection
JE23613	Δ*pduO522* Δ*cobA1465* Δ*eutT1141*	Lab collection
JE25835	Δ*pduO522* Δ*cobA1465* Δ*eutT1141* / pCobA70 (*Se*CobA)	
JE25836	Δ*pduO522* Δ*cobA1465* Δ*eutT1141* / pAbAcaT1	
JE25837	Δ*pduO522* Δ*cobA1465* Δ*eutT1141* / pBAD24	
JE25948	Δ*cobS1313* / pAbCobS1	
JE25949	Δ*cobU1315* / pCV1	
JE25950	Δ*cobU1315* Δ*ycfN112* / pAbCobU1	
JE25951	Δ*cobU1315* Δ*ycfN112* / pCV1	
JE25952	Δ*cobU1315* Δ*ycfN112* / pCobU27 (*Se*CobU)	
JE26300	Δ*eutBC1156* / pCV1	
JE26301	Δ*eutBC1156* / pEut269 (*Se*EutBC)	
JE26302	Δ*eutBC1156* / pAbEutBC1	
JE26303	Δ*eutABC1157* / pCV1	
JE26304	Δ*eutABC1157* / pEut269 (*Se*EutBC)	
JE26305	Δ*eutABC1157* / pAbEutBC1	
JE26306	Δ*eutSPQTDMNEJGHABCLK* (*zfa3648**Tn*10***zfa3649*) / pCV1	
JE26307	Δ*eutSPQTDMNEJGHABCLK* (*zfa3648**Tn*10***zfa3649*) / pEut269 (*Se*EutBC)	
JE26308	Δ*eutSPQTDMNEJGHABCLK* (*zfa3648**Tn*10***zfa3649*) / pAbEutBC1	
JE7088	Δ*metE2702 araB9*	
Derivatives of strain JE7088		
JE20198	Δ*cobB1375 cobT1379*::*kan*$^+$	Lab collection
JE26016	Δ*cobB1375 cobT1379*::*kan*$^+$ / pCV1	
JE26017	Δ*cobB1375 cobT1379*::*kan*$^+$ / pCobT140 (*Se*CobT)	
JE26018	Δ*cobB1375 cobT1379*::*kan*$^+$ / pAbCobT1	
Derivatives of *Acinetobacter baumannii* str. 17978		
JE26013	IS*Aba1* (3,825,518-3,826,6706)	
JE26441	Δ*eutBC* / pAbEutBC3	
JE26442	/ pMMB67EH	

[a]All strains were constructed during the course of this work unless otherwise stated

Table 2.2. Plasmids used in this study[b]		
Plasmid	**Description**	**Reference/source**
pMMB67EHKn	Kan^R	(50)
pKD4	Kan^R	(43)
pRecABtet	*recET*$^+$ cloned into pMMB67EH, tet^R	(45)
pFLPtet	FLP recombinase gene cloned into pMMB67EH, tet^R	(45)
pBAD24	Complementation vector P_{araBAD} bla^+	(51)
pCV1	Complementation vector P_{araBAD} bla^+	(44)
pCobU27	*S.* Typhimurium *cobU*$^+$ cloned into pBAD24	Lab collection
pCobS69	*S.* Typhimurium *cobS*$^+$ cloned into pBAD24	Lab collection
pCobT140	*S.* Typhimurium *cobT*$^+$ cloned into pBAD24	Lab collection
pCobA70	*S.* Typhimurium *cobA*$^+$ cloned into pBAD24	Lab collection
pEut269	*S.* Typhimurium *eutBC*$^+$ cloned into pBAD24	Lab collection
pAbCobU1	*A. baumannii cobU*$^+$ cloned into pCV1	This study
pAbCobS1	*A. baumannii cobS*$^+$ cloned into pCV1	This study
pAbCobT1	*A. baumannii cobT*$^+$ cloned into pCV1	This study
pAbAcaT1	*A. baumannii acaT*$^+$ cloned into pCV1	This study
pAbEutBC1	*A. baumannii eutBC*$^+$ cloned into pCV1	This study
pAbEutBC3	*A baumannii eutBC*$^+$ cloned into pMMB67EH	This study

[b]All plasmids were constructed during the course of this work unless otherwise stated

Table 2.3. Primers used in this study[c]	
Primer name	**Primer sequence (5' → 3')**
5' *AbeutB* deletion	ACCAGAAGAAGAGTTTGCAAATATTAAAGCCGCAGAACAAGAACTATAA ATAAAAGGATGTAACTATGAGTTATCGCAATATTGTCGCCAATCAACAG TATCACTTTGCTGACCTAAAAACGTTA GTGT AGGCTGGAGCTGCTTC
3' *AbeutC* deltion	AAGATAATCTCGTTACGCATAAATATTCTGTAGGGAAGAAATATCTACG TGTAACCTGCTATTTAAAATAAAAGCTTTGCGTTTTCATTATGGTCGATA TTTGAAAGTTGATGTTCATCTTTTAA CATATGAATATCCTCCTTAG
5' *AbcobU* pCV1	NNGCTCTTCNTTCATGTTGCAATtgaTTTTAGG
3' *AbcobU* pCV1	NNGCTCTTCNTTATTACTTATCACCTTTTAAAATC
5' *AbcobS* pCV1	NNGCTCTTCNTTCATGACACCTTTTTGGATAGC
3' *AbcobS* pCV1	NNGCTCTTCNTTATCAAACTAAATAAAAATAACTTACGAC
5' *AbcobT* pCV1	NNGCTCTTCNTTCATGAACTGGTGGTTAGAATC
5' *AbcobT* pCV1	NNGCTCTTCNTTATTAGCCAATTTTATTCCCG
5' *AbacaT* pCV1	NNGCTCTTCNTTCatgGGACACCGTTTAAGCAAAATC
3' *AbacaT* pCV1	NNGCTCTTCNTTAttaAATCATCTCATTAATATTTTTTTG
5' *AbeutB* EcoRI	NNN GAATTC atgAGTTATCGCAATATTGTCGCC
5' *AbeutC* SalI	NNNgtcgacTTAAAATAAAAGCTTTGCG
5' *AbeutB* qPCR	ACTTCCTTCCATGATGCCCT
3' *AbeutB* qPCR	TGAGCAGACGAGAGAATTGGT
5' *AbeutC* qPCR	GAACGCCCTGGTTTAAGCTC
3' *AbeutC* qPCR	TCACTCCTGAAAAGCCAAGC
5' *Ab*16S qPCR	TCTGCAACTCGACTCCATGA
3' *Ab*16S qPCR	ACGGCTACCTTGTTACGACT
5' *Abald1* qPCR	GGTTTAGGTGCAGGTGTATGGT
3' *Abald1* qPCR	AGCATGCGCAGGGTAGATG
5' *Abald1-eutH*	GGTGGCTACAAGAAGTCTGGTATTG
3' *Abald1-eutH*	GCTACGCCTAAACCAATCAGG
5' *AbeutH-eutB*	GCAGTCGCTGCTGTGGTC
3' *AbeutH-eutB*	CGCAACATGTTCGGTTGC

5’ *AbeutB-eutC*	CCCGCTCCTGAGTTCTCC
3’ *AbeutB-eutC*	GCTAATTGCTCCGAGAGGTAG

[c]All primers were synthesized by Integrated DNA Technologies (Coralville, IA)

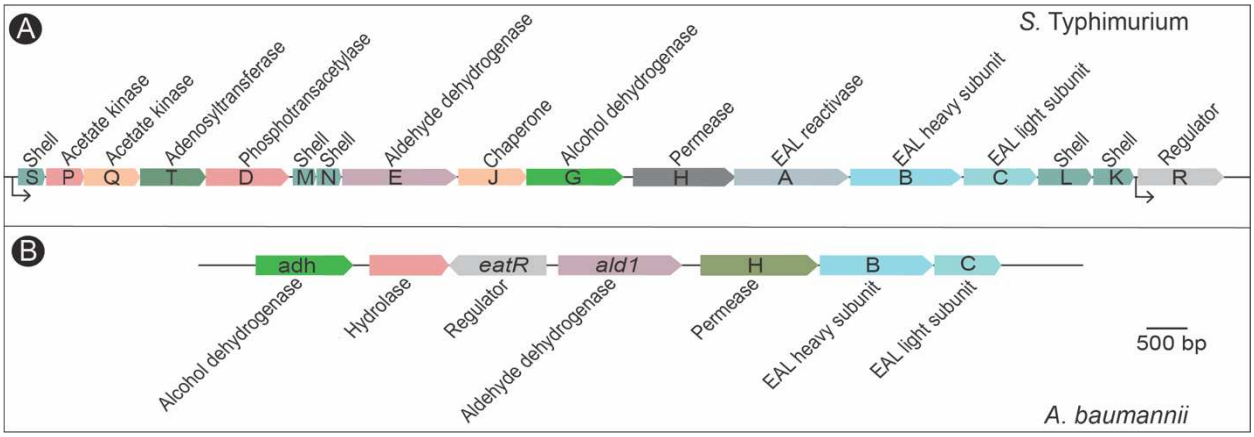

Figure 2.1. Comparison of the *eut* genes in *S.* Typhimurium and *A. baumannii*. A. In *S.* Typhimurium a total of 17 gene functions are needed for ethanolamine utilization (*eut* genes) as a carbon, nitrogen and energy source under certain growth conditions. **B.** In contrast, *A. baumannii* may require seven or less putative *eut* genes to breakdown ethanolamine. Genes are at the scale indicated by the bar.

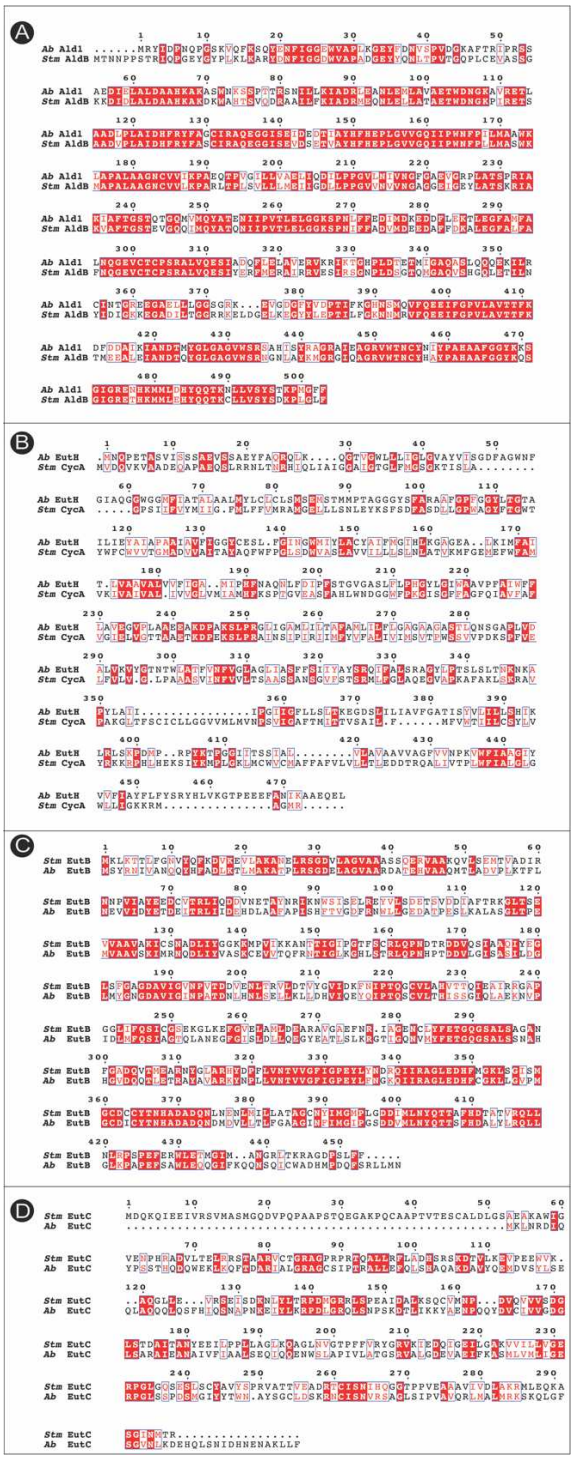

Figure 2.2. Sequence alignment of *eut* associated proteins from *A. baumannii* and *S.* Typhimurium. Identical amino acids are highlighted in red, similar amino acids are boxed in blue. Alignments were generated using Clustal Omega 1.2.3 in Geneious Prime software and ESPript 3 (https://espript.ibcp.fr/ESPript/ESPript/).

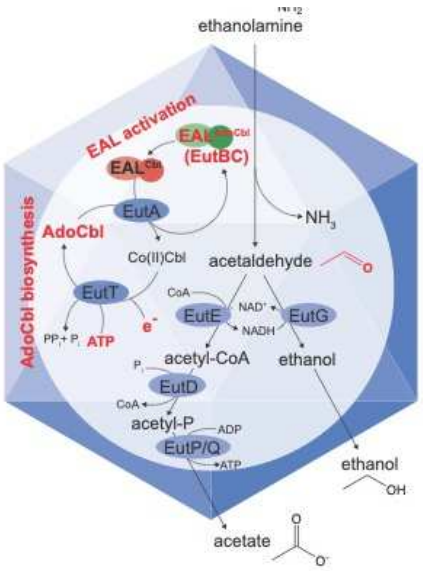

Figure 2.3. The *S.* Typhimurium metabolosome. Indicated in red are the functions present in *A. baumannii*. The genome of this bacterium does not encode any of the shell proteins. Highlighted in red are areas of the pathway studied in this work.

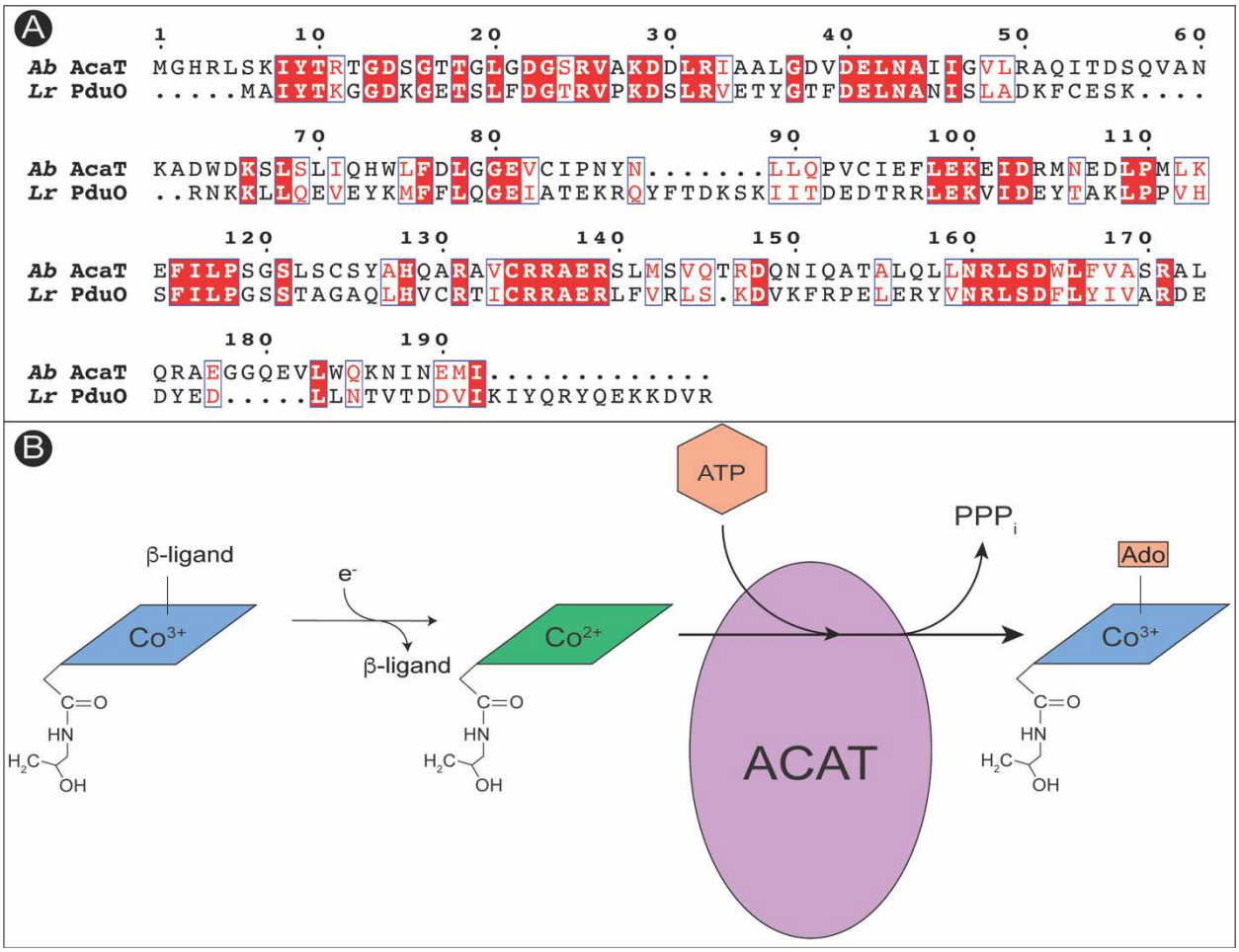

Figure 2.4. *A. baumannii* encodes a putative ATP:Co(I)rrinoid adenosyltransferase (ACAT). (A) Sequence alignment of *A. baumannii* AcaT and *Lactobacillus reuteri* PduO**.** Identical amino acids are highlighted in red, similar amino acids are boxed in blue. Alignments were generated using Clustal Omega 1.2.3 in Geneious Prime software and ESPript 3 (https://espript.ibcp.fr/ESPript/ESPript/). (B) Corrinoid adenosylation pathway. As shown by the scheme, reduction of Co(III) to Co(II) results in a 5-coordinate, Co(II) precursor. The second, one-electron reduction that converts Co(II) to Co(I) occurs after binding of the 5-coordinate, Co(II) precursor to the ATP:Co(I)rrinoid adenolsyltransferase (ACAT) enzyme. As soon as the Co(I) supernucleophile is formed, the attack to the 5' carbon of the ribose of ATP occurs displacing triphosphate and yielding the unique Co-C organometallic bond found in adenosylated corrinoids (52).

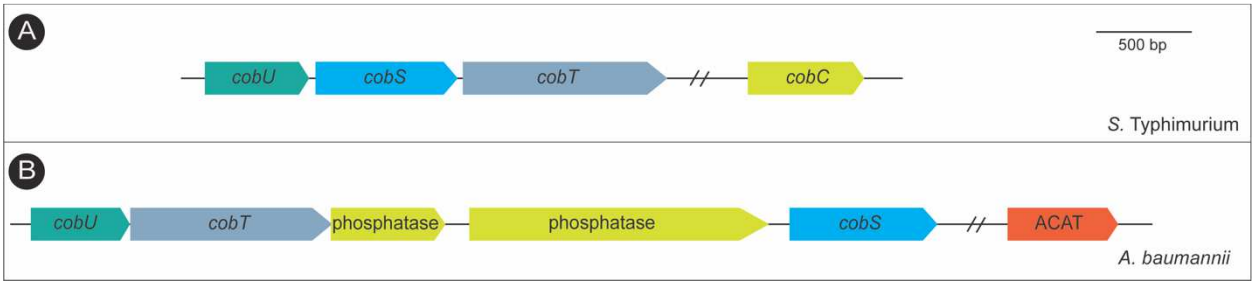

Figure 2.5. Organization of genes encoding nucleotide loop assembly enzymes in *S.* Typhimurium and *A. baumannii*. A. *S.* Typhimurium enzymes have been studied in detail. **B.** The *A. baumannii* genes encode hypothetical proteins, whose enzymatic activities had not been described prior to this work. *cobU* encodes the bifunctional NTP:Ado-cobinamide kinase (EC 2.7.1.156), GTP:AdoCbi-P guanylyltransferase (EC 2.7.7.62); *cobT* encodes nicotinate mononucleotide:dimethylbenzimidazole phosphoribosyltransferase (EC 2.4.2.21), *cobS* encodes AdoCba 5'-P synthase (EC 2.7.8.26), and *cobC* encodes AdoCba 5'-P phosphatase (EC 3.1.3.73). ACAT is the abbreviation for ATP:Co(I)rrinoid adenosyltransferase (EC 2.5.1.17).

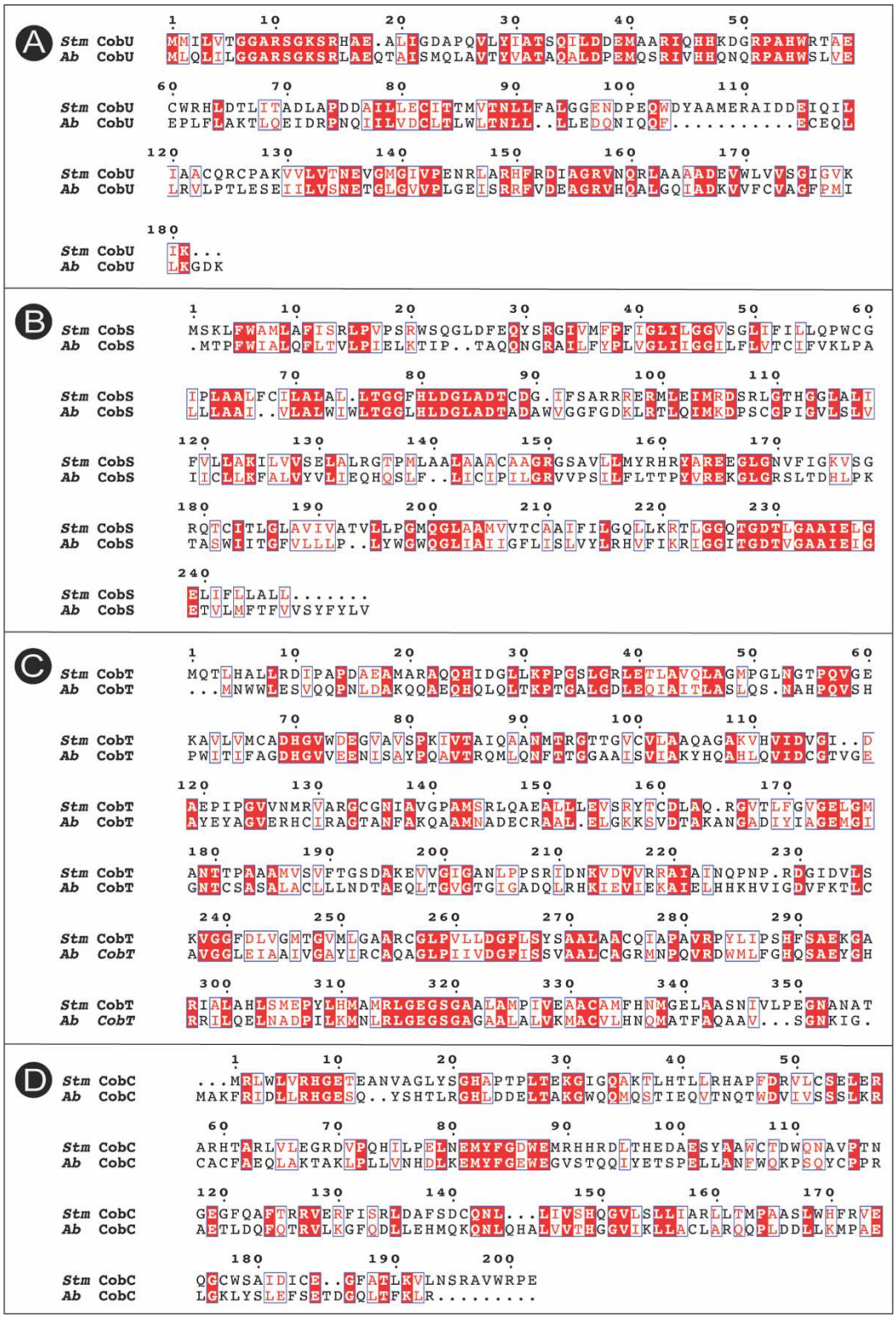

Figure 2.6. Sequence alignment of *A. baumannii* and *S.* Typhimurium NLA enzymes. Identical amino acids are highlighted in red, similar amino acids are boxed in blue. Alignments were generated using Clustal Omega 1.2.3 in Geneious Prime software and ESPript 3 (https://espript.ibcp.fr/ESPript/ESPript/).

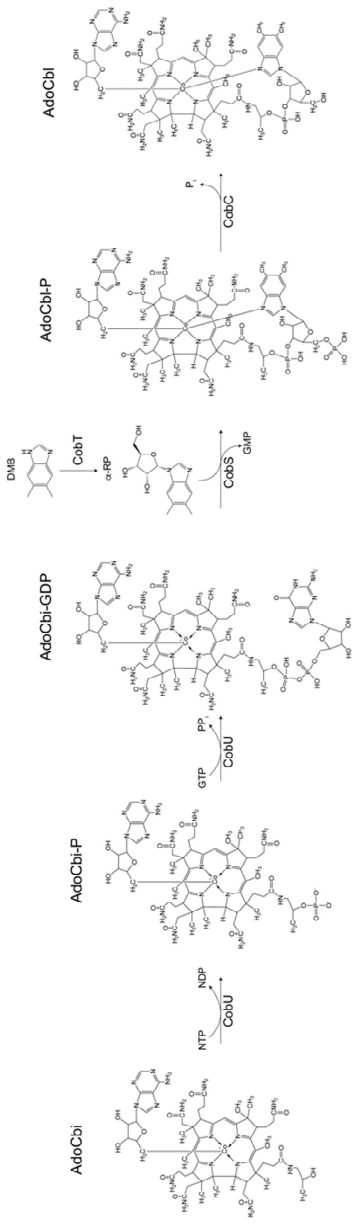

Figure 2.7. The NLA pathway in *S.* Typhimurium. CobU, a bifunctional NTP:Adocobinamide kinase (EC 2.7.1.156), and GTP:AdoCbi-P guanylyltransferase (EC 2.7.7.62), and CobT, a nicotinate mononucleotide:dimethylbenzimidazole phosphoribosyltransferase, generate the substrates for CobS. CobS is a AdoCba 5'-P synthase (EC 2.7.8.26) which condenses these two substrates, and CobC is a AdoCba 5'-P phosphatase (EC 3.1.3.73).

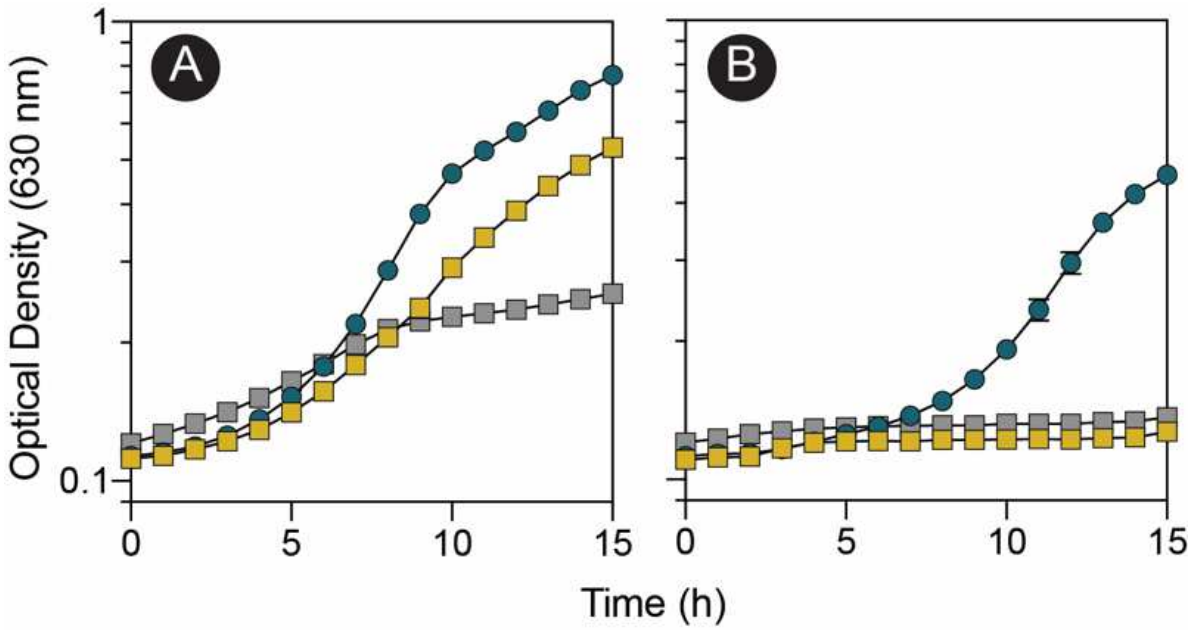

Figure 2.8. *A. baumannii* can use ethanolamine as a sole source of carbon or nitrogen. *A. baumannii* grown on M9 minimal medium with ethanolamine as the sole source of nitrogen (**A**) or carbon and energy (**B**). Wild-type *A. baumannii* 17978 (yellow squares), Δ*eutBC* (gray squares), and Δ*eutBC*/pAbeutBC3 (blue circles). For plasmid maintenance, ampicillin was added to cultures at 100 μg/mL. Experiments were performed in biological and technical triplicate. Error bars represent the standard deviation of replicates.

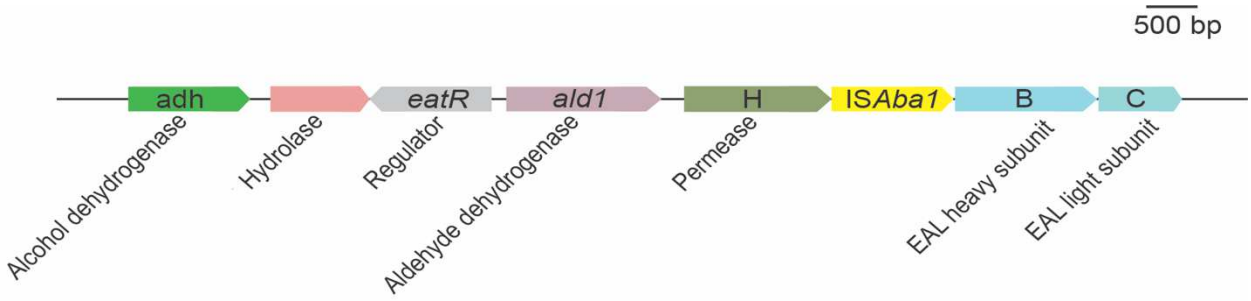

Figure 2.9. Spontaneous insertion of IS*Aba1* upstream of *eutBC* facilitates increased expression sufficient for growth using ethanolamine as a sole carbon source. Genes are presented at scale (see scaling bar).

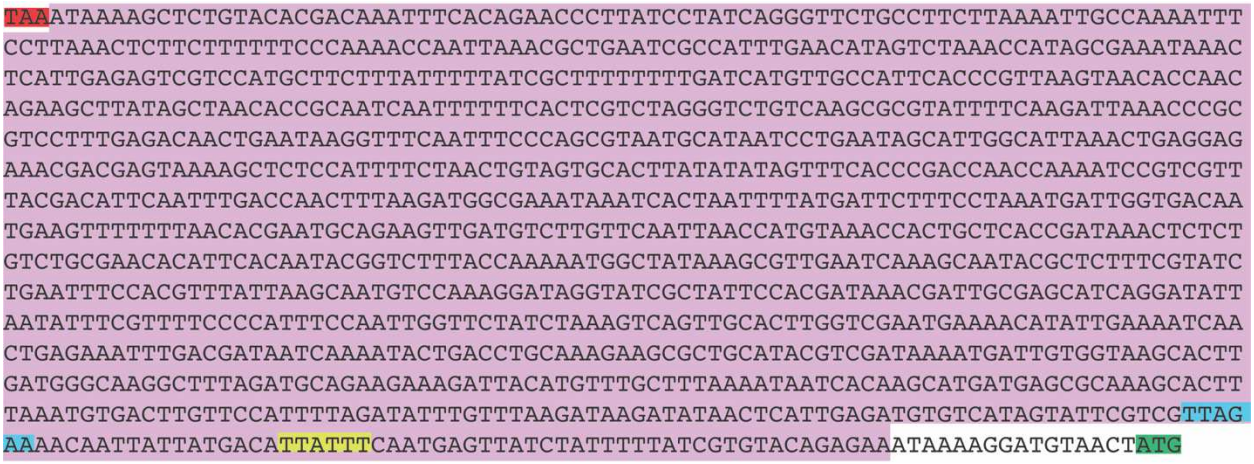

Figure 2.10. IS*Aba1* insertion sequence found upstream of *eutBC* in *A. baumannii* evolved strain. The inserted sequence is shown highlighted in pink. The final 3 nucleotides of *eutH* are highlighted in red. Predicted σ^{70} -35 (blue) and -10 (yellow) are noted (22). The start codon of *eutB* is shown highlighted in green.

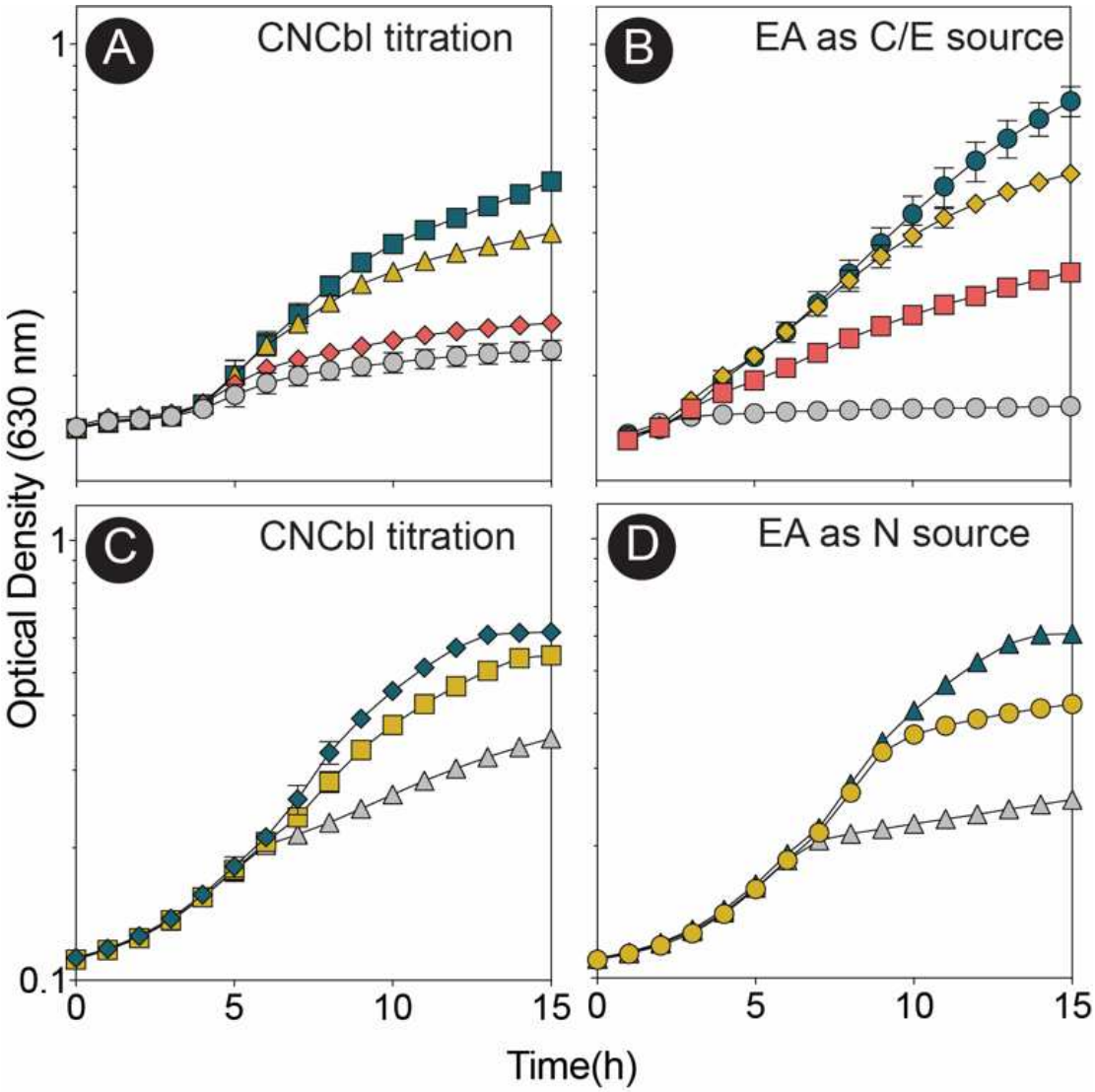

Figure 2.11 Analysis of cobamide and ethanolamine requirement. **Top panels**. Cobalamin and EA requirements of the strain carrying the IS*Aba1* element during growth on EA as a sole carbon source. **A.** CNCbl provided at the following concentrations: none (gray circles); 0.5 nM (orange diamonds); 5 nM (mustard triangles); and 10 nM (blue squares). **B.** EA was tested as carbon and energy source at the following concentrations: none (gray circles); 10 mM (orange squares); 25 mM (mustard diamonds); 75 mM (blue cicles). **Bottom panels**. Cobalamin and EA requirement of the parental *A. baumannii* strain during growth with EA as a sole nitrogen source. **C.** Titration of CNCbl, at the following concentrations: none (gray triangles), 0.5 nM (mustard squares); 5 nM (blue diamonds). **D.** EA concentrations tested: none (gray triangles); 1 mM (mustard circles); 10 mM (blue triangles). In all cases, experiments were performed in biological triplicate with technical triplicates. Error bars indicate the standard deviation of replicates.

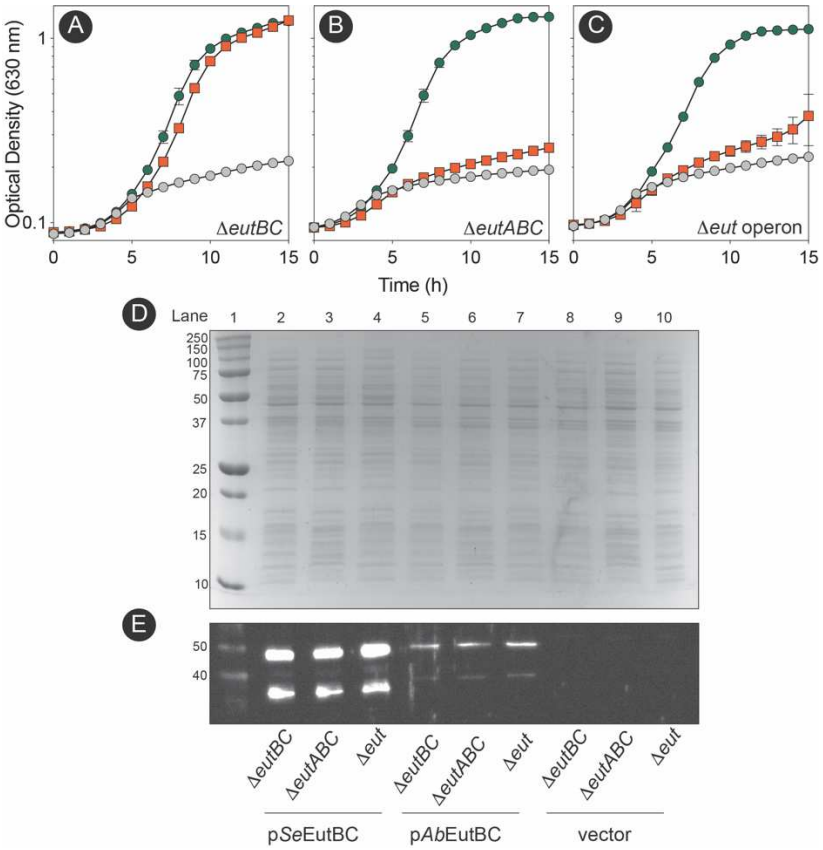

Figure 2.12. The *Ab*EutBC enzyme supports robust growth of *S.* Typhimurium *eut* mutants when ethanolamine is the sole source of nitrogen, and does not require EutA reactivase function to remain active. Strains were grown in minimal medium containing ethanolamine as the sole source of nitrogen. In all panels the growth behaviors of strains carrying plasmid pEUT269 (*S.e. eutBC*$^{+}$) is represented by the orange squares; the strain that carried plasmid pAbEUTBC1 (*A.b. eutBC*$^{+}$) is represented by green circles; and the strain that carried the empty cloning vector is represented by the grey circles. The background of each strain tested is indicated at the bottom right-hand side of the panel. For plasmid maintenance, ampicillin was added to cultures at 100 μg/mL. In all cases, each strain was grown in biological and technical triplicate. Error bars indicate the standard deviation between replicates. (D) SDS-PAGE gel of crude lysate from strains used for growth analysis. Lane 1 contains molecular mass standards reported in kilodaltons (kDa). (E) Anti-EAL Western blot of crude lysate from strains used for growth analysis.

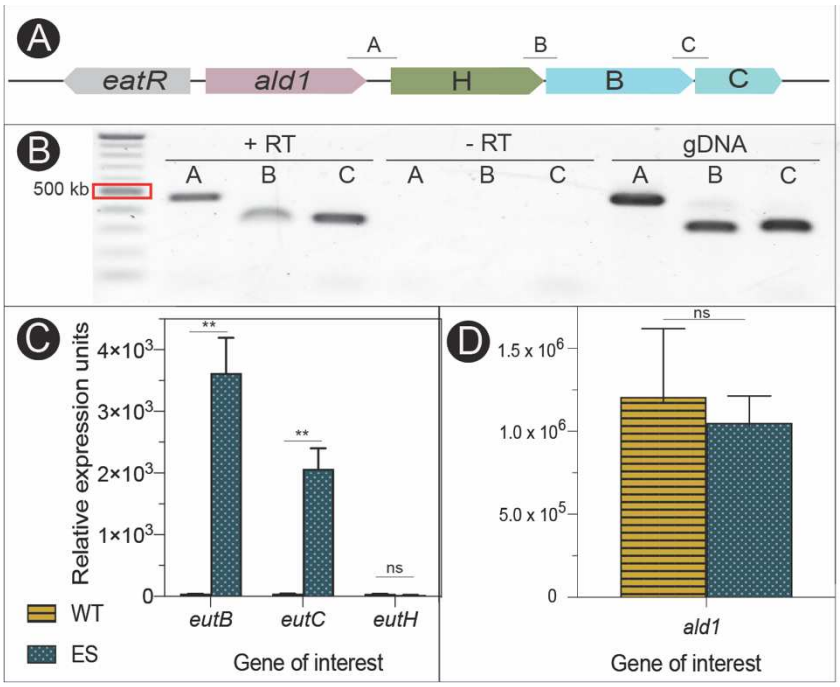

Figure 2.13. Expression of the putative *A. baumannii eut* genes. (A) Schematic of intergenic primers to test the putative *eut* operon. (B) Gel image of amplified products using intergenic primers using RNA extracted from *A. baumannii* incubated with (+ RT) or without (- RT) reverse transcriptase or gDNA as template. (C) RT-qPCR results of *eutB* and *eutC* gene expression in wild-type *A. baumannii* grown on pyruvate (yellow stripes, WT) or the evolved strain grown on ethanolamine as a sole carbon source (blue dots, ES). (D) RT-qPCR results of *ald1* expression in the wild-type *A. baumannii* grown on pyruvate (yellow stripes) or the evolved strain grown on ethanolamine as a sole carbon source (blue dots). ** denotes a *p* value <0.01.

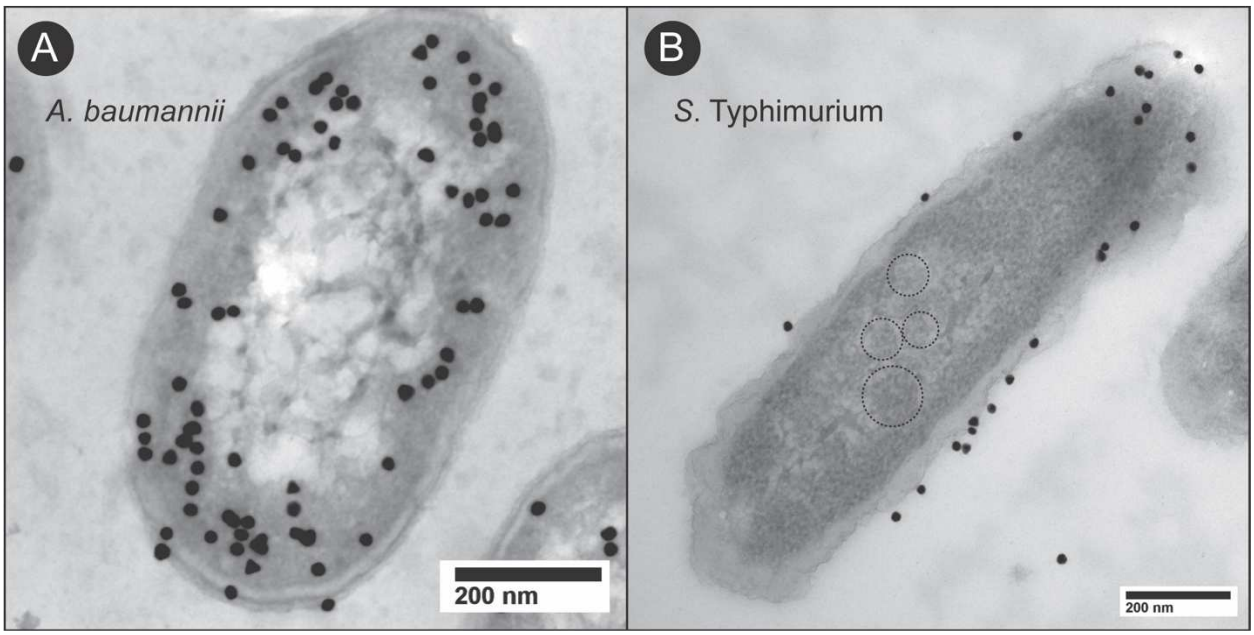

Figure 2.14. *A. baumannii* EutBC localizes to the cell membrane. TEM images of *A. baumannii* Δ*eutBC* (JE26441) (**A**) or *S.* Typhimurium Δ*eutBC* (JE26302) (**B**) grown on EA and expressing *Ab*EutBC *in trans*. For plasmid maintenance, kanamycin (50 μg/mL) was added to *A. baumannii cultures* and ampicillin (100 μg/mL) was added to *S.* Typhimurium cultures. Grids were labeled with a primary antibody generated against *S.* Typhimurium EutBC and a gold-conjugated secondary antibody, and post-stained with uranyl acetate. Metabolosomes are indicated with dotted circles.

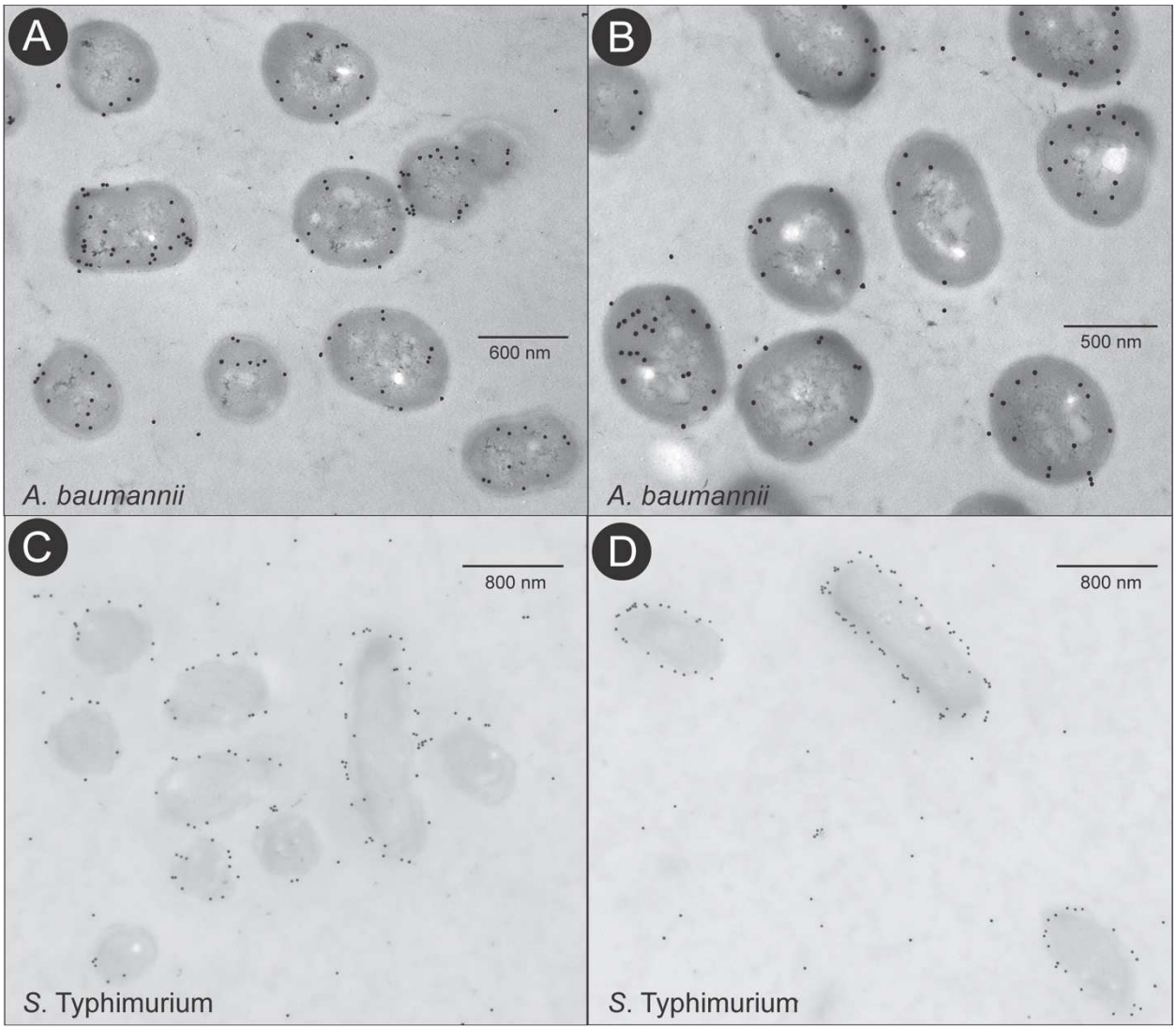

Figure 2.15. Additional images- *A. baumannii* EutBC localizes to the cell membrane. TEM images of *A. baumannii* Δ*eutBC* (JE26441) (**A, B**) or *S.* Typhimurium Δ*eutBC* (JE26302) (**C, D**) grown on EA and expressing *Ab*EutBC *in trans*. For plasmid maintenance, kanamycin (50 μg/mL) was added to *A. baumannii cultures* and ampicillin (100 μg/mL) was added to *S.* Typhimurium cultures. Grids were labeled with a primary antibody generated against *S.* Typhimurium EutBC and a gold-conjugated secondary antibody.

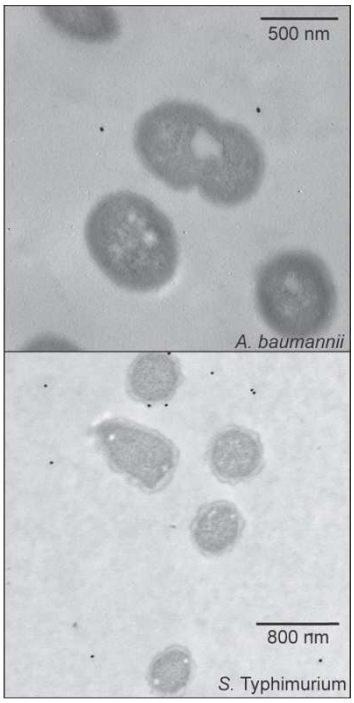

Figure 2.16. TEM nonspecific controls. TEM images of *A. baumannii* Δ*eutBC* (JE26441) (top) or *S.* Typhimurium Δ*eutBC* (JE26302) (bottom) expressing *Ab*EutBC in *trans* grown in minimal medium containing ethanolamine. Cells were processed as described in *Materials and Methods*, and were treated with goat-anti-rabbit IgG-gold secondary antibody in the absence of anti-EutBC primary antibody.

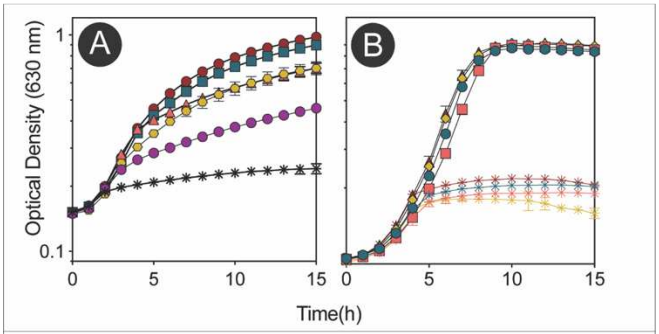

C

Strain	Average maximum growth rate (μ)	Lag time (λ) (h)
Δ*cobS*/ pSeCobS	0.64 ± 0.03	5.4
Δ*cobS*/ pAbCobS	0.69 ± 0.01	5.5
Δ*cobS*/ pCV1	NG	NG
Δ*cobU*/ pSeCobU	0.70 ± 0.03	5.0
Δ*cobU*/ pAbCobU	0.66 ± 0.02	4.9
Δ*cobU*/ pCV1	NG	NG
Δ*cobT*/ pSeCobT	0.64 ± 0.03	4.6
Δ*cobT*/ pAbCobT	0.64 ± 0.03	4.5
Δ*cobT*/ pCV1	NG	NG
ΔACAT/ pSeCobA	0.60 ±0.05	4.5
ΔACAT/ pAbACAT	0.65 ± 0.03	4.6
ΔACAT/ pCV1	NG	NG

Figure 2.17. *A. baumannii* can salvage cobinamide to form a complete cobamide. **A.** EA utilization by *A. baumannii* evolved strain (ES) grown in minimal medium containing EA as the sole source of carbon and energy. To test utilization of various bases, cultures were supplemented with cobalamin (red circles) or salvaging cobinamide with the addition of 5-methoxybenzimidazole (cyan squares), adenine (green triangles), 5,6-dimethylbenzimidazole (yellow hexagons), no base (purple circles) or no cobamide provided (grey diamonds). **B.** Complementation of *A. baumannii* NLA genes in *S.* Typhimurium. Δ*cobS*/pAbCobS (red squares), Δ*cobS*/vector (open, inverted orange triangles), Δ*cobU*/pAbCobU (cyan squares), Δ*cobU*/vector (black diamonds), Δ*cobT*/pAbCobT (green triangles), Δ*cobT*/vector (blue hexagons), ΔACAT/pAbACAT (yellow diamonds), ΔACAT/vector (purple circle). Ampicillin (100 μg/mL) was added to cultures for plasmid maintenance. **C.** Growth behavior of *S.* Typhimurium strains expressing *A. baumannii* genes. Growth rates were determined using online tools (https://scott-h-saunders.shinyapps.io/gompertz_fitting_0v2/).

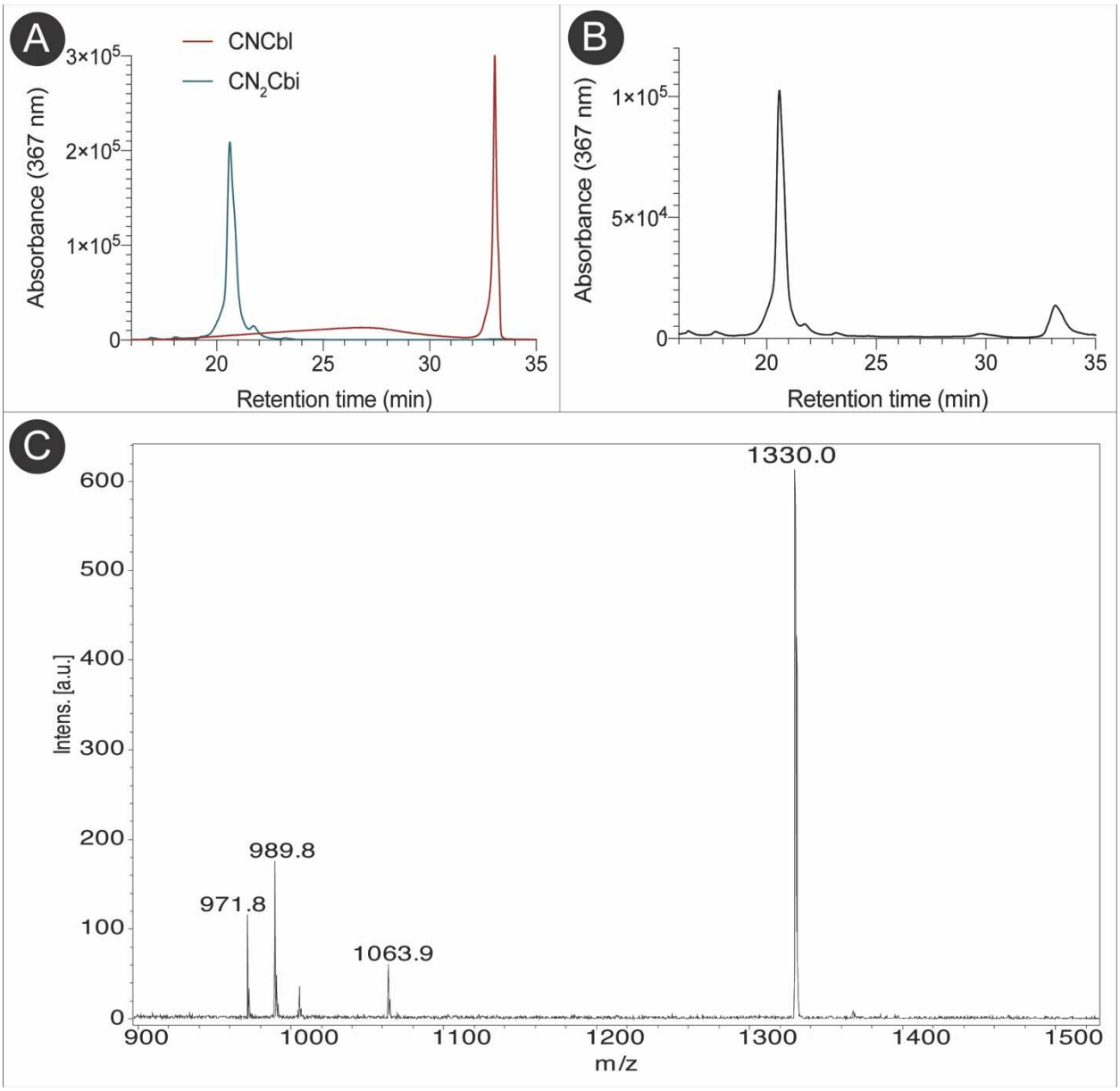

Figure 2.18. Cobamide extracts from *A. baumannii*. A. RP-HPLC chromatogram of pure standards $(CN)_2$Cbi (blue) and CNCbl (red). **B.** RP-HPLC chromatogram of extracts of strain JE26013(*A. baumannii* grown with ethanolamine as a sole carbon source and $(CN)_2$Cbi. **C.** MALDI-TOF mass spectrum of peak isolated at 33 mins.

CHAPTER 3

LITERATURE REVIEW: CORRINOID SALVAGING AND REMODELING IN PROKARYOTES[2]

[2]Elizabeth A. Villa and Jorge C. Escalante-Semerena. 2022. To be submitted to *Molecular Microbiology*.

3.1 ABSTRACT

Cobamides are one of the most complex biomolecules produced in nature and are required by enzymes to perform numerous diverse functions across all domains of life. Most animals and prokaryotes require cobamides, but only a subset of prokaryotes produce cobamides. The *de novo* synthesis pathway requires the production of approximately 30 enzymes and is extremely energy-intensive; as such, many prokaryotic organisms depend on assimilation of preformed corrin-ring precursors to make a coenzyme, or remodel complete cobamides. In this review, we discuss the diverse strategies utilized by bacterial and archaeal organisms to assimilate cobamides or cobamide precursors to form cobamide coenzymes in the absence of a *de novo* pathway. We discuss cobamide transport and salvaging, also known as nucleotide loop assembly, as well as a number of remodeling systems that have been identified in bacteria and archaea.

3.2 INTRODUCTION

Coenzyme B_{12} (CoB_{12}), also known as adenosylcobalamin (AdoCbl), and other cobamides are required by diverse enzymes in eukaryotes and prokaryotes to perform a variety of metabolic reactions including methyl transfers, carbon skeleton rearrangements, and elimination reactions (1). These coenzymes are also used by some bacteria as photoreceptors involved in carotenogenesis or DNA photolyase (2-4). Despite this widespread requirement, bioinformatics analyses suggest that *de novo* synthesis is restricted to a subset of prokaryotes. Alternatively, many organisms rely on salvaging of incomplete precursors or remodeling of complete cobamides (5).

Cobamides consist of a cyclic tetrapyrrole containing a central cobalt ion equatorially coordinated to the nitrogen atoms of the pyrrole rings. This part of the molecule is also referred to as the corrin ring. In the biologically active coenzyme known as adenosylcobalamin (AdoCbl), the cobalt participates in a weakly covalent bond with a 5'-deoxyadenosine group derived from ATP (Figure 3.1). This bond is critical to AdoCbl-based radical chemistry, and is located on the upper face of the corrin ring (a.k.a. *Co*β). AdoCbl also has an axial ligand on the lower, alpha face (a.k.a. *Co*α), and in this cobamide the ligand is 5,6-dimethylbenzimidazole (DMB) (6-8). Alternative nucleobases may be substituted for DMB, and the preference for a base varies between microbial organisms and the specificity of the cobamide-requiring enzyme (9-12). The nucleobase is tethered to the corrin ring by a structure known as the nucleotide loop.

Because of the complex structure of cobamides, the biosynthetic pathway is an energy-intensive process and requires about 30 enzymes. This number is an estimate and may vary from organism to organism. We note that, at the time of this writing, the complete set of cobamide biosynthetic genes and corresponding enzymes has not been experimentally validated in any one organism. However, the different branches of the biosynthetic pathway have been studied in depth in *Salmonella enterica, Bacillus megaterium,* and *Pseudomonas aeruginosa.* Briefly, the corrin ring is assembled first, followed by an adenosylation reaction in which the upper ligand is attached to the cobalt ion (13-16). The late steps of cobamide biosynthesis involve the activation and attachment of the base on the lower face of the ring structure, a process known as nucleotide loop assembly (NLA) (17, 18).

While most bacteria require cobamides, many lack the suite of enzymes needed for *de novo* synthesis. Shelton *et al.* found genes encoding B_{12}-dependent enzymes in the genomes of 86% of gut bacteria; however, only 37% of these were predicted to have a functional *de novo* biosynthesis pathway (19). The human gut contains various cobamides, but cobamide-dependent enzymes may specifically bind a subset or even a single cobamide, leading to preferential use by different organisms within a mixed population (9). Thus, cobamide availability and exchange may regulate interactions within microbial communities (12, 20).

In this review we investigate the prevalence and diversity of systems used by prokaryotes to salvage incomplete corrinoid precursors, and to remodel exogenously available cobamides to suit their requirements. We address the physiological importance of these processes for growth and survival.

3.3 ROLE OF COBAMIDES IN PROKARYOTES

Cobamide-dependent enzymes are necessary for a number of diverse processes in prokaryotes. Notably, methanogenic archaea utilize cobamide-dependent methyltransferase enzymes during methanogenesis (21-23). Cobamides are used by bacteria for a number of functions, including metabolism of ethanolamine, glycerol, and propanediol (24-29). Other cobamide-dependent enzymes are involved in tRNA modifications, dehalogenations, and one-carbon metabolism (30-33). Humans and other animals utilize a cobamide-dependent methylmalonyl-CoA mutase in metabolism, and defects to, or absence of this enzyme can lead to severe neurological effects and are often fatal (34).

3.4 COBAMIDE TRANSPORT AND ADENOSYLATION

Due to the complexity and large size of the corrin ring, import of the ring precursor into the cell is an active, energy-dependent process. In Gram-negative organisms, transport across the outer membrane is facilitated by the calcium-dependent transporter BtuB, and is dependent on energy generated through interactions with the outer membrane protein TonB (35-39). Transport through the inner membrane occurs through the ABC transporter BtuFCD. BtuF binds cobamides and/or corrinoids in the periplasm and delivers them to the BtuCD complex in the inner membrane (40-45). In many cases, a single *btuF* gene product binds and transports a number of incomplete corrinoids or cobamides. However, *Bacteroides thetaiotamicron* utilizes three homologous BtuF proteins with various specificities. Although seemingly redundant, multiple *btuF* alleles imparted a colonization advantage to *B. thetaiotamicron* in a mouse model (46). *B. thetaiotamicron* also utilizes the surface lipoprotein BtuG2 to bind Cbl with high affinity and interact with BtuB to facilitate transport into the periplasm. (47). Therefore, multiple copies of genes encoding transport proteins with various cobamide specificities may be advantageous to growth under some conditions.

Upon reaching the cytoplasm, cobamides and corrinoids are adenosylated at the upper (Co*β*) position. In *Salmonella enterica* subsp. *enterica* sv Typhimurium str. LT2 (hereafter *S.* Typhimurium), this reaction is typically catalyzed by the housekeeping adenosyltransferase CobA (13, 48, 49). *S.* Typhimurium utilizes two additional adenosyltransferases, EutT and PduO, which are required for ethanolamine and propanediol metabolism, respectively (27, 50, 51). Nucleotide loop assembly enzymes

specifically use incomplete corrinoids with the adenosyl ligand as substrates, so this critical step must take place prior to addition of the lower alpha ligand.

3.5 ASSIMILATION OF INCOMPLETE PRECURSORS (SALVAGING)

Precursor salvaging in bacteria. Some prokaryotes can synthesize cobamides *de novo* or salvage complete or incomplete corrinoids that can be converted into cobamides. *S.* Typhimurium synthesizes cobamides *de novo* only under anoxic conditions. However, under normoxic conditions, this bacterium retains the biosynthetic capability of converting precursors that have a complete ring structure into active adenosylcobamides, the final product of the pathway (52, 53). In *S.* Typhimurium, during anoxic cobamide biosynthesis, the cobalt ion is inserted into the corrin ring early in the process. In contrast, *Pseudomonas denitrificans* synthesizes cobamides *de novo* in the presence of oxygen, and the cobalt ion is inserted into the ring in the late stages of the pathway (5, 54). Cobamide-requiring organisms that cannot synthesize cobamides *de novo* rely on salvaging incomplete precursors from the environment.

This review focuses on different approaches used by prokaryotes to salvage precursors and remodel complete cobamides to contain a specific nucleobase. As discussed below, some organisms may also start the nucleobase remodeling process using cobinamide, which is an incomplete corrinoid cells can import and convert into cobamides.

The late steps of cobamide biosynthesis, a.k.a. the nucleotide loop assembly (NLA) pathway. Organisms possessing a complete NLA pathway but lacking most or all of the

ring biosynthesis genes require a fully-formed, complete corrin ring in order to salvage via NLA enzymes (Figure 3.1, solid black arrows) (19). In bacteria, salvaging of the precursor cobinamide (Cbi) requires the bifunctional kinase (EC 2.7.7.62)/guanylyltransferase (EC 2.7.1.156), which first phosphorylates and then guanylylates the corrinoid substrate (18, 24, 55-60). This enzyme is referred to as CobU in *S. enterica* or CobP in *P. denitrificans.*

The nucleobase is activated by a phosphoribosyltransferase (CobT in *S. enterica* or CobU in *P. denitrificans*; EC 2.4.2.21) that generates α-ribazole-P (α-RP) by transferring the phosphoribosyl group of nicotinate mononucleotide (NaMN) to DMB (24, 61-64). Subsequently, the *S. enterica* AdoCbl 5'-P synthase enzyme CobS (CobV in *P. denitrificans*) (EC 2.7.8.26) condenses the activated AdoCbi-GDP and α-RP to form AdoCbl-P (18, 24, 65). Interestingly, CobS and CbiB, the final enzyme of the *de novo* synthesis pathway, are integral inner membrane proteins (66, 67). Reports suggest that these enzymes may serve as a point of interaction for other NLA enzymes and may act as an anchor around which these enzymes can localize to facilitate efficient exchange of corrinoid intermediates (66-68). In the final step of B_{12} biosynthesis, the phosphatase CobC (EC 3.1.3.73) cleaves the phosphate from the nucleotide to yield AdoCbl (18, 69, 70). As *de novo* synthesis requires approximately 30 enzymes, while salvaging and remodeling may require 5 or fewer, modifying available cobamides or precursors may be energetically advantageous even to an organism capable of *de novo* synthesis.

Synthesis of the α-ribazole moiety. The nucleotide loop of AdoCbl is derived from DMB. Multiple DMB synthesis pathways have been identified. In organisms capable of

synthesizing B_{12} in the presence of oxygen, the C1 carbon of FMN is converted into the C2 carbon of DMB by the enzyme BluB (Figure 3.1, top right purple circle) (71-76). Previous work has indicated the presence of a system for the anaerobic synthesis of DMB, but the enzyme(s) involved in this pathway have not yet been identified (10). A possible source of α-ribazole (α-R) is α-*5,6*-dimethylbenzimidazole adenine dinucleotide (*α*-DAD) which can be cleaved to form α-RP (77).

Firmicutes utilize an alternative system, CblTS, through which α-R is salvaged (78-80). CblT is a α-R transporter that imports α-R into the cytoplasm, and CblS is a α-R kinase which activates α-R for addition to the corrinoid ring in place of CobT. In *S. enterica*, CobT directly converts DMB into α-RP, however studies suggest that *S. enterica* also possesses a system for α-R biosynthesis from DMB that has not yet been identified (79).

3.6 REMODELING IS ESSENTIAL FOR COBINAMIDE SALVAGING IN ARCHAEA

Cobamide salvaging and remodeling in archaea. Archaeal enzymes are represented by yellow circles with black text in Figure 3.1. Unlike the bifunctional bacterial *cobU/cobP*, archaeal genomes contain a GTP::adenosylcobinamide-phosphate guanylyltransferase (CobY), a functional homologue for exclusively the guanylyltransferase activity of CobU (58, 81-84). Because CobY lacks kinase activity, Cbi cannot be directly converted into Cbi-P by this enzyme. Instead, archaeal salvaging of Cbi proceeds through hydrolysis of the aminopropanol group on the lower face of the ring by the enzyme CbiZ to form Cby (Figure 3.1, 3.2). CobD catalyzes the conversion of L-threonine-phosphate to aminopropanol-phosphate (AP-P) (85, 86). Cby and AP-P are then condensed by CbiB

to yield cobinamide-phosphate (Cbi-P), the substrate for CobY (67, 81-83, 87, 88). Following the transfer of GMP from GTP by CobY, CobS is able to condense cobinamide-GDP (Cbi-GDP) with an α-RP to yield a cobamide-phosphate derivative, which is dephosphorylated by the CobC homologue in archaea, CobZ (89). Thus, remodeling activity of CbiZ is essential both to salvage the incomplete precursor Cbi as well as to remodel complete cobamides (87, 88).

CbiS, an archaeal CbiZ-CobZ fusion protein. Some archaeal species have been identified in which the amidohydrolase CbiZ is fused to the archaeal phosphatase and final enzyme in cobamide biosynthesis, CobZ. These enzyme functions are illustrated in a yellow circle with black outline in Figure 3.1. This fusion, referred to as CbiS, was first identified in the hyperthermophile *Methanopyrus kandleri* (90). The amidohydrolase portion of CbiS shows remarkably little cobamide specificity, and is capable of cleaving nucleotide loops containing various nucleobases. Importantly, CbiS can also convert cobinamide into cobyric acid despite the absence of a nucleotide loop. An interesting question that remains unanswered is how the activity of the CbiS enzyme is modulated so it does not cleave newly synthesized cobamides.

The fusion of the first and last enzymes involved in cobamide remodeling (*i.e.,* CbiZ, CobZ) found in CbiS is intriguing, and supports a long-held hypothesis that cobamide synthesis and salvaging enzymes are co-localized within the cell to facilitate efficient exchange of valuable intermediates. Interestingly, this fusion has only been identified in extremophiles, primarily hyperthermophiles, suggesting that fusion of these

two enzymes may contribute to thermal stability or protection from other environmental stressors (90).

3.7 COBAMIDE REMODELING IN BACTERIA

Adenosylcobinamide (AdoCbi) hydrolase (CbiZ)-dependent remodeling in bacteria. Genes encoding remodeling enzymes have been identified in both bacteria and archaea, however homologues of *cbiZ* are found in archaea much more frequently than in bacteria likely due to the dependence of corrin ring precursor salvaging on the remodeling enzyme (91). Note that CbiZ (EC 3.5.1.90) is shown in yellow text with a purple circle in Figure 3.1 as this enzyme is found in both bacteria and archaea. It is suggested that *cbiZ* originated in archaea and was horizontally transferred to bacteria. Remodeling cobamides to incorporate a preferred base is dependent on functional NLA gene products, which activate and attach the preferred nucleobase to the corrin ring. Remodeling may be an important process for intestinal bacteria, as cobalamin analogues have been detected at much higher abundance than cobalamin in the human gut (9). Following hydrolysis by CbiZ, the enzymes CbiB, CobD, CobU, CobS and CobC are necessary to yield the biologically active, remodeled coenzyme (69).

Less than 10% of bacterial genomes contain *cbiZ,* however species containing this gene are widely distributed and do not seem to diverge from a single common ancestor (91). It is not currently understood why some bacteria have acquired multiple Cbi salvaging systems, *cbiZ* and *cobU/cobP*, or if one system is used preferentially under certain conditions. It is possible that some bacterial species have retained *cbiZ* due to an environmental abundance of cobamide analogues containing a nucleobase that makes it

unusable by that organism. In this case, salvaging through *cobU/cobP* would be ineffective, and remodeling by first removing the base by CbiZ and replacement of the preferred nucleobase through the NLA pathway would be required. Below are some notable bacterial species that can remodel complete cobamides. We discuss the roles of cobamides in these organisms, and predict that the requirement for a preferred nucleobase led to the retention of remodeling enzymes in the genome following horizontal gene transfer from other prokaryotes.

The α-proteobacterium *Rhodobacter sphaeroides* is able to ferment, photosynthesize, and respire aerobically and anaerobically (92). The genome of *R. sphaeroides* encodes homologues to genes found in pathway for aerobic biosynthesis of cobalamin (93). *R. sphaeroides* utilizes cobamide-dependent enzymes for a number of cellular processes, including methionine synthesis (94). Pseudocobalamin (psCbl), a Cbl analogue containing adenine in place of DMB, cannot be used by *R. sphaeroides*, and is instead remodeled by CbiZ to form Cbl (95).

Dehalococcoides species are of particular interest for their role in detoxification of groundwater contaminants including trichloroethane and perchloroethane through organohalide respiration (96, 97). Dechlorination reactions are catalyzed by cobamide-dependent reductive dehalogenases (30). *Dehalococcoides* genomes lack cobamide biosynthetic genes, so these organisms are restricted to salvaging precursors such as Cbi or remodeling alternative cobamides in the absence of specific cobamides (98). The genomes of *Dehalococcoides* species have multiple copies of *cbiZ,* ranging in number from three to eight copies (91, 98, 99). Only cobalamin or 5-methoxybenzimidazole-cobamide ([5-MeBza]-Cba) support dechlorination reactions in *D. mccartyi,* however

cobamides containing purinyl and phenolyl bases could be remodeled to cobalamin if the preferred benzimidazole base was provided (98). Interestingly, *cbiZ* alleles of *Dehalococcoides* share more sequence similarity with archaeal homologues in *Methanosarcina mazei*, and contain no significant similarity to *cbiZ* alleles found in bacteria such as the gene found in *R. sphaeroides* (91). The physiological importance of remodeling is indicated by the many copies of *cbiZ* encoded in the genome, however the reason for so many copies and diversity in number is not yet understood.

An alternative cobamide remodeling approach is provided by the phosphodiesterase CbiR. The mucin-degrading organism *Akkermansia muciniphila* is of particular interest as a beneficial gut microbe that may strengthen the host gut barrier by stimulating production of mucus (100, 101). Cobamides and cobamide precursors are a valuable resource in the gut, as a majority of gut bacteria utilize cobamide-dependent enzymes (19). A novel phosphodiesterase CbiR was identified in *A. muciniphila* capable of remodeling various cobamides to form psCbl (Figure 3.1, black small dashed arrow). The intermediate precursor formed by CbiR is AdoCbi-P, the substrate for CobU. CbiR homologues were identified in the genomes of organisms across at least 22 phyla, suggesting a widespread alternative mechanism for cobamide salvage (102).

A bifunctional AdoCbl 5'-P synthase from Vibrio cholerae (VcCobS). Recently, a putative novel activity for the *Vibrio cholerae* AdoCbl 5'-P synthase CobS was reported (103). The authors used crude cell extracts of a strain of *E. coli* that overexpressed the *V. cholerae cobS* gene and concluded that *V. cholerae* CobS can directly remodel pseudocobalamin

(psCbl) into cobalamin. Heterologous expression of *V. cholerae* CobS in *Escherichia coli* resulted in conversion of psCbl to Cbl, a result that was suggesting that in *V. cholerae*, CobS is not only capable of synthase activity, but also recognition and replacement of the lower ligand of pseudoCbl (Figure 3.1, black dashed arrows) (103, 104). Furthermore, this process is directly carried out by CobS and does not require CbiB or CobU to form the complete cobamide structure (104). This is the first report of remodeling activity by any CobS enzyme, and additional investigation using pure *Vc*CobS protein should be performed to verify this activity.

3.8 CONCLUDING REMARKS

The ability to salvage cobamide precursors or remodel complete cobamides can provide a competitive advantage to organisms within a microbiome. Synthesizing complete cobamides *de novo* is an energetically intensive process, and many organisms that utilize cobamide-dependent enzymes lack the *de novo* synthesis pathway. Salvage or remodeling is energetically favorable to the cell. Prokaryotes have developed various strategies for remodeling complete cobamides, as detailed in this work. The contribution of cobamides to a competitive advantage in microbiomes such as the human gut is not well understood. Multiple analogues of cobalamin are present in the gut, however access to a preferred cobamide may be limited (9). The ability to salvage precursors or remodel diverse cobamides based on abundance in the environment may provide a competitive advantage to prokaryotes in multispecies communities.

3.9 REFERENCES

1. Bryant DA, Hunter CN, Warren MJ. 2020. Biosynthesis of the modified tetrapyrroles-the pigments of life. J Biol Chem 295:6888-6925.
2. Jost M, Fernandez-Zapata J, Polanco MC, Ortiz-Guerrero JM, Chen PY, Kang G, Padmanabhan S, Elias-Arnanz M, Drennan CL. 2015. Structural basis for gene regulation by a B12-dependent photoreceptor. Nature 526:536-541.
3. Bridwell-Rabb J, Drennan CL. 2017. Vitamin B12 in the spotlight again. Curr Opin Chem Biol 37:63-70.
4. Padmanabhan S, Jost M, Drennan CL, Elias-Arnanz M. 2017. A new facet of vitamin B12: Gene regulation by cobalamin-based photoreceptors. Annu Rev Biochem 86:485-514.
5. Rodionov DA, Vitreschak AG, Mironov AA, Gelfand MS. 2003. Comparative genomics of the vitamin B_{12} metabolism and regulation in prokaryotes. J Biol Chem 278:41148-41159.
6. Woodward RB. 1973. The total synthesis of vitamin B_{12}. Pure Appl Chem 33:145-177.
7. Eschenmoser A, Wintner CE. 1977. Natural product synthesis and vitamin B_{12}. Science 196:1410-1420.
8. Battersby AR. 2000. Tetrapyrroles: the pigments of life. Nat Prod Rep 17:507-526.
9. Allen RH, Stabler SP. 2008. Identification and quantitation of cobalamin and cobalamin analogues in human feces. Am J Clin Nutr 87:1324-1335.

10. Renz P. 1999. Biosynthesis of the 5,6-dimethylbenzimidazole moiety of cobalamin and of other bases found in natural corrinoids, p 557-575. *In* Banerjee R (ed), Chemistry and Biochemistry of B12. John Wiley & Sons, Inc., New York.

11. Chan CH, Escalante-Semerena JC. 2011. ArsAB, a novel enzyme from *Sporomusa ovata* activates phenolic bases for adenosylcobamide biosynthesis. Mol Microbiol 81:952-967.

12. Jeter VL, Mattes TA, Beattie NR, Escalante-Semerena JC. 2019. A new class of phosphoribosyltransferases involved in cobamide biosynthesis Is found in methanogenic archaea and cyanobacteria. Biochemistry 58:951-964.

13. Escalante-Semerena JC, Suh SJ, Roth JR. 1990. *cobA* function is required for both de novo cobalamin biosynthesis and assimilation of exogenous corrinoids in *Salmonella typhimurium*. J Bacteriol 172:273-280.

14. Suh S, Escalante-Semerena JC. 1995. Purification and initial characterization of the ATP:corrinoid adenosyltransferase encoded by the *cobA* gene of *Salmonella typhimurium*. J Bacteriol 177:921-925.

15. Mera PE, Escalante-Semerena JC. 2010. Dihydroflavin-driven adenosylation of 4-coordinate Co(II) corrinoids: are cobalamin reductases enzymes or electron transfer proteins? J Biol Chem 285:2911-2917.

16. Debussche L, Couder M, Thibaut D, Cameron B, Crouzet J, Blanche F. 1991. Purification and partial characterization of Cob(I)alamin adenosyltransferase from *Pseudomonas denitrificans*. J Bacteriol 173:6300-6302.

17. Escalante-Semerena JC, Johnson MG, Roth JR. 1992. The CobII and CobIII regions of the cobalamin (vitamin B12) biosynthetic operon of Salmonella typhimurium. J Bacteriol 174:24-29.

18. Maggio-Hall LA, Escalante-Semerena JC. 1999. In vitro synthesis of the nucleotide loop of cobalamin by *Salmonella typhimurium* enzymes. Proc Natl Acad Sci U S A 96:11798-11803.

19. Shelton AN, Seth EC, Mok KC, Han AW, Jackson SN, Haft DR, Taga ME. 2019. Uneven distribution of cobamide biosynthesis and dependence in bacteria predicted by comparative genomics. ISME J 13:789-804.

20. Magnusdottir S, Ravcheev D, de Crecy-Lagard V, Thiele I. 2015. Systematic genome assessment of B-vitamin biosynthesis suggests co-operation among gut microbes. Front Genet 6:148.

21. Taylor CD, Wolfe RS. 1974. A simplified assay for coenzyme M (HSCH2CH2SO3). Resolution of methylcobalamin-coenzyme M methyltransferase and use of sodium borohydride. J Biol Chem 249:4886-4890.

22. DiMarco AA, Bobik TA, Wolfe RS. 1990. Unusual coenzymes of methanogenesis. Annu Rev Biochem 59:355-94.

23. Grahame DA. 1989. Different isozymes of methylcobalamin:2-mercaptoethanesulfonate methyltransferase predominate in methanol- versus acetate-grown *Methanosarcina barkeri*. J Biol Chem 264:12890-12894.

24. Cameron B, Blanche F, Rouyez MC, Bisch D, Famechon A, Couder M, Cauchois L, Thibaut D, Debussche L, Crouzet J. 1991. Genetic analysis, nucleotide sequence, and products of two Pseudomonas denitrificans cob genes encoding

nicotinate-nucleotide: dimethylbenzimidazole phosphoribosyltransferase and cobalamin (5'-phosphate) synthase. J Bacteriol 173:6066-6073.

25. Roof DM, Roth JR. 1988. Ethanolamine utilization in *Salmonella typhimurium*. J Bacteriol 170:3855-3863.

26. Stojiljkovic I, Baumler AJ, Heffron F. 1995. Ethanolamine utilization in *Salmonella typhimurium*: nucleotide sequence, protein expression, and mutational analysis of the *cchA cchB eutE eutJ eutG eutH* gene cluster. J Bacteriol 177:1357-1366.

27. Sheppard DE, Penrod JT, Bobik T, Kofoid E, Roth JR. 2004. Evidence that a B12-adenosyl transferase is encoded within the ethanolamine operon of *Salmonella enterica*. J Bacteriol 186:7635-7644.

28. Daniel R, Bobik TA, Gottschalk G. 1998. Biochemistry of coenzyme B12-dependent glycerol and diol dehydratases and organization of the encoding genes. FEMS Microbiol Rev 22:553-66.

29. Toraya T, Kuno S, Fukui S. 1980. Distribution of coenzyme B12-dependent diol dehydratase and glycerol dehydratase in selected genera of *Enterobacteriaceae* and *Propionibacteriaceae*. J Bacteriol 141:1439-`442.

30. Glod G, Angst W, Holliger C, Schwarzenbach RP. 1996. Corrinoid-mediated reduction of tetrachloroethene, trichloroethene, and trichlorofluoroethene in homogeneous aqueous solution: Reaction kinetics and reaction mechanisms. Environ Sci Technol 31:253-260.

31. Frey B, McCloskey J, Kersten W, Kersten H. 1988. New function of vitamin B_{12}: cobamide-dependent reduction of epoxyqueuosine to queuosine in tRNAs of *Escherichia coli* and *Salmonella typhimurium*. J Bacteriol 170:2078-2082.

32. Drummond JT, Matthews RG. 1993. Cobalamin-dependent and cobalamin-independent methionine synthases in *Escherichia coli*: two solutions to the same chemical problem. Adv Exp Med Biol 338:687-692.

33. Drummond JT, Huang S, Blumenthal RM, Matthews RG. 1993. Assignment of enzymatic function to specific protein regions of cobalamin-dependent methionine synthase from *Escherichia coli*. Biochemistry 32:9290-9295.

34. Banerjee R, Chowdhury S. 1999. Methylmalonyl-CoA mutase, p 707-729. *In* Banerjee R (ed), Chemistry and Biochemistry of B12. John Wiley & Sons, Inc., New York.

35. Kadner RJ, Liggins GL. 1973. Transport of vitamin B12 in *Escherichia coli:* genetic studies. J Bacteriol 115:514-521.

36. Gudmundsdottir A, Bell PE, Lundrigan MD, Bradbeer C, Kadner RJ. 1989. Point mutations in a conserved region (TonB box) of Escherichia coli outer membrane protein BtuB affect vitamin B12 transport. J Bacteriol 171:6526-6533.

37. Shultis DD, Purdy MD, Banchs CN, Wiener MC. 2006. Outer membrane active transport: structure of the BtuB:TonB complex. Science 312:1396-1399.

38. Bradbeer C, Reynolds PR, Bauler GM, Fernandez MT. 1986. A requirement for calcium in the transport of cobalamin across the outer membrane of Escherichia coli. J Biol Chem 261:2520-2523.

39. Ferguson AD, Amezcua CA, Halabi NM, Chelliah Y, Rosen MK, Ranganathan R, Deisenhofer J. 2007. Signal transduction pathway of TonB-dependent transporters. Proc Natl Acad Sci U S A 104:513-518.

40. DeVeaux LC, Kadner RJ. 1985. Transport of vitamin B12 in *Escherichia coli*: cloning of the btuCD region. J Bacteriol 162:888-896.

41. Borths EL, Poolman B, Hvorup RN, Locher KP, Rees DC. 2005. *In vitro* functional characterization of BtuCD-F, the *Escherichia coli* ABC transporter for vitamin B12 uptake. Biochemistry 44:16301-16309.

42. Korkhov VM, Mireku SA, Veprintsev DB, Locher KP. 2014. Structure of AMP-PNP-bound BtuCD and mechanism of ATP-powered vitamin B12 transport by BtuCD-F. Nat Struct Mol Biol 21:1097-1099.

43. Van Bibber M, Bradbeer C, Clark N, Roth JR. 1999. A new class of cobalamin transport mutants (*btuF*) provides genetic evidence for a periplasmic binding protein in *Salmonella typhimurium*. J Bacteriol 181:5539-5541.

44. Borths EL, Locher KP, Lee AT, Rees DC. 2002. The structure of *Escherichia coli* BtuF and binding to its cognate ATP binding cassette transporter. Proc Natl Acad Sci U S A 99:16642-16647.

45. Cadieux N, Bradbeer C, Reeger-Schneider E, Koster W, Mohanty AK, Wiener MC, Kadner RJ. 2002. Identification of the periplasmic cobalamin-binding protein BtuF of *Escherichia coli*. J Bacteriol 184:706-717.

46. Degnan PH, Barry NA, Mok KC, Taga ME, Goodman AL. 2014. Human gut microbes use multiple transporters to distinguish vitamin B12 analogs and compete in the gut. Cell Host Microbe 15:47-57.

47. Wexler AG, Schofield WB, Degnan PH, Folta-Stogniew E, Barry NA, Goodman AL. 2018. Human gut Bacteroides capture vitamin B12 via cell surface-exposed lipoproteins. Elife 7.

48. Suh SJ, Escalante-Semerena JC. 1993. Cloning, sequencing and overexpression of *cobA* which encodes ATP:corrinoid adenosyltransferase in *Salmonella typhimurium*. Gene 129:93-97.

49. Moore TC, Newmister SA, Rayment I, Escalante-Semerena JC. 2012. Structural insights into the mechanism of four-coordinate cob(II)alamin formation in the active site of the *Salmonella enterica* ATP:co(I)rrinoid adenosyltransferase (CobA) enzyme: Critical role of residues Phe91 and Trp93. Biochemistry 51:9647-9657.

50. Buan NR, Escalante-Semerena JC. 2006. Purification and initial biochemical characterization of ATP:Cob(I)alamin adenosyltransferase (EutT) enzyme of *Salmonella enterica*. J Biol Chem 281:16971-16977.

51. Johnson CL, Pechonick E, Park SD, Havemann GD, Leal NA, Bobik TA. 2001. Functional genomic, biochemical, and genetic characterization of the *Salmonella pduO* gene, an ATP:cob(I)alamin adenosyltransferase gene. J Bacteriol 183:1577-1584.

52. Jeter RM. 1990. Cobalamin-dependent 1,2-propanediol utilization by *Salmonella typhimurium*. J Gen Microbiol 136:887-896.

53. Jeter RM, Olivera BM, Roth JR. 1984. *Salmonella typhimurium* synthesizes cobalamin (vitamin B_{12}) de novo under anaerobic growth conditions. J Bacteriol 159:206-213.

54. Blanche F, Thibaut D, Debussche L, Hertle R, Zipfel F, Muller G. 1993. Parallels and decisive differences in vitamin-B12 biosyntheses. Angew Chem Int Ed Engl 32:1651-1653.

55. O'Toole GA, Escalante-Semerena JC. 1993. *cobU*-dependent assimilation of nonadenosylated cobinamide in cobA mutants of *Salmonella typhimurium*. J Bacteriol 175:6328-6336.

56. O'Toole GA, Escalante-Semerena JC. 1995. Purification and characterization of the bifunctional CobU enzyme of *Salmonella typhimurium* LT2. Evidence for a CobU-GMP intermediate. J Biol Chem 270:23560-23569.

57. Blanche F, Debussche L, Famechon A, Thibaut D, Cameron B, Crouzet J. 1991. A bifunctional protein from *Pseudomonas denitrificans* carries cobinamide kinase and cobinamide phosphate guanylyltransferase activities. J Bacteriol 173:6052-6057.

58. Thomas MG, Thompson TB, Rayment I, Escalante-Semerena JC. 2000. Analysis of the adenosylcobinamide kinase/adenosylcobinamide-phosphate guanylyltransferase (CobU) enzyme of *Salmonella typhimurium* LT2. Identification of residue His-46 as the site of guanylylation. J Biol Chem 275:27576-27586.

59. Thompson TB, Thomas MG, Escalante-Semerena JC, Rayment I. 1999. Three-dimensional structure of adenosylcobinamide kinase/adenosylcobinamide phosphate guanylyltransferase (CobU) complexed with GMP: evidence for a substrate-induced transferase active site. Biochemistry 38:12995-3005.

60. Thompson TB, Thomas MG, Escalante-Semerena JC, Rayment I. 1998. Three-dimensional structure of adenosylcobinamide kinase/adenosylcobinamide phosphate guanylyltransferase from Salmonella typhimurium determined to 2.3 A resolution. Biochemistry 37:7686-95.

61. Trzebiatowski JR, Escalante-Semerena JC. 1997. Purification and characterization of CobT, the nicotinate-mononucleotide:5,6-dimethylbenzimidazole phosphoribosyltransferase enzyme from *Salmonella typhimurium* LT2. J Biol Chem 272:17662-17667.

62. Trzebiatowski JR, O'Toole GA, Escalante-Semerena JC. 1994. The *cobT* gene of *Salmonella typhimurium* encodes the NaMN: 5,6-dimethylbenzimidazole phosphoribosyltransferase responsible for the synthesis of N1-(5-phospho-alpha-D-ribosyl)-5,6-dimethylbenzimidazole, an intermediate in the synthesis of the nucleotide loop of cobalamin. J Bacteriol 176:3568-3575.

63. Cheong CG, Escalante-Semerena JC, Rayment I. 1999. The three-dimensional structures of nicotinate mononucleotide:5,6- dimethylbenzimidazole phosphoribosyltransferase (CobT) from *Salmonella typhimurium* complexed with 5,6-dimethybenzimidazole and its reaction products determined to 1.9Å resolution. Biochemistry 38:16125-16135.

64. Cheong CG, Escalante-Semerena JC, Rayment I. 2001. Structural investigation of the biosynthesis of alternative lower ligands for cobamides by nicotinate mononucleotide: 5,6-dimethylbenzimidazole phosphoribosyltransferase from *Salmonella enterica*. J Biol Chem 276:37612-37620.

65. O'Toole GA, Rondon MR, Escalante-Semerena JC. 1993. Analysis of mutants of defective in the synthesis of the nucleotide loop of cobalamin. J Bacteriol 175:3317-3326.

66. Maggio-Hall LA, Claas KR, Escalante-Semerena JC. 2004. The last step in coenzyme B(12) synthesis is localized to the cell membrane in bacteria and archaea. Microbiology 150:1385-1395.

67. Zayas CL, Claas K, Escalante-Semerena JC. 2007. The CbiB protein of *Salmonella enterica* is an integral membrane protein involved in the last step of the de novo corrin ring biosynthetic pathway. J Bacteriol 189:7697-7708.

68. Jeter VL, Escalante-Semerena JC. 2021. Insights into the relationship between cobamide synthase and the cell membrane. mBio 12.

69. Zayas CL, Escalante-Semerena JC. 2007. Reassessment of the late steps of coenzyme B_{12} synthesis in *Salmonella enterica*: Evidence that dephosphorylation of adenosylcobalamin-5'-phosphate by the CobC phosphatase is the last step of the pathway. J Bacteriol 189:2210-2218.

70. O'Toole GA, Trzebiatowski JR, Escalante-Semerena JC. 1994. The *cobC* gene of *Salmonella typhimurium* codes for a novel phosphatase involved in the assembly of the nucleotide loop of cobalamin. J Biol Chem 269:26503-26511.

71. Taga ME, Larsen NA, Howard-Jones AR, Walsh CT, Walker GC. 2007. BluB cannibalizes flavin to form the lower ligand of vitamin B12. Nature 446:449-453.

72. Gray MJ, Escalante-Semerena JC. 2007. Single-enzyme conversion of $FMNH_2$ to 5,6-dimethylbenzimidazole, the lower ligand of B_{12}. Proc Natl Acad Sci U S A 104:2921-2926.

73. Keck B, Munder M, Renz P. 1998. Biosynthesis of cobalamin in *Salmonella typhimurium*: transformation of riboflavin into the 5,6-dimethylbenzimidazole moiety. Arch Microbiol 171:66-68.

74. Campbell GR, Taga ME, Mistry K, Lloret J, Anderson PJ, Roth JR, Walker GC. 2006. *Sinorhizobium meliloti bluB* is necessary for production of 5,6-dimethylbenzimidazole, the lower ligand of B12. Proc Natl Acad Sci U S A 103:4634-4369.

75. Pollich M, Klug G. 1995. Identification and sequence analysis of genes involved in late steps of cobalamin (vitamin B12) synthesis in *Rhodobacter capsulatus.* J Bacteriol 177:4481-4487.

76. Collins HF, Biedendieck R, Leech HK, Gray M, Escalante-Semerena JC, McLean KJ, Munro AW, Rigby SE, Warren MJ, Lawrence AD. 2013. *Bacillus megaterium* has both a functional BluB protein required for DMB synthesis and a related flavoprotein that forms a stable radical species. PLOS ONE 8:e55708.

77. Maggio-Hall LA, Escalante-Semerena JC. 2003. Alpha-5,6-Dimethylbenzimidazole adenine dinucleotide (alpha-DAD), a putative new intermediate of coenzyme B12 biosynthesis in *Salmonella typhimurium*. Microbiology 149:983-990.

78. Gray MJ, Escalante-Semerena JC. 2010. A new pathway for the synthesis of alpha-ribazole-phosphate in *Listeria innocua*. Mol Microbiol 77:1429-1438.

79. Mattes TA, Escalante-Semerena JC. 2017. *Salmonella enterica* synthesizes 5,6-dimethylbenzimidazolyl-(DMB)-alpha-riboside. Why some Firmicutes do not require the canonical DMB activation system to synthesize adenosylcobalamin. Mol Microbiol 103:269-281.

80. Mattes TA, Malalasekara L, Escalante-Semerena JC. 2021. Functional Studies of alpha-Riboside Activation by the alpha-Ribazole Kinase (CblS) from Geobacillus kaustophilus. Biochemistry doi:10.1021/acs.biochem.1c00119.

81. Woodson JD, Peck RF, Krebs MP, Escalante-Semerena JC. 2003. The cobY gene of the archaeon *Halobacterium* sp. strain NRC-1 is required for de novo cobamide synthesis. J Bacteriol 185:311-316.

82. Otte MM, Escalante-Semerena JC. 2009. Biochemical characterization of the GTP:adenosylcobinamide-phosphate guanylyltransferase (CobY) enzyme of the hyperthermophilic archaeon *Methanocaldococcus jannaschii*. Biochemistry 48:5882-5889.

83. Newmister SA, Otte MM, Escalante-Semerena JC, Rayment I. 2011. Structure and mutational analysis of the archaeal GTP:AdoCbi-P guanylyltransferase (CobY) from *Methanocaldococcus jannaschii*: Insights into GTP binding and dimerization. Biochemistry 50:5301-5313.

84. Singarapu KK, Otte MM, Tonelli M, Westler WM, Escalante-Semerena JC, Markley JL. 2015. Solution structural studies of GTP:Adenosylcobinamide-phosphate guanylyltransferase (CobY) from *Methanocaldococcus jannaschii*. PLoS One 10:e0141297.

85. Brushaber KR, O'Toole GA, Escalante-Semerena JC. 1998. CobD, a novel enzyme with L-threonine-*O*-3-phosphate decarboxylase activity, is responsible for the synthesis of (*R*)-1-amino-2-propanol *O*-2-phosphate, a proposed new intermediate in cobalamin biosynthesis in *Salmonella typhimurium* LT2. J Biol Chem 273:2684-2691.

86. Tavares NK, Zayas CL, Escalante-Semerena JC. 2018. The *Methanosarcina mazei* MM2060 gene encodes a bifunctional kinase/decarboxylase enzyme involved in cobamide biosynthesis. Biochemistry 57:4478-4495.

87. Woodson JD, Escalante-Semerena JC. 2004. CbiZ, an amidohydrolase enzyme required for salvaging the coenzyme B_{12} precursor cobinamide in archaea. Proc Natl Acad Sci USA 101:3591-3596.

88. Woodson JD, Zayas CL, Escalante-Semerena JC. 2003. A new pathway for salvaging the coenzyme B_{12} precursor cobinamide in archaea requires cobinamide-phosphate synthase (CbiB) enzyme activity. J Bacteriol 185:7193-7201.

89. Zayas CL, Woodson JD, Escalante-Semerena JC. 2006. The *cobZ* gene of *Methanosarcina mazei* Gö1 encodes the nonorthologous replacement of the α-ribazole-5'-phosphate phosphatase (CobC) enzyme of *Salmonella enterica*. J Bacteriol 188:2740-2743.

90. Woodson JD, Escalante-Semerena JC. 2006. The *cbiS* gene of the archaeon *Methanopyrus kandleri* AV19 encodes a bifunctional enzyme with adenosylcobinamide amidohydrolase and alpha-ribazole-phosphate phosphatase activities. J Bacteriol 188:4227-4235.

91. Gray MJ, Tavares NK, Escalante-Semerena JC. 2008. The genome of *Rhodobacter sphaeroides* strain 2.4.1 encodes functional cobinamide salvaging systems of archaeal and bacterial origins. Mol Microbiol 70:824-836.

92. Mackenzie C, Eraso JM, Choudhary M, Roh JH, Zeng X, Bruscella P, Puskas A, Kaplan S. 2007. Postgenomic adventures with *Rhodobacter sphaeroides*. Annu Rev Microbiol 61:283-307.

93. Gray MJ, Escalante-Semerena JC. 2009. In vivo analysis of cobinamide salvaging in *Rhodobacter sphaeroides* strain 2.4.1. J Bacteriol 191:3842-3851.

94. Cauthen SE, Pattison JR, Lascelles J. 1967. Vitamin B(12) in photosynthetic bacteria and methionine synthesis by *Rhodopseudomonas spheroides*. Biochem J 102:774-781.

95. Gray MJ, Escalante-Semerena JC. 2009. The cobinamide amidohydrolase (cobyric acid-forming) CbiZ enzyme: a critical activity of the cobamide remodelling system of *Rhodobacter sphaeroides*. Mol Microbiol 74:1198-1210.

96. Magnuson JK, Romine MF, Burris DR, Kingsley MT. 2000. Trichloroethene reductive dehalogenase from Dehalococcoides ethenogenes: sequence of tceA and substrate range characterization. Appl Environ Microbiol 66:5141-7.

97. Löffler FE, Edwards EA. 2006. Harnessing microbial activities for environmental cleanup. Curr Op Biotech 17:274-284.

98. Yi S, Seth EC, Men YJ, Stabler SP, Allen RH, Alvarez-Cohen L, Taga ME. 2012. Versatility in corrinoid salvaging and remodeling pathways supports corrinoid-dependent metabolism in *Dehalococcoides mccartyi*. Appl Environ Microbiol 78:7745-7752.

99. Yan J, Bi M, Bourdon AK, Farmer AT, Wang PH, Molenda O, Quaile AT, Jiang N, Yang Y, Yin Y, Simsir B, Campagna SR, Edwards EA, Löffler FE. 2018. Purinyl-

cobamide is a native prosthetic group of reductive dehalogenases. Nat Chem Biol 14:8-14.

100. Derrien M, Belzer C, de Vos WM. 2017. *Akkermansia muciniphila* and its role in regulating host functions. Microb Pathog 106:171-181.

101. Derrien M, Van Baarlen P, Hooiveld G, Norin E, Muller M, de Vos WM. 2011. Modulation of mucosal immune response, tolerance, and proliferation in mice colonized by the mucin-degrader *Akkermansia muciniphila*. Front Microbiol 2:166.

102. Mok KC, Sokolovskaya OM, Nicolas AM, Hallberg ZF, Deutschbauer A, Carlson HK, Taga ME. 2020. Identification of a novel cobamide remodeling enzyme in the beneficial human gut bacterium *Akkermansia muciniphila*. mBio 11.

103. Ma AT, Tyrell B, Beld J. 2020. Specificity of cobamide remodeling, uptake and utilization in *Vibrio cholerae*. Mol Microbiol 113:89-102.

104. Ma AT, Beld J. 2021. Direct Cobamide Remodeling via Additional Function of Cobamide Biosynthesis Protein CobS from Vibrio cholerae. J Bacteriol 203:e0017221.

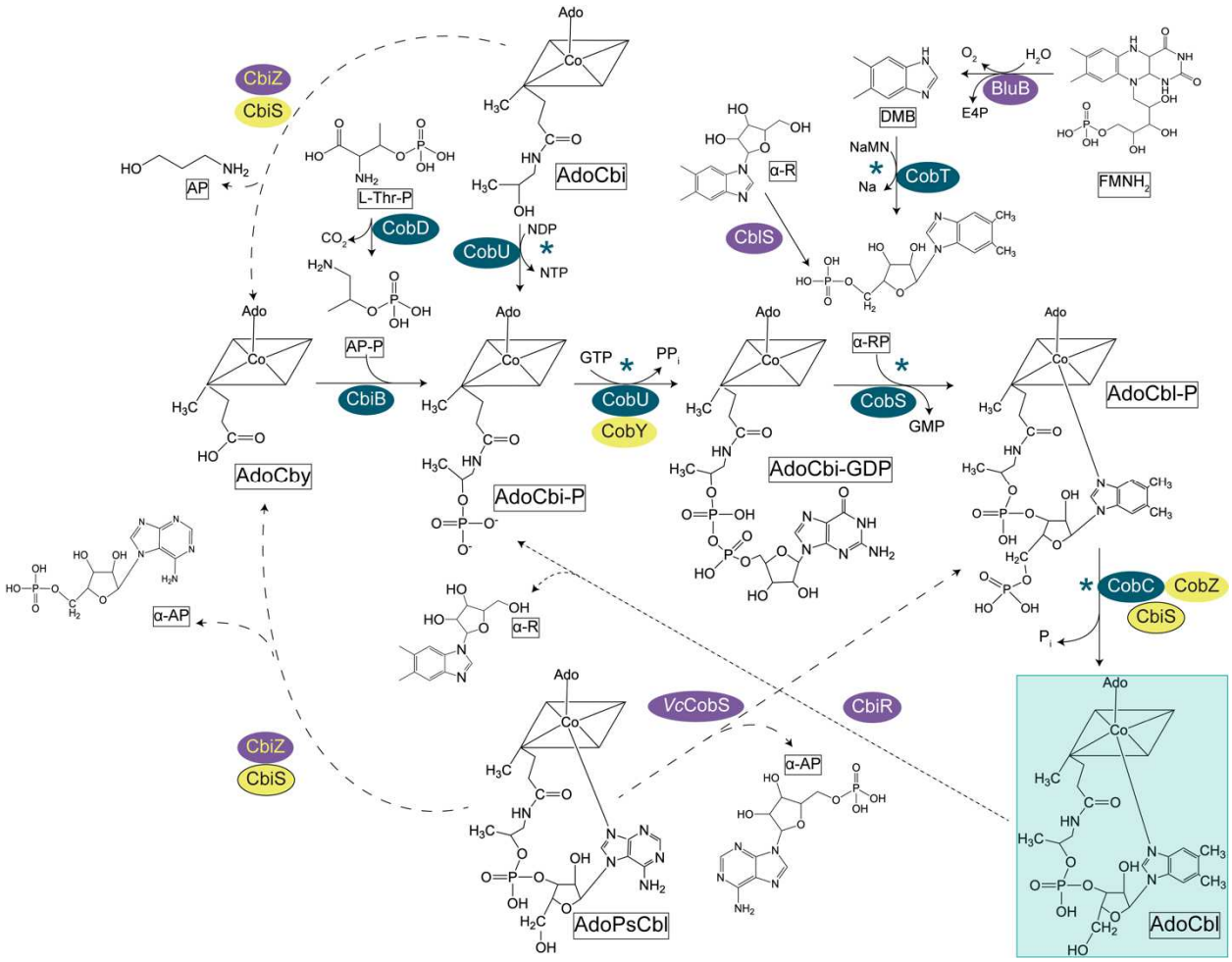

Figure 3.1. Salvaging and remodeling pathways in prokaryotes. The structures of pathway intermediates are shown with the corrin ring simplified to a rhombus. *S.* Typhimurium enzymes are shown in white text, dark blue circles. Other bacterial homologues are shown in white text, purple circles. Steps of the NLA pathway are marked with an asterisk. Archael homologues are shown in black text, yellow circles. CbiZ is found in both archaea and bacteria, so is shown in a purple circle with yellow text. Remodeling steps are shown in a dashed line. Coenzyme B_{12} is marked in a blue square.

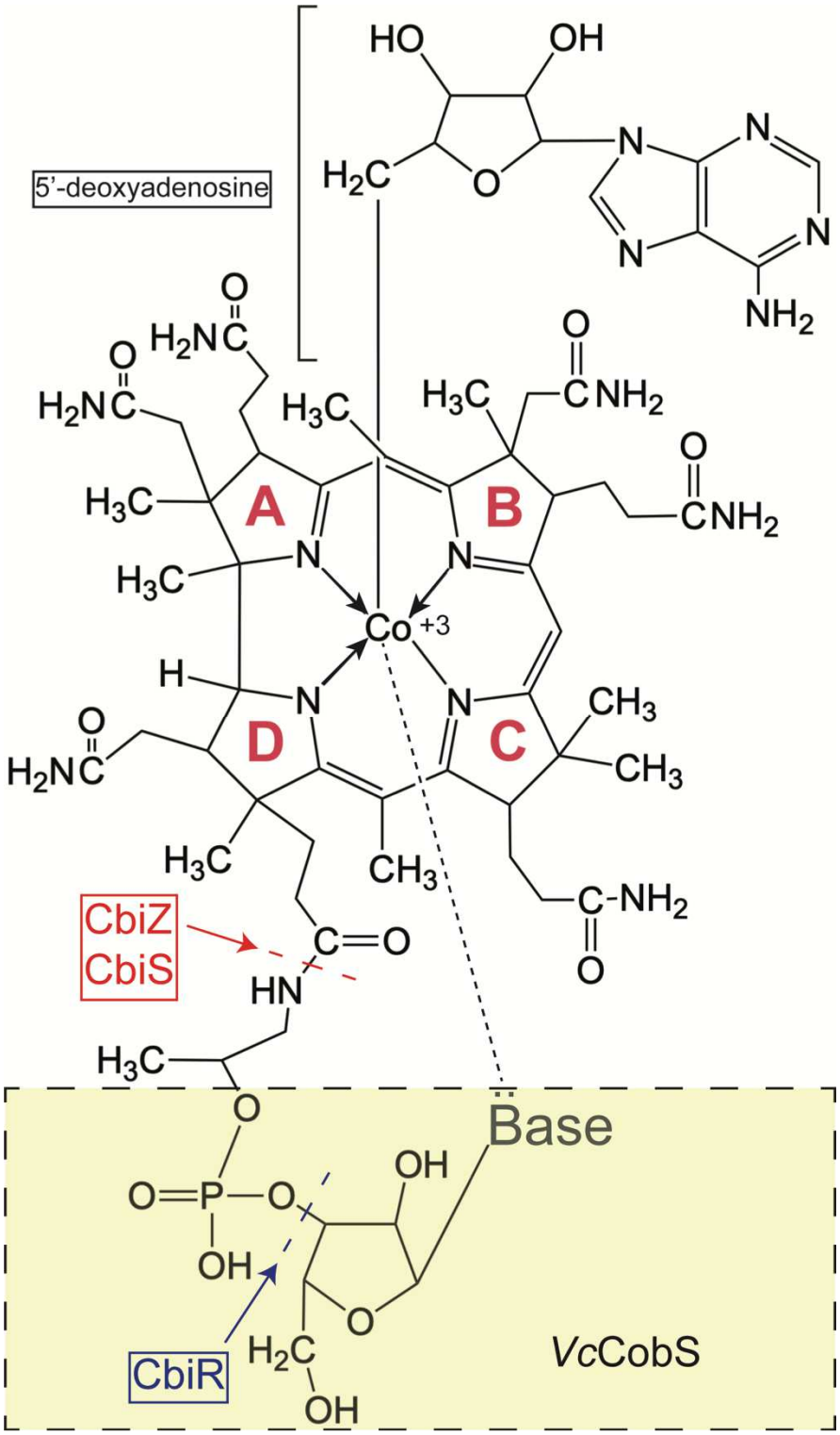

Figure 3.2. AdoCba structure cleavage sites of remodeling enzymes. "Base" denotes the location of interchangeable nucleobases. *Vc*CobS has been proposed to remove the entire nucleotide loop containing adenine as a base (shown in yellow box) and replace with α-RP containing DMB. Cleavage sits for other remodeling enzymes are shown.

CHAPTER 4

A METHOD FOR THE PRODUCTION, PURIFICATION AND LIPOSOME RECONSTITUTION OF COBAMIDE SYNTHASE[3]

[3]Villa E.A. and Escalante-Semerena, J.C. 2022. *Methods in Enzymology.*

Reprinted here with permission from the publisher.

4.1 ABSTRACT

Cobamides are essential for the performance of a variety of reactions such methyl transfers, carbon skeleton rearrangements, and eliminations in both prokaryotes and eukaryotes. However, cobamide biosynthesis is limited to a subset of bacteria and archaea. The biosynthesis pathway culminates with the activation and attachment of a lower ligand to the corrin ring; this branch of the pathway is known as nucleotide loop assembly (NLA) pathway. The cobamide synthase (CobS) enzyme is the penultimate step in NLA pathway, and catalyzes the attachment of an α-ribotide to the activated corrin ring. While other NLA enzymes have been well-studied, studies of CobS have proven difficult to date. CobS is an integral membrane protein, and limitations have been largely due to difficulties in protein purification. Here we provide a method to purify CobS, reconstitute protein in proteoliposomes, and assay for its activity.

4.2 KEYWORDS

Coenzyme B_{12}, Cobamide synthase, CobS, nucleotide loop assembly, cobamide, proteoliposome, membrane-associated metabolism

4.3 INTRODUCTION- B_{12} AND THE NUCLEOTIDE LOOP ASSEMBLY (NLA) PATHWAY.

Adenosylcobamides (AdoCbas) are complex biomolecules whose *de novo* synthesis requires approximately 30 enzymes (1). AdoCbas are made up of a central Co ion with four equatorial bonds to the pyrrolic nitrogens of cyclic tetrapyrroles, and two axial ligands. The upper ligand is a 5'-deoxyadenosyl group derived from ATP, and the lower

ligand is usually to a nitrogenous nucleobase (*i.e.,* purines, or derivatives of benzimidazole) and in a few instances phenol or *p-cresol* (2-4). One commonly-found AdoCba is coenzyme B_{12} (CoB_{12}), a.k.a. adenosylcobalamin (AdoCbl), in which 5,6-dimethylbenzimidazole (DMB) is integrated as the lower ligand. *De novo* CoB_{12} biosynthesis is restricted to a subset of prokaryotes. In biosynthesis, the cobalt-containing cyclic tetrapyrrole, or corrin ring, is formed first and subsequently adenosylated (see Chapter 4). The late steps of CoB_{12} biosynthesis, also known as the nucleotide loop assembly (NLA) pathway, involve the activation and attachment of the lower ligand (Figure 1). In *Salmonella enterica*, the NLA pathway is comprised of the gene products of the *cbiB* gene, the *cobUST* operon and the *cobC* gene. Briefly the NLA pathway reactions are the following:

1) ATP + adenosylcobyric acid + (*R*)-1-aminopropan-2-yl phosphate = ADP + phosphate + adenosylcobinamide phosphate (AdoCbi-P)

   The reaction is catalyzed by the AdoCbi-P synthase (EC 6.3.1.10), a.k.a. CbiB.

2) GTP + adenosylcobinamide phosphate = diphosphate + adenosylcobinamide-GDP (AdoCbi-GDP)

   The reaction is catalyzed by the AdoCbi kinase/AdoCbi-P guanylyltransferase (EC 2.7.7.62), a.k.a. CobU.

3) β-nicotinate D-ribonucleotide + 5,6-dimethylbenzimidazole = nicotinate + α-ribazole 5'-phosphate (α-RP).

   The reaction is catalyzed by the nicotinate-nucleotide—dimethylbenzimidazole phosphoribosyltransferase (EC 2.4.2.21), a.k.a. CobT.

4) AdoCbi-GDP + α-RP = GMP + adenosylcobalamin 5'-phosphate (AdoCbl-P)

The reaction is catalyzed by the AdoCbl-P synthase (EC 2.7.8.26), a.k.a. CobS.

5) AdoCbl-P + H_2O = AdoCbl + phosphate

The reaction is catalyzed by the AdoCbl-P phosphatase (EC 3.1.3.73), a.k.a. CobC

The CobU and CobT enzymes have been well-studied (5-7), however, extensive studies of CobS are lacking. In the genomes of all B_{12} producers sequenced to date, CobS is an integral membrane protein whose overproduction compromises cell survival (8, 9) and thus purification efforts have proven difficult. Here we describe a useful scheme for purification of CobS using detergent to maintain solubility throughout the purification process. Subsequent reconstitution of CobS into proteoliposomes for further study have revealed differences in enzyme efficiency when compared to protein solubilized in detergent. This method is of use to improve our understanding of the CobS enzyme and could prove useful in the purification and study of other membrane proteins.

4.4 CLONING, OVEREXPRESSION AND PURIFICATION OF COBAMIDE SYNTHASE (COBS)

The CobS enzyme from *Salmonella enterica* used in the following method was purified as described elsewhere (10). This method could be implemented to study CobS from other organisms as well. These vectors are recommended and are available upon request. Buffers, strains, and plasmids used in this method are detailed in Table 4.1.

4.4.1 Cloning and overexpression of *cobS*.

4.4.1.1 cobS cloning. Plasmid pCOBS5 encoding *S. enterica cobS* was constructed by cloning *S. enterica cobS* into pET15b using NcoI and HindIII restriction

sites. This resulted in the encoded CobS fused to an N-terminal hexahistidine (H_6) tag (9).

4.4.1.2 cobS overexpression.

Day 1. Electroporate plasmid pCOBS5 encoding *cobS* into your preferred strain. We have used *E. coli* C41 (λDE3) with success. Plate to selective medium and incubate at 37°C overnight.

Day 2. Inoculate a 10 mL overnight culture (~16 h), grow overnight at 37°C with shaking.

Day 3. Inoculate a 2-L culture of Terrific Broth (tryptone, (24 g/L), yeast extract (24 g/L), glycerol (4 mL/L, or 54 mM), KH_2PO_4 (17 mM), $MgSO_4$ (2 mM) supplemented with appropriate antibiotic. Use of a baffled flask is recommended to improve aeration. Grow to mid-log (approximate optical density (OD) at 600 nm = 0.6), then induce *cobS* expression by adding the inducer appropriate for your vector of choice. Allow induced culture to incubate for 3 h at 37°C with shaking. Remove a sample (500 μL) of the culture to verify overexpression. Analyze the 500 μL sample with SDS-PAGE (11) to verify that CobS has been overproduced, indicated by a band at ~26 kDa. If CobS overproduction is successful, harvest the remainder of the culture by centrifugation at 4ºC. Discard supernatant and store cell pellet at -80°C.

4.5 COBS PURIFICATION.

4.5.1 Ni-NTA affinity purification. The purification scheme is illustrated in Figure 4.1.

4.5.1.1 CobS purification was described elsewhere (10). Thaw cell pellets and resuspend in 30 mL of Buffer A (Tris•HCl (0.1 M), pH 7.9) and lyse the cells using a cell disruptor or French press. We have used a cell disruptor set to 1.72 x 10^5 kPa. Following lysis, add 0.5 mL of Protease Inhibitor Cocktail (Sigma), then centrifuge lysate at 5000 x *g* for 15 min at 4°C.

4.5.1.2 Remove supernatant into a new tube and centrifuge at 75,000 x *g* for 90 min to separate cell membranes. Using a glass homogenizer, resuspend membranes in 10 mL of Buffer A. Once resuspended, add 3-(3-cholamidopropyl) dimethylammonio)-1-propanesulfonate (CHAPS) to a final concentration of 20 mM. Incubate on ice for 1 h, then centrifuge at 75,000 x *g* for 30 min at 4°C. Resuspend insoluble fraction containing CobS in Buffer B [Tris•HCl (0.1 M) pH 7.9, NaCl (0.5 M), imidazole (20 mM)] using a glass homogenizer, then slowly add 1,2-dihexanoyl-*sn*-glycero-3-phosphocholine (DHPC) to a final concentration of 15 mM. Incubate on ice for 1 h, then centrifuge at 75,000 x *g* for 30 min at 4°C.

Tip: During this time, equilibrate a 2-mL bed volume of affinity purification resin by first washing with 10 volumes of water and then 10 volumes of Buffer B. We have used HisPur Ni-NTA resin (Fisher Scientific) with success.

4.5.1.3 Mix supernatant containing solubilized H_6-CobS with resin and incubate at 4°C using a tube rotator for at least 2 h, then pour slurry into a column. Allow the cell-free extract (CFE) to flow through, then wash with five column volumes of Buffer C [Tris•HCl (0.1 M), pH 7.9, NaCl (0.5 M), imidazole (20

mM), DHPC (15 mM)] followed by five column volumes of Buffer D [Tris•HCl (0.1 M), pH 7.9, NaCl (0.5 M), imidazole (60 mM), DHPC (15 mM)]. Elute protein with five column volumes of Buffer E [Tris•HCl (0.1M), pH 7.9, NaCl (0.5 M), imidazole (0.5 M), DHPC (15 mM)], and collect flowthrough of each column volume in a separate glass tube.

4.5.2 Identify fractions containing CobS by loading each fraction and resolving proteins on a 12% SDS-PAGE gel.

4.5.3 Remove imidazole by adding fractions containing CobS to a desalting column such as Zeba™ Spin Desalting Column (Fisher Scientific). Add glycerol to a final concentration of 10% (v/v), and flash-freeze in liquid N_2. Store frozen protein at -80°C.

4.6 RECONSTITUTION OF COBS INTO LIPOSOMES

4.6.1 Liposome formation

4.6.1.1 Combine lipids (Avanti Polar Lipids) in a small glass tube (recommended 10 x 75 mm (Fisher)) and dry under a stream of nitrogen gas. We have used the following composition with success: 1-palmitoyl-2-oleoyl-glycero-3-phosphocholine (POPC, 80% mol/mol), 1-palmitoyl-2-oleoyl-*sn*-glycero3-phospho-L-serine (POPS, 10% mol/mol), 1-palmitoyl-2-oleoyl-*sn*-glycero-3 phosphoethanolamine (POPE, 9.5% mol/mol), Lissamine™ Rhodamine B 1,2-dihexadecanoyl-*sn*-glycero-phosphoethanolamine (Rh-DHPE, 0.5% mol/mol). A total of 1 μmol lipid at this point will yield a final concentration of 2 mM after drying and reconstituting in buffer.

Tip: Rotate tube under nitrogen stream to ensure that lipids dry in an even layer and avoid “clumping.” Once lipids are dry, cover tube with Parafilm immediately to prevent introduction of moisture.

4.6.1.2 Dry tubes further in a vacuum centrifuge at 30°C uncovered for a minimum of 1 h or up to overnight. Dried lipids will appear as a film on the bottom of the glass tube. Add 500 μL of Buffer F [4-(2-hydroxyethyl)-1-piperazineethanesulfonic acid buffer (HEPES-NaOH, pH 7.4), NaCl (500 mM), glycerol [10% (v/v)], CHAPS (40 mM)] and mix by vortex until dried lipids are reconstituted. This may take several minutes per tube. Transfer suspended lipids to 1.7 mL Eppendorf tubes and keep on ice.

4.6.1.3 Add protein to reconstituted lipids at the desired concentration. A ratio of 2 μM protein: 2 mM lipids has been used with success. Gently mix protein and lipids by pipetting, and incubate tube on a tube rotator at 4°C for 1 h, then transfer lipids to desired dialysis membrane. We have used 20 MWCO Slide-A-Lyzer dialysis cassette with success. Dialyze thrice in 1 L of Buffer F at 4°C for a minimum of 3 h each or up to overnight to allow proteoliposomes to form. If detergent removal is necessary, dialysis may be extended over several days.

4.7 PROTEOLIPOSOME ISOLATION

4.7.1 Remove protein-lipid mixture from dialysis cassette into a 15 mL conical tube. Add an equal volume of Buffer G [Histodenz (80% w/v), HEPES-NaOH, pH 7.4 (20 mM), NaCl (150 mM), glycerol (10% (v/v)] and gently invert at least 20 times to

mix. Transfer mix to ultracentrifuge tube. Overlay lipid-protein mix with Buffer H [Histodenz (30% w/v), HEPES-NaOH, pH 7.4 (20 mM), NaCl (150 mM), glycerol (10% v/v)]. We recommend use of polyallomer tubes ultracentrifuge tubes (13 x 51 mm, Beckman Coulter) and a total volume of 4 mL. To the top of each tube, add 200 μL of Buffer I [HEPES-NaOH, pH 7.4 (20 mM), NaCl (150 mM), glycerol (10% v/v)].

4.7.2 Separate proteoliposomes by ultracentrifugation at 200,000 x *g* at 4°C for at least 3 h or up to overnight. Following ultracentrifugation, remove the top pink layer containing proteoliposomes into a separate tube. Quantify lipid concentration by measuring fluorescence of rhodamine at 540 nm (excitation)/586 nm (emission). Protein concentration can be calculated using 12% SDS-PAGE and Western blot using known concentrations of pure protein as standards. Store liposomes at 4°C and use within one week.

Tip: Commercially available anti-6X His antibodies (Sigma) can be used to detect tagged CobS protein in Western blot.

4.8 PROTEOLIPOSOME QUALITY CONTROLS

4.8.1 Population dispersal

Homogeneity of the proteoliposome population should be assessed by measuring particle size. A monodispersed population is ideal. Varying the ratio between protein and lipid used to form proteoliposomes can lead to changes in particle size, and should be optimized to determine the optimal ratio to yield the most homogeneous population. Dynamic light scattering (DLS) is a useful technique to

assess particle size and homogeneity in proteoliposome populations, and employs changes in light intensity as a measurement of aggregation.

4.8.2 Protein orientation

Proteins can insert into the lipid bilayer in two orientations, starting with the *N*-terminus on either the outside or inside of the proteoliposome structure [Figure 4.3; modified from a figure published elsewhere (10)]. To assess protein function in the proteoliposome, it is necessary to know the percentage of the population in which the active site is exposed and accessible to substrate. We have employed a proteolytic digest to assess protein orientation and allow accurate quantification of accessible protein. Protease selection should be tailored to the protein to be studied. For *S. enterica*, trypsin (Sigma-Aldrich), chymotrypsin (Sigma-Aldrich), and protease K (Fisher Scientific) were used. Reaction products can be analyzed by SDS-PAGE and subsequent Western blotting with antibodies against the protein of study.

4.9 ACTIVITY ASSAYS

The substrates of CobS are not commercially available and thus must be synthesized (5, 9).

4.9.1 Preparation of substrates

4.9.1.1 Synthesis of AdoCbi-GDP

AdoCbi-GDP was prepared as described elsewhere. Briefly, commercially-available $(CN)_2$Cbi was first incubated with CobA from *S. enterica*, the housekeeping adenosyltransferase, and ATP to yield AdoCbi. This was then incubated with *S. enterica* CobU and GTP to yield AdoCbi-GDP. Reaction conditions are further detailed elsewhere (5, 12). Cbi-GDP may be separated from Cbi by the following HPLC method, using mobile phase (MP) A [KH_2PO_4 (0.1 M), pH 6.5, KCN (10 mM)] and mobile phase B [KH_2PO_4 (0.1 M), pH 8, KCN (10 mM): acetonitrile in a 1:1 ratio. Equilibrate column to 98% MP A/ 2% MP B. Follow sample injection with a 5-minute linear gradient to 95% A / 5% B, then apply a 9-min linear gradient to 80% MP A / 20% MP B. Continue to develop the column for 12.5 min at 80% A / 20% B. Next, apply an 11.5-min linear gradient to 65% MP A / 35% MP B, and finally apply a 7-min linear gradient to 100% MP B.

4.9.1.2 Adenosylation of Cbi-GDP

Because the Co-C bond of adenosylcobamides is sensitive to light, it is unlikely that the population of Cbi-GDP isolated will be adenosylated following HPLC purification. The adenosylation reaction should be repeated by incubating with CobA and ATP prior to use. To calculate the adenosylation efficiency we refer the reader to Chapter 4.

4.9.1.3 Synthesis of α-ribazole-5'-phosphate (α-RP)

α-RP may be synthesized by incubating *S. enterica* CobT with DMB and NaMN and α-RP can be purified by HPLC (see Chapter 29) (13). α-RP may be separated from substrate using a Phenomenex Kinetix C18 column. We

recommend developing the column with the following mobile phases: MP A, ammonium acetate (20 mM); MP B acetonitrile (100%); MP C H_2O. Equilibrate column to 97% MP A / 3% MP B. After injecting sample, allow to develop for 5 min at 97% MP A/ 3% MP B. Follow with a 12-min linear gradient to 60% MP A / 40% MP B. Follow with a 5-min linear gradient to 80% MP B / 20% MP C and allow to develop at 80% MP B/ 20% MP C for 5 min.

4.9.2 Cobamide synthase activity assay

CobS activity can be assayed in multiple ways. We will describe a continuous manner using spectrophotometric measurements, and an endpoint assay using a bioassay strain for product detection. Recommended reaction conditions are as follows: Buffer J [2-[4-(2-hydroxyethyl)piperazin-1-yl]ethanesulfonic acid (HEPES) buffer (20 mM, pH 7.4)], NaCl (150 mM), glycerol (10% [v/v]), α-RP (200 μM), AdoCbi-GDP (500 μM), MgCl (2mM) and proteoliposome complex to a final concentration of 0.33 mM lipid.

Tip: Improved activity has been observed in reconstituted CobS (10). Pure solubilized protein can be assayed by the described method to compare changes in activity.

4.9.2.1 Cobamide synthase continuous assay

The activity of CobS can be tested by measuring the decrease in absorbance of the substrate AdoCbi-GDP at 459 nm in a 96-well quartz microtiter plate. Activity of CobS can be calculated using Beer-Lambert's equation $A = \varepsilon cL$ with the AdoCbi-GDP extinction coefficient of ε_{459} = 3,352 M^{-1} cm^{-1} (10).

4.9.2.2 Endpoint assays- Adenosylcobalamin-5'-phosphate (AdoCbl-P) synthesis

For an endpoint assay, the above reaction components should be incubated at 37°C for 1 h or desired time point. Stop reactions by adding KCN to a final concentration of 2.4 μM and incubating at 90°C for 10 min.

4.9.2.3 AdoCbl synthesis

If Cbl is the preferred product, incubate AdoCbl-P with commercially available alkaline phosphatase.

4.9.2.4 Bioassay

Formation of Cbl-P or Cbl can be assessed by providing reaction components to a *S. enterica metE* and *cobS*-deficient strain. Briefly, cells from an overnight culture should be washed with sterile PBS. An aliquot of 200 μL can be added to 4 mL of melted 0.7% (w/v) agar, mixed, and overlaid on no-carbon E (NCE) medium (14) supplemented with Wolfe's trace minerals (15) $MgSO_4$ (1 mM) and glycerol (22 mM). Once cooled, 1 μL of reaction product can be spotted on overlay. Incubate at 37°C overnight. The following day, assess growth to determine presence of Cbl or Cbl-P (16).

Tip: Reaction products can be fractionated using RP-HPLC and products can be verified using mass spectrometry (13).

4.10 REFERENCES

1. Costa FG, Greenhalgh ED, Brunold TC, Escalante-Semerena JC. 2020. Mutational and functional analyses of substrate binding and catalysis of the *Listeria monocytogenes* EutT ATP:Co(I)rrinoid adenosyltransferase. Biochemistry 59:1124-1136.
2. Chan CH, Escalante-Semerena JC. 2011. ArsAB, a novel enzyme from *Sporomusa ovata* activates phenolic bases for adenosylcobamide biosynthesis. Mol Microbiol 81:952-967.
3. Johnson MG, Escalante-Semerena JC. 1992. Identification of 5,6-dimethylbenzimidazole as the *Coα* ligand of the cobamide synthesized by *Salmonella typhimurium*. Nutritional characterization of mutants defective in biosynthesis of the imidazole ring. J Biol Chem 267:13302-13305.
4. Anderson PJ, Lango J, Carkeet C, Britten A, Kräutler B, Hammock BD, Roth JR. 2008. One pathway can incorporate either adenine or dimethylbenzimidazole as an alpha-axial ligand of B_{12} cofactors in *Salmonella enterica*. J Bacteriol 190:1160-1171.
5. O'Toole GA, Escalante-Semerena JC. 1995. Purification and characterization of the bifunctional CobU enzyme of *Salmonella typhimurium* LT2. Evidence for a CobU-GMP intermediate. J Biol Chem 270:23560-23569.
6. Trzebiatowski JR, Escalante-Semerena JC. 1997. Purification and characterization of CobT, the nicotinate-mononucleotide:5,6-dimethylbenzimidazole phosphoribosyltransferase enzyme from *Salmonella typhimurium* LT2. J Biol Chem 272:17662-17667.

7. O'Toole GA, Trzebiatowski JR, Escalante-Semerena JC. 1994. The *cobC* gene of *Salmonella typhimurium* codes for a novel phosphatase involved in the assembly of the nucleotide loop of cobalamin. J Biol Chem 269:26503-26511.
8. Maggio-Hall LA, Claas KR, Escalante-Semerena JC. 2004. The last step in coenzyme B(12) synthesis is localized to the cell membrane in bacteria and archaea. Microbiology 150:1385-1395.
9. Maggio-Hall LA, Escalante-Semerena JC. 1999. In vitro synthesis of the nucleotide loop of cobalamin by *Salmonella typhimurium* enzymes. Proc Natl Acad Sci U S A 96:11798-11803.
10. Jeter VL, Escalante-Semerena JC. 2021. Insights into the relationship between obamide synthase and the cell membrane. mBio 12.
11. Laemmli UK. 1970. Cleavage of Structural Proteins during Assembly of Head of Bacteriophage-T4. Nature 227:680-685.
12. Blanche F, Thibaut D, Couder M, Muller JC. 1990. Identification and quantitation of corrinoid precursors of cobalamin from Pseudomonas denitrificans by high-performance liquid chromatography. Anal Biochem 189:24-9.
13. Jeter VL, Mattes TA, Beattie NR, Escalante-Semerena JC. 2019. A new class of phosphoribosyltransferases involved in cobamide biosynthesis Is found in methanogenic archaea and cyanobacteria. Biochemistry 58:951-964.
14. Berkowitz D, Hushon JM, Whitfield HJ, Jr., Roth J, Ames BN. 1968. Procedure for identifying nonsense mutations. J Bacteriol 96:215-220.
15. Balch WE, Wolfe RS. 1976. New approach to the cultivation of methanogenic bacteria: 2-mercaptoethanesulfonic acid (HS-CoM)-dependent growth of

Methanobacterium ruminantium in a pressurized atmosphere. Appl Environ Microbiol 32:781-791.

16. Zayas CL, Escalante-Semerena JC. 2007. Reassessment of the late steps of coenzyme B_{12} synthesis in *Salmonella enterica*: Evidence that dephosphorylation of adenosylcobalamin-5'-phosphate by the CobC phosphatase is the last step of the pathway. J Bacteriol 189:2210-2218.
17. Jeter VL, Escalante-Semerena JC. 2021. Insights into the relationship between cobamide synthase and the cell membrane. mBio 12.

Table 4.1. Buffers, strains and plasmids needed for the described procedures		
Buffer Name	**Composition**	**Recommended for**
Buffer A	Tris•HCl (0.1 M, pH 7.9)	CobS purification- reconstitution
Buffer B	Tris•HCl (0.1 M) pH 7.9, NaCl (0.5 M), imidazole (20 mM)	CobS purification- bind buffer
Buffer C	Tris•HCl (0.1 M, pH 7.9), NaCl (0.5 M), imidazole (20 mM), DHPC (15 mM)	CobS purification- bind buffer
Buffer D	Tris•HCl (0.1 M, pH 7.9), NaCl (0.5 M), imidazole (60 mM), DHPC (15 mM)	CobS purification- wash buffer
Buffer E	[Tris•HCl (0.1M, pH 7.9), NaCl (0.5 M), imidazole (0.5 M), DHPC (15 mM)	CobS purification- elution buffer
Buffer F	4-(2-hydroxyethyl)-1-piperazineethanesulfonic acid buffer (HEPES-NaOH, pH 7.4), NaCl (500 mM), glycerol [10% (v/v)], 3-[(3-cholamidopropyl)dimethyl**a**mmonio]-1-propanesulfonate (CHAPS, 40 mM)	Lipid reconstitution, dialysis
Buffer G	Histodenz (80% w/v), HEPES-NaOH, (20 mM, pH 7.4), NaCl (150 mM), glycerol (10% (v/v)	Proteoliposome isolation-separation
Buffer H	Histodenz (30% w/v), HEPES-NaOH, (20 mM, pH 7.4), NaCl (150 mM), glycerol (10% v/v)	Proteoliposome isolation-separation
Buffer I	HEPES-NaOH, (20 mM, pH 7.4), NaCl (150 mM), glycerol (10% v/v)	Proteoliposome isolation-separation
Buffer J	HEPES buffer (20 mM, pH 7.4)	Cobamide synthase activity assay
Strain	**Genotype**	**Source**
JE6663 *E. coli* C41 (λDE3)	F *–ompT hsdSB (rB-mB-) gal dcm* (λDE3)	Avanti
JE8248	*metE205 ara-9 ΔcobS1313*	Laboratory collection
Plasmid	**Genotype**	**Source**
pCobS5	*S. enterica cobS*$^{+}$ cloned into pET15b. The plasmid encodes a H_6-CobS protein (*i.e.,* N-terminally tagged)	(9)

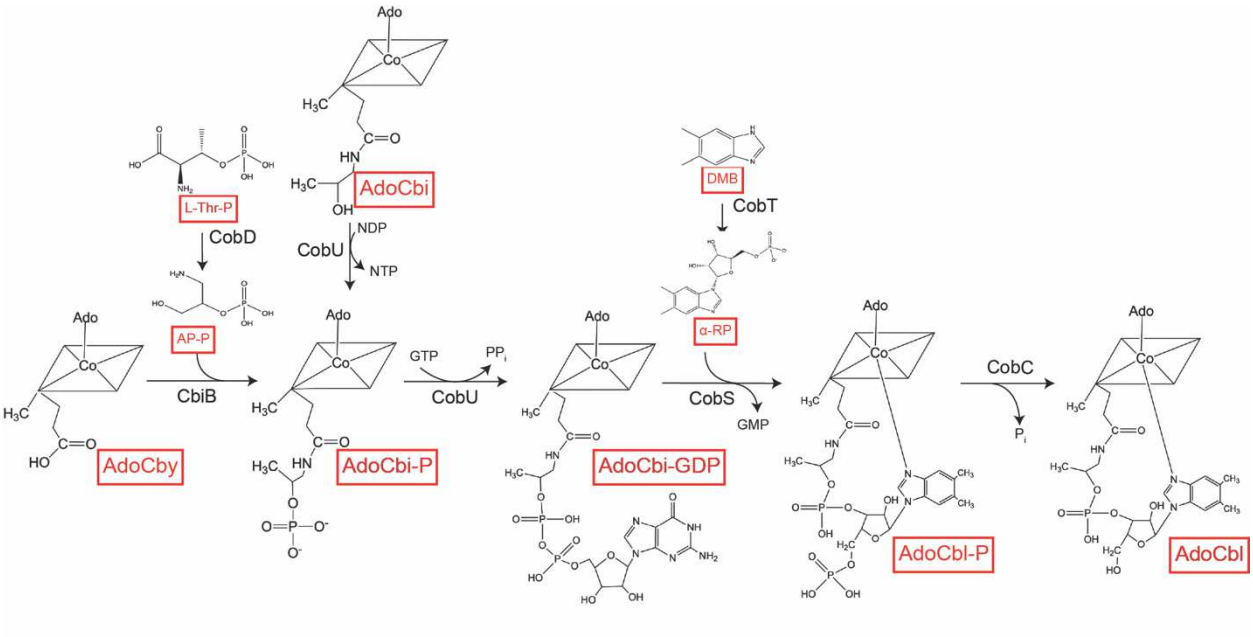

Figure 4.1 The NLA pathway in S. *enterica*. Abbreviations: AdoCby, adenosylcobyric acid; L-Thr-P, L-threonine-phosphate; AP-P, aminopropanol- phosphate; AdoCbi, adenosylcobinamide; AdoCbi-P, adenosylcobinamide-phosphate; AdoCbi-GDP, adenosylcobinamide-GDP; AdoCbl-P, adenosylcobalamin-5'-phosphate; AdoCbl, adenosylcobalamin.

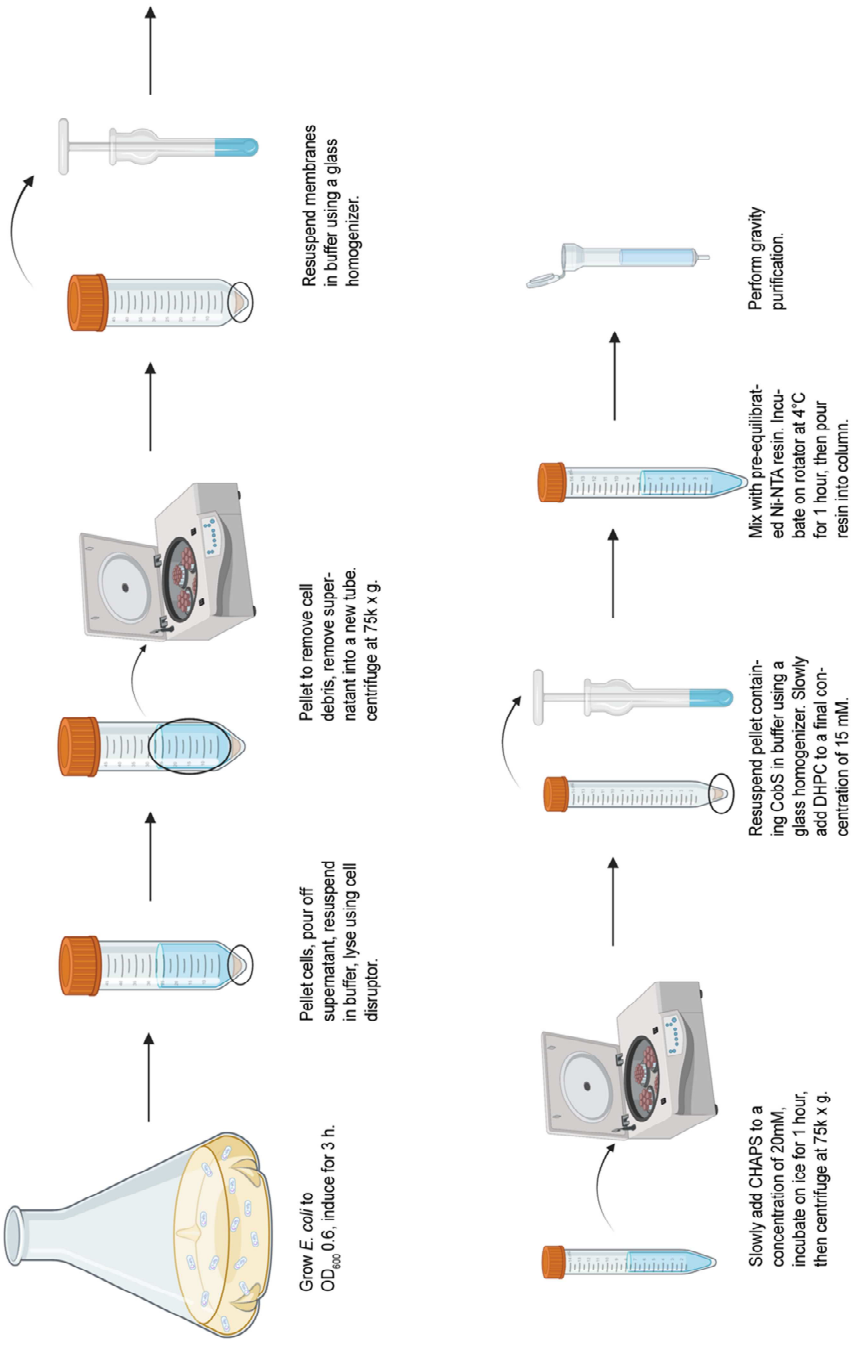

Figure 4.2 Overexpression and purification scheme for CobS. Created using BioRender.com.

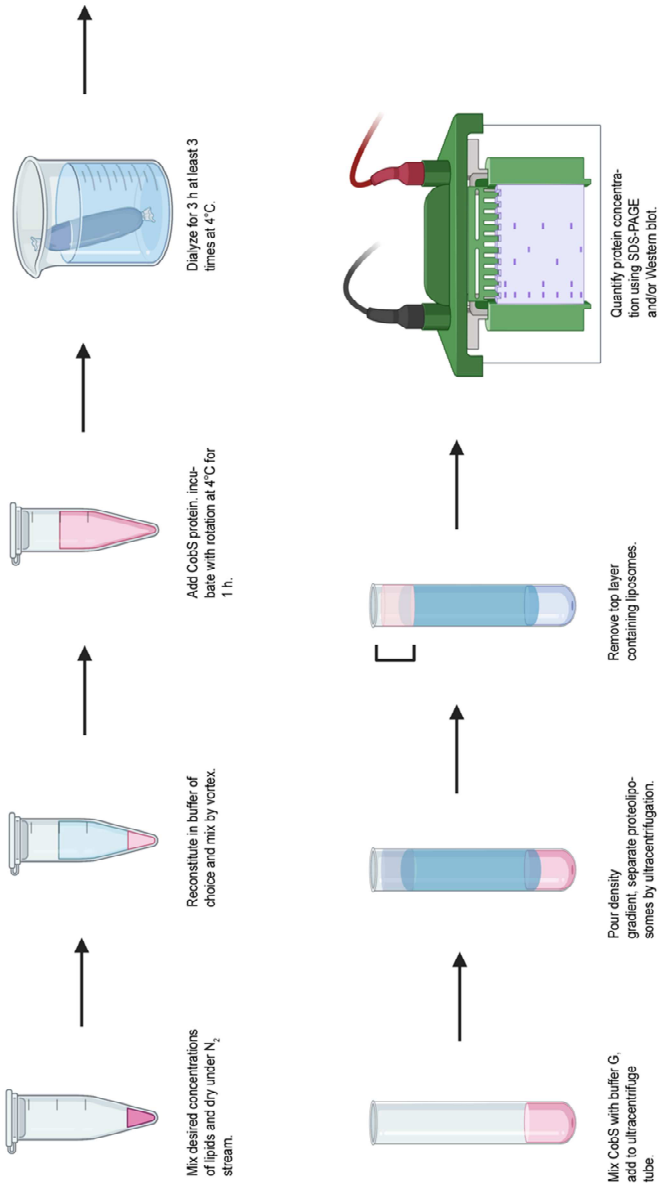

Figure 4.3 CobS-containing proteoliposome reconstitution and separation. Created using BioRender.com

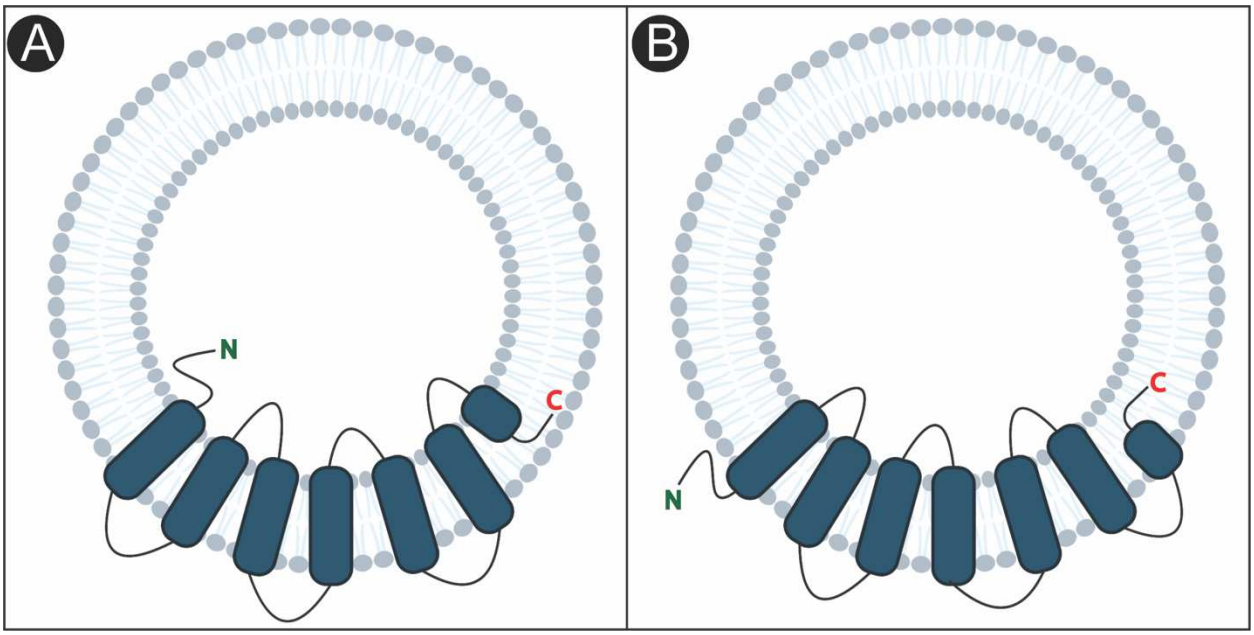

Figure 4.4. CobS can insert into the liposome in two orientations. The N-terminus is shown in green, the C-terminus is shown in red. (A) Insertion with the N-terminus in the lumen of the liposome. (B) Insertion with the N-terminus located on the outside of the lipid bilayer. Created using BioRender.com. Modified from (17).

CHAPTER 5

INSIGHTS INTO THE MEMBRANE-ASSOCIATED INTERACTION BETWEEN THE KINASE/ GUANYLYLTRANSFERASE COBU AND COBALAMIN-5'-PHOSPHATE SYNTHASE COBS[4]

[4]Villa E.A. and Escalante-Semerena, J.C. 2022. To be submitted to *mBio*.

5.1 ABSTRACT

The activation and attachment of the lower ligand of coenzyme B_{12} is known as nucleotide loop assembly, or NLA. The NLA pathway is an essential step in the formation of a biologically active coenzyme. This pathway involves both the activation of the corrin ring and the activation of the base to be added. Early work on the NLA pathway suggested that the enzymes involved form a multiprotein complex, but work to elucidate the interactions involved in complex formation has proven challenging. Two NLA enzymes, CbiB and CobS, are integral membrane proteins, and we hypothesize that together they serve as anchor points around which other NLA enzymes can localize to facilitate efficient exchange of intermediates. Here, we report observations of the interactions between the adenosylcobinamide kinase/ adenosylcobinamide-phosphate guanylyltransferase CobU and cobalamin-5'-phosphate synthase, CobS. We show that the CobU Glu^{80} and Cys^{81} facilitate an interaction with a CobS cytoplasmic loop. We use variant proteins to further assess these interactions with CobS incorporated into a proteoliposome in order to expand our knowledge of this intriguing multienzyme complex.

5.2 INTRODUCTION

Cobamides such as coenzyme B_{12} (or adenosylcobalamin, AdoCbl) are required by prokaryotic and eukaryotic enzymes to perform catabolic and anabolic processes including carbon skeleton rearrangements, methyl group transfers and elimination reactions (1). Although the coenzyme is critical to eukaryotes, *de novo* synthesis of cobamides is only performed by some prokaryotes. AdoCbl is a complex molecule composed of a cyclic tetrapyrrole with a central cobalt ion. In the biologically active

coenzyme, the cobalt atom is bound to a 5'-deoxyadenosine as an upper (Co*β*) ligand and coordinated to a nucleotide base as the lower (Co*α*) ligand. The nucleotide base is tethered to the ring by a structure known as the nucleotide loop.

Nucleotide loop assembly (NLA) and attachment occurs late in coenzyme B_{12} biosynthesis (2). Four enzymes comprise the NLA pathway, illustrated in Figure 1, which in *Salmonella* are: i) a bifunctional kinase/guanylyltransferase (CobU, EC 2.7.1.156, 2.7.7.62) that activates the ring into its GDP derivative through a CobU-GMP intermediate (3-8), ii) a phosphoribosyltransferase (CobT, EC 2.4.2.21) that activates the base into a unique α-ribotide (9-11)), iii) a synthase (CobS, EC 2.7.8.26) that joins the activated base and ring together to yield AdoCbl-P (2, 12), and iv) a phosphatase (CobC, EC 3.1.3.73) that dephosphorylates AdoCbl-P to yield the final product of the pathway, AdoCbl (12, 13). NLA enzymes are required for both salvaging of corrinoid precursors and *de novo* synthesis of complete cobamides, and as such are critical to AdoCbl-requiring prokaryotes.

Studies in *Pseudomonas denitrificans* have demonstrated that NLA enzymes may form a multiprotein complex (8). CobS and the final step of the *de novo* synthesis pathway, CbiB (EC 6.3.1.10), are both polytopic integral membrane proteins, and membrane association may serve as a point of localization for NLA enzymes (14-16). The membrane topology of CobS determined by PhoA and LacZ fusions is illustrated in Figure 5.2A (15). CobS is made up of six transmembrane domains, with three loops extending into the cytoplasm and periplasm (Figure 5.2 A, B). The C-terminus is predicted to be anchored within the membrane bilayer. We predict that one or more of the cytoplasmic

loops may serve as a site of interaction between CobS and other cytoplasmic NLA enzymes including CobU, CobT, and CobC (20).

Previous studies in our lab have identified a subset of mutants in *cobU* which not only prevent Cbl formation when provided with the CobU substrate cobinamide (Cbi), but also are unable to grow when provided with the CobU product Cbi-GDP. This is unexpected and intriguing, because it suggests that these changes cause disruptions to CobU that extend beyond catalytic activity. We hypothesize that these variant proteins have been altered at critical sites that disrupt interaction with other NLA proteins. As such, that these variant proteins are unable to interact with enzymes that are downstream in the NLA pathway, preventing access to the substrate for subsequent enzymes. We suggest that changes to some sites in CobU inhibits critical protein-protein interactions, and not simply catalytic activity, disrupting the NLA pathway and preventing the formation of the complete cobamide.

In this work, we investigate the characteristics of interactions between CobU and CobS using variant CobU proteins in order to elucidate essential sites of interactions between these enzymes. We assess effects caused by variant protein expression on cell growth. We also directly investigate binding and interactions of CobU and CobS enzymes using CobS cytoplasmic loops and full-length CobS reconstituted into liposomes (17, 18).

5.3 RESULTS AND DISCUSSION

Substitutions to Glu^{80}, Cys^{81} prevent growth on Cbi. Previous studies have reported that Glu^{80} and Cys^{81} form a non-prolyl *cis* bond (6, 19). This type of bond is uncommon, and typically only found in cases where a structural or catalytic advantage is imparted by

this conformation (6, 20). These amino acids also weakly interact with the 3'- hydroxyl group of the ribose ring of GMP when CobU has self-guanylylated (5). Despite the proximity to the GMP-binding site, the conformation of Glu^{80} and Cys^{81} are essentially identical in the apo- and GMP-complexed enzyme (6). These amino acids are conserved in these positions across CobU proteins from various organisms. The amino acid sequence from some organisms contains an aspartic acid in place of glutamic acid at position 80, indicating that some advantage is imparted by a negative charge at this position (Figure 5.3). Cys^{81} is conserved across all CobU enzymes analyzed.

Our data show that a negative charge is important at position 80, as a substitution to aspartate had no significant effect on growth (Figure 5.4A, Table 5.4, μ= 0.76)). Introducing a lysine or proline to position 80 completely prevented growth on Cbi, the CobU substrate. This is consistent with a previous observation in our lab in which a strain generated by hydroxylamine mutagenesis encoding substitution of a lysine at position 80 resulted in a nonfunctional *cobU* gene product (Escalante J.C., unpublished). This strain was unable to grow on both Cbi and Cbi-GDP. The failure of proline to compensate at position 80 suggests that the conformation alone imparted by a *cis* bond at this position may be insufficient to restore function. Substitution of Cys^{81} with an alanine or serine resulted in a growth defect on Cbi (μ= 0.13 and 0.04, respectively), though the effect was less severe than the lysine or proline substitutions for Glu^{80} (Figure 5.4, Table 5.5). Interestingly, the observed phenotype for Cys^{81} changes was more severe in the serine substitution, despite the similar conformation of serine and cysteine. From this evidence we can conclude that the substitution of the sulfhydryl group of serine with a hydroxyl group is more severe than removal of this group altogether. These results suggest that

the changes made to Glu^{80} and Cys^{81} are both detrimental to CobU function *in vivo*, but may affect the mechanism in unique ways.

Substitutions to Glu^{80}, Cys^{81} prevent growth on Cbi-GDP, the CobU product. Intriguingly, we observed that changes to Glu^{80} cause a growth defect not only on the CobU substrate, but also when these strains are provided with the CobU product, Cbi-GDP (Figure 5.4 B, Table 5.5). As observed on Cbi, a change from glutamic acid to aspartic acid at position 80 had no change on CobU function (μ= 0.58). Substituting a lysine or proline at this position again inhibited growth, even when provided with the CobU product, Cbi-GDP. This is unexpected, because although $CobU^{E80K}$ is catalytically inactive (Figure 5.4 C), providing Cbi-GDP eliminates the need for catalysis by CobU. Furthermore, a *cobU* strain carrying pBAD24 (the vector-only control) is also unable to grow on Cbi-GDP. We find this especially intriguing because providing Cbi-GDP bypasses the need for CobU catalysis; therefore, the function and presence of this protein altogether would be expected to be irrelevant.

We observed a decrease in the growth rate of strains in which Cys^{81} was changed to an alanine or serine (Figure 5.4, Table 5.5). Perhaps expectedly, the effect was less severe than what we observed on Cbi (Figure 5.4 A and B). While we observed a decrease in the growth rate (μ=0.32 and 0.2, respectively), these cultures did eventually reach density near that of those expressing CobU. Thus, while the CobU Cys^{81} variants seem to function less efficiently, the change is not substantial enough to prevent growth on Cbi-GDP.

These observations support our hypothesis that the role of CobU in nucleotide loop assembly extends beyond simply catalyzing the production of a pathway intermediate. We suggest that CobU-CobS interactions are a critical step of the NLA pathway. The removal of a negative charge at position 80 prevents CobU from critical interactions with CobS that is not ameliorated by providing Cbi-GDP, thereby circumventing the requirement for catalysis. This suggests that additional problems arise in these variant proteins; for example, perhaps CobU must properly position Cbi-GDP for the subsequent enzyme in the pathway, CobS, or CobU variants interact with CobS in a way that blocks other NLA enzyme interactions. This is supported by previous observations that a strain carrying a *cobU* deletion cannot grow on Cbi-GDP, suggesting that the presence of CobU is still necessary even when catalysis is not. We observed that Cys^{81} substitutions are more severe during growth in the presence of Cbi than Cbi-GDP, which may be the result of impaired catalytic function or altered interactions. The Cys^{81} variants demonstrate a reduced growth rate compared to CobU even on Cbi-GDP, which suggests that additional effects such as interactions with subsequent enzymes may be affected, but less severely than in the case of Glu^{80} changes.

CobU binds to the cytoplasmic loop 1 of CobS. Because of difficulties purifying the full-length protein, we tested initial interactions using synthesized peptides of the cytoplasmic loops (Figure 5.2). CobU was purified to >98% purity (Figure 5.5). We analyzed these interactions using SDS-PAGE and Western blotting, probing with primary antibodies against CobU or CobS. CobU is approximately 19.9 kDa (Figure 5.5, 5.6 lane 3, top). When CobU was incubated with the CL1 peptide, then crosslinked using

formaldehyde, an additional band around 23 kDa develops (Figure 5.6, lane 2,). This increase is consistent with the size of a CobU monomer bound to CL1 peptide (3.2 kDa, Figure 5.7, lane 2). The primary antibody generated against CobS also reacts with this 23 kDa molecular weight band (Figure 5.6, lane 2, bottom). This interaction is sensitive to reduction, and is not maintained if the reaction mixture is mixed with a loading buffer containing 2-mercaptoethanol (BME) prior to gel loading (Figure 5.6, lanes 5 and 6 compared to lanes 2 and 3). The appearance of a faint band of approximately 40 kDa in the anti-CobU Western (Figure 5.6) is likely the CobU dimer that is maintained under the denaturing conditions of the gel due to the presence of crosslinker. We further probed the strength of this interaction by testing if the CobU-CL1 complex can be maintained in the absence of a crosslinker. Strikingly, the 23 kDa band representing the CobU-CL1 peptide is still present under these conditions (Figure 5.7, lane 3 and lane 7). We conclude that this must be a substantially strong interaction in order to be maintained both through boiling and in denaturing conditions of the SDS-PAGE gel tested, even in the absence of a crosslinking agent.

The observed sensitivity of this complex to reduction suggests that this interaction may be due to disulfide bond formation. The amino acid sequence of CobU contains four cysteines (Figure 5.2). Only one cysteine is present in the CL1 peptide sequence, corresponding to Cys^{88} of the full-length CobS protein. We assessed this interaction using CobU Glu^{80} and Cys^{81} variants to test our hypothesis that the amino acids at this location modulate interactions with CobS. The strength of 23 kDa CobU-CL1 band was reduced when the peptide was incubated and crosslinked with the $CobU^{C81S}$ variant protein (Figure 5.8, lane 6). Interestingly, the strength of the interaction between the $CobU^{E80K}$ variant

was similar to wild-type CobU at this level of detection (Figure 5.7, lanes 2 and 4). Strikingly, the CobU^{C81S}-CL1 interaction is completely abolished when crosslinker was absent (Figure 5.9, lane 6). CobU^{E80K} remains capable of binding the peptide (Figure 5.9, lane 4). Furthermore, a darker band developed in the CobU^{E80K}-incubated sample compared to wild-type CobU (Figure 5.9, lanes 4 and 6). A quantitative assay is necessary to determine whether the introduction of a positive charge in this region in the CobU^{E80K} variant may result in stronger binding to the CL1 peptide than we observe in CobU. We conclude that under the conditions tested, Glu^{80} and Cys^{81} facilitate interactions between CobU and the CL1 region of CobS.

CobU binds to CobS in a proteoliposome. Previous work in our lab has determined that CobS can be reconstituted into a proteoliposome, and that other NLA enzymes interact with this proteoliposome to form a complex (17, 18, 20). Two types of liposomes were used to test the incorporation of CobS and subsequent binding of CobU. The procedure utilized to assess interactions requires two high-speed centrifugation steps to separate proteoliposomes through a density gradient (17, 18). In the first step, proteoliposomes containing CobS are isolated (first floatation). This is followed by an incubation with other NLA enzyme(s), here CobU, and an additional separation by high-speed centrifugation (second floatation). Previous experiments utilized a mix of POPC, POPE, POPS, and Rh-DHPE ("lipid mix") to form CobS proteoliposomes. We compared CobS integration into liposomes formed by this mixture to *E. coli* polar lipid extract and found that while CobS can integrate into liposomes formed from both lipid mixtures (Figure 5.10, lanes 2 and 4, bottom), a stronger signal is detected after the second

floatation for the in the lipid mix used previously compared to *E. coli* polar lipids (Figure 5.10, lanes 6 and 8, bottom). We also observed more CobU protein associated with the proteoliposome formed by the previously used lipid mix (Figure 5.10, lanes 6 and 8, top). No CobU associated with empty liposome formed in the absence of CobS (Figure 5.10, lanes 7 and 9.)

The previously used lipid mixture was used to test the interactions between $CobU^{E80K}$ and $CobU^{C81S}$ with CobS-proteoliposome (Figure 5.11). A markedly stronger band was observed for $CobU^{E80K}$ compared to CobU. Using densitometry, the strength of $CobU^{E80K}$ was determined to be ~6.5-fold stronger than the signal for CobU or $CobU^{C81S}$. A quantitative assay is being developed to allow us to determine the amount of CobU that is bound to the CobS liposome. Our preliminary evidence suggests that $CobU^{E80K}$ interacts more strongly with the CobS-proteoliposome complex, and this may be responsible for the detrimental growth phenotype that is observed in strains expressing this variant (Figure 5.4). Contrary to our observations using the CobS CL1 peptide, the signal for $CobU^{C81S}$ bound to the CobS-proteoliposome was approximately equal to the signal for CobU. This conflicts with our observation that $CobU^{C81S}$ could not interact with the CobS CL1 peptide. This could be due to the accessibility of the cysteine in the peptide, which may be improperly folded/unfolded; however, the participation of Cys^{81} in the *cis* bond formed with Glu^{80} may be important for CobS interactions.

5.4 CONCLUDING REMARKS

The evidence in this work supports the hypothesis that CobU interacts with CobS, and that Glu^{80} and Cys^{81} of CobU are involved in these interactions. We propose a model

in which CobU interacts with both integral membrane proteins in the nucleotide loop assembly pathway, CbiB and CobS (Figure 5.12). One possibility is that CobU interactions with each are transient, allowing CobU to accept substrate from CbiB, catalyze the formation of Cbi-GDP, and then pass off this product to CobS (Figure 5.12 A). In this model, CobU oscillates between the two integral membrane proteins. A second possibility is that CobU remains bound to both enzymes concurrently (Figure 5.12 B). We have previously observed that CobU-CobS interactions may be less strong than CobT-CobS (21). In both proposed models, CobU may remain sufficiently strongly anchored to the membrane through additional interactions with CbiB.

Our findings regarding $CobU^{E80K}$ and $CobU^{C81S}$ variants suggests that these two sites are important in facilitating CobU-CobS interactions. The observed interactions of $CobU^{C81S}$ with the CobS CL1 peptide may be an artefact of the *in vitro* system used, but is informative in that this observation suggests that CobU Cys^{81} and CobS Cys^{88} are in sufficiently close proximity to form this bond under these conditions. The absence of C^{88} or any cysteine in the length of CL1 sequence among CobS homologues suggests that Cys-Cys disulfide bond formation is not the physiologically relevant interaction needed between CobU and CobS (Figure 2B). Consistent with this observation, a *cobS* mutant producing $CobS^{C88A}$ has a growth phenotype indiscernible from the wild-type allele. An assay to accurately quantify the amount of enzyme bound to CobS-proteoliposomes is essential to verify the effects that we have observed, and development of this assay is currently underway.

Previous data has also suggested that CobS undergoes a conformational change after binding α-RP, and that this change may increase the affinity of CobS for Cbi-GDP

(17). The strong interaction observed between CobU^{E80K} and CobS may affect NLA in multiple ways. The first model assumes that Cbi-GDP binding by CobS is preceded by a CobT-CobS interaction in which CobT delivers α-RP. Binding of α-RP induces a conformational change in CobS, which provides access for Cbi-GDP to the corrin binding site. In this model, CobU^{E80K} may remain bound to CobS in a conformation that prevents CobT from interacting with CobS to deliver α-RP, preventing a critical conformational change necessary for Cbi-GDP binding and thereby locking CobS into a conformation in which it cannot accept the corrinoid substrate (Figure 5.12 C). Alternatively, CobS-CobT interactions may be unencumbered, but the stronger association of CobU^{E80K} may promote an orientation in which the CobS corrinoid binding site is no longer accessible (Figure 5.12 D). Finally, CobU may be necessary to properly position the corrinoid substrate in an orientation to make it accessible to CobS. CobU^{E80K} may be unable to bind Cbi-GDP, or is otherwise unable to deliver the corrinoid to CobS (Figure 5.12 E). This hypothesis is compelling, and supported by our observation that a strain lacking *cobU* is unable to grow even when provided with Cbi-GDP. Based on our findings, we suggest that CobU interacts with CobS in a way that facilitates access of Cbi-GDP to the CobS corrin binding site. CobU may position the substrate in an orientation to facilitate access by CobS. Alternatively, CobU-CobS binding may induce a conformational change in CobS, making the corrinoid binding site accessible.

Ultimately, we would like to observe the complex formed by NLA enzymes. Despite our attempts, CbiB has not been successfully overexpressed and purified. We hypothesize that CbiB colocalizes with NLA enzymes, and that together CbiB and CobS form anchor points around which the other NLA enzymes can localize. Obtaining CbiB

protein is essential to further our understanding of interactions among NLA enzymes, and we are currently attempting to overexpress CobD and CbiB in tandem based on the observation that CbiB is stabilized by CobD. We propose that cryo-electron microscopy would provide the most detailed information about the NLA complex. CbiB is the final NLA enzyme needed to perform these experiments, and work is under way to obtain pure protein.

5.5 MATERIALS AND METHODS

Bacterial strains and plasmid construction. The genotypes of all strains used are listed in Table 5.1. All plasmids used in this work are listed in Table 5.2. Plasmids containing CobU and CobS variants were constructed using Pfu Ultra II per the manufacturer's instructions (Agilent Technologies). All plasmids were verified by sequencing analysis (Eton Biosciences). All primers used in the work are listed in Table 5.3.

Growth conditions, media, and chemicals. Unless otherwise noted, all chemicals used were commercially available high-purity compounds. LB or TB was used as rich medium for *E. coli*, and NB was used as rich medium for *S.* Typhimurium. Where indicated, growth analysis was performed in a minimal medium of no-carbon essential (NCE) supplemented with $MgSO_4$ (1 mM), and Wolfe's trace minerals (22) with glycerol (22 mM) added to the growth medium as the sole source of carbon. Corrinoids or cobamides were added to the medium at the concentrations designated in figure legends. Dicyanocobinamide and cyanocobalamin were purchased from Sigma. Cobinamide-GDP and ado-cobinamide-GDP were prepared as previously described (4, 5, 23). DMB (Sigma) was added to

medium at a concentration of 150 μM. Growth analysis was performed in a 96-well microtiter dish. A single colony was used to inoculate rich medium and grown overnight. A 1% (v/v) inoculum from this culture was used to inoculate 200 μL of minimal medium. Plates were incubated with shaking at 37 °C and monitored at 630 nm. All growth experiments were performed in biological triplicate and technical triplicate. Ampicillin (100 ug/mL) was added to cultures for plasmid maintenance. Expression of CobU and CobU variants was induced by the addition of arabinose at 0.5 mM.

Purification of CobU and CobU variants. CobU was purified as described elsewhere with minor modifications (5). *E. coli* BL21-λDE3 transformed with a plasmid encoding CobU or a variant was grown in Terrific Broth (TB) [tryptone (12g/L), yeast extract [24g/L], glycerol (4mL/L), $MgSO_4$ (2mM), KH_2PO_4 (17mM), K_2HPO_4 (72mM)] at 37 °C with shaking at 200 rpm to an OD_{600}=06-0.8. Expression was induced by the addition of IPTG to a final concentration of 1 mM, and incubated under the previous conditions for 3 h. Cultures were harvested by centrifugation at 6000 x g for 15 min at 4 °C in an Avanti J-20 XPI centrifuge. Cell pellets were resuspended in Buffer A [Tris-HCl (50 mM, pH 8), 1,4-dithiolthreitol (DTT, 10 mM), phenylmethylsulfonyl fluoride (PMSF, 200 μM), ethylenediaminetetraacetic acid (EDTA, 1mM) containing 10% (w/v) glycerol and stored at -80 °C overnight.

The following day, the resuspension was thawed on ice and cells were lysed by sonication with a Q500 Ultrasonic Processor (Qsonica) set to 50% amplitude, 2 s on/2 s off for 5 min repeated thrice. The lysate was clarified by centrifugation at 34,000 x g for 30 minutes at 4 °C in an Avanti J-25I centrifuge equipped with a JA-25.50 rotor.

Ammonium sulfate [$(NH_4)_2SO_4$, 30% w/v) was added to the clarified lysate slowly with stirring at 4 °C followed by an incubation for 30 min. Precipitated protein was pelleted by centrifugation in an Avanti J-25I centrifuge equipped with a JA-25.50 rotor at 14,000 x g at 4 °C for 20 min. The supernatant was removed, and $(NH_4)_2SO_4$ was added slowly to a final concentration of 55% (w/v). After a 30 min incubation at 4 °C, protein was pelleted as previously described. The pellet was resuspended in Buffer A, and dialyzed thrice in 1 L Buffer A for at least 3 h each at 4 °C to remove ammonium sulfate.

Dialyzed lysates were passed through a 0.44 μm filter and loaded to a HiTrap DEAE FF column (GE Healthcare Life Sciences) on an AKTA Pure Fast Protein Liquid Chromatography (FPLC) system (GE Healthcare Life Sciences) equilibrated with Buffer A. The column was washed with 5 column volumes (CV) of Buffer A, and CobU was eluted using a 500 mL (10 CV) linear gradient of 0-500 mM NaCl in Buffer A. Elution factions were loaded to a 15% SDS-PAGE gel, and fractions containing CobU were pooled and dialyzed in storage buffer [Tris-HCl (50 mM, pH 8), DTT (5 mM), NaCl (0.1M) and glycerol (5% w/v). The dialyzed protein was drop frozen in liquid N_2 and stored at -80 °C.

Protein concentration was determined by Bradford assay (BioRad) following the manufacturer's instructions. Percent purity of the proteins used in the work was determined by loading 1 μg of protein to a 15% SDS-PAGE gel. The gel was stained with Coomassie and analyzed by densitometry using TotalLab TL100 v2009 software.

Thin-layer chromatography. CobU activity was tested using TLC as described (4, 5). Reaction buffer contained Tris (0.1M, pH 8 at 37 °C), $MgCl_2$ (2.5 mM), GTP (4.5 mM),

AdoCbi (300 μM) and CobU (2 μM). Reactions were incubated in the dark overnight at 37 °C. Products were separated using ascending TLC. A silica-coated TLC plate (Whatman, 20 x 20 cm) was equilibrated in a solvent system of isobutyric acid: water: ammonium hydroxide (66:33:1) and dried. At the bottom of the plate, 5 μL of the reaction was spotted and allowed to dry. The TLC plate was replaced in the chamber pre-equilibrated with the solvent system and run for approximately 6 h.

CobU-CobS interactions and Western blotting. Purified CobU was extensively dialyzed in crosslinking buffer made up of HEPES (4-(2-hydroxyethyl)- 1-piperazineethanesulfonic acid buffer, GoldBio) (50mM, pH 7.5) and NaCl (500 mM). Lyophilized peptides of cytoplasmic loops were reconstituted in the same buffer. CobU (15 μM) and CobS CL1 peptide (45 μM) were mixed and brought to a total volume of 500 μL with HEPES (50 mM, pH 7.5) and NaCl (500 mM). The reaction mixture was incubated for one or two hours at room temperature with nutation. Where indicated, samples were crosslinked by the addition of formaldehyde (1%, v/v) to these reactions. Crosslinked reactions were quenched by the addition of glycine (25 mM) for 15 min at 4 °C. Reaction samples were then mixed with non-reducing loading buffer [Tris pH 6.8 (300 mM), glycerol (60%, v/v), 12 mM ethylenediaminotetracetic acid (EDTA, 12 mM), and bromophenol blue (0.05% w/v)] or reducing loading buffer reducing loading buffer [Tris pH 6.8 (300 mM), glycerol (60%, v/v), 12 mM ethylenediaminotetracetic acid (EDTA, 12 mM), and 2-mercaptoethanol (BME, 864 mM), and bromophenol blue (0.05% w/v)] and incubated for 5 min at 95 °C. Samples were then loaded to a 15% (w/v) SDS-PAGE gel (24). SuperSignal Molecular Weight Protein Ladder (ThermoFisher) was used as the molecular

marker. A constant voltage of 200 V was applied for approximately 35 min. A transfer to a PVDF membrane was performed using a Trans-Blot Turbo system (Bio-Rad Laboratories). The membrane was then incubated in blocking buffer containing 0.5% (w/v) nonfat milk in PBST [phosphate-buffered saline; Na_2HPO_4 (10 mM, pH 7.2), NaCl (15 mM), and Tween 20 (0.1%, v/v, Millipore Sigma)] for 1 hour at room temperature (24 °C). New blocking buffer was applied and primary antibody generated against either CobU or CobS was added at 1:2000 (v/v) and incubated overnight at 4 °C with rotation. Membranes were washed thrice with PBST, then incubated in PBST containing goat anti-rabbit IgG horseradish peroxidase conjugate (1:10,000 [v/v], Invitrogen) at room temperature for 1 h with shaking. Membranes were washed thrice with PBST, then developed using SuperSignal West Pico PLUS Chemiluminescent Substrate (ThermoFisher) for 5 min at room temperature with shaking. Membranes were imaged using a UVP ChemStudio (analytikjena).

CobS-liposome formation. Liposomes were generated as detailed in Chapter 4. Interactions between CobU and CobS were tested by performing flotation assays. A five-fold molar excess of pure CobU was added to CobS proteoliposome and incubated at room temperature (24 °C) with nutation for 1 h. This mixture was mixed with an equal volume of buffer containing HEPES (20 mM pH 7.4 at 4 °C), NaCl (150 mM) and Histodenz (80% w/v) and moved into a polyallomer ultracentrifuge tube (Beckman Coulter, 13 x 51 mm). 2.5 mL of buffer containing HEPES (20 mM pH 7.4), NaCl (150 mM) and Histodenz (30% w/v) was overlayed, followed by a 150 μL overlay of HEPES (20 mM pH 7.4), NaCl (150 mM). Proteoliposomes were isolated by centrifugation at

214,000 x g for 3 h at 4 °C in a Optima MAX-XP ultracentrifuge fitted with a TLS-55 rotor. The top layer containing proteoliposomes was removed and used for subsequent assays. Western blots were performed as described above.

5.6 REFERENCES

1. Roth JR, Lawrence JG, Bobik TA. 1996. Cobalamin (coenzyme B12): synthesis and biological significance. Annu Rev Microbiol 50:137-181.
2. O'Toole GA, Rondon MR, Escalante-Semerena JC. 1993. Analysis of mutants of defective in the synthesis of the nucleotide loop of cobalamin. J Bacteriol 175:3317-3326.
3. O'Toole GA, Escalante-Semerena JC. 1993. *cobU*-dependent assimilation of nonadenosylated cobinamide in cobA mutants of *Salmonella typhimurium*. J Bacteriol 175:6328-6336.
4. O'Toole GA, Escalante-Semerena JC. 1995. Purification and characterization of the bifunctional CobU enzyme of *Salmonella typhimurium* LT2. Evidence for a CobU-GMP intermediate. J Biol Chem 270:23560-23569.
5. Thomas MG, Thompson TB, Rayment I, Escalante-Semerena JC. 2000. Analysis of the adenosylcobinamide kinase/adenosylcobinamide-phosphate guanylyltransferase (CobU) enzyme of *Salmonella typhimurium* LT2. Identification of residue His-46 as the site of guanylylation. J Biol Chem 275:27576-27586.
6. Thompson TB, Thomas MG, Escalante-Semerena JC, Rayment I. 1999. Three-dimensional structure of adenosylcobinamide kinase/adenosylcobinamide phosphate guanylyltransferase (CobU) complexed with GMP: evidence for a substrate-induced transferase active site. Biochemistry 38:12995-3005.
7. Blanche F, Debussche L, Famechon A, Thibaut D, Cameron B, Crouzet J. 1991. A bifunctional protein from *Pseudomonas denitrificans* carries cobinamide kinase

and cobinamide phosphate guanylyltransferase activities. J Bacteriol 173:6052-6057.

8. Cameron B, Blanche F, Rouyez MC, Bisch D, Famechon A, Couder M, Cauchois L, Thibaut D, Debussche L, Crouzet J. 1991. Genetic analysis, nucleotide sequence, and products of two Pseudomonas denitrificans cob genes encoding nicotinate-nucleotide: dimethylbenzimidazole phosphoribosyltransferase and cobalamin (5'-phosphate) synthase. J Bacteriol 173:6066-6073.

9. Trzebiatowski JR, O'Toole GA, Escalante-Semerena JC. 1994. The *cobT* gene of *Salmonella typhimurium* encodes the NaMN: 5,6-dimethylbenzimidazole phosphoribosyltransferase responsible for the synthesis of N1-(5-phospho-alpha-D-ribosyl)-5,6-dimethylbenzimidazole, an intermediate in the synthesis of the nucleotide loop of cobalamin. J Bacteriol 176:3568-3575.

10. Chen P, Ailion M, Weyand N, Roth J. 1995. The end of the *cob* operon: evidence that the last gene (*cobT*) catalyzes synthesis of the lower ligand of vitamin B12, dimethylbenzimidazole. J Bacteriol 177:1461-1419.

11. Trzebiatowski JR, Escalante-Semerena JC. 1997. Purification and characterization of CobT, the nicotinate-mononucleotide:5,6-dimethylbenzimidazole phosphoribosyltransferase enzyme from *Salmonella typhimurium* LT2. J Biol Chem 272:17662-17667.

12. Zayas CL, Escalante-Semerena JC. 2007. Reassessment of the late steps of coenzyme B_{12} synthesis in *Salmonella enterica*: Evidence that dephosphorylation of adenosylcobalamin-5'-phosphate by the CobC phosphatase is the last step of the pathway. J Bacteriol 189:2210-2218.

13. O'Toole GA, Trzebiatowski JR, Escalante-Semerena JC. 1994. The *cobC* gene of *Salmonella typhimurium* codes for a novel phosphatase involved in the assembly of the nucleotide loop of cobalamin. J Biol Chem 269:26503-26511.

14. Zayas CL, Claas K, Escalante-Semerena JC. 2007. The CbiB protein of *Salmonella enterica* is an integral membrane protein involved in the last step of the de novo corrin ring biosynthetic pathway. J Bacteriol 189:7697-7708.

15. Maggio-Hall LA, Claas KR, Escalante-Semerena JC. 2004. The last step in coenzyme B(12) synthesis is localized to the cell membrane in bacteria and archaea. Microbiology 150:1385-1395.

16. Maggio-Hall LA, Escalante-Semerena JC. 1999. In vitro synthesis of the nucleotide loop of cobalamin by *Salmonella typhimurium* enzymes. Proc Natl Acad Sci U S A 96:11798-11803.

17. Jeter VL, Escalante-Semerena JC. 2021. Insights into the relationship between cobamide synthase and the cell membrane. mBio 12.

18. Jeter VL, Escalante-Semerena JC. 2022. Elevated levels of an enzyme involved in coenzyme B12 biosynthesis kills *Escherichia coli*. mBio 13:e0269721.

19. Thompson TB, Thomas MG, Escalante-Semerena JC, Rayment I. 1998. Three-dimensional structure of adenosylcobinamide kinase/adenosylcobinamide phosphate guanylyltransferase from Salmonella typhimurium determined to 2.3 A resolution. Biochemistry 37:7686-95.

20. Herzberg O, Moult J. 1991. Analysis of the steric strain in the polypeptide backbone of protein molecules. Proteins: Structure, Function, and Bioinformatics 11:223-229.

21. Jeter VL. 2020. Cobamide Biosynthesis Is Anchored to the MembraneUniversity of Georgia.

22. Balch WE, Fox GE, Magrum LJ, Woese CR, Wolfe RS. 1979. Methanogens: reevaluation of a unique biological group. Microbiol Rev 43:260-296.

24. Suh S, Escalante-Semerena JC. 1995. Purification and initial characterization of the ATP:corrinoid adenosyltransferase encoded by the *cobA* gene of *Salmonella typhimurium*. J Bacteriol 177:921-925.

25. Laemmli UK. 1970. Cleavage of structural proteins during the assembly of the head of bacteriophage T4. Nature 227:680-685.

26. Cronan JE. 2006. A family of arabinose-inducible *Escherichia coli* expression vectors having pBR322 copy control. Plasmid 55:152-157.

Table 5.1. Strains used in this study[a]		
Strain	**Genotype**	**Reference/source**
***Salmonella enterica* subsp. *enterica* sv. Typhimurium str. LT2 strains**		
JE3892	*E. coli* BL21 (λDE3) F- *ompT gal dcm lon hsdSB*(*rB-mB-*) λ(DE3 [*lacI lacUV5-T7 gene 1 ind1 sam7 nin5*])	Lab collection
JE6583	*metE205 araB9*	Lab collection
JE8249	*metE205 araB9 cobU1315 (*Δ*cobU)*	Lab collection
JE24507	*metE205 araB9 cobU1315*/ pBAD24	
JE24508	*metE205 araB9 cobU1315*/ pCobU27	
JE24628	*metE205 araB9 cobU1315*/ pCobU35	
JE24629	*metE205 araB9 cobU1315*/ pCobU36	
JE24630	*metE205 araB9 cobU1315*/ pCobU37	
JE24631	*metE205 araB9 cobU1315*/ pCobU38	
JE24632	*metE205 araB9 cobU1315*/ pCobU39	

[a]All strains were constructed during the course of this work unless otherwise stated

Table 5.2 Plasmids used in this study[b]		
Plasmid	**Description**	**Reference/source**
pBAD24	Complementation vector P_{araBAD} *bla*$^{+}$	(25)
pCobU27	*S.* Typhimurium *cobU* cloned into the KpnI and HindIII restriction sites of pBAD24	Lab collection
pCobU35	*S.* Typhimurium *cobU1480* coding for CobU^{E80D} cloned into pBAD24	
pCobU36	*S.* Typhimurium *cobU340* coding for CobU^{E80K} cloned into pBAD24	
pCobU37	*S.* Typhimurium *cobU1481* coding for CobU^{E80P} cloned into pBAD24	
pCobU38	*S.* Typhimurium *cobU1482* coding for CobU^{C81A} cloned into pBAD24	
pCobU39	*S.* Typhimurium *cobU1483* coding for CobU^{C81S} cloned into pBAD24	
pJO52	*S.* Typhimurium *cobU* cloned into pT7-7 using *NdeI* and *HindIII* restriction sites	(4)
pCobU57	*S.* Typhimurium *cobU340* coding for CobU^{E80K} cloned into pT7-7 at *NdeI* and *HindIII* restriction sites	
pCobU60	*S.* Typhimurium *cobU1483* coding for CobU^{C81S} cloned into pT7-7 at *NdeI* and *HindIII* restriction sites	

[b]All plasmids were constructed during the course of this work unless otherwise stated

Table 5.3. Primers used in this study[c]	
Primer name	**Primer sequence (5' → 3')**
CobU E80K 1	CCATGGTGGTAATACATTTCAGCAAAATCGCGTCGTC
CobU E80K 2	GACGACGCGATTTTGCTGAAATGTATTACCACCATGG
CobU C81S 1	ACGCGATTTTGCTGGAAAGTATTACCACCATGGTG
CobU C81S 2	CACCATGGTGGTAATACTTTCCAGCAAAATCGCGT
CobU E135K 1	CCATTCCCACCTTATTTGTCACCAGTACCACTTTCG
CobU E135K 2	CGAAAGTGGTACTGGTGACAAATAAGGTGGGAATGG
CobU E80D 1	ATGGTGGTAATACAATCCAGCAAAATCGCGTCGTC
CobU E80D 2	GACGACGCGATTTTGCTGGATTGTATTACCACCAT
CobU C81A 1	TGACGACGCGATTTTGCTGCCATGTATTACCACCATGGTG
CobU C81A 2	CGTCACCATGGTGGTAATAGCTTCCAGCAAAATCGCGTCG

[c]All primers were purchased from Integrated DNA Technologies (IDT)

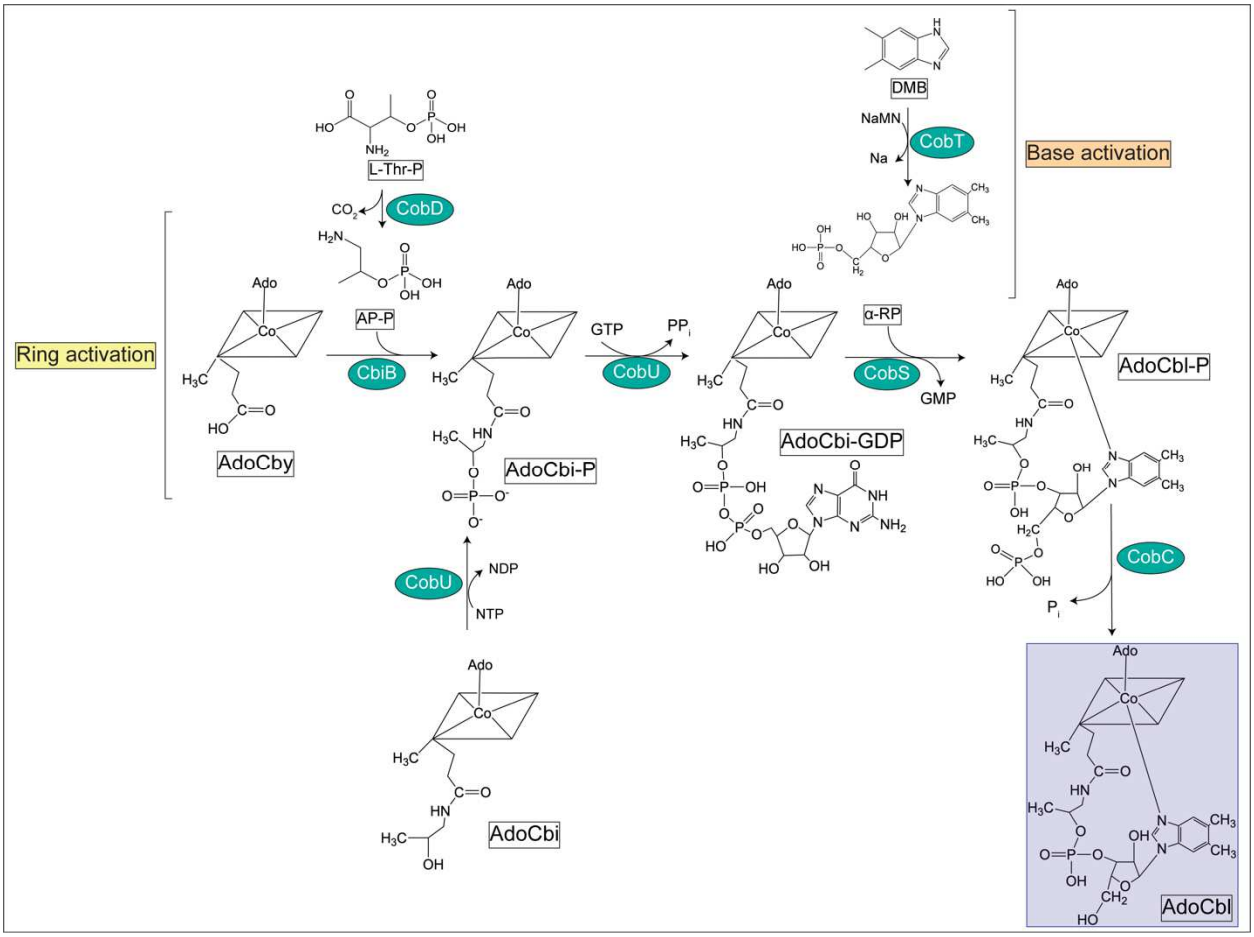

Figure 5.1. Nucleotide loop assembly in *S.* Typhimurium. The structures of pathway intermediates are shown with the corresponding name in a black box. The names of *S.* Typhimurium enzymes are shown in teal circles. The biologically active coenzyme, AdoCbl (coenzyme B_{12}) is shown in a blue box. Steps involved in base activation (orange) and ring activation (yellow) are marked with brackets. Abbreviations stand for: L-Thr, L-threonine; L-Thr-P, L-threonine-phosphate; AP-P, aminopropanol-phosphate; AdoCby, adenosylcobyric acid; AdoCbi, adenosylcobinamide; AdoCbi-P, adocobinamide-phosphate; AdoCbi-GDP, adenosylcobinamide-GDP; DMB, 5,6-dimethylbenzimidazole; α-RP, a-ribazole-phosphate; AdoCbl-P, adenosylcobalamin-phosphate; AdoCbl, adenosylcobalamin.

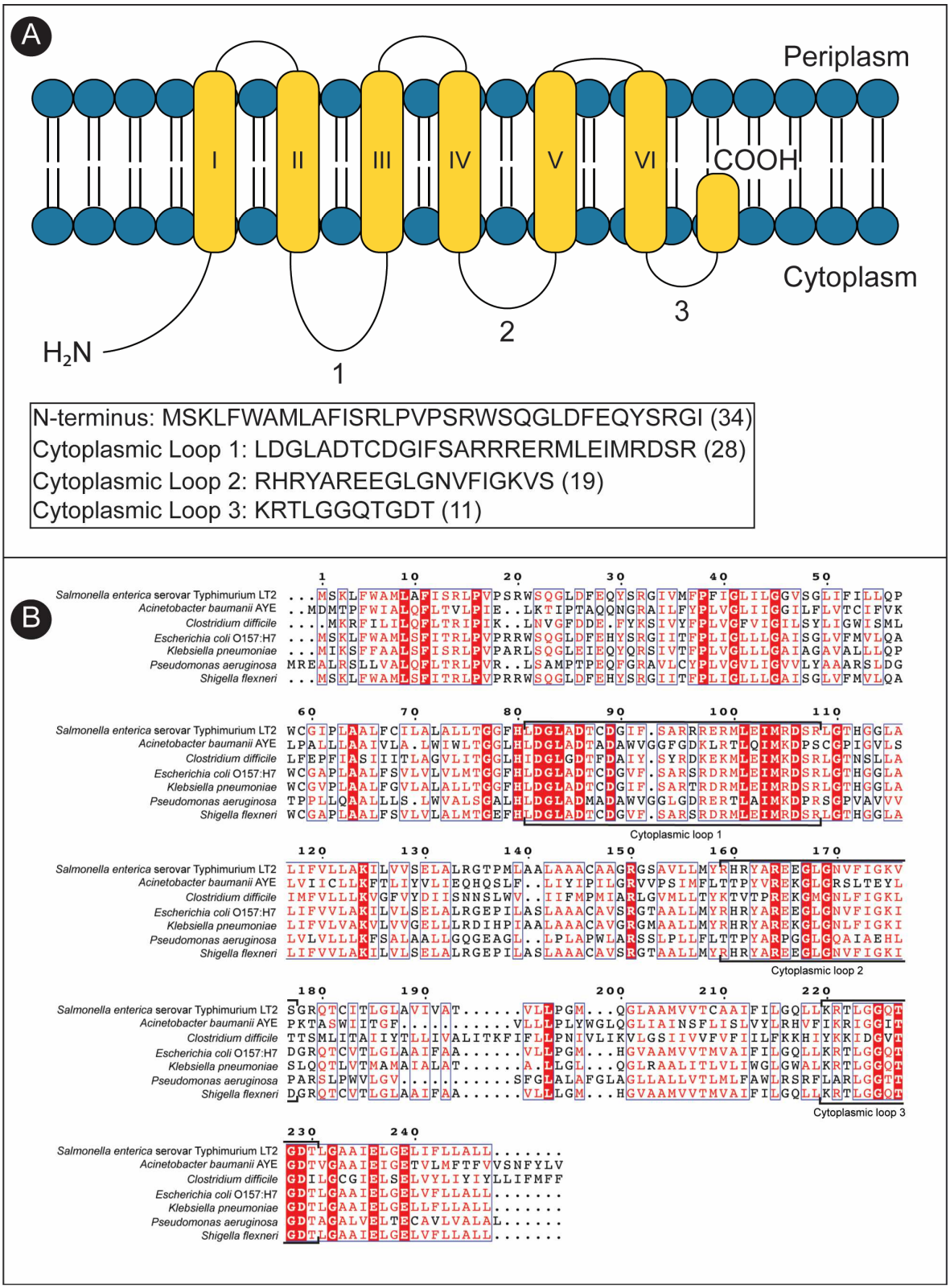

Figure 5.2 Structure and sequence alignment of the integral membrane protein CobS. (A) Schematic of the structure of CobS. Transmembrane regions are illustrated in yellow, and periplasmic or cytoplasmic loops are illustrated by a black line. The N-

terminus is located in the cytoplasm. The final 17 amino acids are predicted to be located within the inner membrane bilayer. (B) Sequence alignment of CobS enzymes. Identical amino acids are highlighted in red, similar amino acids are shown in red text. Regions of similarity are boxed in blue. Cytoplasmic loop regions are indicated by a black bracket. Alignments were generated using Clustal Omega 1.2.3 in Geneious Prime software and ESPript 3 (https://espript.ibcp.fr/ESPript/ESPript/).

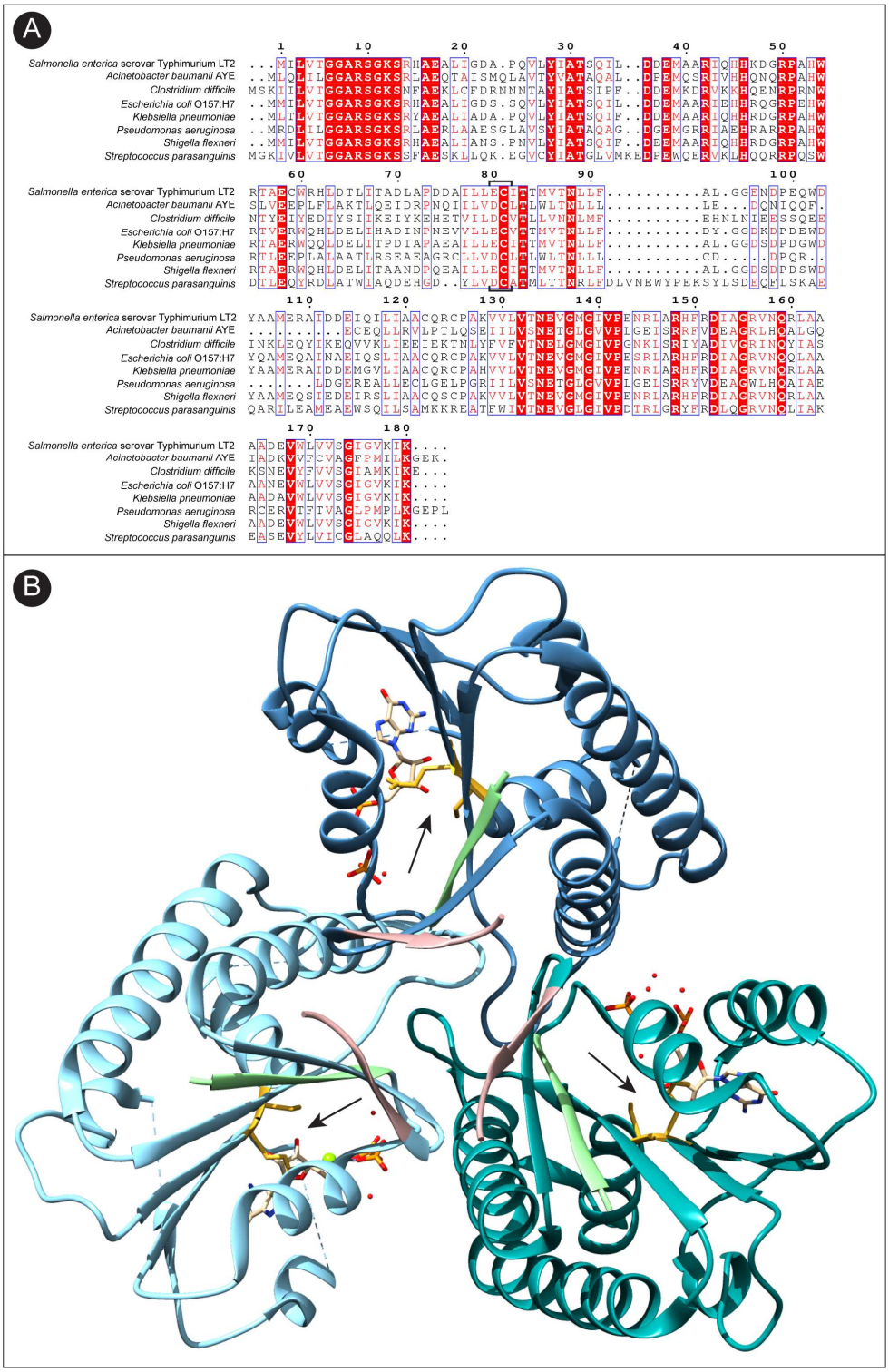

Figure 5.3. Sequence alignment and structure of CobU. (A) Sequence alignment of CobS enzymes. Identical amino acids are highlighted in red, similar amino acids are shown in red text. Regions of similarity are boxed in blue. Glu^{80} and Cys^{81} are indicated by black brackets. Alignments were generated using Clustal Omega 1.2.3 in Geneious

Prime software and ESPript 3 (https://espript.ibcp.fr/ESPript/ESPript/). (B) Structure of the CobU-GMP trimer. Each monomer is illustrated in a different shade of blue. The first five N-terminal amino acids are depicted in green, the last five C-terminal amino acids are shown in pink. The side chains of Glu^{80} and Cys^{81} are shown in gold. The structure of GMP is shown in tan. Pyrophosphate is shown in orange, and magnesium ions are shown in lime green.

Table 5.4. Comparison of bacterial CobU sequences[d]		
Bacterial species	Percent identity to *S.* Typhimurium	Percent identity to *S.* Typhimurium
Acinetobacter baumannii	37%	55%
Clostridium difficile	40%	60%
Escherichia coli O157:H7	82%	91%
Klebsiella pneumoniae	87%	93%
Pseudomonas aeruginosa	36%	54%
Shigella flexneri	85%	92%
Streptococcus parasanguinis	39%	57%

[d] Alignments were generated and analyzed for similarity/identity using Clustal Omega 1.2.3 in Geneious Prime software

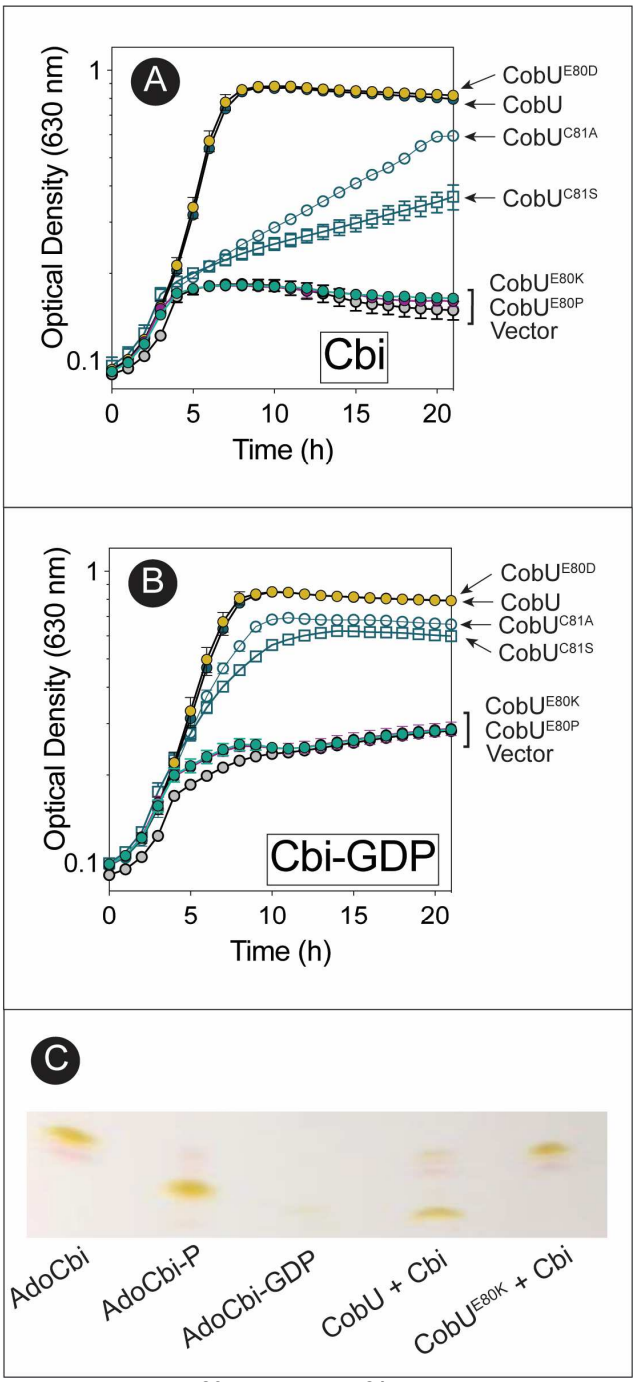

Figure 5.4 Changes to CobU Glu^{80} and Cys^{81} alter growth in *S.* Typhimurium. All experiments were performed in an *S.* Typhimurium *cobU1315* (Δ*cobU*) background. Cultures were provided with 15 nM $(CN)_2$Cbi (A) or 15 nM $(CN)_2$Cbi-GDP (B). In both cases, 150 μM DMB was added. Strains expressing the following are shown: CobU (dark blue circle), CobU^{E80D} (yellow circle), CobU^{E80K} (teal circle), CobU^{E80P} (purple circle), CobU^{C81A} (blue open circle), CobU^{C81S} (blue open square) empty vector (grey circle). In all cases, growth was restored by the addition of 15 nM CNCbl. Error bars represent the standard deviation of technical triplicates. (C) TLC to assess CobU activity *in vitro*.

Table 5.5 Growth analysis of strains expressing CobU variants[e]			
Plasmid	15 nM Cbi, 150uM DMB	15nM Cbi-GDP, 150uM DMB	15nM Cbl
pBAD24	NG	NG	0.87 ± 0.02
pCobU27	0.73 ± 0.04	0.55 ± 0.01	0.87 ± 0.06
E80D	0.76 ± 0.06	0.58 ± 0.02	0.89 ± 0.06
E80K	NG	NG	0.90 ± 0.03
E80P	NG	NG	0.90 ± 0.04
C81A	0.13 ± 0.0	0.32 ± 0.01	0.89 ± 0.05
C81S	0.04 ± 0.0	0.2 ± 0.01	0.97 ± 0.08

[e]All strains are a *S.* Typhimurium *metE205 ara-9 cob1315* background. Cells were grown at 37 °C with shaking in 96-well microtiter plates in NCE minimal medium and monitored for 16 h as described above. Growth rate (μ) of three biological replicates in technical triplicate shown with the corresponding standard deviation between all replicates. Growth rates were determined using online tools (https://scott-h-saunders.shinyapps.io/gompertz_fitting_0v2/).

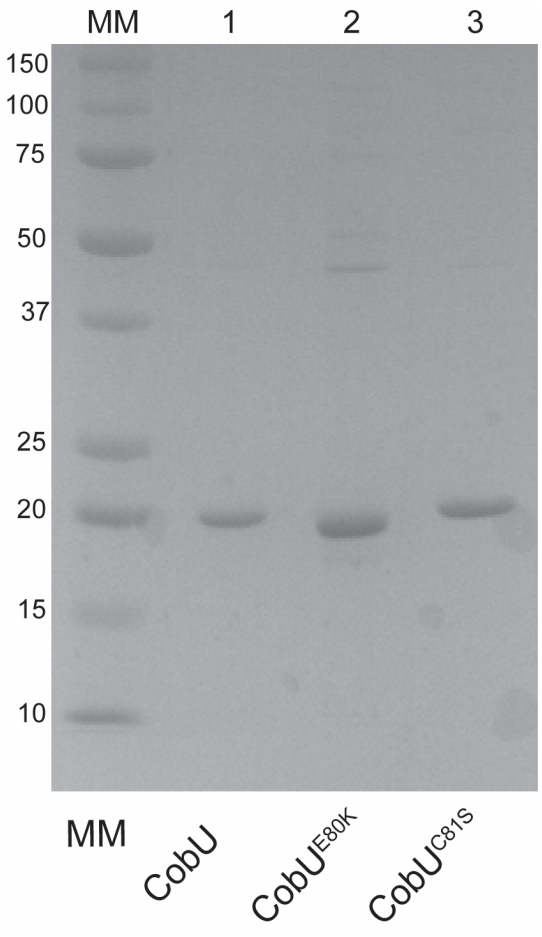

Figure 5.5 Purity of proteins used in this study. Protein concentration was determined by Bradford assay and were diluted such that 6 μL containing 1 μg was loaded to a 15% SDS-PAGE gel. The gel was stained with Coomassie and analyzed by densitometry using TotalLab TL100 v2009 software. The purity of each protein is as follows: CobU, >98%; $CobU^{E80K}$, 90%; $CobU^{C81S}$, >98%.

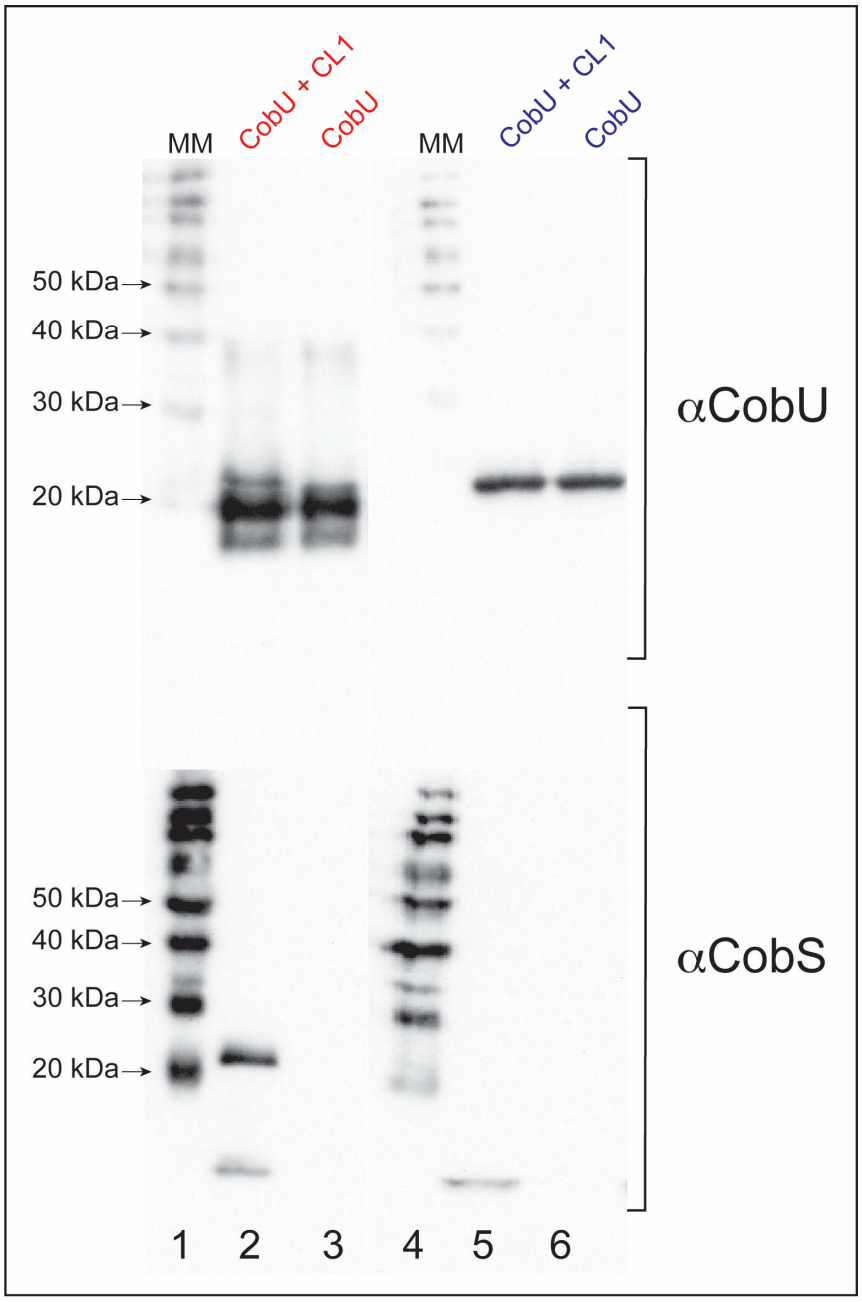

Figure 5.6. Formaldehyde crosslinking of CobU and CobS CL1 peptide. Western blot of membranes incubated with αCobU (top) or αCobS (bottom). The interaction reaction was allowed to proceed for one hour. MM denotes the molecular mass marker. Prior to loading, reactions were mixed with non-reducing (red label) or reducing (blue label) loading buffer and were not heated. The molecular mass for CobU is 19.9 kDa, the molecular mass for the CobS CL1 peptide is 3.2 kDa. Lane contents are as follows: lane 1, molecular marker; lane 2, CobU + CL1; lane 3, CobU; lane 4, molecular marker; lane 5, CobU + CL1 (reduced); lane 6, CobU (reduced). Lane contents are identical for the top and bottom gel. The corresponding primary antibody used for each blot is noted on the right side of the image.

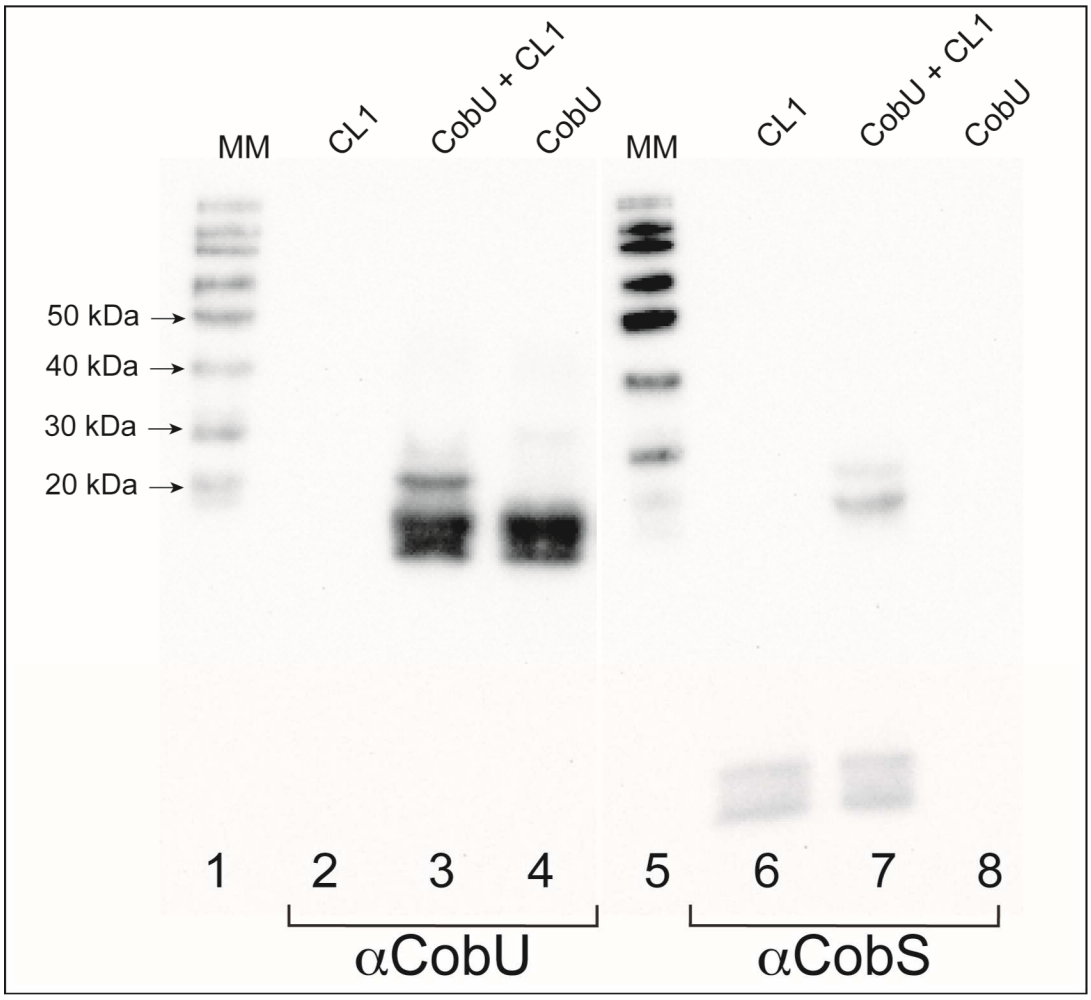

Figure 5.7. CobU interacts with cytoplasmic loop 2 of CobS in the absence of crosslinker. Western blot of membranes incubated with αCobU (top) or αCobS (bottom). The interaction reaction was allowed to proceed for two hours. MM denotes the molecular mass marker. Prior to loading SDS-PAGE gel, samples were incubated with a non-reducing loading buffer and heated for 5 mins at 95 °C. The molecular mass for CobU is 19.9 kDa, the molecular mass for the CobS CL1 peptide is 3.2 kDa. Lane contents are: lane 1, molecular marker; lane 2 CobS CL1; lane 3, CobU + CobS CL1; lane 4, CobU; lane 5, molecular marker; lane 6, CobS CL1; lane 7, CobU + CobS CL1; lane 8, CobU.

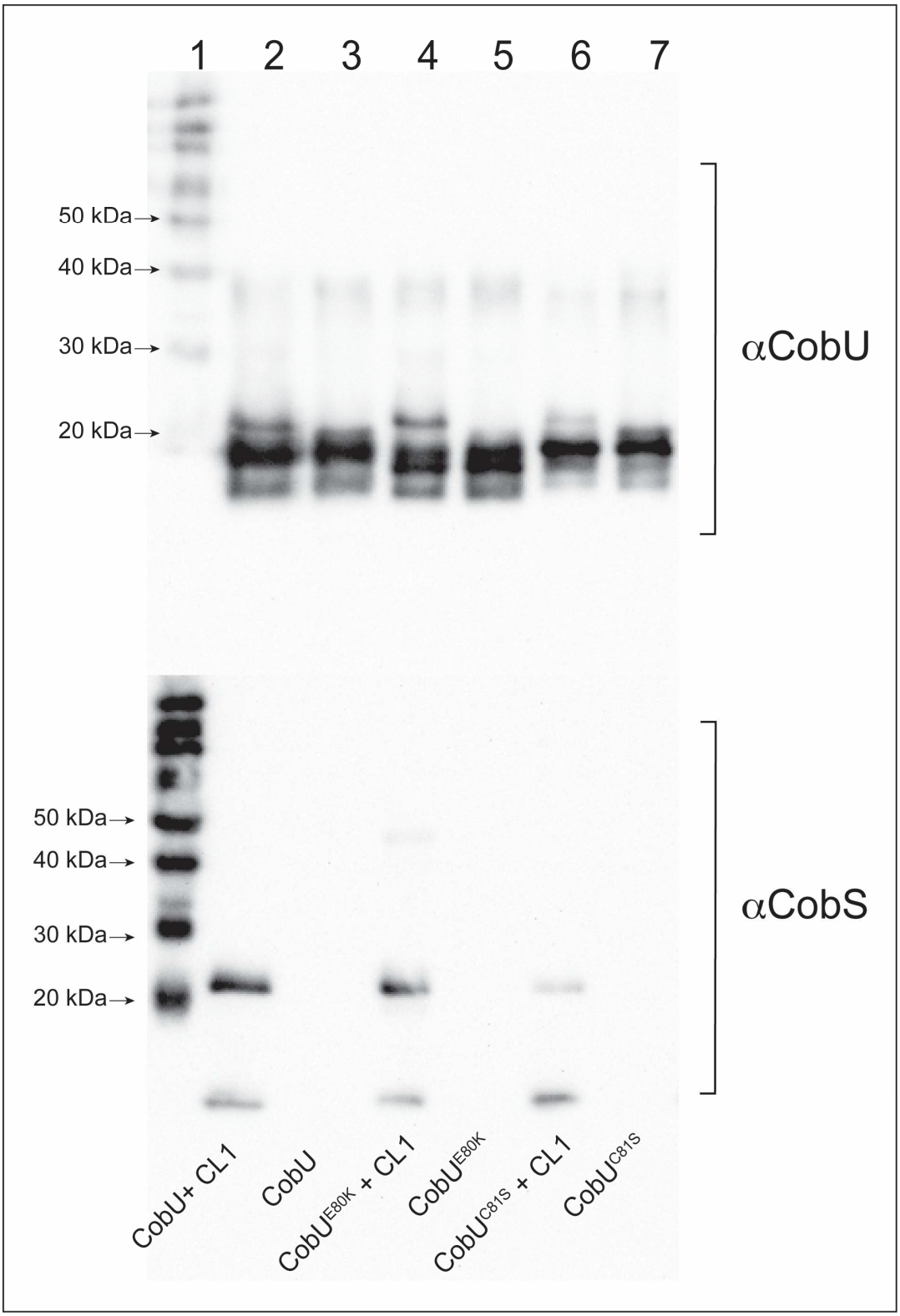

Figure 5.8. CobU^{C81S} reduces interaction with the CobS CL1 peptide when crosslinked with formaldehyde. Western blot of membranes incubated with αCobU (top) or αCobS (bottom). The reaction was allowed to proceed for one hour. MM denotes

the molecular mass marker. Prior to loading, reactions were mixed with non-reducing loading buffer. The molecular mass for CobU is 19.9 kDa, the molecular mass for the CobS CL1 peptide is 3.2 kDa. Lane contents are as follows: lane 1, molecular marker; lane 2, CobU + CobS CL1; lane 3, CobU; lane 4, $CobU^{E80K}$ + CobS CL1; lane 5, $CobU^{E80K}$; lane 6, $CobU^{C81S}$ + CobS CL1; lane 7, $CobU^{C81S}$. Lane contents are identical for the top and bottom membrane. The corresponding primary antibody used for each blot is noted on the right side of the image.

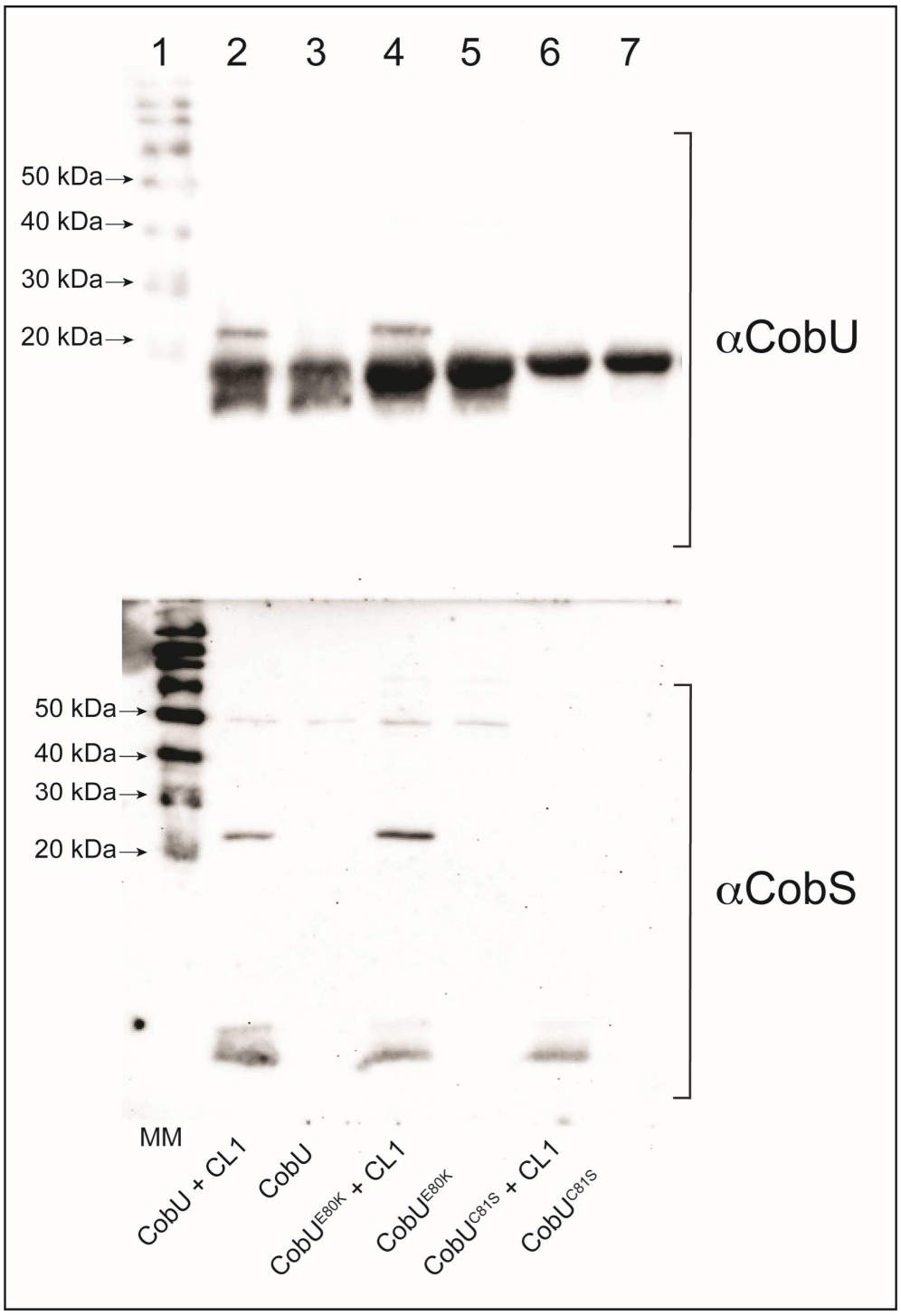

Figure 5.9. CobU^{C81S}- CobS CL1 interaction is prevented in the absence of crosslinker. Western blot of membranes incubated with αCobS (bottom) or αCobU (top). MM denotes the molecular mass marker. The molecular mass for CobU is 19.9 kDa, the molecular mass for the CobS CL1 peptide is 3.2 kDa. Lane contents are as follows: lane 1, molecular marker; lane 2, CobU + CobS CL1; lane 3, CobU; lane 4, CobU^{E80K} + CobS CL1; lane 5, CobU^{E80K}; lane 6, CobU^{C81S} + CobS CL1; lane 7, CobU^{C81S}.

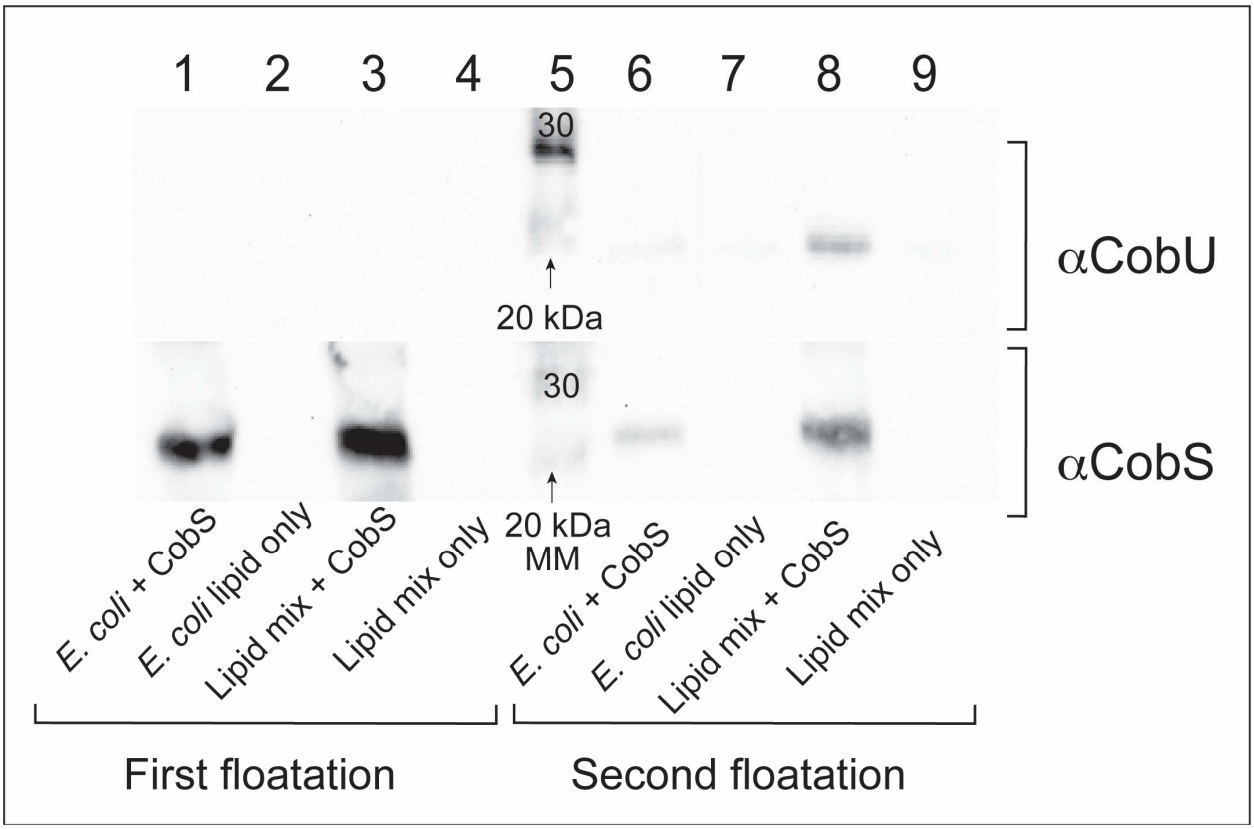

Figure 5.10 CobU interacts with CobS in proteoliposomes of various compositions. To test interactions, proteoliposomes undergo two separations using ultra-centrifugation through a density gradient ("floatation" assays). The first floatation separates CobS-proteoliposomes from unincorporated CobS protein (left, "first floatation"). These proteoliposomes are incubated with CobU, and a second floatation is performed to identify only CobU bound to CobS in the proteoliposome (right). The membranes were incubated with αCobU (top) or αCobS (bottom).

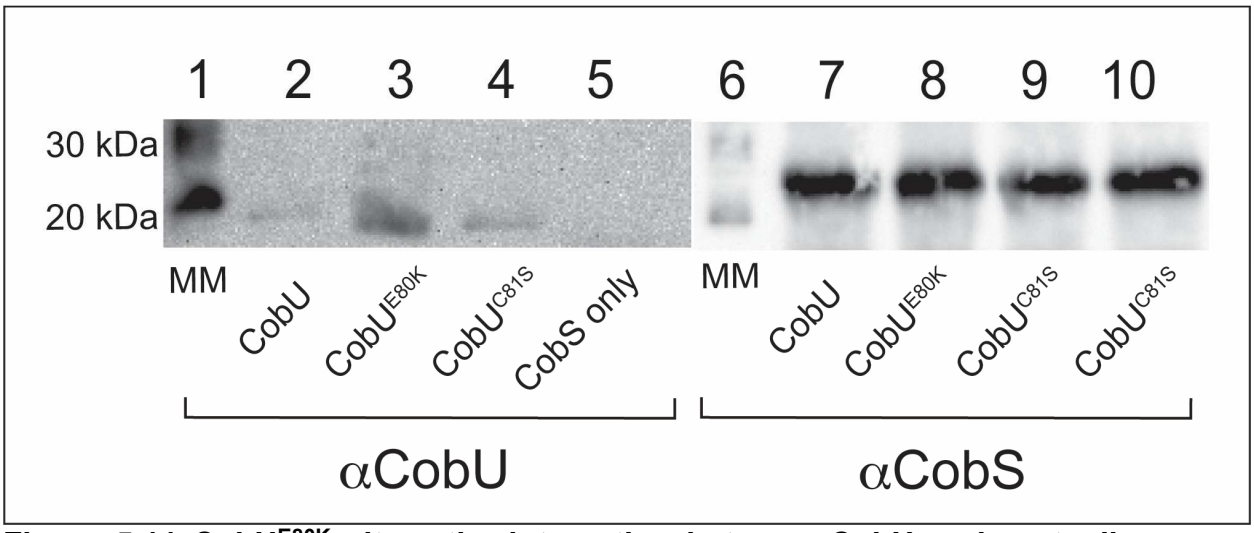

Figure 5.11 CobU^{E80K} alters the interaction between CobU and proteoliposome-incorporated CobS. Western blot image of isolated fractions following CobU and CobU variants were incubated with CobS-containing proteoliposomes and isolated by ultracentrifugation through a density gradient. Membranes were incubated with αCobU (left) or αCobS (right). Densitometry of the bands was performed using TotalLab TL100 v2009 software.

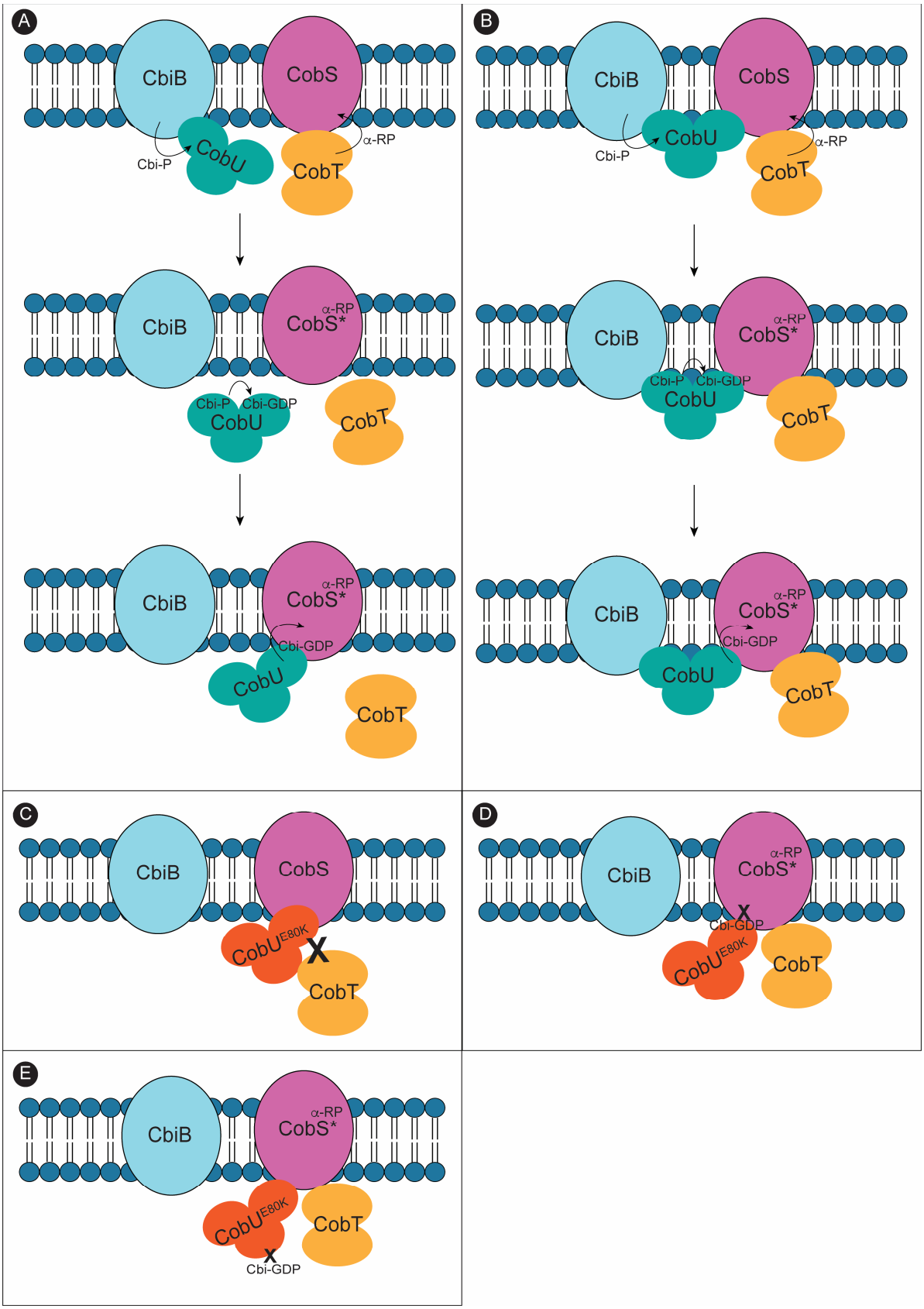

Figure legend on next page

Figure 5.12. Proposed model of interactions between NLA enzymes. CobU may associated with CbiB individually (A) or concurrently (B). We propose that $CobU^{E80K}$ may alter these interactions by preventing CobT binding and the conformational change induced in the presence of a-RP (C), occlusion of the Cbi-GDP binding site in CobS (D) or $CobU^{E80K}$ may be unable to bind Cbi-GDP (E).

CHAPTER 6

CORRINOID REMODELING BY THE *METHANOPYRUS KANDLERI* AMIDOHYDROLASE CBIS[5]

[5]Villa E.A. and Escalante-Semerena, J.C. 2022. To be submitted to *Molecular Microbiology*.

6.1 ABSTRACT

Archaeal species salvage the cobamide precursor cobinamide through a unique mechanism which requires remodeling. In bacteria, cobinamide can be phosphorylated and subsequently guanylylated by a single bifunctional enzyme, CobU, the adenosylcobinamide kinase/ guanylyltransferase. Archaea utilize an alternative pathway requiring two enzymes. First, the amidohydrolase CbiZ cleaves the lower aminopropanol linker, and assimilation into the nucleotide loop assembly (NLA) pathway depends on the cobinamide-phosphate synthase CbiB. Interestingly, genomes from archaea isolated from extreme environments, such as hyperthermophiles, contain a fusion protein known as CbiS in which this CbiZ amidohydrolase is fused to the archaeal adenosylcobalamin5'-phosphate phosphatase CobZ. This fusion is of particular interest because it physically links the first and last enzyme required for archaeal salvaging, suggesting that it is advantageous for enzymes of this pathway to be colocalized within the cell, and that this fusion may impart an advantage under extreme growth conditions.

In this work, we examine the biochemical parameters of CbiS from *Methanopyrus kandleri*. CbiS restores growth in a *Salmonella* strain incapable of cobinamide kinase activity. Because little is known about the structure of this enzyme, we use site directed mutagenesis of conserved amino acids to determine critical residues for CbiS amidohydrolase function.

6.2 INTRODUCTION

Coenzyme B_{12} (also known as adenosylcobalamin, AdoCbl) and its derivatives, known as cobamides, are used as cofactors by enzymes to perform a variety of cellular processes in both prokaryotes and eukaryotes; however *de novo* synthesis is only

performed by some prokaryotes (1, 2). Cobamides are complex molecules composed of a cobalt-containing cyclic tetrapyrrole (corrin ring) coordinated to both an upper (*Co*β) and lower (*Co*α) ligand (3). The term *cobamide* is used to refer to all complete structures regardless of the organic base incorporated into the lower ligand. In coenzyme B_{12}, the nucleobase contains 5,6-dimethylbenzimidazole (DMB) (4, 5). Many prokaryotes are able to import and assimilate the corrin ring if a corrin-ring containing precursor is available in the environment. Forming the biologically active coenzyme requires activation and attachment of a nucleotide base-containing loop on the lower face of the ring in a process known as Nucleotide Loop Assembly (NLA) (6, 7). Figure 6.1 illustrates the difference between the NLA pathways in bacteria and archaea. Archaea depend on cobamides to perform methanogenesis from H_2, CO_2, methanol and acetate (8, 9). Archaeal genomes contain functional homologs for a number of enzymes involved in *de novo* synthesis in bacteria, but lack the bifunctional CobU (EC 2.7.1.156, 2.7.7.62) enzyme used by bacteria salvage the incomplete precursor known as cobinamide (Cbi) (10-12). In *S.* Typhimurium, the precursor cobinamide can be assimilated into the nucleotide loop assembly pathway by this single enzyme, CobU, which phosphorylates and guanylylates Cbi (13, 14). The archaeal homologue CobY is only capable guanylylation (15). Instead, two enzymes are needed for cobinamide assimilation. First, the amidohydrolase CbiZ (EC 3.5.1.90) cleaves the aminopropanol group from the lower face of the corrin ring generating the *de novo* intermediate cobyric acid (Cby) (16, 17). Subsequently, cobyric acid is condensed with aminopropanol-P by the synthase CbiB (EC 6.3.1.10) to form cobinamide-P (12, 18). Nucleotide loop assembly then proceeds as follows: CobY (EC 2.7.1.156), guanylylates the ring corrin with a GMP to form AdoCbi-GDP (11, 15) ; CobS (EC 2.7.8.26) condenses

AdoCbi-GDP with an α-ribazole-P (α-RP) generated by CobT (EC 2.4.2.21) to form AdoCbl-P (6, 19-22); finally, CobZ, the archaeal homologue of the phosphatase CobC (EC 3.1.3.73), removes the 5'-phosphate to form AdoCbl (23-25) (Figure 6.1).

In this work, we analyze the biochemical characteristics of *Methanopyrus kandleri* CbiS, a fusion protein containing both CbiZ and CobZ (16). CbiS homologues have been identified in hyperthermophilic archaea, suggesting that fusion of these two enzymes may aid in survival of stressful environmental conditions. Providing CbiS restores growth in a *Salmonella enterica* subsp. *enterica* sv. Typhimurium str. LT2 (hereafter referred to as *S.* Typhimurium) strain lacking CobU kinase activity,, demonstrating that the amidohydrolase and phosphatase activities of this enzyme are functional in bacteria (16). In this work, we use site-directed mutagenesis to investigate amino acids that are necessary for catalysis, stability, and oligomerization of the enzyme, and hypothesize that the CbiZ-CobZ fusion increases thermal stability. Because CbiZ and CobZ are required at distinct locations in the NLA pathway, we propose that NLA enzymes are localized together and interact to facilitate efficient exchange of intermediates.

6.3 RESULTS AND DISCUSSION

Residues required for Cbi salvaging *in vivo*. Several conserved amino acids found in the amidohydrolase domain of CbiS homologues (Figure 6.2) were selected for targeted mutational analysis to assess functionality in *vivo. S.* Typhimurium strains harboring a deletion of *cobU* and *ycfN* and heterologously expressing the archaeal cobinamide guanylyltransferase CobY (pCobY38) are unable to salvage Cbi due to the absence of CobU kinase activity (Figure 6.3) (16). Instead, growth is dependent on provision of Cby,

which can be converted directly to Cbi-P by CbiB. As CobY lacks the kinase activity of CobU homologues, Cbi-P is the only known substrate. Providing p*Mk*CbiS13 restores the ability of this strain to salvage Cbi through hydrolysis of the AP from the central ring to yield Cby, demonstrating that CbiS amidohydrolase activity is functional *in vivo* (Figure 6.3). Strains harboring plasmids encoding amino acid changes T76A, T96A, T117A, N119A, E142K, K144E, T162A, T164A, D165K and G182A do not permit growth when provided with Cbi, suggesting that these residues are critical for the amidohydrolase function of CbiS. Providing Cby to strains containing any variant plasmid corrected growth. S26A, V195T and V199T variants demonstrated reduced growth rate, but still functioned sufficient well to support Cbi salvaging-dependent growth (Table 6.4).

The structure of CbiS has not been solved. This enzyme is intriguing, as the fusion of CbiZ and CobZ, the first and last enzymes, respectively, in the archaeal salvaging pathway, is typically only observed in organisms that survive in extreme conditions. Thus, this fusion may improve thermal stability or enzyme efficiency in such a way that it provides a competitive advantage in these environments.

Assay for *Mk*CbiS activity. *Mk*CbiS was purified in order to assess *in vitro* activity. His_6-CbiS was determined to be 86% pure using analysis by SDS-PAGE and densitometry (Figure 6.4). A subset of variants were also purified to test activity *in vitro* (Fig. 6.5). Using RP-HPLC, we observed an elution time of approximately 20 minutes for $(CN)_2$Cbi, a substrate of *Mk*CbiS. When incubated with *Mk*CbiS, an additional elution peak develops at approximately 12 minutes, which corresponds with the retention time of Cby. Variants $CbiS^{T76A}$, $CbiS^{V118A}$, and $CbiSG^{182A}$ produced no detectable Cby, consistent with the

observed loss of functionality *in vivo.* CbiS^{V120A} and CbiS^{I121A} showed reduced activity, producing 38% and 21%, respectively, compared to CbiS (Figure 6.5). This finding is consistent with the observed growth behavior of strains producing these variant proteins (Figure 6.3) which supported growth, albeit to a lower degree than CbiS.

***Mk*CbiS is a tetramer in the presence of Cbl.** The oligomeric state of purified CbiS was determined using size exclusion chromatography. As shown in Figure 6.6, when compared to standards, *Mk*CbiS incubated with CNCbl elutes at a retention time corresponding to a molecular mass of 158 kDa, which corresponds to a tetrameric oligomer. Interestingly, none of the altered amino acids resulted in a change in the oligomeric state of the enzyme. As shown in Figure 6.6A, all variant proteins tested eluted with a molecular mass similar to the wild-type enzyme. We conclude that although some of these variant proteins are inactive, they still form a tetrameric structure; this suggests that disruption of these sites does not inhibit subunit-subunit contacts to a degree that the oligomer is prevented from forming.

***Mk*CbiS can be reconstituted in a proteoliposome.** Previous work has suggested that CobC may contain a transmembrane domain (26). During purification, we observed that a population of *Mk*CbiS is insoluble. To determine whether CbiS may be membrane-associated, we tested whether CbiS becomes incorporated into a proteoliposome. We found that when incubated with a lipid mix and incubated to allow liposomes to form, CbiS separates with the liposome structures when separated by ultra-centrifugation through a density gradient, illustrated by the presence of a band of ~40 kDa in the lane loaded with

liposome incubated with CbiS (Figure 6.7, lane 2) compared to empty liposome (Figure 6.7, lane 1). Further analysis is necessary to determine whether CbiS is fully inserted into the liposome, or simply associates strongly enough with the liposome to allow the protein to co-migrate. Regardless, this observation suggests that membrane-association may be an important additional physiological characteristic for *Mk*CbiS.

6.4 CONCLUDING REMARKS

At this point, little is known about the structure of CbiS. We have not identified the location of the binding site(s) or any structural characteristics that may provide an advantage in the fusion protein. The data presented here illustrate a number of critical residues for CbiS activity. Preliminary experiments have identified conditions in which CbiS forms crystals, although further optimization is necessary to obtain high-quality crystals. If successful, obtaining a crystal structure will be optimal to expand our understanding of this unique enzyme. The variants identified here demonstrate reduced or no activity *in vivo*, and can be assessed for structural changes causing detrimental effects including inhibition of catalytic activity, substrate binding, or oligomer formation. Likewise, additional experiments are necessary to determine if CbiS inserts into a proteoliposome or is simply strongly associated with the liposome structure. This can be accomplished by performing trypsin digests to determine how much of *Mk*CbiS is exposed when associated with the proteoliposome. If *Mk*CbiS is inserted in the proteoliposome, this experiment will also allow us to determine the orientation of *Mk*CbiS, and from this information we can identify transmembrane domains.

The emergence of a fusion protein that encompasses the first and last enzyme involved in nucleotide loop assembly is intriguing (Figure 6.1). Little is known about the advantages imparted by fusing these two enzymes, but we hypothesize that colocalization may provide an advantage in extreme environments. We suggest that in extremophiles, this fusion may serve to assist in membrane localization to improve efficient catalysis and perhaps to provide additional thermal stability. We have observed that CobS and CobC associate (26). It is logical that the archaeal homologue CobZ would also associate with NLA enzymes, and therefore we suggest that the CbiZ-CobZ fusion would localize similarly. Elucidating the multienzyme complex formed by NLA enzymes is of particular interest, and it is possible that in *M. kandleri* CbiS is a component of that complex in archaea. Furthermore, CbiS has been shown to convert cobalamin into cobyric acid *in vitro*; however, sufficient cobalamin is present in the cell to support growth when CbiS is heterologously expressed. Insight into the interplay between CbiS other NLA enzymes will elucidate how the complete coenzyme is sequestered and protected from amidohydrolase activity, and will provide insight into the broader context of interactions that take place between NLA enzymes.

6.5 MATERIALS AND METHODS

Bacterial strains and growth conditions. Unless otherwise noted, all chemicals used were commercially available high-purity compounds. *E. coli* DH5α was used for plasmid construction. Unless otherwise noted, cultures were grown at 37 °C with shaking at 180 rpm. All strains used in this work are listed in Table 6.1. LB was used as rich medium for *E. coli* unless otherwise noted. Difco Nutrient Broth (NB) was used as rich medium for *S.*

Typhimurium intended for growth analysis. Growth analysis was performed using minimal medium containing no-carbon essential (NCE), Wolfe's trace minerals (cite) and 1mM $MgSO_4$. Glycerol (22mM) was added to the medium as the sole carbon source. Where indicated, ampicillin and kanamycin were added to cultures for plasmid maintenance at 100 μg/mL and 50 μg/mL, respectively. Corrinoids were added to the growth medium at a concentration of 5nM. Dicyanoobinamide ($[CN]_2$Cbi) and cyanocobalamin (CNCbl) were purchased from Sigma. Cobyric acid (Cby) was a gift from Paul Renz (Universit¨at-Hohenheim, Stuttgart, Germany). DMB was purchased from Sigma. Growth assays were performed by subculturing 1% (v/v) from an overnight culture grown in rich medium into 200 μL minimal medium in a 96-well microtiter dish (Falcon). The dish was incubated at 37 °C with shaking and monitored at 630 nm. Each experiment was performed in biological and technical triplicate.

Plasmid construction. Plasmids are listed in Table 6.2. *Mk*CbiS was codon-optimized for expression in *E. coli* by GeneScript USA. The codon-optimized sequence was excised from pMkCbiS12 and cloned into pTEV5 using *NheI* and *EcoR*I restriction sites. Primers are listed in Table 6.3. All primers were synthesized by Integrated DNA Technologies (IDT) (Coralville, IA). Plasmids encoding variants of CbiS were constructed by amplifying with Pfu Ultra II (Agilent Technologies) per the manufacturer's instructions.

Overexpression and purification of *Mk*CbiS. *E. coli* BL21-λDE3 cells containing pMkCbiS13 were grown in at 37 °C with shaking at 200 rpm in Terrific Broth [tryptone (12g/L), yeast extract [24g/L], glycerol (4mL/L), $MgSO_4$ (2mM), KH_2PO_4 (17mM), K_2HPO_4

(72mM)] to an OD_{600}=0.8 at which point expression was induced through addition of IPTG to a final concentration of 1mM. Cultures were incubated with IPTG with shaking at 150 rpm at 20 °C for an additional 18 h. Cells were harvested by centrifugation at 6000 rpm for 15 mins at 4°C in an Avanti J-20 XPI centrifuge. Cell pellets were resuspended in Buffer A (20mM Na_2HPO_4, pH 7.4, 500mM NaCl, 20mM imidazole). DNase and lysozyme were added to a final concentration of 0.025 mM and 1mM, respectively. Cells were lysed using a Cell disruptor (Constant systems) at 25 kpsi. The lysate was collected and cleared by centrifuging at 43000 x g for 1h in an Avanti J-25I centrifuge equipped with a JA-25.50 rotor. Lysates were passed through a 0.44 μm filter and loaded to a HisTrap Fast-Flow column (GE Healthcare Life Sciences) on an AKTA Pure Fast Protein Liquid Chromatography (FPLC) system (GE Healthcare Life Sciences) equilibrated with Buffer A (20mM Na_2HPO_4, pH 7.4, 500mM NaCl, 20mM imidazole). His-CbiS was eluted from the column using an imidazole gradient (20-500 mM). For storage, elution fractions containing His-CbiS, as identified by SDS-PAGE, were pooled and dialyzed against Buffer B (20mM Tris base, pH 7.4, 500 mM NaCl, 30% glycerol). Protein was drop frozen in liquid N_2 and stored at -80 °C.

Protein concentration was determined using a Bradford assay (BioRad). The purity of CbiS was determined using SDS-PAGE. Dilutions were performed so that the following total amount of protein was loaded per well: 2.5 μg, 1.25 μg. 0.625 μg, 0.3125 μg, 0.156 μg. The gel was stained with Coomassie and analyzed by densitometry using TotalLab TL100 v2009 software.

***In vitro* CbiS amidohydrolase assay.** Assays were performed in 1 mL reaction mixtures containing 500mM KH_2PO_4 pH 9, and 60 μM corrinoid substrate. Reaction mixtures were flushed with N_2 gas and incubated anoxically in dim lighting at 90 °C. Reactions were allowed to proceed for 1 h unless otherwise noted. Following incubation, reaction mixtures were flash frozen and stored at -80 °C. To identify corrinoids, reaction mixtures were thawed and debris was separated by centrifuging at 16,000 x g for 10 min at room temperature in an Eppendorf Centrifuge 5418. The supernatant was removed and analyzed. Mixtures were separated by RP-HPLC on a Shimadzu Prominence UFLC SPD-M30A equipped with a Synergi 4m Hydro-RP 80A 150 x 4.6 mm column equilibrated with 97% mobile phase A (MP A) [KH_2PO_4 (0.1 M, pH 6.5), KCN (10 mM)]/ 3% mobile phase B (MP B) [KH_2PO_4 (0.1 M, pH 8), KCN (10 mM). After injection of the sample, a five-minute linear gradient was applied to 75% MP A/ 25% MP B, followed by a 15 min linear gradient to 65% MP A/ 35% MP B, followed by a 5 min isocratic step at 65% MP A/ 35% MP B. This was followed by a 2.5 min linear gradient to 100% MP B, concluding with a 5 min isocratic step at 100% B. Cobamides and corrinoids were identified by monitoring the fluorescence at 367 nm.

Size-exclusion chromatography. Size-exclusion chromatography was performed using an AKTA Pure Fast Protein Liquid Chromatography (FPLC) system (GE Healthcare Life Sciences) equipped with a Superose 12 10/300 column. The column was equilibrated with a buffer composed of Tris (20 mM, pH 7.4) and NaCl (500 mM). Gel filtration standards (BioRad) were used to generate a standard curve and contained a mix of the following proteins: γ-globulin (158 kDa), ovalbumin (44 kDa), myoglobin (17 kDa) and

vitamin B_{12} (1.35 kDa). Purified *Mk*CbiS or variant protein was injected to the equilibrated column. Peaks were analyzed using UNICORN 7.1 software. Molecular mass was calculated using retention time.

Liposome preparation. Proteoliposomes were prepared as described in Chapter 4 and 5. The lipids used in this study were a mix of POPC (80% v/v), POPS (10% v/v), POPE (9.5% v/v), and Rh-DHPE (0.5% v/v). Proteoliposomes were isolated by centrifugation at 200,000 x g for 3 h at 4 °C in a Optima MAX-XP ultracentrifuge fitted with a MLS-50 rotor.

6.6 REFERENCES

1. Escalante-Semerena JC, Warren MJ. 2008. Biosynthesis and use of cobalamin (B_{12}). *In* Böck A, Curtiss III R, Kaper JB, Karp PD, Neidhardt FC, Nyström T, Slauch JM, Squires CL (ed), *EcoSal - Escherichia coli* and *Salmonella*: cellular and molecular biology. ASM Press, Washington, D. C.
2. Roth JR, Lawrence JG, Bobik TA. 1996. Cobalamin (coenzyme B12): synthesis and biological significance. Annu Rev Microbiol 50:137-181.
3. Battersby AR. 2000. Tetrapyrroles: the pigments of life. Nat Prod Rep 17:507-526.
4. Woodward RB. 1973. The total synthesis of vitamin B_{12}. Pure Appl Chem 33:145-177.
5. Eschenmoser A, Wintner CE. 1977. Natural product synthesis and vitamin B_{12}. Science 196:1410-1420.
6. Zayas CL, Escalante-Semerena JC. 2007. Reassessment of the late steps of coenzyme B_{12} synthesis in *Salmonella enterica*: Evidence that dephosphorylation of adenosylcobalamin-5'-phosphate by the CobC phosphatase is the last step of the pathway. J Bacteriol 189:2210-2218.
7. O'Toole GA, Rondon MR, Escalante-Semerena JC. 1993. Analysis of mutants of defective in the synthesis of the nucleotide loop of cobalamin. J Bacteriol 175:3317-3326.
8. DiMarco AA, Bobik TA, Wolfe RS. 1990. Unusual coenzymes of methanogenesis. Annual review of biochemistry 59:355-394.
9. Grahame DA. 1989. Different isozymes of methylcobalamin: 2-mercaptoethanesulfonate methyltransferase predominate in methanol-versus

acetate-grown Methanosarcina barkeri. Journal of Biological Chemistry 264:12890-12894.

10. Thomas MG, Escalante-Semerena JC. 2000. Identification of an alternative nucleoside triphosphate: 5'- deoxyadenosylcobinamide phosphate nucleotidyltransferase in *Methanobacterium thermoautotrophicum* ΔH. J Bacteriol 182:4227-4233.

11. Woodson JD, Peck RF, Krebs MP, Escalante-Semerena JC. 2003. The cobY gene of the archaeon *Halobacterium* sp. strain NRC-1 is required for de novo cobamide synthesis. J Bacteriol 185:311-316.

12. Woodson JD, Zayas CL, Escalante-Semerena JC. 2003. A new pathway for salvaging the coenzyme B_{12} precursor cobinamide in archaea requires cobinamide-phosphate synthase (CbiB) enzyme activity. J Bacteriol 185:7193-7201.

13. O'Toole GA, Escalante-Semerena JC. 1995. Purification and characterization of the bifunctional CobU enzyme of *Salmonella typhimurium* LT2. Evidence for a CobU-GMP intermediate. J Biol Chem 270:23560-23569.

14. Thomas MG, Thompson TB, Rayment I, Escalante-Semerena JC. 2000. Analysis of the adenosylcobinamide kinase/adenosylcobinamide-phosphate guanylyltransferase (CobU) enzyme of *Salmonella typhimurium* LT2. Identification of residue His-46 as the site of guanylylation. J Biol Chem 275:27576-27586.

15. Otte MM, Escalante-Semerena JC. 2009. Biochemical characterization of the GTP:adenosylcobinamide-phosphate guanylyltransferase (CobY) enzyme of the

hyperthermophilic archaeon *Methanocaldococcus jannaschii*. Biochemistry 48:5882-5889.

16. Woodson JD, Escalante-Semerena JC. 2006. The *cbiS* gene of the archaeon *Methanopyrus kandleri* AV19 encodes a bifunctional enzyme with adenosylcobinamide amidohydrolase and alpha-ribazole-phosphate phosphatase activities. J Bacteriol 188:4227-4235.

17. Woodson JD, Escalante-Semerena JC. 2004. CbiZ, an amidohydrolase enzyme required for salvaging the coenzyme B12 precursor cobinamide in archaea. Proceedings of the National Academy of Sciences 101:3591-3596.

18. Zayas CL, Claas K, Escalante-Semerena JC. 2007. The CbiB protein of *Salmonella enterica* is an integral membrane protein involved in the last step of the de novo corrin ring biosynthetic pathway. J Bacteriol 189:7697-7708.

19. Trzebiatowski JR, Escalante-Semerena JC. 1997. Purification and characterization of CobT, the nicotinate-mononucleotide:5,6-dimethylbenzimidazole phosphoribosyltransferase enzyme from *Salmonella typhimurium* LT2. J Biol Chem 272:17662-17667.

20. Trzebiatowski JR, O'Toole GA, Escalante-Semerena JC. 1994. The *cobT* gene of *Salmonella typhimurium* encodes the NaMN: 5,6-dimethylbenzimidazole phosphoribosyltransferase responsible for the synthesis of N^1-(5-phospho-alpha-D-ribosyl)-5,6-dimethylbenzimidazole, an intermediate in the synthesis of the nucleotide loop of cobalamin. J Bacteriol 176:3568-3575.

21. Maggio-Hall LA, Escalante-Semerena JC. 1999. In vitro synthesis of the nucleotide loop of cobalamin by *Salmonella typhimurium* enzymes. Proc Natl Acad Sci U S A 96:11798-11803.

22. Maggio-Hall LA, Claas KR, Escalante-Semerena JC. 2004. The last step in coenzyme B(12) synthesis is localized to the cell membrane in bacteria and archaea. Microbiology 150:1385-1395.

23. McGoldrick HM, Roessner CA, Raux E, Lawrence AD, McLean KJ, Munro AW, Santabarbara S, Rigby SE, Heathcote P, Scott AI, Warren MJ. 2005. Identification and characterization of a novel vitamin B12 (cobalamin) biosynthetic enzyme (CobZ) from *Rhodobacter capsulatus*, containing flavin, heme, and Fe-S cofactors. J Biol Chem 280:1086-1094.

24. Zayas CL, Woodson JD, Escalante-Semerena JC. 2006. The *cobZ* gene of *Methanosarcina mazei* Gö1 encodes the nonorthologous replacement of the α-ribazole-5'-phosphate phosphatase (CobC) enzyme of *Salmonella enterica*. J Bacteriol 188:2740-2743.

25. O'Toole GA, Trzebiatowski JR, Escalante-Semerena JC. 1994. The *cobC* gene of *Salmonella typhimurium* codes for a novel phosphatase involved in the assembly of the nucleotide loop of cobalamin. J Biol Chem 269:26503-26511.

26. Jeter VL. 2020. Cobamide Biosynthesis Is Anchored to the MembraneUniversity of Georgia.

Table 6.1. Strains used in this study[a]		
Strain	**Genotype**	**Reference/source**
***Salmonella enterica* subsp. *enterica* sv. Typhimurium str. LT2 strains**		
JE3892	*E. coli* BL21 (λDE3) F- *ompT gal dcm lon hsdSB*(*rB-mB-*) λ(DE3 [*lacI lacUV5-T7 gene 1 ind1 sam7 nin5*])	Lab collection
JE6583	*metE205 araB9*	
JE8312	*metE205 ara-9 cob1315 ycfN112* (Δ*cobU* Δ*ycfN*) / p*cobY*38 (*M. mazei cobY*+, kan+)	Lab collection
Derivatives of strain JE8312		
JE24684	*cob1315 ycfN112* (Δ*cobU* Δ*ycfN*) / p*cobY*38 /pTEV5 (*bla*+)	Lab collection
JE24685	*cob1315 ycfN112* (Δ*cobU* Δ*ycfN*) / p*cobY*38 /p*Mk*CbiS13	Lab collection
JE25383	*cob1315 ycfN112* (Δ*cobU* Δ*ycfN*) / p*cobY*38 /p*Mk*CbiS21	
JE25384	*cob1315 ycfN112* (Δ*cobU* Δ*ycfN*) / p*cobY*38 /p*Mk*CbiS22	
JE25385	*cob1315 ycfN112* (Δ*cobU* Δ*ycfN*) / p*cobY*38 /p*Mk*CbiS23	
JE25386	*cob1315 ycfN112* (Δ*cobU* Δ*ycfN*) / p*cobY*38 /p*Mk*CbiS24	
JE25387	*cob1315 ycfN112* (Δ*cobU* Δ*ycfN*) / p*cobY*38 /p*Mk*CbiS25	
JE25388	*cob1315 ycfN112* (Δ*cobU* Δ*ycfN*) / p*cobY*38 /p*Mk*CbiS26	
JE25389	*cob1315 ycfN112* (Δ*cobU* Δ*ycfN*) / p*cobY*38 /p*Mk*CbiS27	
JE25390	*cob1315 ycfN112* (Δ*cobU* Δ*ycfN*) / p*cobY*38 /p*Mk*CbiS28	
JE25391	*cob1315 ycfN112* (Δ*cobU* Δ*ycfN*) / p*cobY*38 /p*Mk*CbiS29	
JE25392	*cob1315 ycfN112* (Δ*cobU* Δ*ycfN*) / p*cobY*38 /p*Mk*CbiS30	
JE25393	*cob1315 ycfN112* (Δ*cobU* Δ*ycfN*) / p*cobY*38 /p*Mk*CbiS31	
JE25394	*cob1315 ycfN112* (Δ*cobU* Δ*ycfN*) / p*cobY*38 /p*Mk*CbiS32	
JE25395	*cob1315 ycfN112* (Δ*cobU* Δ*ycfN*) / p*cobY*38 /p*Mk*CbiS33	
JE25396	*cob1315 ycfN112* (Δ*cobU* Δ*ycfN*) / p*cobY*38 /p*Mk*CbiS34	
JE25397	*cob1315 ycfN112* (Δ*cobU* Δ*ycfN*) / p*cobY*38 /p*Mk*CbiS35	

JE25398	*cob1315 ycfN112* (Δ*cobU* Δ*ycfN*) / p*cobY*38 /p*Mk*CbiS36	

[a]All strains were constructed during the course of this work unless otherwise stated

Table 6.2 Plasmids used in this study[b]		
Plasmid	**Description**	**Reference/source**
pTEV5	Overexpression vector resulting in a rTEV-cleavable N-terminal His_6 tag (*bla+)*	
p*Mk*CbiS12	Codon-optimized sequence of *M. kandleri cbiS* in the EcoRV site of pUC57	GeneScript USA
p*Mk*CbiS13	*M. kandleri cbiS* (codon-optimized) cloned into pTEV5 using NheI and EcoRI restriction sites	Lab collection
p*Mk*CbiS21	*M. kandleri cbiS* coding for $CbiS^{T76A}$ (codon-optimized) cloned into pTEV5	
p*Mk*CbiS22	*M. kandleri cbiS* coding for $CbiS^{G182A}$ (codon-optimized) cloned into pTEV5	
p*Mk*CbiS23	*M. kandleri cbiS* coding for $CbiS^{V118A}$ (codon-optimized) cloned into pTEV5	
p*Mk*CbiS24	*M. kandleri cbiS* coding for $CbiS^{V120A}$ (codon-optimized) cloned into pTEV5	
p*Mk*CbiS25	*M. kandleri cbiS* coding for $CbiS^{I121A}$ (codon-optimized) cloned into pTEV5	
p*Mk*CbiS26	*M. kandleri cbiS* coding for $CbiS^{S26A}$ (codon-optimized) cloned into pTEV5	
p*Mk*CbiS27	*M. kandleri cbiS* coding for $CbiS^{T96A}$ (codon-optimized) cloned into pTEV5	
p*Mk*CbiS28	*M. kandleri cbiS* coding for $CbiS^{T117A}$ (codon-optimized) cloned into pTEV5	
p*Mk*CbiS29	*M. kandleri cbiS* coding for $CbiS^{N119A}$ (codon-optimized) cloned into pTEV5	
p*Mk*CbiS30	*M. kandleri cbiS* coding for $CbiS^{E142K}$ (codon-optimized) cloned into pTEV5	
p*Mk*CbiS31	*M. kandleri cbiS* coding for $CbiS^{K144E}$ (codon-optimized) cloned into pTEV5	
p*Mk*CbiS32	*M. kandleri cbiS* coding for $CbiS^{T162A}$ (codon-optimized) cloned into pTEV5	
p*Mk*CbiS33	*M. kandleri cbiS* coding for $CbiS^{T164A}$ (codon-optimized) cloned into pTEV5	
p*Mk*CbiS34	*M. kandleri cbiS* coding for $CbiS^{D165K}$ (codon-optimized) cloned into pTEV5	
p*Mk*CbiS35	*M. kandleri cbiS* coding for $CbiS^{V195T}$ (codon-optimized) cloned into pTEV5	
p*Mk*CbiS36	*M. kandleri cbiS* coding for $CbiS^{V199T}$ (codon-optimized) cloned into pTEV5	

[b]All plasmids were constructed during the course of this work unless otherwise stated

Table 6.3. Primers used in this study[c]	
Primer name	**Primer sequence (5' → 3')**
MkCbiS T76A 5'	GATACTCTGGCATTTCTGGCAGCGGCCGATGTAG
MkCbiS T76A 3'	CTACATCGGCCGCTGCCAGAAATGCCAGAGTATC
MkCbiS G182A 5'	CGGTGGCCGGCGCGCAGAAGCTG
MkCbiS G182A 3'	CAGCTTCTGCGCGCCGGCCACCG
MkCbiS V118A 5'	GGCAATGACATTTGCGGTGCCCGGCCC
MkCbiS V118A 3'	GGGCCGGGCACCGCAAATGTCATTGCC
MkCbiS V120A 5'	CACCACGGCAATGGCATTTACGGTGCCCG
MkCbiS V120A 3'	CGGGCACCGTAAATGCCATTGCCGTGGTG
MkCbiS I121A 5'	TCCCACCACGGCAGCGACATTTACGGTGCCCG
MkCbiS I121A 3'	CGGGCACCGTAAATGTCGCTGCCGTGGTGGGA
MkCbiS T96A 5'	GTTACCAAACCCCGCTGCAGCAACAGCAAAGACAT
MkCbiS T96A 3'	ATGTCTTTGCTGTTGCTGCAGCGGGGTTTGGTAAC
MkCbiS T117A 5'	ATGACATTTACGGCGCCCGGCCCGCC
MkCbiS T117A 3'	GGCGGGCCGGGCGCCGTAAATGTCAT
MkCbiS N119A 5'	CACGGCAATGACAGCTACGGTGCCCGGCCC
MkCbiS N119A 3'	GGGCCGGGCACCGTAGCTGTCATTGCCGTG
MkCbiS E142K 5'	CCATGACATTTAGCCTTGACCGCCCAAGTCAGG
MkCbiS E142K 3'	CCTGACTTGGGCGGTCAAGGCTAAATGTCATGG
MkCbiS K144E 5'	CAGGACTCCATGACACTCAGCCTCGACCGCCCAAG
MkCbiS K144E 3'	CTTGGGCGGTCGAGGCTGAGTGTCATGGAGTCCTG
MkCbiS T162A 5'	AGTCTGTGGTGGCGCCCAGGCACGG
MkCbiS T162A 3'	CCGTGCCTGGGCGCCACCACAGACT
MkCbiS T164A 5'	GCTACAGAGTCTGCGGTGGTGCCCAGG
MkCbiS T164A 3'	CCTGGGCACCACCGCAGACTCTGTAGC
MkCbiS D165K 5'	AACCGCTACAGACTTTGTGGTGGTGCCCAGGC
MkCbiS D165K 3'	GCCTGGGCACCACCACAAAGTCTGTAGCGGTT
MkCbiS V195T 5'	CGTCGTCTGATGTCAGCGACGGAGGAAGCGGTTGTGACC
MkCbiS V195T 3'	GGTCACAACCGCTTCCTCCGTCGCTGACATCAGACGACG
MkCbiS V199T 5'	CACCTGCGGTCACAGCCGCTTCCTCTACC
MkCbiS V199T 3'	GGTAGAGGAAGCGGCTGTGACCGCAGGTG

[c]All primers were purchased from Integrated DNA Technologies (IDT)

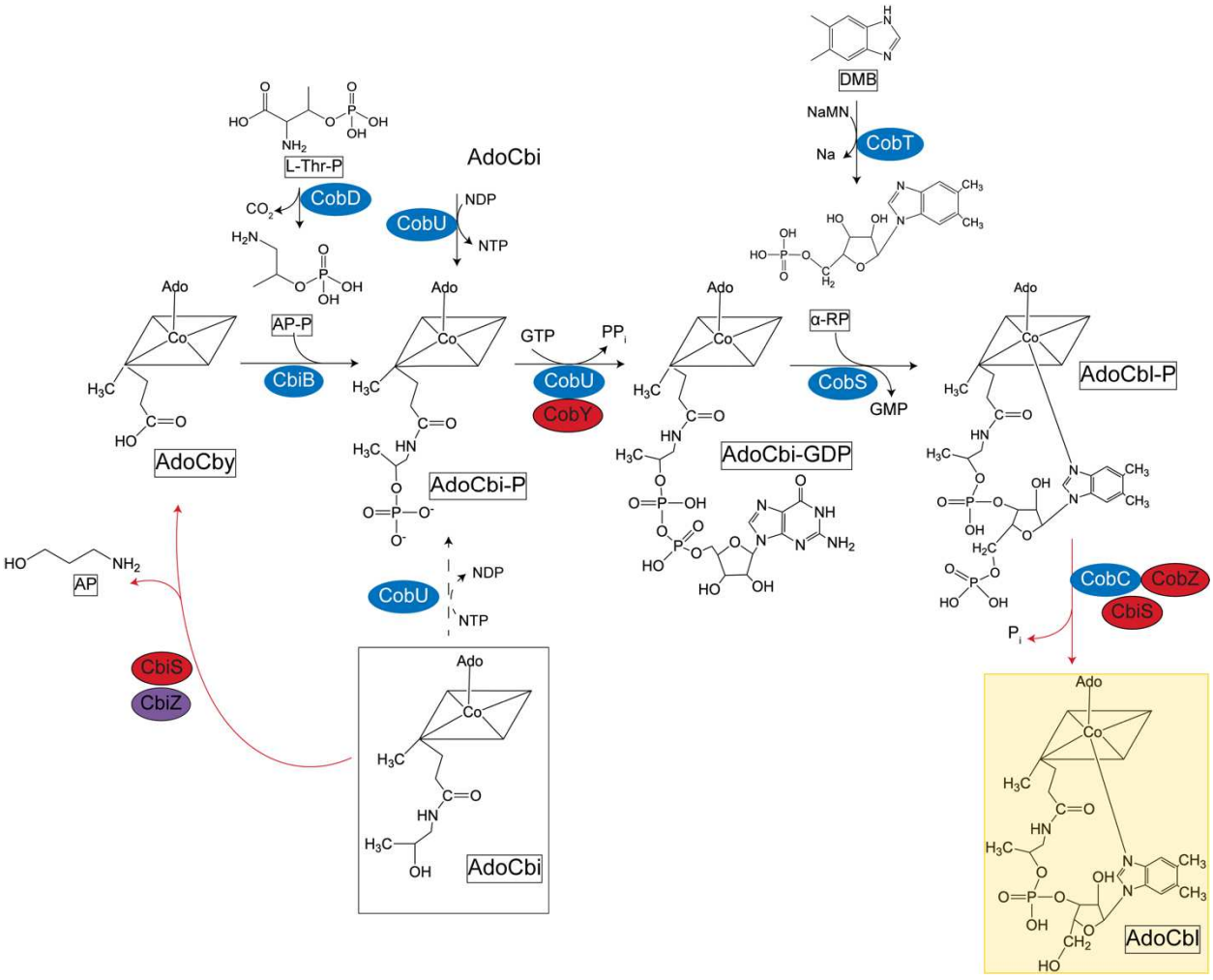

Figure 6.1. Salvaging of the corrinoid precursor cobinamide requires remodeling in archaea. The CbiS substrate cobinamide is shown in a black box. Archaeal enzymes are shown in a red circle, bacterial homologues are shown in a blue circle. Reactions catalyzed by CbiS are illustrated with a red arrow. The CobU kinase function absent in the archaeal homologue is illustrated by a broken arrow. The complete coenzyme is shown in a gold box. Abbreviations are as follows: AdoCbi, adenosyl-cobinamide; AP, aminopropanol; AdoCby, adenosylcobyric acid; L-Thr-P, L-threonine-phosphate; AP-P, aminopropanol-phosphate; AdoCbi-P, adenosylcobinamide-phosphate; AdoCbi-GDP, adenosylcobinamide-GDP; DMB, 5,6-dimethylbenzimidazole; a-RP, a-ribazole-5'-phosphate; AdoCbl-P, adenosylcobalamin-phosphate; AdoCbl, adenosylcobalamin.

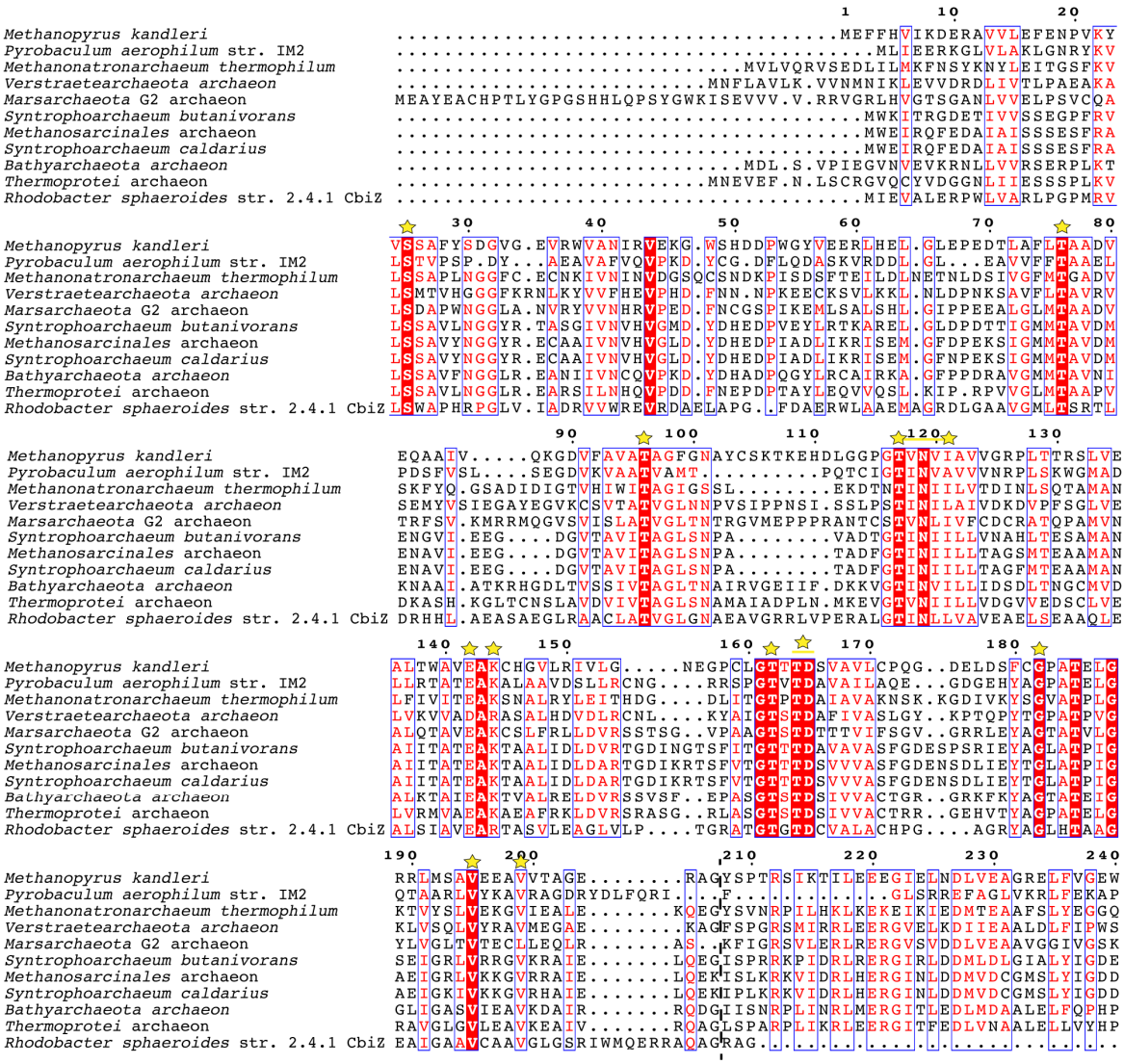

Figure 6.2. Alignment of the amidohydrolase domain of *Mk*CbiS with archaeal and bacterial homologues. Identical amino acids are boxed in red with white text. Regions of similarity are boxed in blue. Similar amino acids are shown in red text. Amino acids that are changed in this work are denoted with a gold star. The termination of the 207-amino acid amidohydrolase domain is marked with a black dashed line. Alignment was generated in Geneius Prime and illustrated using ESPript3.

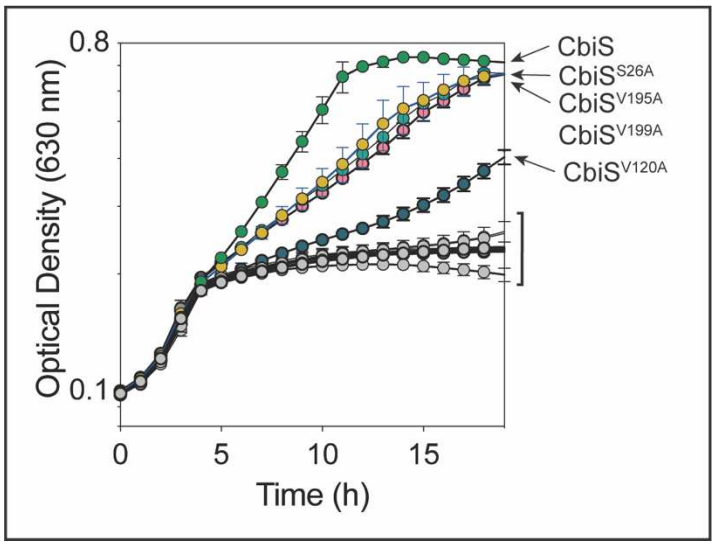

Figure 6.3. Amino acids required for CbiS amidohydrolase activity. Heterologous expression of *Mk*CbiS variants in a *S.* Typhimurium. In all cases, *Mk*CbiS-expressing plasmids were introduced into a *metE205 ara-9 cob1315 ycfN112* (Δ*cobU* Δ*ycfN*) / p*cobY*38 background. Cells were grown at 37 °C with shaking in 96-well microtiter plates in NCE minimal medium supplemented with 1mM $MgSO_4$, 22mM glycerol, 1mM arabinose, 150 μM DMB and 15 nM $(CN)_2$Cbi. Strains producing the following progeins are shown: CbiS (green circles), $CbiS^{S26A}$ (yellow circles), $CbiS^{V120A}$ (dark blue circles) $CbiS^{V195A}$ (teal circles) $CbiS^{V199A}$ (pink circles). Experiments were performed thrice in technical triplicate. Error bars represent the standard deviation of technical triplicates. For simplicity, strains expressing CbiS variants that did not support growth on Cbi are all labeled with a gray dot and denoted with a bracket. These variants are: T76A, T96A, T117A, N119A, E142K, K144E, T162A, T164A, D165K and G182A, and pBAD24 (empty vector).

Table 6.4 Growth analysis of *S.* Typhimurium strains expressing CbiS variants[d]		
Variant	15 nM CNCbi 150uM DMB	5 nM CNCby 150uM DMB
*Mk*CbiS (p*Mk*CbiS13)	0.113 ± 0.021	0.62 ± 0.02
VOC (pTEV5)	NG	0.64 ± 0.03
CbiS^{S26A} (p*Mk*CbiS26)	0.066 ± 0.010	0.61 ± 0.02
CbiS^{T76A} (p*Mk*CbiS21)	0.097 ± 0.008	0.64 ± 0.03
CbiS^{T96A} (p*Mk*CbiS27)	NG	0.62 ± 0.01
CbiS^{T117A} (p*Mk*CbiS28)	NG	0.64 ± 0.02
CbiS^{V118A} (p*Mk*CbiS23)	0.043 ± 0.002	0.65 ± 0.02
CbiS^{N119A} (p*Mk*CbiS29)	NG	0.65 ± 0.02
CbiS^{V120A} (p*Mk*CbiS24)	0.064 ± 0.001	0.66 ± 0.03
CbiS^{I121A} (p*Mk*CbiS25)	0.046 ± 0.004	0.66 ± 0.02
CbiS^{E142K} (p*Mk*CbiS30)	NG	0.67 ± 0.01
CbiS^{K144E} (p*Mk*CbiS31)	NG	0.65 ± 0.01
CbiS^{T162A} (p*Mk*CbiS32)	NG	0.68 ± 0.01
CbiS^{T164A} (p*Mk*CbiS33)	NG	0.68 ± 0.03
CbiS^{D165K} (p*Mk*CbiS34)	NG	0.71 ± 0.03
CbiS^{G182A} (p*Mk*CbiS22)	NG	0.64 ± 0.01
CbiS^{V195T} (p*Mk*CbiS35)	0.080 ± 0.018	0.72 ± 0.02
CbiS^{V199T} (p*Mk*CbiS36)	0.069 ± 0.003	0.72 ± 0.02

[d]All strains originated from a *S.* Typhimurium *metE205 ara-9 cob1315 ycfN112* (Δ*cobU* Δ*ycfN*) / p*cobY*38 background. Cells were grown at 37 °C with shaking in 96-well microtiter plates in NCE minimal medium as described above. Growth rate (μ) of three biological replicates in technical triplicate shown with the corresponding standard deviation between all replicates.

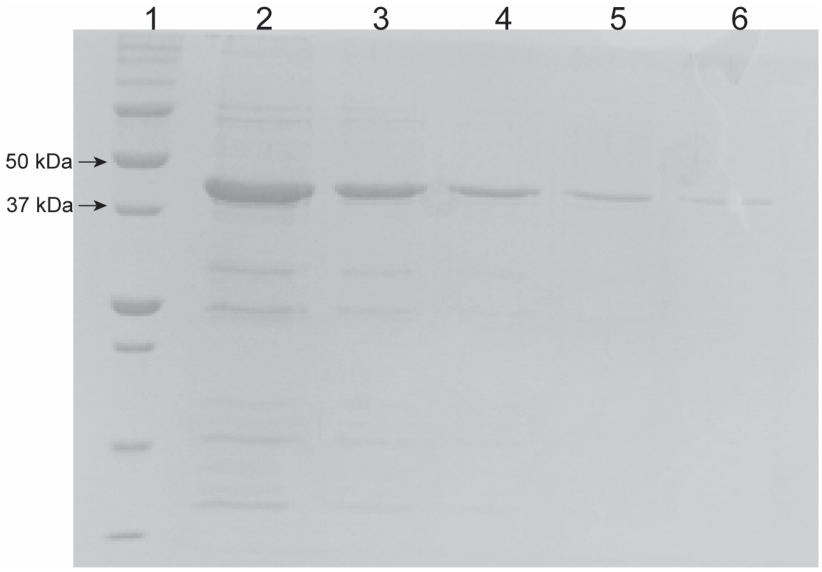

Figure 6.4. Purity of *Mk*CbiS used in this study. *Mk*CbiS was loaded to a 15% SDS-PAGE gel in the following amounts: lane 2, 2.5 μg; lane 3, 1.25 μg; lane 4, 0.625 μg; lane 5, 0.313 μg; lane 6, 0.156 μg. The lanes were analyzed using Total Lab TL100 software. The percent purity of the 40 kDa band corresponding to *Mk*CbiS was determined to be as follows: lane 2, 56%; lane 3, 86%; lane 4, 86%; lanes 5 and 6, 100%.

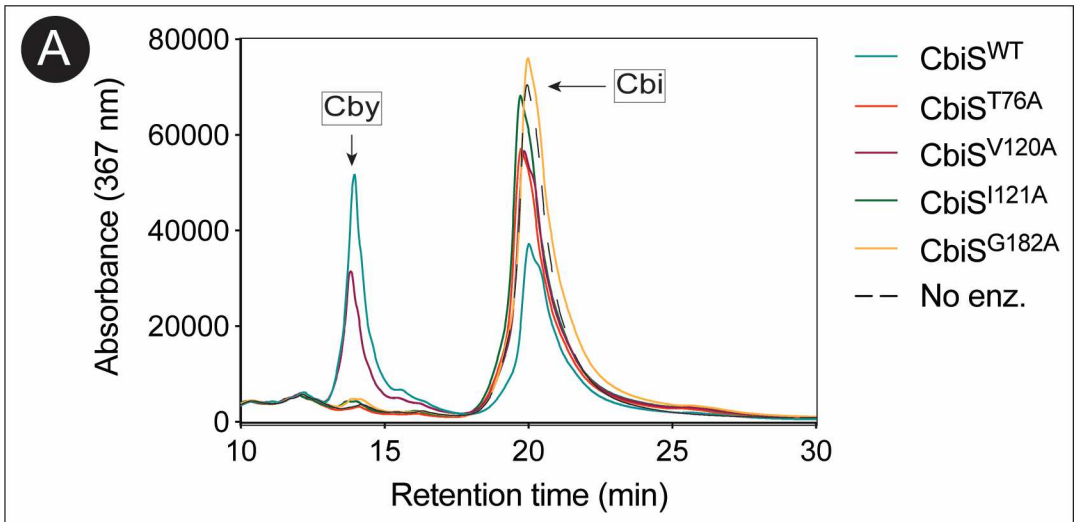

B

Variant	Relative activity
T76A	N/A
V120A	38%
I121A	21%
G182A	N/A

Figure 6.5. Activity of CbiS variants *in vitro*. (A) HPLC chromatogram of the reaction products when $(CN)_2$Cbi (60 μM) was incubated with *MkCbiS* (teal) or the following variants: T76A (red); V120A (maroon); I121A (green); G182A (orange); and no enzyme control (black, dashed line). (B) Relative activity of variants compared to *Mk*CbiS. Relative activity was calculated by compiling the area under the curve at the retention time corresponding to Cby (12 min) divided by wild-type. Each analysis was performed in triplicate. N/A denotes no detectable area under the curve compared to no enzyme control.

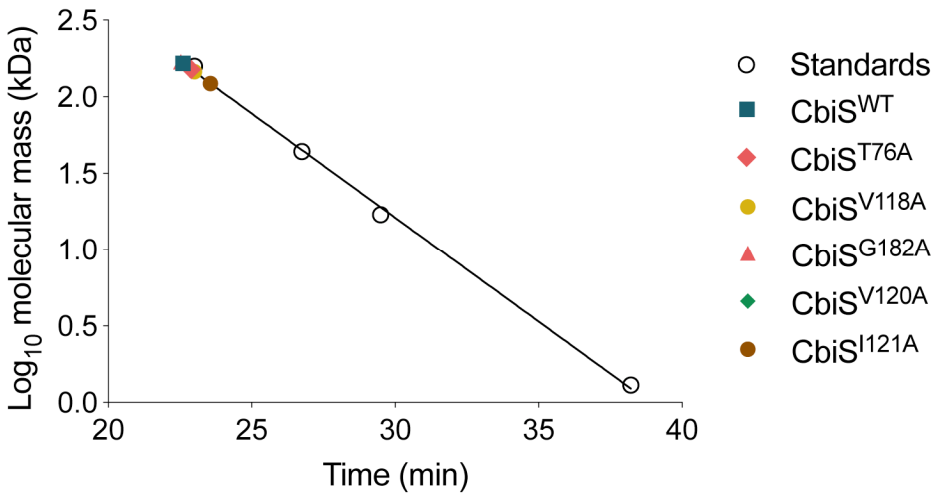

Figure 6.6. Oligomeric state of *Mk*CbiS and variants. CbiS and variants were plotted to a standard curve generated using Biorad gel filtration standards of the following size: γ-globulin (158 kDa), ovalbumin (44 kDa), myoglobin (17 kDa) and vitamin B_{12} (1.35 kDa. All CbiS variants shown here are predicted to be tetramers.

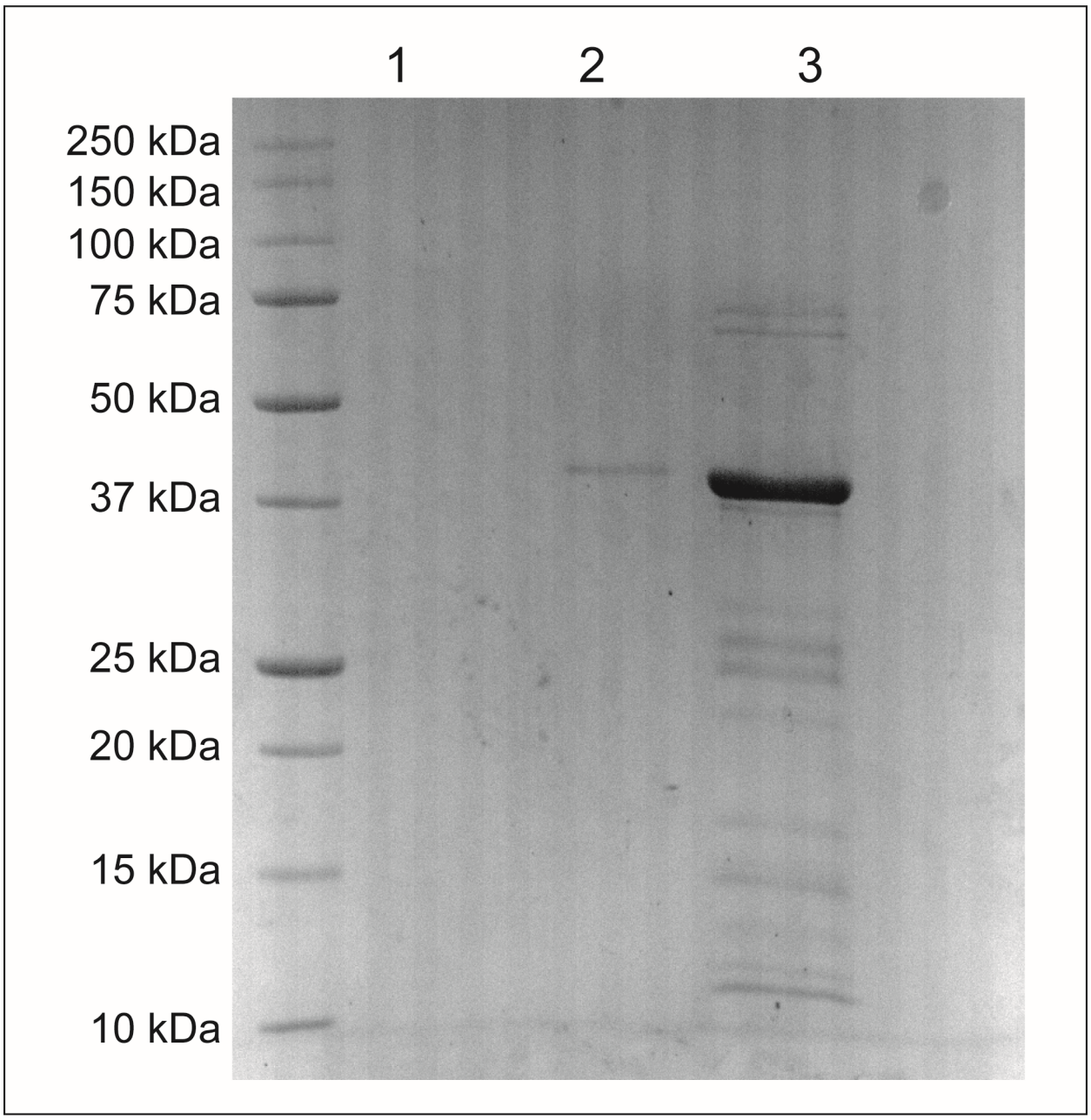

Figure 6.7 CbiS associates with liposomes. SDS-PAGE gel image of liposomes separated by ultra-centrifugation through a density gradient. Lanes include: empty liposome (lane 1), liposome incubated with *Mk*CbiS (lane 2), or pure *Mk*CbiS (lane 3).

CHAPTER 7

CONCLUDING REMARKS AND RECOMMENDED FUTURE DIRECTIONS

7.1 SUMMARY

The preceding work encompasses investigation of utilization and biosynthesis of cobamides in bacteria and archaea. Chapter 2 describes a novel system for ethanolamine utilization used by *Acinetobacter baumannii* that takes place in the absence of a metabolosome structure, and identifies a unique association of the ethanolamine-ammonia lyase (EAL) enzyme complex made up of EutBC with the cell membrane.

Chapter 3 reviews the current literature on the nucleotide loop assembly (NLA) pathway, its role in salvaging of corrinoid precursors, and remodeling of both precursors and complete cobamides. Chapter 4 describes a method for reconstituting membrane proteins into proteoliposomes, in this case the cobamide-phosphate synthase CobS.

In Chapter 5, we further dissect the associations between the adenosylcobinamide kinase/ adenosylcobinamide-phosphate guanylyltransferase CobU with CobS. Our observations suggest that CobU Glu^{80} and Cys^{81}, which form a *cis* peptide bond, have a role in facilitating this interaction. We show that some changes to the amino acids at these locations is detrimental to cell growth. We further show that CobU interacts with the first cytoplasmic loop (CL1) of CobS *in vitro*. Our data suggest that Glu^{80} also has a role in the association of CobU with the full-length CobS protein reconstituted in proteoliposomes.

In Chapter 6, we describe studies of the CbiZ-CobZ fusion CbiS from *Methanopyrus kandleri.* We attempted to expand our limited understanding of this archaeal fusion protein by constructing site-directed mutants resulting in single amino acid changes that result in reduced or inhibition of growth in *S.* Typhimurium. We assess how some of these changes affect catalytic activity. We show that CbiS associates with liposomes, and suggest a role for CbiS in a multienzyme complex formed by NLA enzymes.

A unique system for ethanolamine utilization in *A. baumannii*. We were first attracted to study ethanolamine catabolism in *A. baumannii* due to the identification of a drastically reduced *eut* operon compared to the 17-gene operon found in *Salmonella enterica* subsp. *enterica* sv. Typhimurium str. LT2 (hereafter *S.* Typhimurium). Initial studies determined that *A. baumannii* can utilize ethanolamine as a nitrogen source, but not a carbon source. Our work identified spontaneous mutants that gain the ability to catabolize ethanolamine as a sole carbon source through the insertion of the IS*Aba1* element upstream of *eutBC*, leading to increased *eutBC* expression. We showed that heterologous expression of *Ab*EutBC alone is sufficient to support ethanolamine catabolism in a *S.* Typhimurium strain in which the entire 17-gene *eut* operon has been deleted. We confirmed that the *A. baumannii* AcaT and NLA enzymes CobU, CobS, and CobT are functional and capable of salvaging the precursor cobinamide to form cobamides with various bases as the lower ligand, and that EutBC can utilize multiple cobamides as coenzymes. Using transmission electron microscopy and immunogold labeling, we determined that EutBC localizes to peripheral regions of the cell and to the inner membrane in *A. baumannii* and *S.*

Typhimurium. To our knowledge, this is the first report of an organism that does not produce a metabolosome. Understanding how the acetaldehyde generated in this process is prevented from causing cellular damage in the absence of a physical structure is of great interest.

Elucidating interactions between NLA enzymes. A long-standing hypothesis in the field of coenzyme B_{12} research is that NLA enzymes form a multiprotein complex. This model was proposed in the early 1990's, however studying complex formation has proven difficult. Recent advancements in our protein purification procedure have allowed us to obtain pure CobS, which can be reconstituted into a proteoliposome and used to analyze these interactions. In this work, we focus on the interactions between CobU and CobS. We show that changes to CobU Glu^{80} and C^{81} can cause severe growth defects in *S.* Typhimurium, even when cells are provided with Cbi-GDP. This indicates an additional role for CobU, perhaps in delivery of the substrate for CobS. We present evidence that $CobU^{E80K}$ and $CobU^{C81S}$ alter the interactions between CobU and the first cytoplasmic loop (CL1) of CobS. Furthermore, preliminary evidence suggests that $CobU^{E80K}$ actually promotes a stronger association with CobS. We hypothesize that the strain expressing this variant is unable to grow because CobS does not have access to Cbi-GDP. This may be due to an inability of CobT to provide a-RP, occlusion of the Cbi-GDP binding site, or the inability of CobU to bind Cbi-GDP in an orientation that facilitates CobS access.

Understanding cobamide salvaging in hyperthermophilic archaea. Our studies have expanded the information about the bifunctional fusion protein CbiS. We have identified

several amino acids that are critical for CbiS function when expressed in *S.* Typhimurium. Efforts are underway to develop conditions in which high-quality crystals can be formed to be used in X-ray crystallography and to allow us to determine the structure of this intriguing enzyme. The variants described in this work can be crystallized as well, and the structures compared to CbiS to gain insight into the ramifications of the amino acid substitutions tested here.

7.2 RECOMMENDATIONS FOR FUTURE DIRECTIONS

Ethanolamine catabolism in *A. baumannii.* Current work is underway to further understand the physiological relevance of ethanolamine catabolism in *A. baumannii.* The marked absence of a metabolosome raises the question of how *A. baumannii* is able to prevent cell damage from acetaldehyde production. While we know that EAL is localized to the membrane, and it is possible that other enzymes colocalize to promote efficient quenching of reactive intermediates. The alcohol and aldehyde dehydrogenases encoded upstream of the *eut* genes may provide a rapid response to acetaldehyde generation. Efforts should focus on purifying these enzymes, as well as determining subcellular localization. Alternatively, a Tn-seq would identify other essential steps for ethanolamine utilization in this organism using an unbiased approach.

Other pathogens benefit from the capability to catabolize ethanolamine. Future studies should include identifying co-expressed genes when *A. baumannii* is growing in the presence of ethanolamine to determine whether ethanolamine catabolism contributes to pathogenesis.

The NLA complex. The studies discussed in Chapter 5 provide information to expand our understanding of the nature of CobU-CobS interactions. Interestingly, previous work has shown that CobU does not bind as strongly to proteoliposome-reconstituted CobS as some of the other NLA enzymes. This is unexpected, as CobU provides the substrate for CobS, and so we would anticipate a strong interaction between these two enzymes. We propose that instead, CobU also associates with the integral membrane protein CbiB, reducing the need for a strong association with CobS. CobU may be bound to both CbiB and CobS at the same time, or may oscillate between the two proteins to facilitate this exchange.

Currently, we are limited in our ability to assess NLA interactions because CbiB has not yet been successfully purified. Our current efforts are focused on overexpressing and purifying CbiB, and obtaining this protein is critical to our investigation of this system. Our ultimate goal is to use cryo-electron microscopy in order to visualize the complex, which would include CbiB, CobS, CobD, CobU, CobT, and CobC. We suggest that these proteins colocalize to the inner membrane to promote efficient exchange of intermediates, as corrinoid intermediates are valuable and require substantial energy input to synthesize. We do not yet know the extent to which enzymes involved in B_{12} biosynthesis interact, but we envision a system in which not only NLA enzymes, but the Btu ABC-transport system, the adenosyltransferase CobA, and other related enzymes all localize in close proximity. The use of liposomes has expanded our ability to test interactions between CobS and many of these other enzymes. Using cryo-EM to obtain a visual of the NLA complex would provide insight into this suspected complex that has been under question in the field for over 30 years.

7.3 CONCLUSION

In the previous chapters, I have identified a metabolosome-free system for ethanolamine utilization in *Acinetobacter baumannii*, probed membrane-associated interactions between NLA enzymes, and identified characteristics of an archaeal fusion protein. Together, this dissertation expands our knowledge about both biosynthesis and use of cobamide coenzymes in bacteria and archaea. I hope that these findings serve as steps to continue the growth in this field. Thank you for reading!

APPENDIX A

IDENTIFICATION OF COBU AND COBS MUTANTS UNABLE TO CONVERT COBINAMIDE INTO COBALAMIN[6]

[6]Villa, E.A. and Escalante-Semerena, J.C. 2022. To be submitted to *Journal of Bacteriology.*

A.1 INTRODUCTION

The nucleotide loop assembly (NLA) pathway is essential to forming a biologically active cobamide coenzyme. This process includes enzymes encoded by the *cobUST* operon as well as *cobC*, and is illustrated in Figure A.1. CobU (EC 2.7.1.156, 2.7.7.62) is a bifunctional adenosylcobinamide kinase/ adenosylcobinamide-phosphate guanylyltransferase, catalyzing the reaction of adenosylcobinamide to adenosylcobinamide-GDP (1-6). CobT (CobT, EC 2.4.2.21) is a phosphoribosyltransferase, which activates a base, in this case 5,6-dimethylbenzimidazole (DMB), into α-ribazole-phosphate (α-RP) to serve as the lower ligand (Coα) (6-8). CobS (EC 2.7.8.26) condenses the activated ring and base to form cobalamin-5'phosphate (6, 9-12). In the final step of the pathway, the phosphatase CobC (EC 3.1.3.73) cleaves the 5'-phosphate from the ribose ring to yield the complete coenzyme (13).

We have previously identified mutations in *cobU* that produce a CobU protein incapable of converting Cbi to Cbi-GDP. Several of these mutants do not recover growth even when supplied with Cbi-GDP. We suggest that in these cases, the CobU proteins produced are otherwise impaired in a critical process necessary for NLA, and hypothesize that this is due to disrupted interactions with the subsequent enzyme in the pathway, CobS. The structures and amino acid sequences of CobS and CobU are shown in Figure A.2 and A.3, respectively.

In this work, we report mutations in both *cobU* and *cobS* that prevent conversion of cobinamide into cobalamin. The *cobS* mutations discussed result in N- or C- terminal truncations. CobS is a polytopic integral membrane protein in which the N-terminus is

predicted to be located in the cytoplasm, while the C-terminus is predicted to be embedded in the inner membrane (Figure A.2) (12). We show here that these regions are essential to produce a functional enzyme. The *cobU* mutations described also prevent growth on the product, Cbi-GDP. CobU forms a trimer, illustrated in Figure A.3 A. Subunit-subunit contacts occur at Ala^{8}-Gly^{11}, Glu^{135}-Ile^{140}, and Asp^{152}- the C-terminus (179 aa) terminus (5). The variants described here have disruptions in these regions. Glu^{135} extends towards the hydrophobic core formed by the C-terminus (Figure A.3 A). We suggest that additional disruptions to the NLA pathway occur when the variant proteins described here are expressed, such as prevention of trimer formation and critical protein-protein interactions with other NLA enzymes.

A.2 RESULTS AND DISCUSSION

CobS N- and C-terminal truncations incapable of converting cobinamide into cobalamin are sensitive to the presence of DMB. An N-terminal truncation in which a methionine is placed before the amino acid at position 6 ($CobS^{N5}$), deleting the first five amino acids shows reduced growth compared to a 2- amino acid truncation or full-length CobS (Figure A.4 A, teal compared to dark blue or open circles). However, when provided with DMB, this strain is capable of reaching the same density as full-length CobS (Figure A.4 B, teal compared to open circles). In the presence of DMB, a truncation of 8 amino acids ($CobS^{N8}$) can be tolerated (Figure A.4 B, yellow circles). A strain expressing $CobS^{N9}$, denoting a truncation of the first 9 amino acids, is incapable of growth regardless of access to DMB.

The final 5 C-terminal amino acids are critical for CobS activity. Strains expressing truncations of the final 3 amino acids have a growth phenotype indiscernible from full-length CobS (Figure A.4, C and D). In the absence of DMB, removal of the last four amino acids ($CobS^{243}$) still permits growth, but to a reduced density compared to full-length CobS (Figure A.4 C, pink circles). Providing DMB allows the strain expressing $CobS^{243}$ to reach a density similar to full-length CobS. Removing all 5 C-terminal amino acids ($CobS^{242}$) prevents growth regardless of provision of DMB.

The observed phenotype in which growth of strains expressing N-terminal truncations of CobS is restored by the addition of DMB suggests that the N-terminus may contain either the α-RP binding site or a site of interaction for CobT. A truncation of more than 4 C-terminal interactions prevented growth regardless of DMB provision. The C-terminus contains many hydrophobic amino acids, and removal of more than 4 may prevent anchoring of this region into the membrane, preventing enzyme function.

$CobU^{E135}$ and the C-terminus are required for conversion of cobinamide and cobinamide-GDP into cobalamin. Glu^{135} was identified as an important amino acid in CobU because a mutant unable to grow on Cbi or Cbi-GDP was isolated and determined to encode $CobU^{E135K}$. This is consistent with our observation that a strain expressing $CobUE^{135K}$ is not capable of converting cobinamide or cobinamide-GDP into cobalamin (Figure A.5 A and B, orange circles.) Likewise, substituting an alanine at position 135 also prevented growth on both intermediates (Figure A.4 A and B, green). An aspartic acid, glutamine, or valine in this position resulted in a phenotype indiscernible from CobU (Figure A.5 A and B, yellow, teal, and dark blue circles compared to open circles). The

strain expressing CobU^{E135V} reached a slightly lower density when provided with Cbi-GDP (Figure A.5 B, teal circles).

In the same mutant hunt, a strain was isolated and identified to encode a CobU truncation at Trp^{169}. Substitution of Trp^{169} with a glycine does not affect the ability to convert precursors into cobalamin (Figure A.5 C, D, light blue circles compared to open circles), however a truncation of the final 10 amino acids (CobU^{170}, green circles) prevents growth when providing cobinamide or cobinamide-GDP. Likewise, a strain expressing a truncation removing the 6 final amino acids (CobU^{174}) cannot grow on cobinamide or cobinamide-GDP. CobU^{177}, in which the final 3 amino acids are removed, is not impaired when provided with either intermediate.

In the CobU trimer, subunit-subunit contacts occur at Ala^{8}-Gly^{11}, Glu^{135}-Ile^{140}, and Asp^{152}- the C-terminus (5). We observe here that mutations in these regions may inhibit growth on both the CobU substrate Cbi and the product Cbi-GDP. We hypothesize that this intriguing phenotype is due to an additional role for CobU in positioning Cbi-GDP in a way that makes it accessible to CobS. The observed mutations may prevent proper CobU oligomer formation and/or conformational changes that disrupt interactions with CobS. For example, it is possible that the CobU trimer cannot form in the C-terminal truncation, as too much of the central hydrophobic core region is removed. We suggest that CobU is necessary to deliver Cbi-GDP to CobS, and the changes described herein alter the conformation of CobU such that CobS is unable to access Cbi-GDP.

A.3 CONCLUDING REMARKS

Here, we show that the N- and C-terminus are critical for CobS activity. Based on the phenotypes described here, we suggest that the first 8 N-terminal amino acids are involved in α-RP binding or interactions with CobT. Removing the final 5 amino acids of the C-terminus prevents CobS function. We hypothesize that this is due to improper CobS conformation, as the C-terminus has been shown to be located in the inner membrane.

The work described here suggests that CobU is necessary for Cbi-GDP to be converted into Cbl. This is quite striking, as providing a *cobU* deletion with the product of CobU catalysis would be expected to bypass the requirement for this enzyme. We suggest that without CobU, CobS is prevented from accessing the substrate Cbi-GDP. A number of mechanisms could be responsible for the impairment of CobS access to Cbi-GDP by CobU variants. These are discussed further in Chapter 5.

A.4 MATERIALS AND METHODS

Bacterial strains and plasmid construction. The genotypes of all strains used are listed in Table A.1. All plasmids used in this work are listed in Table A.2. Plasmids containing CobU and CobS variants were constructed using Pfu Ultra II per the manufacturer's instructions (Agilent Technologies). Plasmids containing *cobS* truncations were constructed by amplifying genomic DNA purified from *S.* Typhimurium using primers listed in Table A.3. Amplified fragments were cloned into a BspQI-compatible vector as previously described (14). All plasmids were verified by sequencing analysis (Eton Biosciences).

Growth conditions, media, and chemicals. Unless otherwise noted, all chemicals used were commercially available high-purity compounds. NB or LB was used as rich medium for *S.* Typhimurium. Where indicated, growth analysis was performed in a minimal medium of no-carbon essential (NCE) supplemented with $MgSO_4$ (1 mM), and Wolfe's trace minerals (15). Glycerol (22 mM) was added to the growth medium as the sole carbon source. Corrinoids or cobamides were added to the medium at the concentrations designated in figure legends. Dicyanocobinamide ($[CN]_2$Cbi) and cyanocobalamin (CNCbl) were purchased from Sigma. Cobinamide-GDP and AdoCobinamide-GDP were prepared as previously described (1, 6, 16). DMB was purchased from Sigma. Growth analysis was performed in a 96-well microtiter dish. A 1% (v/v) inoculum was removed from a culture grown overnight in rich medium and used to inoculate 200 μL of minimal medium. Plates were incubated with shaking at 37 °C and monitored at 630 nm. All growth experiments were performed in biological triplicate and technical triplicate. Error bars represent the standard deviation of technical triplicates. Ampicillin (100 μg/mL) was added to cultures for plasmid maintenance. Expression of CobU or CobS variants was induced by the addition of arabinose at 0.5 mM.

A.5 REFERENCES

1. O'Toole GA, Escalante-Semerena JC. 1993. *cobU*-dependent assimilation of nonadenosylated cobinamide in cobA mutants of *Salmonella typhimurium*. J Bacteriol 175:6328-6336.
2. O'Toole GA, Escalante-Semerena JC. 1995. Purification and characterization of the bifunctional CobU enzyme of *Salmonella typhimurium* LT2. Evidence for a CobU-GMP intermediate. J Biol Chem 270:23560-23569.
3. Thomas MG, Thompson TB, Rayment I, Escalante-Semerena JC. 2000. Analysis of the adenosylcobinamide kinase/adenosylcobinamide-phosphate guanylyltransferase (CobU) enzyme of *Salmonella typhimurium* LT2. Identification of residue His-46 as the site of guanylylation. J Biol Chem 275:27576-27586.
4. Thompson TB, Thomas MG, Escalante-Semerena JC, Rayment I. 1999. Three-dimensional structure of adenosylcobinamide kinase/adenosylcobinamide phosphate guanylyltransferase (CobU) complexed with GMP: evidence for a substrate-induced transferase active site. Biochemistry 38:12995-3005.
5. Thompson TB, Thomas MG, Escalante-Semerena JC, Rayment I. 1998. Three-dimensional structure of adenosylcobinamide kinase/adenosylcobinamide phosphate guanylyltransferase from Salmonella typhimurium determined to 2.3 A resolution. Biochemistry 37:7686-95.
6. O'Toole GA, Rondon MR, Escalante-Semerena JC. 1993. Analysis of mutants of defective in the synthesis of the nucleotide loop of cobalamin. J Bacteriol 175:3317-3326.

7. Trzebiatowski JR, Escalante-Semerena JC. 1997. Purification and characterization of CobT, the nicotinate-mononucleotide:5,6-dimethylbenzimidazole phosphoribosyltransferase enzyme from *Salmonella typhimurium* LT2. J Biol Chem 272:17662-17667.

8. Trzebiatowski JR, O'Toole GA, Escalante-Semerena JC. 1994. The *cobT* gene of *Salmonella typhimurium* encodes the NaMN: 5,6-dimethylbenzimidazole phosphoribosyltransferase responsible for the synthesis of N1-(5-phospho-alpha-D-ribosyl)-5,6-dimethylbenzimidazole, an intermediate in the synthesis of the nucleotide loop of cobalamin. J Bacteriol 176:3568-3575.

9. Jeter VL, Escalante-Semerena JC. 2021. Insights into the relationship between cobamide synthase and the cell membrane. mBio 12.

10. Jeter VL, Escalante-Semerena JC. 2022. Elevated levels of an enzyme involved in coenzyme B12 biosynthesis kills *Escherichia coli*. mBio 13:e0269721.

11. Zayas CL, Escalante-Semerena JC. 2007. Reassessment of the late steps of coenzyme B_{12} synthesis in *Salmonella enterica*: Evidence that dephosphorylation of adenosylcobalamin-5'-phosphate by the CobC phosphatase is the last step of the pathway. J Bacteriol 189:2210-2218.

12. Maggio-Hall LA, Claas KR, Escalante-Semerena JC. 2004. The last step in coenzyme B(12) synthesis is localized to the cell membrane in bacteria and archaea. Microbiology 150:1385-1395.

13. O'Toole GA, Trzebiatowski JR, Escalante-Semerena JC. 1994. The *cobC* gene of *Salmonella typhimurium* codes for a novel phosphatase involved in the assembly of the nucleotide loop of cobalamin. J Biol Chem 269:26503-26511.

14. VanDrisse CM, Escalante-Semerena JC. 2016. New high-cloning-efficiency vectors for complementation studies and recombinant protein overproduction in *Escherichia coli* and *Salmonella enterica*. Plasmid 86:1-6.

15. Balch WE, Fox GE, Magrum LJ, Woese CR, Wolfe RS. 1979. Methanogens: reevaluation of a unique biological group. Microbiol Rev 43:260-296.

16. Maggio-Hall LA, Escalante-Semerena JC. 1999. In vitro synthesis of the nucleotide loop of cobalamin by *Salmonella typhimurium* enzymes. Proc Natl Acad Sci U S A 96:11798-11803.

17. Cronan JE. 2006. A family of arabinose-inducible *Escherichia coli* expression vectors having pBR322 copy control. Plasmid 55:152-157.

Table A.1. Strains used in this study[a]		
Strain	**Genotype**	**Reference/source**
***Salmonella enterica* subsp. *enterica* sv. Typhimurium str. LT2 strains**		
JE3892	*E. coli* BL21 (λDE3) F- *ompT gal dcm lon hsdSB*(*rB-mB-*) λ(DE3 [*lacI lacUV5-T7 gene 1 ind1 sam7 nin5*])	Lab collection
JE6583	*metE205 araB9*	Lab collection
JE8248	*metE205 araB9 cobS1313 (ΔcobS)*	Lab collection
JE15888	*metE205 araB9 cobS1313/* pCobS69	Lab collection
JE16852	*metE205 araB9 cobS1313/* pBAD24	Lab collection
JE25696	*metE205 araB9 cobS1313*/ pCobS110	Lab collection
JE25697	*metE205 araB9 cobS1313*/ pCobS111	Lab collection
JE25700	*metE205 araB9 cobS1313*/ pCobS114	Lab collection
JE25701	*metE205 araB9 cobS1313*/ pCobS115	Lab collection
JE25702	*metE205 araB9 cobS1313*/ pCobS116	Lab collection
JE25703	*metE205 araB9 cobS1313*/ pCobS117	Lab collection
JE25704	*metE205 araB9 cobS1313*/ pCobS118	Lab collection
JE8249	*metE205 araB9 cobU1315 (ΔcobU)*	Lab collection
JE24507	*metE205 araB9 cobU1315*/ pBAD24	
JE24508	*metE205 araB9 cobU1315*/ pCobU27	
JE24633	*metE205 araB9 cobU1315*/ pCobU40	
JE24634	*metE205 araB9 cobU1315*/ pCobU41	
JE24635	*metE205 araB9 cobU1315*/ pCobU42	
JE24789	*metE205 araB9 cobU1315*/ pCobU45	
JE24790	*metE205 araB9 cobU1315*/ pCobU46	
JE24791	*metE205 araB9 cobU1315*/ pCobU47	
JE24792	*metE205 araB9 cobU1315*/ pCobU48	
JE24796	*metE205 araB9 cobU1315*/ pCobU52	
JE24797	*metE205 araB9 cobU1315*/ pCobU53	

[a]All strains were constructed during the course of this work unless otherwise stated

Table A.2 Plasmids used in this study[b]		
Plasmid	**Description**	**Reference/source**
pBAD24	Complementation vector P_{araBAD} *bla*$^{+}$	(17)
pCobU27	*S.* Typhimurium *cobU* cloned into the KpnI and HindIII restriction sites of pBAD24	Lab collection
pCobS69	*S.* Typhimurium *cobS* cloned into pBAD24	Lab collection
pCobS110	*S.* Typhimurium *cobS1492* coding for N-terminal truncation encoding $CobS^{3-247}$ cloned into pBAD24	Lab collection
pCobS111	*S.* Typhimurium *cobS1493* coding for N-terminal truncation encoding $CobS^{5-247}$ cloned into pBAD24	Lab collection
pCobS114	*S.* Typhimurium *cobS1494* coding for C-terminal truncation encoding $CobS^{1-242}$ cloned into pBAD24	Lab collection
pCobS115	*S.* Typhimurium *cobS1495* coding for C-terminal truncation encoding $CobS^{1-243}$ cloned into pBAD24	Lab collection
pCobS116	*S.* Typhimurium *cobS1496* coding for C-terminal truncation encoding $CobS^{1-244}$ cloned into pBAD24	Lab collection
pCobS117	*S.* Typhimurium *cobS1497* coding for C-terminal truncation encoding $CobS^{1-245}$ cloned into pBAD24	Lab collection
pCobS118	*S.* Typhimurium *cobS1498* coding for C-terminal truncation encoding $CobS^{1-246}$ cloned into pBAD24	Lab collection
pCobS127	*S.* Typhimurium *cobS1499* coding for N-terminal truncation encoding $CobS^{8-247}$ cloned into pBAD24	
pCobS128	*S.* Typhimurium *cobS1500* coding for N-terminal truncation encoding $CobS^{9-247}$ cloned into pBAD24	
pCobU40	*S.* Typhimurium *cobU1484* coding for $CobU^{E135A}$ cloned into pBAD24	
pCobU41	*S.* Typhimurium *cobU1485* coding for $CobU^{E135D}$ cloned into pBAD24	
pCobU42	*S.* Typhimurium *cobU323* coding for $CobU^{E135K}$ cloned into pBAD24	
pCobU45	*S.* Typhimurium *cobU1486* coding for C-terminal truncation encoding $CobU^{1-177}$ cloned into pBAD24	
pCobU46	*S.* Typhimurium *cobU1487* coding for $CobU^{W169G}$ cloned into pBAD24	
pCobU47	*S.* Typhimurium *cobU1488* coding for C-terminal truncation encoding $CobU^{1-170}$ cloned into pBAD24	
pCobU48	*S.* Typhimurium *cobU1489* coding for C-terminal truncation encoding $CobU^{1-174}$ cloned into pBAD24	
pCobU52	*S.* Typhimurium *cobU1490* coding for $CobU^{E135Q}$ cloned into pBAD24	
pCobU53	*S.* Typhimurium *cobU1491* coding for $CobU^{E135V}$ cloned into pBAD24	

[b]All plasmids were constructed during the course of this work unless otherwise stated

Table A.3. Primers used in this study[c]	
Primer name	**Primer sequence (5' → 3')**
CobS M8 pCV1 5'	NNGCTCTTCNTTCATGCTCGCTTTTATTAGCCGC
CobS L9 pCV1 5'	NNGCTCTTCNTTCATGGCTTTTATTAGCCGCTTG
CobS pCV1 3'	NNGCTCTTCNTTATCATAACAGAGCCAGCAGAAAG
CobU E135A 1	ATCCCCATTCCCACCGCATTTGTCACCAGTACC
CobU E135A 2	GGTACTGGTGACAAATGCGGTGGGAATGGGGAT
CobU E135D 1	CGATCCCCATTCCCACATCATTTGTCACCAGTAC
CobU E135D 2	GTACTGGTGACAAATGATGTGGGAATGGGGATCG
CobU E135K 1	CCATTCCCACCTTATTTGTCACCAGTACCACTTTCG
CobU E135V 1	ATCCCCATTCCCACCACATTTGCTACCAGTACC
CobU E135V 2	GGTACTGGTGACAAATGTGGTGGGAATGGGGAT
CobU E135Q 1	CGAAAGTGGTACCAAATCAGGTGGGAATGG
CobU E135Q 2	CCATTCCCACCTGATTTGTCACCAGTACCACTTTCG
CobU 170 1	GGATGAGGTCTGGTGATGAGTCTCAGGTATT
CobU 170 2	AATACCTGAGACTCATCACCAGACCTCATCC
CobU 174 1	TGGCTGGTAGTCTCATGATGAGGAGTCAAAATT
CobU 174 2	AATTTTGACTCCTCATCATGAGACTACCAGCCA
CobU 177 1	GTCTCAGGTATTGGATGAAAAATTAAATGA
CobU 177 2	TCATTTAATTTTTCATCCAATACCTGAGAC

[c]All primers were purchased from Integrated DNA Technologies (IDT)

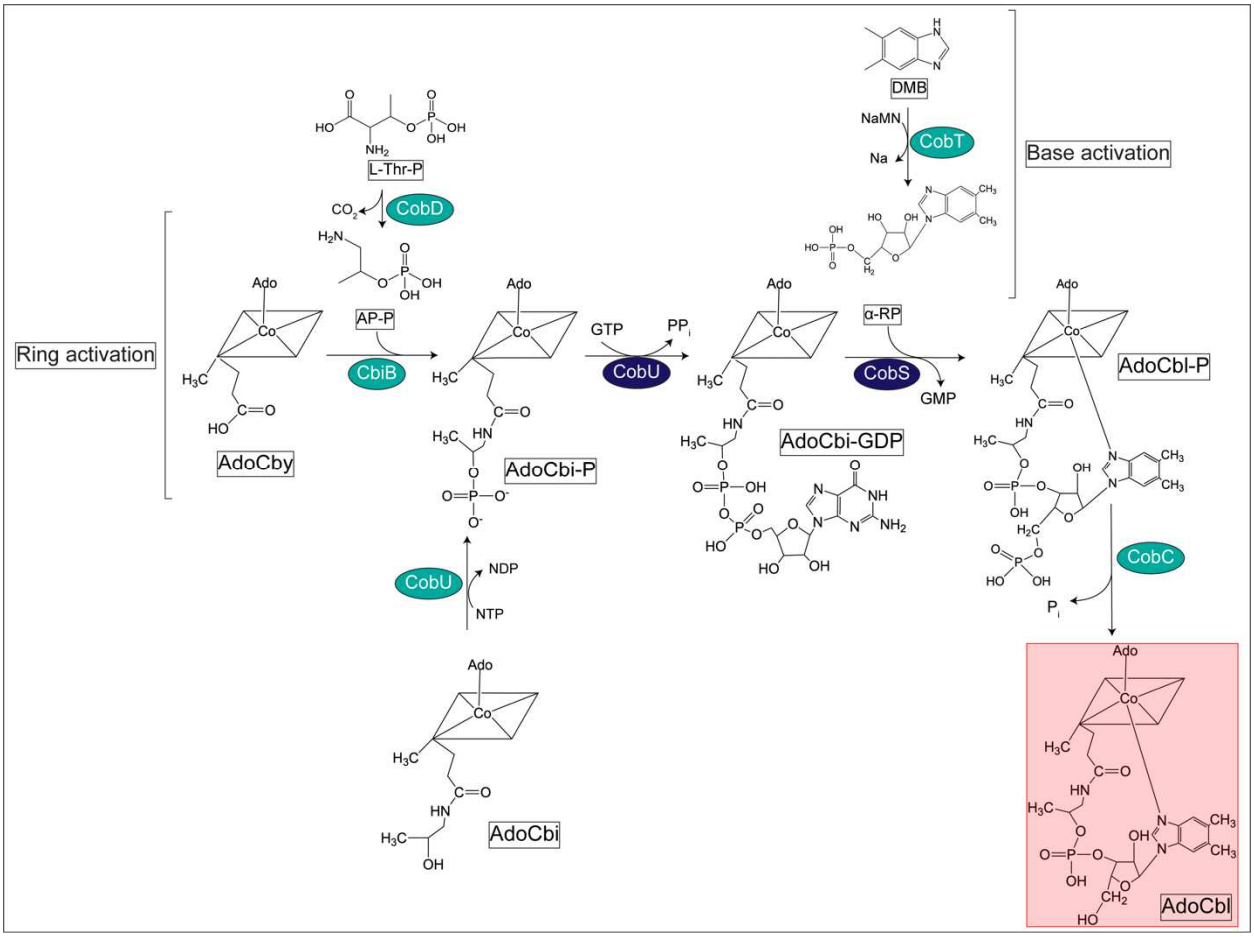

Figure A.1. Nucleotide loop assembly pathway. The chemical structures of intermediates with the corrin ring simplified to a rhombus structure are shown here. Coenzyme B_{12} is shown in a red square. Abbreviations represent: L-Thr, L-threonine; L-Thr-P, L-threonine-phosphate; AP-P, aminopropanol-phosphate; AdoCby, adenosylcobyric acid; AdoCbi, adenosylcobinamide; AdoCbi-P, adocobinamide-phosphate; AdoCbi-GDP, adenosylcobinamide-GDP; DMB, 5,6-dimethylbenzimidazole; α-RP, a-ribazole-phosphate; AdoCbl-P, adenosylcobalamin-phosphate; AdoCbl, adenosylcobalamin.

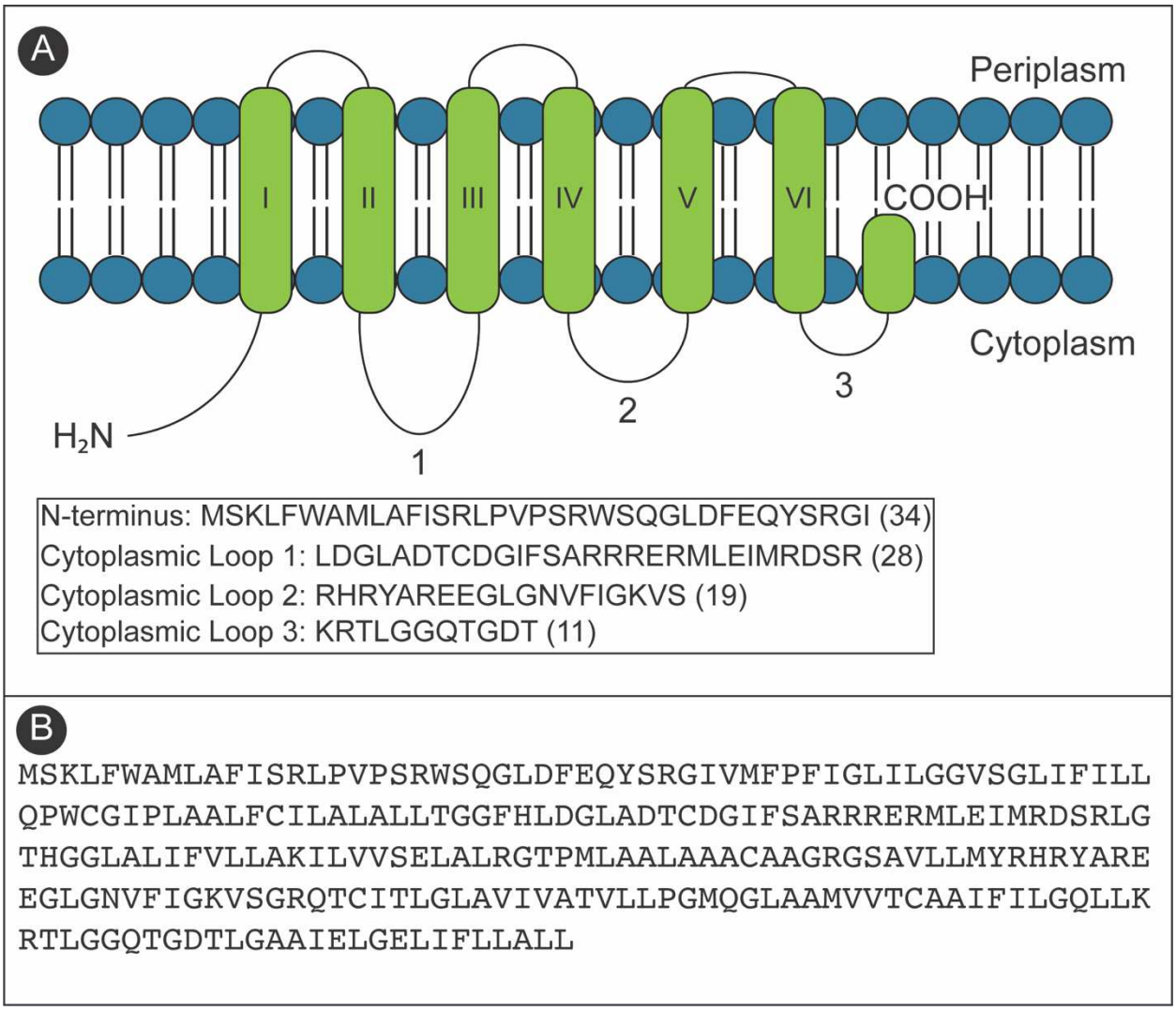

Figure A.2. CobS predicted structure and sequence. Transmembrane domains are indicated in green, cytoplasmic or periplasmic regions are shown with a black line. The N-terminus (34 amino acids) is predicted to be in the cytoplasm. The C-terminus (17 amino acids) is predicted to be embedded in the membrane (12).

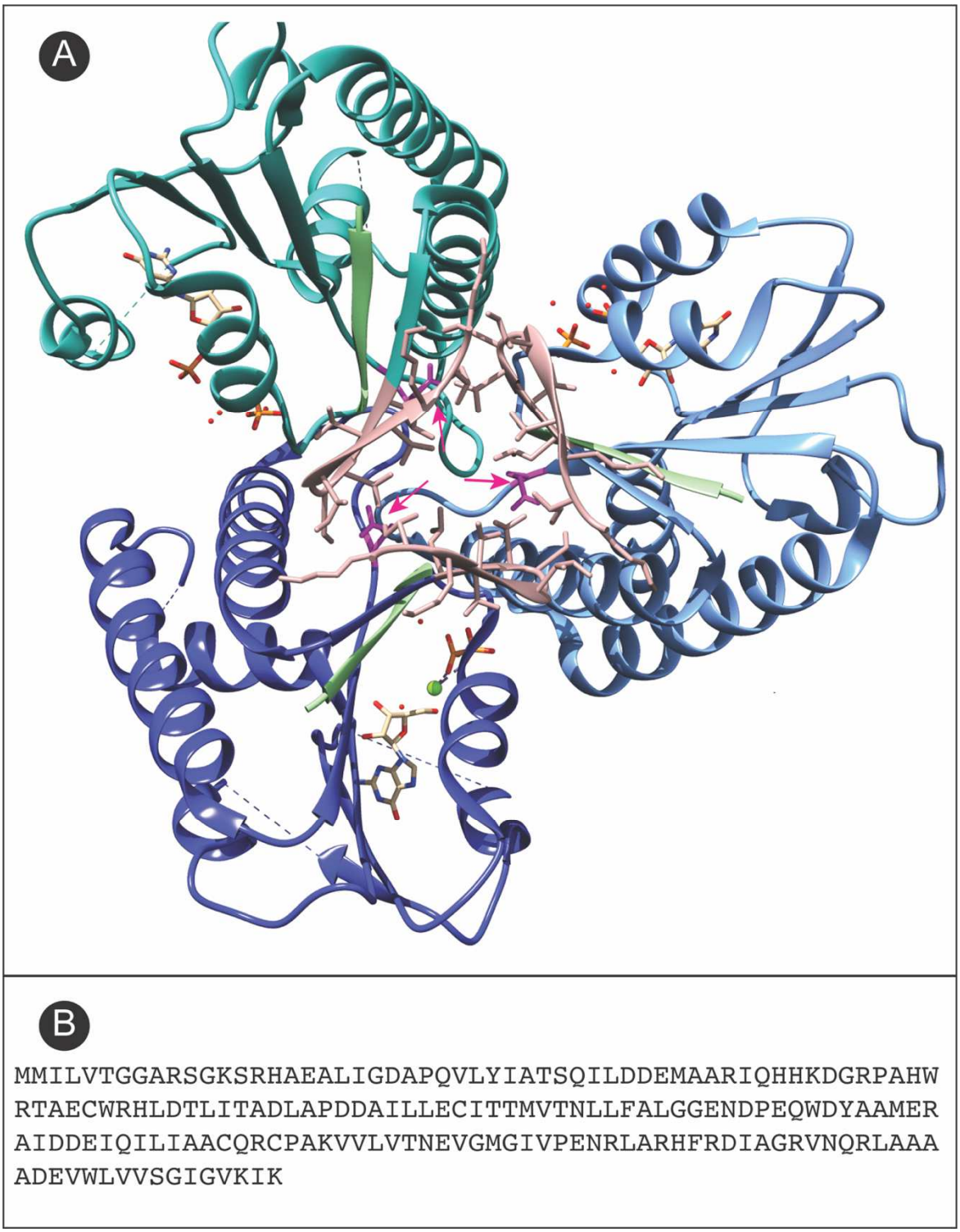

Figure A.3 Structure and sequence of CobU. (A) The CobU trimer is shown with each monomer represented by a different shade of blue. The first five N-terminal amino acids are shown in green. The side chain of Glu^{135} is shown in orange. The final ten C-terminal amino acids are shown in pink. The structure of GMP is shown in tan. Pyrophosphate is shown in orange, and magnesium ions are shown in lime green.

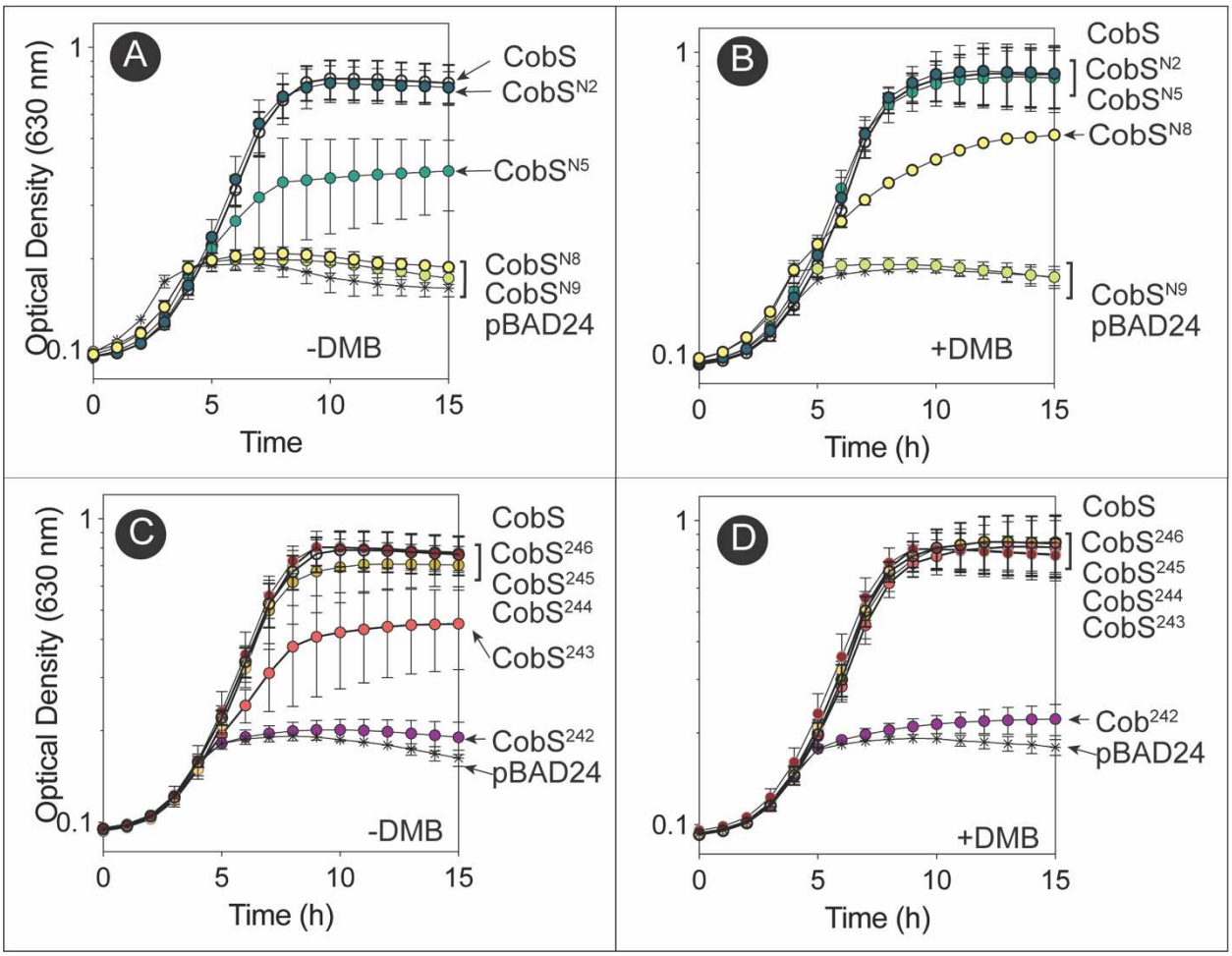

Figure A4. CobS N- and C-terminal truncations. All experiments were performed in an *S.* Typhimurium *cobS1313* (Δ*cobS*) background. Strains expressing CobS N-terminal truncations (top, A and B) or C-terminal truncations (bottom, C, D) were grown in minimal medium supplemented with 5 nM $(CN)_2$Cbi. Where indicated, DMB was added at 150 μM. In all cases, growth was restored by the addition of 15 nM CNCbl. Strains expressing CobS or variants are noted with the following icons for panels A and B: CobS (open circle), $CobS^{N2}$ (dark blue circle), $CobS^{N5}$ (teal circle), $CobS^{N8}$ (yellow circle), $CobS^{N9}$ (lime circle), empty vector (asterisks). Strains expressing CobS or variants are noted with the following icons for panels C and D: CobS (open circles), $CobS^{242}$ (purple circles), $CobS^{243}$ (pink circles), $CobS^{244}$ (yellow circles), $CobS^{245}$ (red circles), $CobS^{246}$ (orange circles), empty vector (asterisks). Error bars represent the standard deviation of technical triplicates.

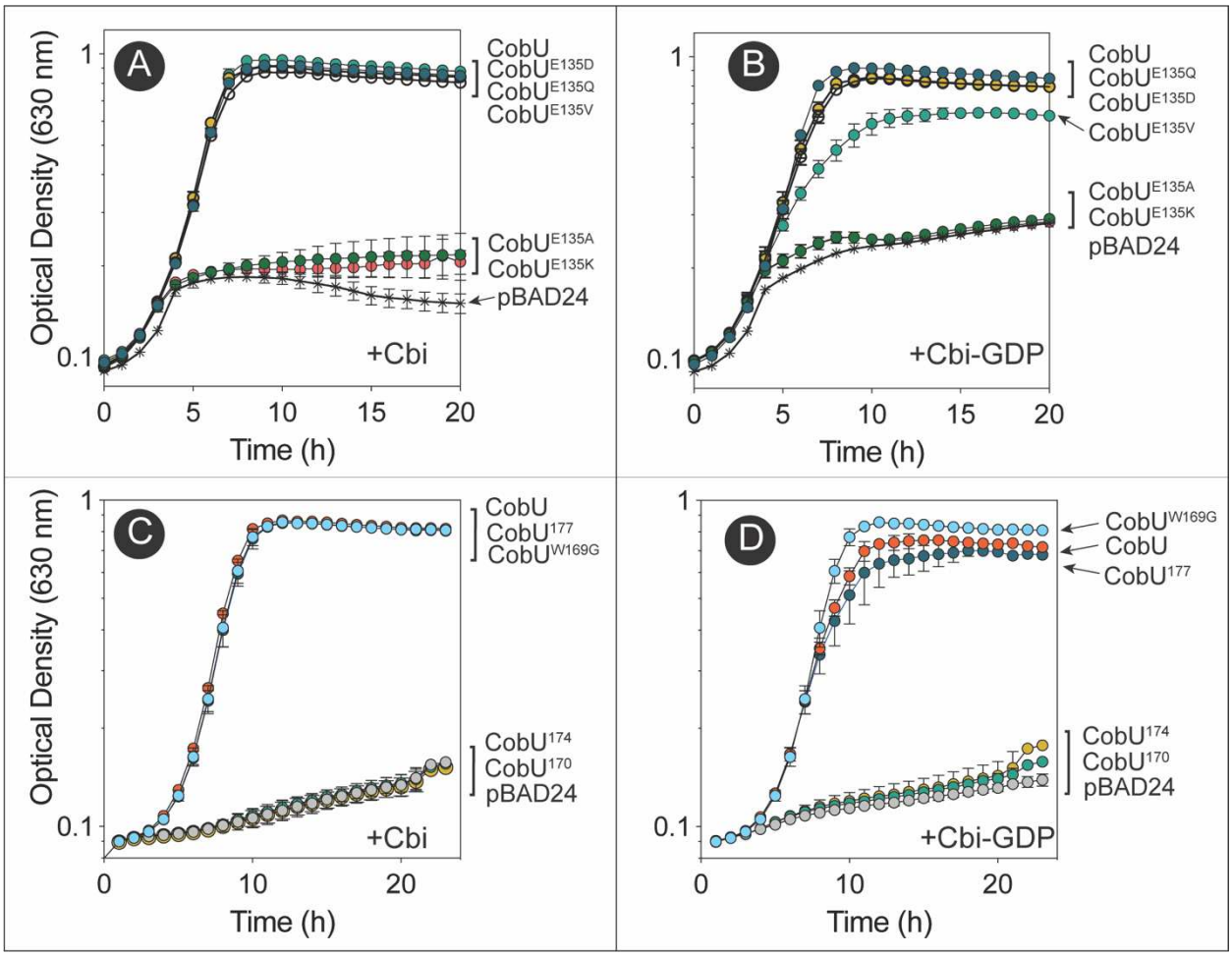

Figure A5. Strains expressing CobU^{E135} variants and C-terminal truncations are unable to convert cobinamide or cobinamide-GDP to cobalamin. All experiments were performed in an *S.* Typhimurium *cobU 1315* (Δ*cobU*) background. Strains expressing CobU^{E135} variants (A, B) or C-terminal truncations (C, D). Cultures were provided with 150 μM DMB and 15 nM $(CN)_2$Cbi (A, C) or 15 nM $(CN)_2$Cbi-GDP (B, D). In all cases, growth was restored by the addition of 15 nM CNCbl. Strains expressing CobU or variant proteins in panels A and B are represented by: CobU (open circles), CobUE^{135A} (dark green circles), CobU^{E135D} (yellow circles), CobUE^{135K} (orange circles), CobUE^{135Q} (dark blue circles), CobUE^{135V} (teal circles). Strains expressing CobU or variant proteins in panels C and D are represented by: CobU (orange circle), CobU^{W169G} (blue circle), CobU^{177} (dark blue circle), CobU^{174} (yellow circle), CobU^{170} (teal circles), empty vector (grey circles). Error bars represent the standard deviation of technical triplicates.